Flow Cytometry Quantitation of Dopamine Receptor D2 Loss as a Sensitive Measure of Huntington's Disease Progression in Mouse Neurons

by

Zachary R. Crook

B.A., University of Colorado (2007)

Submitted to the Department of Biology
in Partial Fulfillment of the Requirements for the Degree of

Doctor of Philosophy in Biology

at the

MASSACHUSETTS INSTITUTE OF TECHNOLOGY

September 2013

Signature of Author……..
Department of Biology
June 17, 2013

Certified by…….
David Housman
Virginia and D.K. Ludwig Professor for Cancer Research
Thesis Supervisor

Accepted by……...
Stephen Bell
Professor of Biology
Co-chair of Graduate Committee

Flow Cytometry Quantitation of Dopamine Receptor D2 Loss as a Sensitive Measure of Huntington's Disease Progression in Mouse Neurons

by

Zachary R. Crook

Submitted to the Department of Biology in September 2013,
in Partial Fulfillment of the Requirements for the Degree of
Doctor of Philosophy in Biology

ABSTRACT

Mouse models of Huntington's Disease (HD) are often used for testing potential therapeutic compounds. These experiments require substantial investments in time and resources, and have yet to produce any intervention that has made a significant impact on disease progression in the clinic. In evaluating potential therapeutics, there is an unmet need for a rapid, highly quantitative measure of disease progression in the HD mouse model brain. Such an assay would help make preclinical trials more efficient. To address this need, I have developed a novel technique for measuring the progression of transcriptional dysregulation, a phenotype with substantial similarities between mouse models and patients. Specifically, utilizing mice that drive GFP expression under the control of one such dysregulated gene (*Drd2*), I have improved on previous protocols for the isolation and characterization of adult neurons by flow cytometry. *Drd2* is a well-studied marker of a particularly vulnerable population in HD patients, the indirect medium spiny neurons of the striatum. Using this technique, I have demonstrated the ability to accurately and rapidly quantitate *Drd2* transcript levels, as measured by *Drd2* GFP (D2GFP) fluorescence, in several strains of HD model mice. This D2GFP loss is particularly robust, with sufficient power to allow subtle, statistically significant alterations to be observed with very small cohorts. Furthermore, the introduction of this D2GFP transgene does not alter the classic HD pathology in these mice. Finally, I show that D2GFP dysregulation can be either induced or ameliorated genetically by delivering transgenes via adeno associated viral vectors, and that a small molecule with only subtle transcriptional effects (cystamine) fails to rescue D2GFP loss. I hope that this system can be of great utility in the validation of effective therapeutic interventions for HD.

Thesis Supervisor: David Housman
Title: Virginia and D.K. Ludwig Professor for Cancer Research

TABLE OF CONTENTS

CHAPTER 1 – HUNTINGTIN FUNCTION AND MALFUNCTION
Introduction 5
Wild Type Huntingtin Function and Evolution 6
mHTT Aggregates: Toxic, or Byproduct? 11
Insights in to Oligomer Toxicity for mHTT and Other Proteins 14
Sequestration of Proteins in Inclusions 17
mHTT, Misfolded Proteins, and Chaperones in HD 18
Pleiotropic Transcriptional Profile Changes in *mHTT*-Expressing Cells 22
Taking Out the Trash: Autophagy and mHTT 24
mHTT and Mitochondria: Altered Activity, Morphology, and Permeability 26
Excitotoxins and Striatal Vulnerability 29
BDNF Transport Alterations and Striatal Vulnerability 35
Summary 36
Figures 37
Bibliography 47

CHAPTER 2 – ASSESSING HD PROGRESS AND CANDIDATE THERAPIES
Introduction 65
Diagnosing HD and Measuring its Progress 65
Pathology Before Phenoconversion: Premanifest HD 69
The Current Therapeutic Landscape: Small Molecules, Small Effects 73
Cell Grafting for Tissue Replacement or Trophic Factor Supplementation 79
Gene Therapy Delivery of Growth Factors 81
Prevention Rather than Rescue: Knockdown Approaches for HD 83
Summary 86
Bibliograpy 87

CHAPTER 3 – MOUSE MODELS OF HUNTINGTON'S DISEASE
Introduction 100
Behavioral Symptoms in HD Model Mice 102
Neuropathology of Murine Models 104
Cell Autonomous vs. Non-autonomous Pathology 107
Specific Excitotoxicity Responses in Various Models 108
Murine Mitochondria and Energy Imbalance 110
Electrophysiology 111
CAG Expansion 112
Transcriptional Dysregulation: Striking Similarities Among Models 113
From Preclinical to Clinical Treatment of HD 116
Summary 116
Figures and Tables 119
Bibliography 125

CHAPTER 4 – D2GFP FLOW CYTOMETRY ASSAY DEVELOPMENT
Introduction 136
Methods 138
Results 147
Discussion 161
Figures and Tables 169
Bibliography 195

CHAPTER 5 – ASSESSING AAV AND CYSTAMINE MODULATION OF D2GFP LOSS
Introduction 200
Methods 202
Results 206
Discussion 220
Figures and Tables 227
Bibliography 255

CHAPTER 6 – FUTURE DIRECTIONS FOR THE (PRE)CLINIC IN HD
Introduction 260
Toward a UHDRS for Mouse Models 260
Pharmaceutical Interventions: When is the Target Specific Enough? 268
Beating Back mHTT on Multiple Fronts 272
Gene Therapeutics: Risks, Progress Remaining, and Potential 275
Conclusions 278
Bibliography 279

APPENDIX: TARGETING HTT RNA SECONDARY STRUCTURE
Introduction 284
Methods 286
Results 288
Discussion 293
Figures 297
Bibliography 307

ACKNOWLEDGMENTS 310

Note: Chapter 3 has been modified from the following article: “Crook ZR, Housman DE. Huntington's Disease: Can Mice Lead the Way to Treatment? Neuron. 2011 Feb 10;69(3):423–35.” Chapters 4 and 5 contain material that was published in the following article: “Crook ZR, Housman DE. Dysregulation of dopamine receptor D2 as a sensitive measure for Huntington disease pathology in model mice. Proc Natl Acad Sci USA. 2012 May 8;109(19):7487–92.” All other work is unpublished as of September 2013.

CHAPTER 1 – HUNTINGTIN FUNCTION AND MALFUNCTION

Introduction

Huntington's Disease (HD) is a progressive, fatal neurodegenerative disorder, characterized by motor, cognitive, behavioral, and psychological dysfunction. Affecting approximately 1 in 10,000 people worldwide, HD is caused by an expansion within a poly(CAG) tract in exon 1 of the huntingtin (*HTT*) gene. Age of onset is roughly inversely correlated with the length of the CAG tract (1-3). Disease occurs with 100% penetrance when 40 or more CAG repeats are present (2). Pathology in HD is characterized by progressive neurodegeneration, particularly within the striatum (caudate and putamen). The massive loss of neurons in this region, normally responsible (amongst many things) for facilitation of volitional movement, is believed to lead to the characteristic motor dysfunctions of HD, such as uncontrolled limb and trunk movements, difficulty maintaining gaze, and general lack of balance and coordination (4). Neuronal loss or dysfunction also leads to cognitive problems, behavioral abnormalities, and psychological dysfunction, some of which are reported before motor abnormalities are noticeable. Importantly, some patients present with a more rigid, Parkinsonian form of the disease, most typicaly when age of onset is under 20 (so called juvenile onset cases). These children generally have large repeats, ranging from over 50 repeats up to 180 repeats, the highest observed value in an early juvenile patient (5). The distinctive features of juvenile HD cause many investigators to think of it as a discrete subform of the disease that may involve distinctive pathological processes. Although 20 years have passed since the discovery of the causative gene, there is no disease modifying

treatment for HD. Treatments providing temporary symptom relief are the only interventions currently available to patients. Significant strides have been made in understanding the gene and its dysfunction when mutated, but the complexities of the cellular pathology observed in HD make it clear that curing HD will not be a simple task.

Wild Type Huntingtin Function and Evolution

Encoded by a gene spanning 67 exons over 170 kbp of the genome at Chromosome 4p16.3, huntingtin (HTT) is a 350 kDa protein of ~3140 residues; the length is approximate, due to a coding CAG trinucleotide polymorphism in exon 1 causing a polyglutamine (polyQ) tract of varying length near the protein's N-terminus. The protein can tolerate a wide variance of lengths in this polyQ tract, typically falling between 6 and 33. At 36 or more repeats, the huntingtin protein acquires toxic properties which become increasingly more severe with increases in repeat length (1).

While the lion's share of research in the field is focused, justifiably, on the toxic isoform with 36 or more Q's (here called mutant HTT or mHTT), understanding the disease process and the consequences of targeted therapeutics requires intimate knowledge of the wild type isoform (wtHTT).

HTT expression is ubiquitous, but most highly expressed in the brain and testis (6,7). It has no known paralogs, but clear orthologs of *HTT* are present in all deuterostomes and some protostomes, including Drosophila, and in general it is highly conserved in animals (8). HTT has few characterized domains; its large size and presence at membranes of many organelles has precluded detailed structural analysis (9). However, it has some highly conserved features. The polyQ repeat in exon 1 varies

in length in chordates, but amongst sequenced animals is longest in humans, and its length tends to correlate with greater organismal complexity and phylogenic similarity to primates (10). A polyproline (polyP) repeat follows the polyQ repeat only in mammals, including marsupials. The function of the polyP and polyQ repeats are not clearly defined, as development, behavior, and neuropathology are largely normal in mice bred missing one or the other region (11,12), and it was even reported that homozygous removal of the polyQ region lengthens lifespan (13).

N-terminal to the polyQ tract is a 17-residue region commonly termed N17. It has strong conservation in deuterostomes, particularly in chordates, where only residue 4 changes (either L or M) and all others are identical (10). A tremendous amount is known about the N17 region and will be discussed more in the following sections, particularly in regards to posttranslational modifications. For now, I will simply say that N17 forms an amphipathic α-helix that is involved in membrane binding (14), and its rapid evolution and minimal sequence variation, particularly in vertebrates, implies a crucial functional role for this domain.

The three regions previously discussed (N17, polyQ, and polyP) all reside in exon 1, within the first 100 residues. However, HTT has more than 3000 residues. As a testament to the mystery of HTT's structure, the only documented, conserved domains downstream of exon 1 are HEAT repeats, protein-protein interaction domains whose name in part derives from HTT itself (the "H" in HEAT). HEAT domains consist of repeated helix-turn-helix motifs, each of which forms a hairpin with two hydrophobic faces, but assembled together form a largely soluble superhelix with a hydrophobic core (15). There are four such HEAT domains in HTT, three of which are capable of auto-

interaction or cross-interaction. This leads to one model in which HTT's N-terminus is membrane bound, while the protein folds on itself as HEAT domains interact in antiparallel arrangement (16), allowing dimerization. This is supported by evidence of HTT being observed as either a monomer or dimer in tissue culture and native brain samples (9,15). Potential facilitation of dimerization notwithstanding, these HEAT repeats are most commonly associated with protein-protein interactions in general, and given HTT's diverse set of interaction partners, they are the main reason HTT is commonly referred to as a scaffolding protein (17).

In spite of its large transcript size and 66 introns, regulation of *HTT* at the transcript level is minimal. There is an upstream open reading frame, an alternative 3' untranslated region, and several miRNA target sites (18-20), but none have been strongly implicated in normal HTT function or disease pathology, nor is there any well studied alternative splicing of the transcript. Post-translational modifications, on the other hand, have significant effects on HTT's turnover, localization, and interactions.

There are many locations along the protein that are subject to covalent modifications; most are concentrated within the rapidly evolving N-terminal 600 residue region. Such modifications include phosphorylation, ubiquitination, SUMOylation, acetylation, palmitoylation, and protease cleavage (reviewed in (1,21)), although proteolysis only happens with regularity in mHTT (2,9). Ubiquitination and SUMOylation of lysines within N17 likely control HTT's turnover (3,22-24). Meanwhile, serine and threonine residues within N17 are sites of phosphorylation. Here, more phosphorylation is generally neuroprotective in the mHTT context, promoting mHTT turnover (reviewed in (25)), but basal phosphorylation is lower in mHTT than in wtHTT (4,26,27), and

wtHTT N-terminal phosphorylation is lowest in those cell types that are most vulnerable in HD (striatal and cortical neurons). Outside of the N17 region, proteolysis sites and serine phosphorylation (pS) events are common. Serine 421 has been particularly well studied. Reduced basal pS421 correlates with sensitivity to mHTT toxicity (5,28), and is particularly important for vesicle transport (to be discussed later).

HTT is known to be associated with many organelles and membranes, and palmitoylation, particularly at cysteine 214, appears crucial in this regard. Mutation of this cysteine residue can induce aggregation even in wtHTT, and can increase aggregation of mHTT, amplifying toxicity. Similarly to protective phosphoserine and phosphothreoninie sites, basal C214 palmitoylation is higher in wtHTT than mHTT (1,29). Proteolysis of wtHTT is not well studied. Native protein preparations of wtHTT include monomers and dimers with very limited proteolytic products; only one cleavage product of ~180 kDa is observed in such preparations (6,7,9). Nevertheless, caspase 3 cleavage can occur on wtHTT in certain disease conditions, as excitotoxic stimulus (excess Ca^{2+} influx from hyperactive ionotropic glutamate receptors) results in cleavage of HTT in neurons, while cells expressing extra *wtHTT* are protected from this stimulus (8,30).

Many of these covalent modifications influence HTT's localization and interaction partners. It can be found associated with the cytoskeletion, playing a role in microtubule transport of vesicles and organelles through $p150^{glued}$ and HAP1 of the dynactin complex (9,31). It also has a well-studied role in transcriptional control. The N17 region acts as a nuclear export signal, keeping it primarily in the cytosol or associated with cytosolic organelles (10,14,32), but HTT can directly act on chromatin or transcriptional

machinery (11,12,33). It is known to interact with many transcription factors, including Sp1, CBP, and REST/NRSF, the latter of which is sequestered outside the nucleus, which increases transcription of *BDNF* and other neuronal genes (13,34). On a more global level, unbiased mass spectrometry revealed interaction partners involved in the 14-3-3 network, chaperones, mitochondrial function, synaptic function, calcium signaling, and the actin cytoskeleton, among others (10,17). In addition, it has been found tightly associated with the mitochondria, the ER, and the plasma membrane (14,32,35,36).

Despite this variety of crucial neuronal functions aided by HTT association, not many specific protein-protein interactions are known to depend solely on HTT, and most are unaltered by a polyQ expansion (15,17). This may help explain why neurons can survive decades with a polyQ expansion in HTT. Additionally, while its knockout is embryonic lethal (due to a role in nutrient transfer from extraembryonic tissue) (16,37,38), it is more dispensable within adult mice. Chimaeras of mice with mixtures of *Htt*(+/+) and *Htt*(-/-) cells can survive for months or longer, depending on chimaeric makeup (9,15,39). This is not universal in mouse tissues, because while some peripheral and brain tissues can contain large numbers of healthy *Htt*(-/-) cells, such cells are scarce in the cortex, striatum, palladium, thalamus, and the cerebellar purkinje layer. Nevertheless, this demonstrates that *Htt* is not necessary for neuronal survival, and tolerance of *Htt* loss is not murine-specific, as short hairpin RNA-mediated knockdown of *HTT* in adult primates is not toxic (17,40,41).

Based on its promiscuous interaction partners but ultimate dispensability in most cells, HTT likely has no specific, indispensable function in most adult cells that cannot

be at least partly replaced by redundant scaffolds. However, its conservation, rapid N-terminal evolution, and embryonic necessity suggest it has been adapted by vertebrates (and mammals in particular) to the development of extraembryonic tissues and complex nervous system patterning while maintaining a role in neuronal homeostasis. Overall, it is clear that neuronal and organismal health and development relies on HTT. Nevertheless, apart from the polyQ expansion conferring a toxic gain of function that is relatively subtle and highly context dependent, the embryonic survival and slow, subtle degeneration in *mHTT*-expressing neurons establish that mHTT behaves very similarly overall to wtHTT.

mHTT Aggregates: Toxic, or Byproduct?

After *HTT* was cloned and *mHTT* expressed in mice (a variety of which are illustrated in brief in Figure 1, and explored in detail in Chapter 3) to generate the first genetic animal model (18-20,42), its subcellular localization was investigated. This led to the discovery that *mHTT*-expressing cells contain inclusions, small (~1 μm) aggregates that stain strongly for mHTT and are found in either the cytosol or nucleus, depending on the model. They were also seen in HD patient samples (43) and became one of the hallmarks of neuropathology.

As reviewed by Yamada et al. (44), there are at least nine disorders involving a coding polyglutamine expansion: Huntington's Disease, spinal and bulbar muscular atrophy (SBMA, also known as Kennedy's Disease), dentatorubral-pallidoluysian atrophy (DRPLA), and spinocerebellar ataxia (SCA) 1, 2, 3, 6, 7, and 17. There is no overarching pattern to their linkage or even the function of the proteins involved. This

results in vastly different protein contexts in which the polyQ tracts are embedded, which likely leads to the different regional susceptibilities involved. The SCA diseases tend to cause degeneration in the cerebellum and brainstem, but with variable pathologies, including basal ganglia involvement (striatum and globus pallidus) in SCA1, SCA3, and SCA17. DRPLA strongly affects the globus pallidus and other forebrain subcortical structures, while SBMA is primarily a disease of lower motor neuronal and spinal motor nuclei loss. All of the known polyQ diseases are neurodegenerative (which may be a result of the postmitotic nature of neurons lacking the ability to remove damaged proteins through dilution upon division), and they all demonstrate neuronal intranuclear inclusions and eventual neuronal death as a result of the gain of toxic function imparted by the polyQ expansion.

However, it is worth mentioning that SBMA presents a unique case. Because androgen binding is required for intranuclear translocation of the protein involved (androgen receptor), it only causes disease in males, and is rapidly cleared upon administration of anti-androgen therapies or castration (45,46). The rapid clearance of polyQ SBMA when not sequestered in the nucleus provides another example (apart from HD) in which nuclear accumulation of a polyQ protein appears under conditions of proteotoxic stress. As will be discussed in Chapter 5, though, a mouse model of HD with poor nuclear retention still causes neuropathology (47), suggesting that nuclear translocation is not a requirement for polyQ proteotoxicity.

Like wtHTT, mHTT is largely cytosolic (48), but N-terminal mHTT, either the result of cleavage or due to the expression of an N-terminal fragment of mHTT, can form inclusions in the cell soma or nucleus (49-51). These inclusions are presumed to

be rich in β-sheet amyloid, as they bind thioflavin T and congo red, and the CD spectra of isolated polyQ amyloid is demonstrably β-sheet rich (52). mHTT aggregation is currently thought to begin by seeding of small oligomers, facilitated by the amphipathic helical N17 region and which can be modulated by posttranslational modifications in the region. Once there is a local increase in the concentration of polyQ regions in close apposition, the structure reorganizes to a more regular β-sheet amyloid (53,54). In support of this, congo red, which binds amyloid and mHTT inclusions in patient samples (55), was shown to inhibit the formation of mature amyloid fibrils (56). Many groups theorized that these inclusions were the source of mHTT toxicity; for example, it was tested whether *in vivo* treatment of HD model mice with congo red could prevent toxicity, but the data was inconclusive, as one group showed improvement of weight, survival, and aggregate formation, while a second failed to show any of those improvements (57,58). These, and other studies, caused the field to re-think the relationship between inclusions and HD.

In an elegant imaging study, it was demonstrated that, in PC12 cells transfected with an exon 1 fragment containing 47Q, inclusion formation correlates with survival, rather than toxicity. Instead, soluble mHTT levels are a stronger predictor of death (59). Meanwhile, in mouse models of HD and in two other polyQ disease models, aggregates either fail to correlate with neuron death or actually correlate with survival (60-62). Perhaps most compelling is an N-terminal mouse model known as shortstop (Ss). Ss mice were the result of an unintended truncation in exon 2 during integration of a full-length YAC construct of *mHTT*, resulting in the expression of a short N-terminal protein reminiscent of that in the highly toxic R6/2 line, albeit with some of exon 2 present. Like

R6/2 mice, inclusions are pervasive in neurons, but this line exhibits no behavioral or neuropathological defects (63). Later work showed that Ss constructs *in vitro* don't form soluble oligomers and more readily interact with the chaperone Hsp70, suggesting that oligomers, now thought to be the toxic species, are not a kinetically favorable state for Ss constructs. Other N-terminal mHTT constructs known for toxicity readily form oligomers (64). Yeast models provide additional insight into the regulation of aggregation kinetics, as they suggest there are distinct classes of genes either facilitating small oligomer formation or the transition from oligomers to inclusions. Knockouts in the former pathway were protective, while loss of those in the latter enhanced the 103Q construct's toxicity (65).

All told, there is strong evidence that inclusions appear in the presence of neurotoxic species in patients and most mouse models, but there is stronger evidence that this is little more than the correlative, and that such inclusions may be protective or benign. One might think of the inclusions as the cell's landfill. If there is garbage (mHTT) in the cell, it is better that it ends up in the landfill (inclusions) rather than littering the streets (cytosol and nucleus). If an intervention is altering the size of the landfill / inclusion, this makes it crucial to distinguish whether the trash is being disposed of (for example, by autophagy), which would be healthy, or whether the garbage now isn't getting to the landfill in the first place (remaining as oligomers), increasing toxicity.

Insights into Oligomer Toxicity for mHTT and Other Proteins

There are many aggregation-prone proteins, both disease-associated and artificial, which shed further light on the relationship between oligomers, aggregates,

and toxicity. Studying the kinetics of aggregation in artificial conditions can provide detailed mechanisms of self-association, but these experiments are normally done in the absence of the cellular milieu, let alone the specific environment encountered by the natural protein in a cell type prone to particular sensitivity (e.g. the striatum in HD). Additionally, protein context provides a great deal of control over the pathways to aggregation. All that being said, Bemporad and Chiti (66) have proposed three simplified pathways towards aggregation, based on studies of a number of such proteins in a variety of *in vitro* and *in vivo* model systems. The first involves native-like proteins that self-associate into higher order multimers without gross misfolding, only slowly acquiring β-sheet-rich amyloid structure as they form more regular, higher order structures. In the second, proteins either partially or completely misfold and rapidly form small oligomers, hiding exposed hydrophobic regions from solution. These oligomers then slowly become the nucleation sites for more stable amyloid structures. Finally, the third pathway involves monomer nucleation, where rare misfolding events drive a partially-denatured monomeric protein (poor in exposed hydrophobic regions) into a very stable β-sheet-rich nucleation site, which then rapidly catalyzes both the misfolding and association of other monomers into a mature amyloid.

Such state changes likely are concentration-dependent, as tissue samples containing Alzheimer's Disease (AD)-associated amyloid β (Aβ) plaques show oligomeric species in a halo around the organized amyloid structures (67). These higher molecular weight oligomers may be transient in nature (68), and become more stable the larger they get (69). Intriguingly, the kinetics of these varied pathways might be modulated chemically, as small molecules were shown to drive toxic oligomers into

either larger disordered aggregates, highly structured fibrils, or even dissociated monomers, all of which were less toxic in tissue culture than the original oligomeric species (70).

The particular toxicity of oligomers has been demonstrated in many models of aggregation-prone proteins. Rapidly-formed early amorphous aggregates of two model proteins, the SH3 domain of PI3K and the N-terminal region of bacterial HypF, are much more toxic to mouse fibroblasts than are mature amyloid fibrils when applied to tissue culture media (71). For the HypF protein fragment, its toxicity likely involves Ca^{2+} influx alterations (72), a source of toxicity in mHTT-expressing cells as well. In the case of mHTT, oligomers were seen to associate with Hsp70 in an ATP- and Hsp40-dependent manner in vitro. Furthermore, in cells expressing toxic mHTT exon 1 fragments, overexpression of both Hsp40 and Hsp70 reduced toxicity, increasing the presence of non-toxic oligomers while reducing both toxic oligomers and aggregates. However, the group also found a reduced rate of luciferase refolding by Hsp40 and Hsp70 when mHTT oligomers are present, demonstrating a potential mechanism for protein homeostasis deficits in mHTT-expressing neurons (73).

Such artificial constructs can be neurotoxic to animals. When oligomers of Aβ or α-synuclein (an aggregation-prone protein implicated in protein homeostasis defects in Parkinson's Disease) generated *in vitro* were delivered to the rat brain, toxicity and cognitive problems were observed. In contrast, injection of either monomers of Aβ or of α-synuclein mutants that were prone to rapid amyloid formation had no effect. (74,75). Furthermore, these studies implicating oligomers (but not monomers or mature amyloid) in neurotoxicity are not limited to proteins generated in vitro. At a correlative level, a

common mouse model of AD demonstrates cognitive decline at an age when intracellular Aβ staining is apparent but before more structured plaques or tangles form (76). Furthermore, when such an Aβ oligomer (~56 kDa) found in another AD mouse model was purified, it could induce memory deficits when delivered to the rat brain (77).

None of these studies investigate the cell-type specificity of oligomer sensitivity, but one group generated interesting data to this end in HD models (78). Starting with an Exon 1 mHTT fragment, they generated amyloid fibrils at either 4°C (cold) or 37°C (warm), which had different structural properties. The cold fibrils were more heat labile (producing monomeric species at room temperature over time), rich in loops and turns, and had more surface-exposed glutamines. In contrast, the warm fibrils were more heat-stable, had numerous intermolecular β-sheets, and more buried glutamine residues. Only the unstable, cold fibrils were toxic when bath-applied to tissue culture cells. mHTT aggregates purified from the R6/2 HD mouse model brain were similarly analyzed, and remarkably, the aggregates from the striatum were more similar in biophysical and toxicity profiles to the cold fibrils, while cerebellar mHTT had the characteristics of the warm amyloid. This does not provide a mechanism for the different kinds of aggregation seen, but it is clear that different cell types drive aggregation down different pathways. Perhaps posttranslational modifications like phosphorylation or ubiquitination, which are differentially regulated in various brain structures, control these kinetics in some way.

Sequestration of Proteins in Inclusions

The study of oligomer seeding and amyloid inclusion formation *in vitro* has

helped better define the polyQ-driven kinetics of N-terminal mHTT aggregation, but *in vivo*, these inclusions can have quite complex structures and are not simple amyloid fibrils. The core of such inclusions is largely made of N-terminal mHTT fragments as well as other small proteins including ubiquitin and Hsp40 (79). Ubiquitination of inclusions is not necessary for their formation, though, as both model mice and juvenile cases demonstrate mHTT+ inclusions that stain negative for ubiquitin (43,80,81). The surface of these aggregates, once established, contains full-length wtHTT and mHTT, and also Hsp70, dynamin, the proteasome, and others (79). These more surface-oriented proteins are susceptible to protease digestion, while the core proteins are not.

Many believe that some of the molecular pathology is the result of proteins being titrated out of solution in the cell, caught in these aggregates. Proteins found in aggregates include mTOR, p53, Mdm2, Hsp70, caspases, and nuclear pore proteins (82,83). mHTT also aberrantly interacts with many transcription factors (reviewed in (84)) resulting in transcriptional profile alterations that have wide-ranging effects (to be discussed later). However, bound transcription factors were not found in macroscopic aggregates (85) and soluble monomers found in the nucleus can suppress transcription (86), so sequestration in an aggregate is not required for mHTT to disrupt a transcription factor's function.

mHTT, Misfolded Proteins, and Chaperones in HD

As mentioned above, mHTT is a target for chaperones, proteins that aid in the proper folding or degradation of misfolded proteins. The presence of heat shock proteins (Hsps) and ubiquitin in insoluble inclusions demonstrates that cells are

attempting to refold or mediate degradation of mHTT (82,87), and there is a wealth of data on mHTT's effects on chaperone pathways and vice-versa (Figure 2).

The interaction of Hsps and inclusion bodies seems to be polyQ and age-dependent. Hsps are mainly found on the periphery of inclusion bodies (79), and are only found there in older HD model mice (88). Hsp70 may play an active role in facilitating the degradation of mHTT under normal HD conditions, as its knockout significantly worsens symptoms of HD mice and increases the size of inclusions (89), though it is possible that these effects are indirect through dysregulation of proteostasis. On the other hand, Hsp90 seems to protect mHTT from proteasomal degradation, and its knockdown reduces mHTT levels (90). Basal levels of Hsps may contribute to the specific toxicity of medium spiny neurons (MSNs) in the striatum, as Hsp70 is particularly highly expressed in the cerebellum, a tissue with little to no neuropathology in HD (91).

Drosophila models have been especially instructive for the relationship between Hsp70 proteins, ubiquitination, and neurodegeneration. PolyQ-expanded androgen receptor (AR), HTT, and *MJD1* (the fly homolog for the gene mutated in Machado-Joseph Disease) all cause degeneration of the retina when expressed in the fly eye (92-94). When Hsp70 is overexpressed in the context of many of these polyQ proteins, degeneration is suppressed, while its deletion or dominant negative expression exacerbate the degenerative phenotype. Hsp70 does not function alone in this regard, as the cochaperones HIP and CHIP facilitate ubiquitination of polyQ substrates (94,95). Interestingly, CHIP, an E3 ubiquitin ligase functioning through Hsp70, appears to depend on the protein context for its activity. CHIP overexpression can suppress toxicity

of polyQ mHTT, but not that of a protein only consisting of an HA-tagged polyQ tract of identical length (94). Furthermore, the ubiquitination of polyQ proteins by Hsp70-aided processes also depends on SUMOylation (92). This may be particularly relevant to HD because SUMO, a similar protein to ubiquitin, was recently found to be conjugated to mHTT by Rhes in human cells. Rhes is a striatal-specific protein, and its SUMOylation of mHTT is competitive with pro-survival ubiquitination (96).

Given the interesting data on mHTT's interaction with Hsps (particularly Hsp70), many groups have tested whether the overexpression of Hsps is protective in mammalian HD models. Tissue culture cells overexpressing *Hsc70*, *Hsp40*, and *Hsp84* are protected from a polyQ construct (88,97), but mice were not so easily treated by single-gene overexpression. Unlike data seen in flies, even a massive congenital overexpression of *Hsp70* only modestly rescued the weight loss phenotype of R6/2 mice, without affecting neuropathology (98,99). It's possible that in adult neurons, multiple Hsps need to be overexpressed if a significant alteration of mHTT aggregation kinetics is to be seen. To that end, overexpression of a constitutively active *Hsf1*, a positive regulator of many Hsps, was tried in R6/2 mice. Though this transgene did not express well in the CNS, the mice survived longer and showed reduced inclusion body formation in skeletal muscle (100), indicating that modulating levels of Hsps may be a viable strategy in HD.

However, a note of caution is warranted regarding modulation of proteostasis for a therapeutic option. It is plausible that steady state increases in a person's proteostasis capacity could promote tumorigenesis, as it is well known that many oncoproteins are clients of Hsp90 or other chaperones (101). While tumors are commonly seen to

overexpress chaperone proteins, I am unaware of whether pharmacologic upregulation of chaperone activity has been shown to induce tumorigenesis. However, it is worth mentioning that polyQ disease patients (including both manifest and premanifest HD) have roughly half the rate of cancer, after correcting for age and other factors, as family members without the polyQ expansion (102). It is therefore worth investigating whether mHTT's disruptive effect on proteostasis is preventing chaperone pathways from facilitating hypertrophy and uncontrolled cell division. If this were true, rescue of this pathway may also lead to normalization, or even a further elevation, of cancer incidence rates, though this is purely speculative.

The classical chaperones Hsp40, 70, and 90 are not the only members of the protein folding machinery known to interact with and modify mHTT toxicity. The chaperonin TRiC is a large ~1 MDa complex that actively refolds proteins through sequestration within a cavity, providing an optimal entropic folding environment (103). It may work by exposing client proteins to a highly hydrophilic environment, essentially preventing cargo from "bumping into" other proteins or lipids and allowing secondary and tertiary folding to take place in seclusion. Initially, client protein interaction takes place through the apical lid subunit that tends to bind hydrophobic, disordered proteins. Its interaction with mHTT was established when overexpression of TRiC subunits in yeast prevented N-terminal mHTT constructs from aggregating (104). Interestingly, this only occurred when all 8 subunits were expressed, indicating that this may require an intact complex. Further work, though, showed that the apical domain alone can suppress aggregation and toxicity (105,106), even when applied exogenously to the cell culture media. Clearly the apical domain alone would have a very different function than

an intact TRiC, and it is possible that apical domains of TRiC subunits simply suppress toxicity by interacting with mHTT in such a way that it alters aggregation kinetics rather than actively refolds it.

All told, chaperones and chaperonins are responsible for maintaining protein folding homeostasis, and there is sufficient evidence that not only is protein folding deranged in *mHTT*-expressing cells, but that toxicity can be ameliorated by artificially increasing the cell's capacity to deal with misfolded proteins.

Pleiotropic Transcriptional Profile Changes in *mHTT*-Expressing Cells

Shortly after the cloning of the causative gene, postmortem HD patient brain samples were analyzed for levels of neurotransmitter receptors to investigate the cause of the complex motor and psychiatric symptoms displayed by patients. Several receptors expressed on the vulnerable MSNs demonstrated robust reductions, particularly dopamine receptors D1 and D2 (107,108). Intracellular markers of these neurons were also reduced, namely substance P and enkephalin (109). Even interneurons, spared from cell death, are nonetheless subject to dysregulation in the form of reduced neuronal NOS and somatostatin levels (110). These receptor or antigen reductions were determined to be not simply total tissue loss, but the result of reduced transcripts on a cell-by-cell basis.

Reduced transcript levels of receptors led to studies on the mechanism of transcriptional dysregulation in HD (Figure 3). Many groups have established aberrant interactions between mHTT and the transcription factors CBP, TBP, p53, NCoR, and Sp1, in addition to some of the core transcriptional machinery (84,111). Additionally, the

transcriptional repressor of neuronal genes REST/NRSF, normally sequestered in the cytosol by a complex including wtHTT, cannot efficiently form a complex with mHTT. Due to mHTT's reduced ability to bind HAP1, another component of the REST/NRSF sequestration complex, REST/NRSF now enters the nucleus more freely, reducing the levels of its target neuronal transcripts (112,113).

Given the large number of transcription factors affected by HTT polyQ expansion, global transcriptional profiles are highly informative. In patient tissues studied by array-based transcriptional profiling, many categories of genes are significantly dysregulated. These include synaptic transmission, neurogenesis, ATP synthesis, CNS development, and Ca^{2+} transport, among others (114), and similar alterations are present in blood and skeletal muscle samples from patients (115,116). Studies in mouse models gave similar results, indicating that this is a shared and consistent feature of mammalian *mHTT* expression (117-119). REST/NRSF targets are of particular interest, based on two lines of study. First, it was determined that those genes that have strongest downregulation in HD brain are most highly enriched for being targets of REST/NRSF, suggesting that of all of the transcription factors with altered activity in *mHTT*-expressing neurons, REST/NRSF plays a particularly central role (Reviewed in (120)). Second, a particularly crucial gene for striatal health is *BDNF*, which encodes a neurotrophic factor mainly produced in the cortex and trafficked by afferent projections to the striatum (121). There are four alternative promoters for *BDNF*, and it is promoter II that is responsible for most of the physiological BDNF present in the striatum. REST/NRSF controls transcription from this promoter, resulting in significantly reduced levels of this transcript in HD mice and cell models. (Reviewed in (122)). REST/NRSF-mediated suppression of *BDNF* and

other transcripts is observed in mice and patient samples (34). Loss of wtHTT recapitulated some of these effects in embryonic stem cells, and surprisingly, the transcriptional profiles of HD model mice and patient samples are remarkably similar to that of a heterozygous knockout *BDNF* mouse (119).

Dysregulated REST/NRSF targets (*BDNF* in particular) are not the only disease-relevant dysregulated genes. As an additional example, PGC1α (gene name *PPARGC1A*), a central regulator of mitochondrial biogenesis, activity, and structure, is itself dysregulated in HD. Given striatal cells' particular vulnerability to perturbations of electron transport chain (ETC) function (to be discussed later in the chapter), this may go a long way to explaining striatal vulnerability in HD. mHTT is found at the *PPARGC1A* promoter (123), and its protein levels are reduced in striatal but not cortical samples from HD mice (124). In addition, its loss in wild type animals results in striatal lesions, while its loss in HD mice exacerbates symptoms (123,125). Mitochondrial energetic problems in HD are manifold, and will be discussed in more detail later, but reduced levels of PGC1α only worsen energetic demands on already fragile MSNs.

Taking Out the Trash: Autophagy and mHTT

For all the focus on transcription and translation in modern molecular biology, it's easy to forget that in general, for every protein produced, another is degraded. In protein folding disorders like HD with impaired degradation of a misfolded toxic protein, this process is clearly deranged, if only subtly.

Proteins are largely degraded by either the proteasome, which typically requires interaction with ubiquitinated substrates that are brought to the proteasome by

chaperones, or by the lysosome / autophagosome processes when the protein in question is too large or aggregated to be fed into the proteasome. It is well known that mHTT is often ubiquitinated, particularly in inclusions, and that chaperones also are readily found in association with it (43,79). There is also evidence that impairment of the proteasome worsens mHTT toxicity (126,127); this may be of limited direct relevance, though, as the proteasome is relatively poor at degrading polyQ proteins. The eukaryotic proteasome's three protease activities cut after hydrophobic, basic, and acidic residues, but glutamine fits none of these criteria, and is thus resistant to proteasome-mediated proteolysis (128).

Autophagy, on the other hand, is more amenable to not only degrading polyglutamine-bearing proteins, but at engulfing and disposing of insoluble inclusion bodies (Figure 3). Cells expressing *mHTT* seem to detect this protein homeostasis threat and increase autophagy signals, particularly cathepsins (129), and impairment of proteasome function increases autophagy-mediated degradation of mHTT fragments (130). Increased autophagy through starvation or dietary restriction also reduces the toxic effects of mHTT (130,131).

HTT, being often membrane-associated, is found on autophagosomes (wtHTT, full-length mHTT, and N-terminal mHTT are all seen there) (32,132). Targeting to the autophagosome is carefully regulated by acetylation at K444. This residue is acetylated by CBP and deacetylated by HDAC1, and mutating this residue, preventing acetylation, increases mHTT levels and toxicity *in vitro* and *in vivo* (133). This effect is dependent on macroautophagy (as it is LC3-dependent), which is one of two autophagy pathways relevant to mHTT degradation, the other being chaperone-mediated autophagy.

Macroautophagy plays an important role in removal of toxic mHTT, as LC3 knockdown increases the presence of mHTT aggregates. However, macroautophagy is reduced in general in *mHTT*-expressing cells, while chaperone-mediated autophagy seems to try to compensate, as it increases in such cells. This phenomenon may partly explain the late onset nature of the disease, as this LAMP-2 and Hsc70-dependent chaperone-mediated autophagy pathway becomes less effective in aged HdhQ111 mice (134). Lastly, an essential regulator of autophagy, *ATG7*, houses a SNP that reduces the age of onset in patients (135), giving autophagy additional credibility as a potential therapeutic target.

mHTT and Mitochondria: Altered Activity, Morphology, and Permeability

Mitochondrial function has long been a crucial player in HD pathology (Figure 4), and may be more important to striatal neurons than those of other parts of the brain such as the cortex and cerebellum. Some of the first evidence for this was the demonstration that systemic treatment with 3-nitropropionate (3-NP), a specific mitochondrial Complex II (succinate dehydrogenase) inhibitor, induces neurotoxicity that is reminiscent of HD in terms of its cell-type specificity (136). Intraperitoneal injection of the drug induces striatal lesions (cell death and gliosis) due to death of MSNs but, similarly to brains of HD patients and genetic animal models, the cholinergic interneurons are spared. This made 3-NP treatment a simple, rapid animal and cell model of HD, and its continued study demonstrated further similarities in mitochondrial dysfunction to cells expressing *mHTT*.

3-NP's inhibition of the ETC has many interesting effects, most of which seem to damage MSNs disproportionally. Its overall effects on mitochondrial energetics and ATP

production play a role, as treatment results in depolarization of MSNs but not HD-resistant interneurons (137). Energetics don't tell the whole story though, as the effects of 3-NP can be ameliorated without rescuing succinate dehydrogenase. 3-NP-treated samples generate reactive oxygen species (ROS) and produce DNA oxidative damage (138). Antioxidants and free radical scavengers protect striata from lesions and protein carbonylation (139), so the striatal specificity of 3-NP seems to rely in some part on ROS generation. 3-NP also appears to induce toxicity via sensitization of mitochondrial permability, as inhibitors of the permeability transition pore (PTP) prevent damage in culture (140,141). The effects of disruption of the ETC can were also examined genetically when a restriction enzyme (PstI) was directed to the mitochondria in transgenic mice, producing a condition of chronic mtDNA damage and reducing ETC activity under careful transcriptional control. In this study, as is the case with 3-NP treatment, MSNs of the striatum are particularly sensitive to mtDNA damage / ETC reduced activity. Additionally, the mitochondria specifically were hypersensitive to challenge with Ca^{2+} (142), a response that will be covered in more detail in the next section.

Once the *HTT* gene was cloned and mouse and cell models of *mHTT* expression were more prominent, studying the interplay between mitochondrial function and mHTT was possible. Based on the 3-NP studies and its demonstrated ability to selectively damage MSNs in an HD-like pattern, patient and cell samples were tested for mitochondrial activity. Striatum from late-stage patients demonstrates reduced activity of multiple complexes of the ETC, and DNA oxidation is also increased (143-145). The cortex and cerebellum are relatively spared in this regard, suggesting a mechanism of

those tissues' relative protection from mHTT. Furthermore, ATP levels (reported as the ATP/ADP ratio) were reduced in lymphoblastoid cell lines generated from patients (146). Two points are notable from this study. First, there was exquisite CAG-length-dependence, as the correlation between high repeat length and low ATP/ADP ratio was strikingly strong, and second, there was even a reduction in ATP/ADP ratio in cells expressing *HTT* with high-wild-type repeats (30-35), a range not known to produce neuropathology.

Mouse models of HD show similar ETC abnormalities. Striatal slices in culture from mice expressing an N-terminal transgene have half of the respiratory capacity of their wild type littermates, though interestingly, this effect was rescued by perfusion with succinate, indicating that in spite of 3-NP's ability to mimic HD, it may not specifically be succinate dehydrogenase that is the defective enzyme in HD striatal cells limiting their respiratory capacity (147). R6/2 mice, expressing a particularly lethal *mHTT* transgene, have elevated striatal DNA oxidation and glutathione levels (148,149), and mHTT primes their mitochondria to depolarize more readily upon exposure to 3-NP (137,150). Their sensitivity could be compounded by impaired mtDNA repair, a phenomenon shared between R6/2 mice and 3-NP-treated mice (138). ETC defects are not limited to mouse neurons in the brain, as immortalized striatal precursors from knockin mice behave similarly to patient-derived lymphoblasts by demonstrating reduced ATP/ADP ratios (151).

Many studies have also demonstrated that mitochondrial morphology and movement are altered in HD samples, and not only is this not a simple byproduct of toxicity, but its prevention can ameliorate toxicity. Initially, it was demonstrated that

increased fragmentation and reduced movement are observed in cells expressing *mHTT* (152), possibly relating to aberrant trafficking to the mitochondria of mHTT (153). Further studies have revealed aberrant morphology of mitochondria in HD patient lymphoblastoid cells, myoblasts, and fibroblasts (154,155), effects that are more severe in homozygote samples than heterozygotes. Altered mitochondrial morphology is highly dependent on a subset of genes involved in fission and fusion of the mitochondrial reticulum, and *Drp1* has been studied in some detail in this regard. Drp1, a mitochondrial GTPase enzyme, positively regulates mitochondrial fission (156). Drp1 levels are increased in mid- to late-stage HD patient striata (157,158), and its GTPase activity is increased upon interaction with mHTT (159,160). Phosphorylation of Drp1 suppresses its activity, while both the increased basal levels of calcineurin seen in HD (a phosphatase of Drp1 among many targets) and impairment of its phosphorylation by staurosporine increase its activity and result mitochondrial fragmentation (161). This can be rescued by dominant negative (DN) *Drp1* expression (156), and in fact, DN *Drp1* in a *C. elegans* polyQ model partially rescues its movement defect (162).

Excitotoxins and Striatal Vulnerability

The specificity of neurodegeneration in HD (selectively killing the GABAergic MSNs of the striatum while cholinergic interneurons are spared) is striking. In trying to explain this pattern, a popular hypothesis is that *mHTT*-expressing MSNs are particularly sensitive to the glutamatergic inputs from the cortex. Glutamate normally activates many receptors, among which are ionotropic NMDA receptors and metabotropic mGluR receptors, which lead either directly or indirectly to increases of

intracellular Ca^{2+} (Figure 4). An excellent review on calcium's role in neurodegeneration (163) summarizes it thusly: as Ca^{2+} levels rise in the neuron (from both NMDA receptor influx and from Ca^{2+} escaping the ER by way of hyperactive IP_3 receptors), three things happen. First, calcium-mediated proteases (e.g. calpains) are activated, degrading substrates that can include cytoskeletal components and neurotransmitter receptors. Second, levels of reactive oxygen species rise via perturbations of oxidative phosphorylation. Third, mitochondrial permeability is induced, flooding the cytosol with proapoptotic factors such as cycochrome C. mHTT appears to prime mitochondria for this toxic insult, as mitochondria from HD mouse models (both brain and muscle), patient lymphoblastoid cells, and knockin mouse striatal precursors all permeabilize in response to lower levels of Ca^{2+} than is seen in wild type samples (164-167). In all of these cases, mitochondrial permeability transition pore (mPTP) opening not only releases proapoptotic factors but also depolarizes mitochondria, hampering ATP production, and allows glutathione and calcium to escape, exacerbating damage from ROS and cytosolic Ca^{2+} levels.

The observation that NMDA receptor agonists, many of which are analogs of glutamate, can cause toxicity when administered at highly supraphysiological concentrations (termed "excitotoxicity") (168) led to a great deal of research on how normal excitatory stimuli cause apoptosis when present in excess. One such excitotoxin, kainic acid, specifically lesions the striatum when administered intracranially (169). Kainic acid is not an endogenous metabolite, unlike quinolinic acid (QA), an excitotoxin that is a product of tryptophan metabolism. When administered intrastriatally to rats, QA's effects, much like those of 3-NP, are strikingly similar to HD (albeit

occurring acutely rather than over weeks to years) in that the MSNs are destroyed rapidly but cholinergic interneurons are spared (170,171). This effect is not rodent specific, having been demonstrated in primate brains and additionally establishing that NMDA receptor activation mediates the toxicity, as an antagonist prevented the damage (172). At this point, it was commonly proposed that much of HD pathology stems either a) from endogenous excitotoxic metabolites like QA leading to degeneration of *mHTT*-expressing neurons, or b) because *mHTT*-expressing neurons are hypersensitive to normal glutamate inputs from the cortex.

There is intriguing recent data to suspect the former (endogenous tryptophan metabolites like QA) plays a role. Typically studied by delivery of synthetic QA to the brain, as it is an endogenous metabolite, it has been investigated in animal models whether modulation of steady state tryptophan metabolism may play a role in HD. In fly HD models, administration of 3-hydroxykynurenine (3-HK), a precursor of excitotoxic QA, enhances neurodegeneration, while deletion of the enzyme just upstream of 3-HK, kynurenine monooxygenase (KMO), rescues the effect (173). Furthermore, some benefit to survival and reduction in inflammatory microglial activation were seen in R6/2 mice treated with a specific KMO inhibitor (174).

Much of the HD / excitotoxicity subfield has focused on calcium currents from NMDA receptors (NMDARs). They can be found at the synapse or on the extrasynaptic plasma membrane, where their activation evokes different responses (175), and are heterotetramers composed of two NR1 and two NR2 subunits. NR2 comes in two main subtypes, NR2A and NR2B, and aside from different developmental functions, they appear to elicit different responses to the presence of mHTT. NR2B-containing

NMDARs, both synaptic and extrasynaptic, have higher Ca^{2+} currents in cells expressing mHTT when challenged with chemical agonists or synaptic glutamate (176,177). This may be a minor effect on cellular health compared to the sensitized mPTP on mitochondria of *mHTT*-expressing cells (165,178), but increased NR2B levels compound neurodegeneration (179) and are normally found in tissues that are more vulnerable to mHTT (177).

If increased Ca^{2+} currents are not responsible for excitotoxicity (165), how does NR2B play a role? Subcellular localization and posttranslational modifications of NR2B seem important to the specific response to agonists evoked by their NMDARs. Many studies suggest it is extrasynaptic NMDARs that mediate much of the toxicity from agonism. Synaptic / extrasynaptic localization is regulated by both cleavage of the C-terminus by calpain and dephosphorylation by the phosphatase STEP, which both reduce its synaptic presence (180). This may alter the balance of downstream CREB-mediated transcription pathways, which are activated by synaptic NR2B NMDARs but inhibited by the extrasynaptic ones. (181). Extrasynaptic NR2B-containing NMDARs are more common in HD mice, possibly in part because both STEP and calpain levels are increased in *mHTT*-expressing animals (180,182).

Given the relationship between mHTT and NMDAR activity and locations, many HD model mouse strains have been tested for their response to excitotoxic stimulus, generally via intrastriatal injection of kainic acid or quinolinic acid. The particulars of each strain's response to such stresses is discussed in more detail in Chapter 3 (and summarized in list form by Graham et al. 2009 (183)), but a basic trend is apparent, and the correlation involves mHTT aggregation. As was previously discussed, it is still

unclear what role aggregates play in disease, and it is likely that visible aggregates have little to no role in disease other than as a histological byproduct of polyglutamine stress. However, over many studies, it seems that the appearance of aggregates (but not necessarily visible behavioral symptoms) correlates with a transition from mouse models being hypersensitive to excitotoxicity to being resistant to such insults. While cells with mHTT aggregates are not necessarily as healthy as cells only expressing wtHTT, it seems clear that aggregation is a sign of a cellular attempt to cope with such stress. Both visible aggregation and survival of cells expressing polyQ proteins are influenced by chaperone proteins like Hsp40, Hsp70, and Hsp90, and mice challenged with the mitochondrial toxin 3-NP suffer less damage when overexpressing Hsp70 (184). Given that a) 3-NP and other electron transport chain inhibitors generate prodigious oxidative stress (138), b) excitotoxins largely kill cells through the Ca^{2+} influx from NMDA receptors (172), c) neuronal death from both ETC poisoning and excitotoxic stress can be reduced significantly by inhibiting mitochondrial permeability (140,165), and d) cells and mice that are better capable of promoting aggregation of mHTT survive longer in general (63,64), one can imagine the following path to resistance to excitotoxicity.

--Initially, expression of *mHTT* causes reorganization of NMDAR location, activity, and NR2B/NR2A ratios. This puts neurons under steady state Ca^{2+} elevation, or at least puts them at risk to mitochondrial permeability transition due to mHTT's effect on its sensitivity. Under these conditions (elevated Ca^{2+} and/or mPTP opening sensitivity), *mHTT*-expressing neurons are subject to oxidative stress.

--Increased oxidative stress leads to general protein homeostasis defects (185),

and over time, Hsps are recruited, promoting aggregation of mHTT along the way. This could be aided by a steady-state increase of pro-survival Akt signaling (which can induce HSF1) (186), since NMDAR-dependent Akt activation has been demonstrated in cultured knockin *mHTT*-expressing cells (187).

--When such neurons are later subject to excitotoxicity, they are better equipped to handle acute mitochondrial oxidative stress. Hence, they are resistant to excitotoxicity. *wtHTT*-expressing cells, on the other hand, have no such steady-state elevation in acute oxidative stress response and are normally vulnerable. Meanwhile, cells with mHTT but which are incapable of generating aggregates instead have tremendous amounts of toxic oligomers, which prime mitochondria to permeability under lower Ca^{2+} levels, hence rendering them hypersensitive to excitotoxicity.

Excitotoxicity, despite being an artificial condition, can also inform us about mHTT modifications that may be relevant to steady state conditions. We know that increased levels of non-toxic HTT render cells resistant to excitotoxicity (30,63,188), which in the context of excitotoxins' mitochondrial-mediated toxicity, lends importance to the fact that many proteins involved in mitochondrial function bind with HTT (17). I use the phrase "non-toxic HTT", because in this case, I also mean mHTT that does not cause toxicity, evidenced by caspase-6-resistant (C6R) mHTT (a strain carrying a version of mHTT that is resistant to caspase-6 cleavage, limiting the production of N-terminal fragments) and the previously-mentioned Shortstop (Ss) strain, both of which have an expanded polyQ tract but neither of which induces neurodegeneration *in vivo* or *in vitro* (188,189). Because C6R mHTT has reduced production of toxic N-terminal fragments while Ss mHTT appears to aggregate too readily for toxic oligomers to

occupy a significant population (64), it seems all the more apparent that mHTT fragment oligomers, but not full length mHTT or aggregated mHTT, are what render mitochondria hypersensitive to Ca^{2+} fluctuations. Such Ca^{2+} fluctuations likely occur in the absence of excitotoxicity and are carried out by corticostriatal glutamatergic inputs, because decortication relieves some neurodegeneration in R6/2 mice (190).

Excitotoxic stimulation also informs us about the steady state phosphorylation dynamics of certain disease-relevant residues within HTT. One such residue, serine 421 (S421) has been studied in detail and its phosphorylation influences vesicle transport (discussed in the next section). S421 phosphorylation is reduced after excitotoxic stimulation, and is also seen in YAC128 transgenic mice (191,192). The likely culprits are the phosphatases calcineurin and PP1, which have altered activity in *mHTT*-expressing cells. Calcineurin levels and activity are elevated, directly or indirectly, by mHTT (193). Meanwhile, PP1 is inhibited by activity at the dopamine D1 receptor, whose levels drop over time in HD patients and model mice (192). As phosphorylated S421 is well known to reduce mHTT toxicity (31,194-196), it is clear that excitotoxic stimuli are also acting direcly on HTT (rather than solely on mitochondrial permeability) to contribute to neurodegeneration.

BDNF Transport Alterations and Striatal Vulnerability

While we see that phosphorylation of mHTT S421 rescues cells from excitotoxicity, it also modulates a vesicle trafficking defect seen in HD cortical neurons (31) (Figure 5). These vesicles are carried by the dynactin / microtubule network via a complex involving HTT, HAP1, and $p150^{glued}$. This requires HTT S421 phosphorylation

for proper directional movement along the microtubule network (195). A major cargo delivered by these vesicles is BDNF. Striatal degeneration is seen in *Bdnf* knockout mice, while its overexpression reduces neuropathology in YAC128 HD model mice (121,197). Its altered transcript levels clearly play a role in pathology, but even if transcribed properly, it must be efficiently delivered to the striatum from its site of production in the cortex. Calcineurin-regulated dephosphorylation of phosphoS421 is an attractive target, and inhibition of calcineurin by FK506 rescues phosphoS421 levels and BDNF vesicle transport *in vitro* (198). Delivery of exogenous BDNF may go a long way towards therapy in HD, and it has been demonstrated beneficial in model mice with many delivery modes (197,199-201).

Summary

The above chapter is not an exhaustive list of the dysfunctions induced by mHTT in neurons, yet it is clear that even if reduction of mHTT levels through knockdown approaches are not yet viable and produce complex risks of their own, there are many pathways mediating part of toxicity that are potential targets for therapeutic intervention. I do not believe that any one pathway has particular importance or deserves priority, and there is a need to test any and all approaches quickly and conclusively. In the following chapter, I will explore what therapeutic options have been and are being tried in animals and patients, while Chapter 3 will discuss in detail the mouse models of HD that have been instrumental in the evaluation of candidate therapeutics.

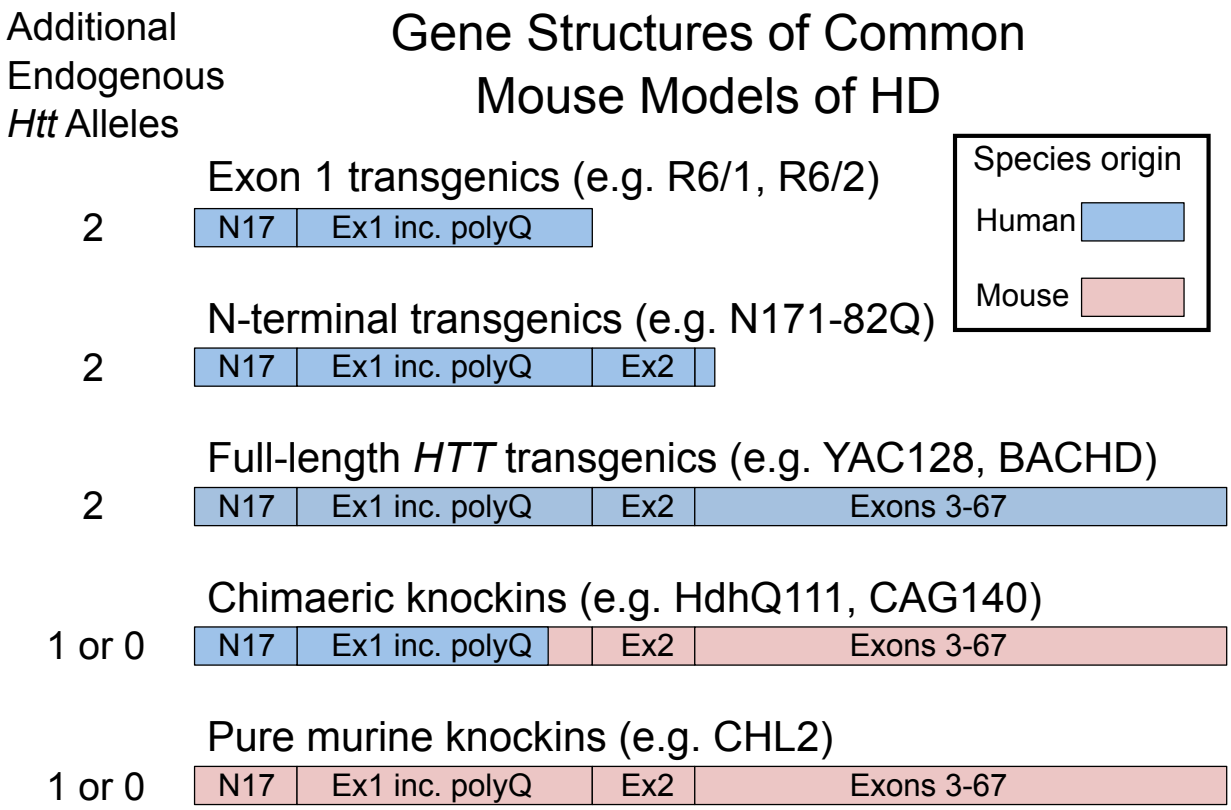

Figure 1: Gene structure of common mouse models of HD. There are many genetic mouse models of HD. Their detailed phenotypic characteristics will be covered in Chapter 3, but in general, they can be divided into 3 categories. Those with the most striking pathology and lethality are the Exon 1 and N-terminal transgenics (R6/2 and N171-82Q are most common). Full-length transgenic strains use human *mHTT* as a transgene under endogenous human transcriptional control. YAC128 has been used most commonly in this group. Knockin strains can be subdivided into those with human DNA in exon 1 (HdhQ111 is a prominent example; CAG140 is also known as HdhQ140) versus those with pure mouse *mHtt* and only an expanded CAG tract knocked in to the endogenous locus, such as CHL2 (also known as HdhQ150). Additional endogenous *Htt* alleles are listed as a reminder that the transgenic strains have both *Htt* alleles present and unaltered, while the knockin strains have 1 (if *mHtt* is heterozygous) or 0 (if *mHtt* is homozygous).

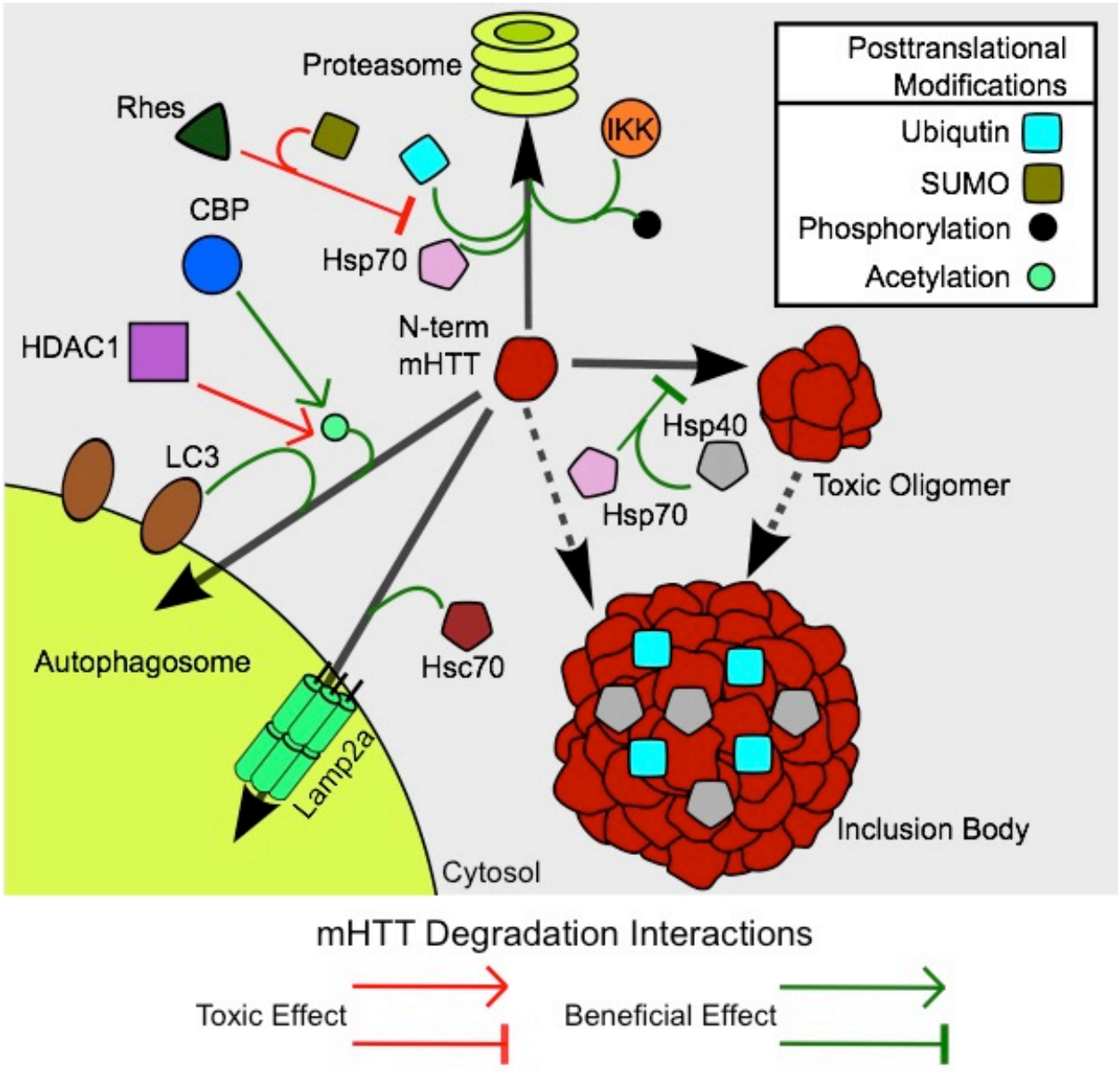

Figure 2: Disposal of mHTT. Cells can safely dispose of mHTT through one of four routes. Inclusion bodies represent a relatively safe place for mHTT. Non-toxic isoforms of mHTT (like Shortstop) bind Hsp70 and Hsp40 readily and do not form toxic oligomer species, and Hsp70/40 overexpression suppresses toxic oligomer formation. However, non-toxic mHTT isoforms still form inclusion bodies, so either Hsp70/40 facilitate oligomer sequestration into inclusion bodies, or they prevent toxic oligomerization, allowing mHTT to join inclusion bodies through alternate pathways. The proteasome can also degrade mHTT after Hsp70-aided ubiquitination and IKK-mediated phosphorylation, while SUMOylation by RHES opposes it. Autophagy can also be employed to destroy mHTT. Acetylated mHTT (regulated by CBP and HDAC1) is a target for LC3-mediated macroautophagy, while Hsc70 promotes passage of mHTT through Lamp2a channels for chaperone-mediated autophagy. These routes of disposal

are clearly insufficient as cells age, but experiments demonstrating enhanced toxicity upon impairment of these pathways demonstrate that they each contribute to survival.

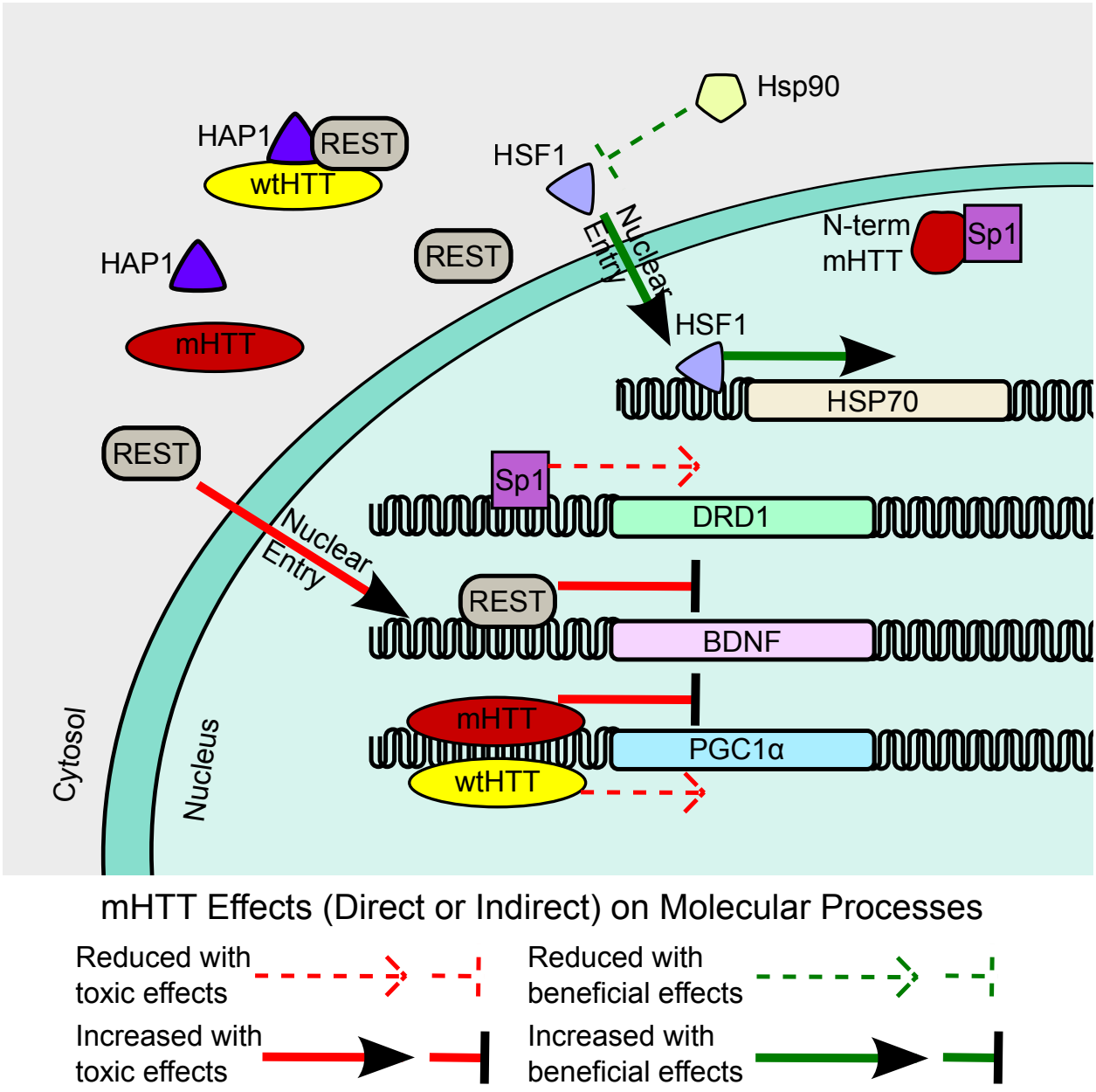

Figure 3: Transcriptional dysregulation by mHTT. Many classes of genes are dysregulated by mHTT. Genes such as *DRD1* have reduced transcription due to sequestration of transcription factor Sp1 by nuclear N-terminal mHTT. *BDNF* levels are repressed by REST/NRSF, which is normally excluded from the nucleus by a complex including wtHTT and HAP1. mHTT also directly represses PGC1α (gene name *PPARGC1A*) expression, a process normally induced by wtHTT. However, the presence of protein folding stress and oxidative stress also cause Hsp90 to release HSF1, allowing it to upregulate heat shock proteins like *HSP70*.

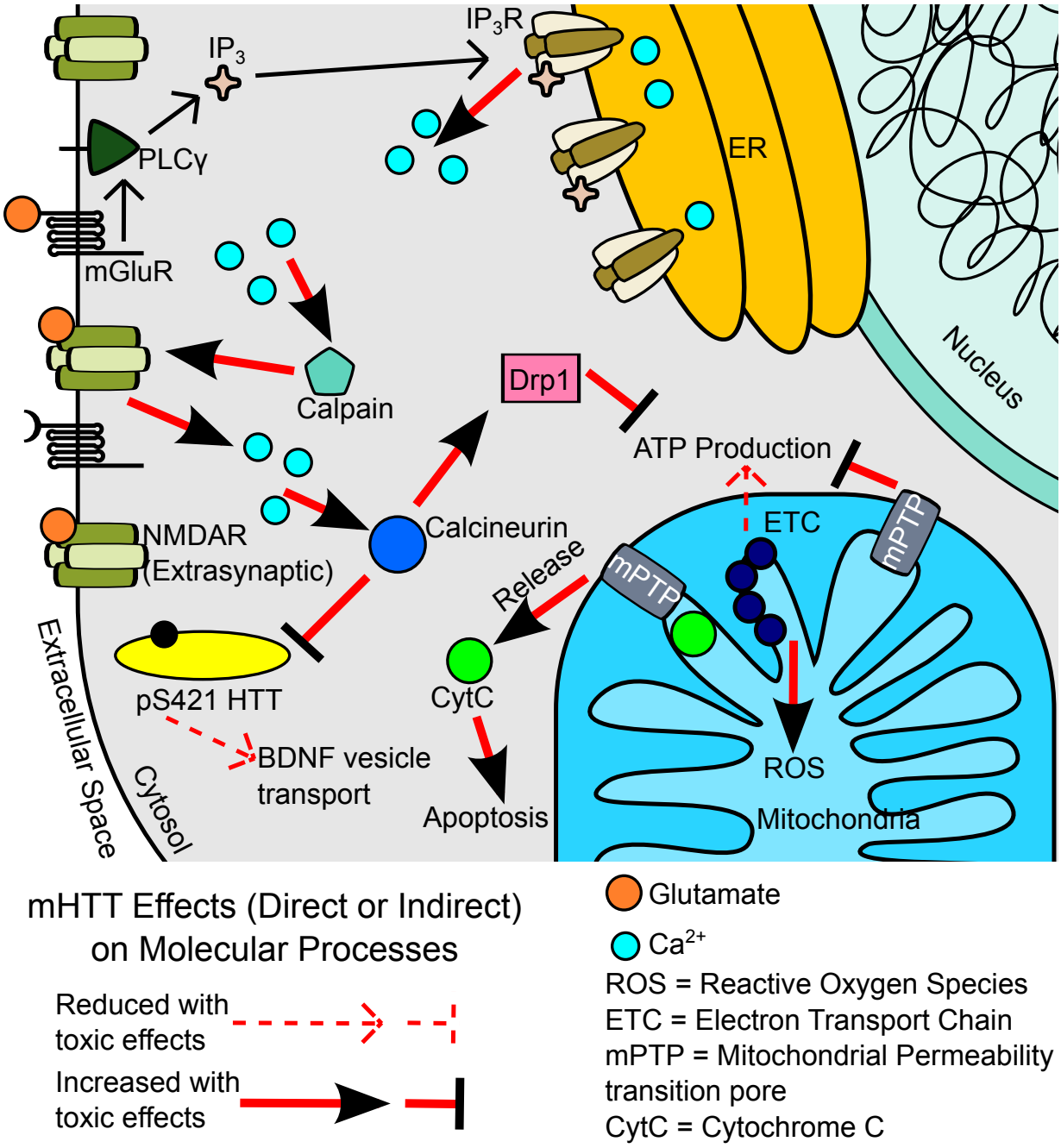

Figure 4: Glutamate Receptors Cause Calcium-mediated Toxicity in HD. Glutamate activates two classes of receptors, leading to toxicity due to hypersensitive mitochondrial permeability transition pores (mPTPs). mGluRs activate PLCγ, causing IP_3 to allow IP_3 receptors on the ER (hypersensitized by mHTT) to release Ca^{2+} into the cytosol. Meanwhile, extrasynaptic NMDARs open to glutamate, allowing Ca^{2+} into the cytosol. This increase of Ca^{2+} leads to many toxic pathways. Calpain activity increases, causing among other things increased extrasynaptic NMDAR presence. The phosphatase calcineurin is also activated, reducing pS421 levels on HTT which hampers the vesicle transport of cargo like BDNF. Calcineurin also activates Drp1,

causing mitochondrial fission that hampers ATP production. More directly, Ca^{2+} causes opening of the mPTP, which has three effects. First, mitochondrial potential drops, reducing ATP production. Second, reactive oxygen species (ROS) production spikes. Third, cytochrome C (CytC) is released, activating apoptotic pathways.

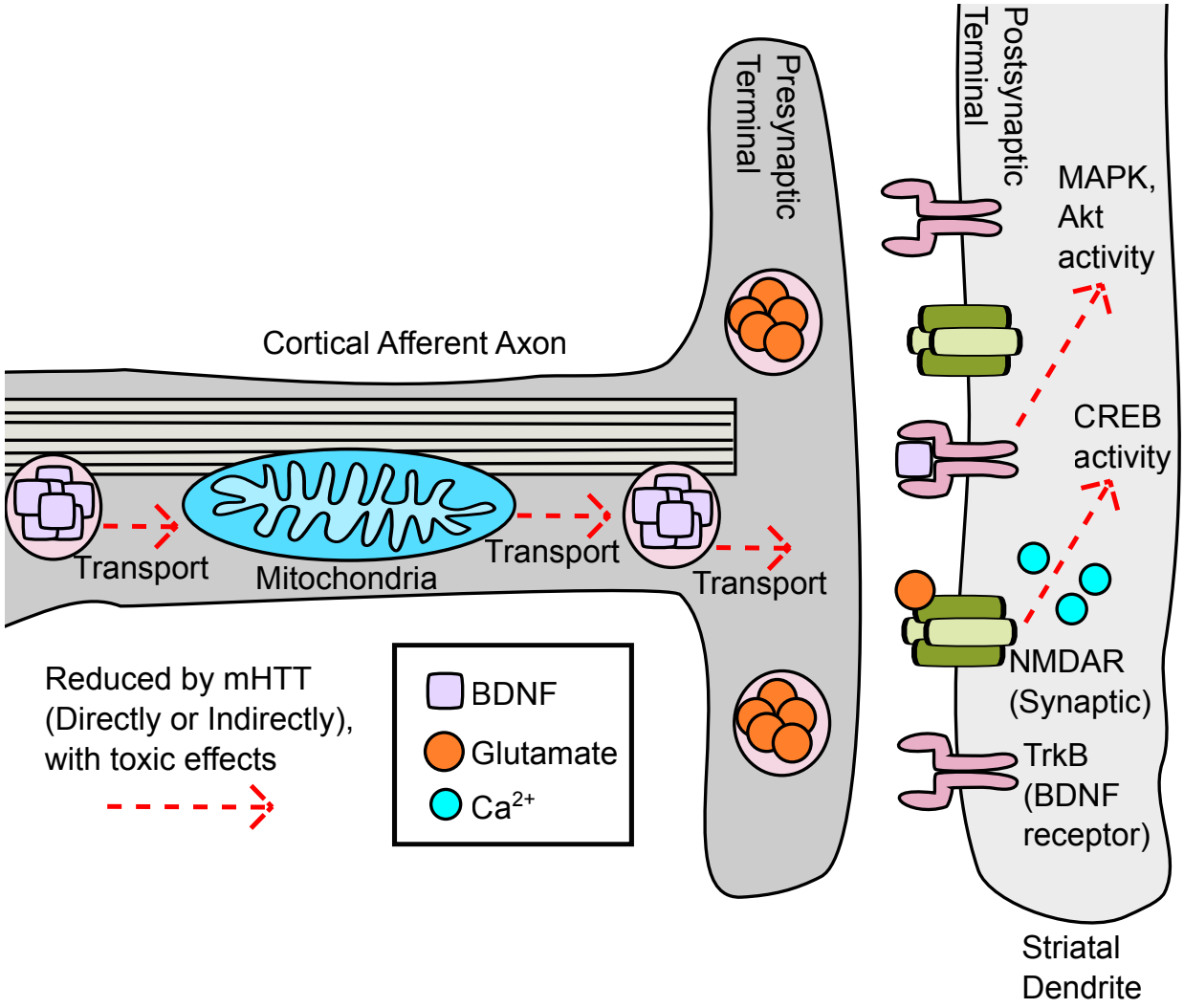

Figure 5: Toxicity at the Synapse. mHTT impairs transport down the axon towards the synapse. Mitochondria are not efficiently trafficked, impairing energetics at the synapse. BDNF also is not efficiently transported, so postsynaptic TrkB receptors less efficiently activate prosurvival MAPK and Akt pathways. Additionally, mHTT results in fewer synaptic NMDARs, so prosurvival CREB activity (specifically the result of synaptic Ca^{2+} influx) is reduced.

Bibliography

1. The Huntington's Disease Collaborative Research Group. A novel gene containing a trinucleotide repeat that is expanded and unstable on Huntington's disease chromosomes. Cell. 1993 Mar 26;72(6):971–83.

2. Nørremølle A, Riess O, Epplen JT, Fenger K, Hasholt L, Sørensen SA. Trinucleotide repeat elongation in the Huntingtin gene in Huntington disease patients from 71 Danish families. Hum Mol Genet. 1993 Sep 1;2(9):1475–6.

3. Myers RH, MacDonald ME, Koroshetz WJ, Duyao MP, Ambrose CM, Taylor SA, et al. De novo expansion of a (CAG)n repeat in sporadic Huntington's disease. Nat Genet. 1993 Oct 1;5(2):168–73.

4. Bates G, Harper P, Jones L. Huntington's Disease. 3rd ed. Oxford University Press, USA; 2002.

5. Sathasivam K, Amaechi I, Mangiarini L, Bates G. Identification of an HD patient with a (CAG)180 repeat expansion and the propagation of highly expanded CAG repeats in lambda phage. Hum Genet. 1997 May;99(5):692–5.

6. Li S-H, Schilling G, Young WS, Li X-J, Margolis RL, Stine OC, et al. Huntington's disease gene (IT15) is widely expressed in human and rat tissues. Neuron. 1993 Nov;11(5):985–93.

7. Strong TV, Tagle DA, Valdes JM, Elmer LW, Boehm K, Swaroop M, et al. Widespread expression of the human and rat Huntington's disease gene in brain and nonneural tissues. Nat Genet. 1993 Nov;5(3):259–65.

8. Gissi C, Pesole G, Cattaneo E, Tartari M. Huntingtin gene evolution in Chordata and its peculiar features in the ascidian Ciona genus. BMC Genomics. 2006;7:288.

9. Sapp E, Valencia A, Li X, Aronin N, Kegel KB, Vonsattel J-P, et al. Native mutant Huntingtin in human brain: Evidence for prevalence of full length monomer. Journal of Biological Chemistry. 2012 Feb 27.

10. Tartari M, Gissi C, Sardo lo V, Zuccato C, Picardi E, Pesole G, et al. Phylogenetic Comparison of Huntingtin Homologues Reveals the Appearance of a Primitive polyQ in Sea Urchin. Molecular Biology and Evolution. 2008 Jan 2;25(2):330–8.

11. Neveklovska M, Clabough EBD, Steffan JS, Zeitlin SO. Deletion of the huntingtin proline-rich region does not significantly affect normal huntingtin function in mice. J Huntingtons Dis. 2012 Jan 1;1(1):71–87.

12. Clabough EBD, Zeitlin SO. Deletion of the triplet repeat encoding polyglutamine within the mouse Huntington's disease gene results in subtle behavioral/motor

phenotypes in vivo and elevated levels of ATP with cellular senescence in vitro. Hum Mol Genet. 2006 Feb 15;15(4):607–23.

13. Zheng S, Clabough EBD, Sarkar S, Futter M, Rubinsztein DC, Zeitlin SO. Deletion of the huntingtin polyglutamine stretch enhances neuronal autophagy and longevity in mice. PLoS Genet. 2010 Feb;6(2):e1000838.

14. Maiuri T, Woloshansky T, Xia J, Truant R. The huntingtin N17 domain is a multifunctional CRM1 and Ran-dependent nuclear and cilial export signal. Hum Mol Genet. 2013 Apr 1;22(7):1383–94.

15. Li W, Serpell LC, Carter WJ, Rubinsztein DC, Huntington JA. Expression and characterization of full-length human huntingtin, an elongated HEAT repeat protein. J Biol Chem. 2006 Jun 9;281(23):15916–22.

16. Palidwor GA, Shcherbinin S, Huska MR, Rasko T, Stelzl U, Arumughan A, et al. Detection of alpha-rod protein repeats using a neural network and application to huntingtin. PLoS Comput. Biol. 2009 Mar;5(3):e1000304.

17. Shirasaki DI, Greiner ER, Al-Ramahi I, Gray M, Boontheung P, Geschwind DH, et al. Network organization of the huntingtin proteomic interactome in mammalian brain. Neuron. 2012 Jul 12;75(1):41–57.

18. Lin B, Rommens JM, Graham RK, Kalchman M, MacDonald H, Nasir J, et al. Differential 3' polyadenylation of the Huntington disease gene results in two mRNA species with variable tissue expression. Hum Mol Genet. 1993 Oct;2(10):1541–5.

19. Sinha M, Ghose J, Bhattarcharyya NP. Micro RNA -214,-150,-146a and-125b target Huntingtin gene. RNA Biol. 2011 Nov;8(6):1005–21.

20. Lee J, Park EH, Couture G, Harvey I, Garneau P, Pelletier J. An upstream open reading frame impedes translation of the huntingtin gene. Nucleic Acids Res. 2002 Dec 1;30(23):5110–9.

21. Ehrnhoefer DE, Wong BKY, Hayden MR. Convergent pathogenic pathways in Alzheimer“s and Huntington”s diseases: shared targets for drug development. Nat Rev Drug Discov. 2011 Nov;10(11):853–67.

22. Kalchman MA, Graham RK, Xia G, Koide HB, Hodgson JG, Graham KC, et al. Huntingtin is ubiquitinated and interacts with a specific ubiquitin-conjugating enzyme. J Biol Chem. 1996 Aug 9;271(32):19385–94.

23. Jana NR, Dikshit P, Goswami A, Kotliarova S, Murata S, Tanaka K, et al. Co-chaperone CHIP associates with expanded polyglutamine protein and promotes their degradation by proteasomes. J Biol Chem. 2005 Mar 25;280(12):11635–40.

24. Steffan JS, Agrawal N, Pallos J, Rockabrand E, Trotman LC, Slepko N, et al. SUMO modification of Huntingtin and Huntington's disease pathology. Science. 2004 Apr 2;304(5667):100–4.

25. Ehrnhoefer DE, Sutton L, Hayden MR. Small changes, big impact: posttranslational modifications and function of huntingtin in Huntington disease. Neuroscientist. 2011 Oct;17(5):475–92.

26. Aiken CT, Steffan JS, Guerrero CM, Khashwji H, Lukacsovich T, Simmons D, et al. Phosphorylation of threonine 3: implications for Huntingtin aggregation and neurotoxicity. Journal of Biological Chemistry. 2009 Oct 23;284(43):29427–36.

27. Thompson LM, Aiken CT, Kaltenbach LS, Agrawal N, Illes K, Khoshnan A, et al. IKK phosphorylates Huntingtin and targets it for degradation by the proteasome and lysosome. The Journal of Cell Biology. 2009 Dec 28;187(7):1083–99.

28. Warby SC, Chan EY, Metzler M, Gan L, Singaraja RR, Crocker SF, et al. Huntingtin phosphorylation on serine 421 is significantly reduced in the striatum and by polyglutamine expansion in vivo. Hum Mol Genet. 2005 Jun 1;14(11):1569–77.

29. Yanai A, Huang K, Kang R, Singaraja RR, Arstikaitis P, Gan L, et al. Palmitoylation of huntingtin by HIP14 is essential for its trafficking and function. Nat Neurosci. 2006 Jun;9(6):824–31.

30. Leavitt BR, van Raamsdonk JM, Shehadeh J, Fernandes H, Murphy Z, Graham RK, et al. Wild-type huntingtin protects neurons from excitotoxicity. J Neurochem. 2006 Feb;96(4):1121–9.

31. Zala D, Colin E, Rangone H, Liot G, Humbert S, Saudou F. Phosphorylation of mutant huntingtin at S421 restores anterograde and retrograde transport in neurons. Hum Mol Genet. 2008 Dec 15;17(24):3837–46.

32. Atwal RS, Xia J, Pinchev D, Taylor J, Epand RM, Truant R. Huntingtin has a membrane association signal that can modulate huntingtin aggregation, nuclear entry and toxicity. Hum Mol Genet. 2007 Nov 1;16(21):2600–15.

33. Benn CL, Sun T, Sadri-Vakili G, McFarland KN, DiRocco DP, Yohrling GJ, et al. Huntingtin modulates transcription, occupies gene promoters in vivo, and binds directly to DNA in a polyglutamine-dependent manner. J Neurosci. 2008 Oct 15;28(42):10720–33.

34. Zuccato C, Belyaev N, Conforti P, Ooi L, Tartari M, Papadimou E, et al. Widespread disruption of repressor element-1 silencing transcription factor/neuron-restrictive silencer factor occupancy at its target genes in Huntington's disease. J Neurosci. 2007 Jun 27;27(26):6972–83.

35. Rockabrand E, Slepko N, Pantalone A, Nukala VN, Kazantsev A, Marsh JL, et

al. The first 17 amino acids of Huntingtin modulate its sub-cellular localization, aggregation and effects on calcium homeostasis. Hum Mol Genet. 2007 Jan 1;16(1):61–77.

36. Kegel KB, Sapp E, Yoder J, Cuiffo B, Sobin L, Kim YJ, et al. Huntingtin associates with acidic phospholipids at the plasma membrane. J Biol Chem. 2005 Oct 28;280(43):36464–73.

37. Dragatsis I, Efstratiadis A, Zeitlin S. Mouse mutant embryos lacking huntingtin are rescued from lethality by wild-type extraembryonic tissues. Development. 1998 Apr;125(8):1529–39.

38. Zeitlin S, Liu JP, Chapman DL, Papaioannou VE, Efstratiadis A. Increased apoptosis and early embryonic lethality in mice nullizygous for the Huntington's disease gene homologue. Nat Genet. 1995 Oct;11(2):155–63.

39. Reiner A, del Mar N, Meade CA, Yang H, Dragatsis I, Zeitlin S, et al. Neurons lacking huntingtin differentially colonize brain and survive in chimeric mice. J Neurosci. 2001 Oct 1;21(19):7608–19.

40. Grondin R, Kaytor MD, Ai Y, Nelson PT, Thakker DR, Heisel J, et al. Six-month partial suppression of Huntingtin is well tolerated in the adult rhesus striatum. Brain. 2012 Apr;135(Pt 4):1197–209.

41. McBride JL, Pitzer MR, Boudreau RL, Dufour B, Hobbs T, Ojeda SR, et al. Preclinical Safety of RNAi-Mediated HTT Suppression in the Rhesus Macaque as a Potential Therapy for Huntington's Disease. Mol Ther. 2011 Dec;19(12):2152–62.

42. Mangiarini L, Sathasivam K, Seller M, Cozens B, Harper A, Hetherington C, et al. Exon 1 of the HD gene with an expanded CAG repeat is sufficient to cause a progressive neurological phenotype in transgenic mice. Cell. 1996 Nov 1;87(3):493–506.

43. DiFiglia M, Sapp E, Chase KO, Davies SW, Bates GP, Vonsattel JP, et al. Aggregation of huntingtin in neuronal intranuclear inclusions and dystrophic neurites in brain. Science. 1997 Sep 26;277(5334):1990–3.

44. Yamada M, Sato T, Tsuji S, Takahashi H. CAG repeat disorder models and human neuropathology: similarities and differences. Acta Neuropathol. 2008 Jan;115(1):71–86.

45. Katsuno M, Adachi H, Kume A, Li M, Nakagomi Y, Niwa H, et al. Testosterone reduction prevents phenotypic expression in a transgenic mouse model of spinal and bulbar muscular atrophy. Neuron. 2002 Aug 29;35(5):843–54.

46. Banno H, Katsuno M, Suzuki K, Takeuchi Y, Kawashima M, Suga N, et al. Phase 2 trial of leuprorelin in patients with spinal and bulbar muscular atrophy.

Ann Neurol. 2009 Feb;65(2):140–50.

47. Gray M, Shirasaki DI, Cepeda C, André VM, Wilburn B, Lu X-H, et al. Full-length human mutant huntingtin with a stable polyglutamine repeat can elicit progressive and selective neuropathogenesis in BACHD mice. J Neurosci. 2008 Jun 11;28(24):6182–95.

48. Hackam AS, Singaraja R, Wellington CL, Metzler M, McCutcheon K, Zhang T, et al. The influence of huntingtin protein size on nuclear localization and cellular toxicity. The Journal of Cell Biology. 1998 Jun 1;141(5):1097–105.

49. Landles C, Sathasivam K, Weiss A, Woodman B, Moffitt H, Finkbeiner S, et al. Proteolysis of mutant huntingtin produces an exon 1 fragment that accumulates as an aggregated protein in neuronal nuclei in Huntington disease. Journal of Biological Chemistry. 2010 Mar 19;285(12):8808–23.

50. Cooper JK, Schilling G, Peters MF, Herring WJ, Sharp AH, Kaminsky Z, et al. Truncated N-terminal fragments of huntingtin with expanded glutamine repeats form nuclear and cytoplasmic aggregates in cell culture. Hum Mol Genet. 1998 May;7(5):783–90.

51. Liu YF. Expression of polyglutamine-expanded Huntingtin activates the SEK1-JNK pathway and induces apoptosis in a hippocampal neuronal cell line. J Biol Chem. 1998 Oct 30;273(44):28873–7.

52. Chen S, Berthelier V, Hamilton JB, O'Nuallain B, Wetzel R. Amyloid-like features of polyglutamine aggregates and their assembly kinetics. Biochemistry. 2002 Jun 11;41(23):7391–9.

53. Thakur AK, Jayaraman M, Mishra R, Thakur M, Chellgren VM, Byeon I-JL, et al. Polyglutamine disruption of the huntingtin exon 1 N terminus triggers a complex aggregation mechanism. Nat. Struct. Mol. Biol. 2009 Apr;16(4):380–9.

54. Wetzel R. Physical chemistry of polyglutamine: intriguing tales of a monotonous sequence. J. Mol. Biol. 2012 Aug 24;421(4-5):466–90.

55. McGowan DP, van Roon-Mom W, Holloway H, Bates GP, Mangiarini L, Cooper GJ, et al. Amyloid-like inclusions in Huntington's disease. NSC. 2000;100(4):677–80.

56. Poirier MA, Li H, Macosko J, Cai S, Amzel M, Ross CA. Huntingtin spheroids and protofibrils as precursors in polyglutamine fibrilization. J Biol Chem. 2002 Oct 25;277(43):41032–7.

57. Wood NI, Pallier PN, Wanderer J, Morton AJ. Systemic administration of Congo red does not improve motor or cognitive function in R6/2 mice. Neurobiology of Disease. 2007 Feb;25(2):342–53.

58. Sánchez I, Mahlke C, Yuan J. Pivotal role of oligomerization in expanded polyglutamine neurodegenerative disorders. Nature. 2003 Jan 23;421(6921):373–9.

59. Arrasate M, Mitra S, Schweitzer ES, Segal MR, Finkbeiner S. Inclusion body formation reduces levels of mutant huntingtin and the risk of neuronal death. Nature. 2004 Oct 14;431(7010):805–10.

60. Bowman AB, Yoo S-Y, Dantuma NP, Zoghbi HY. Neuronal dysfunction in a polyglutamine disease model occurs in the absence of ubiquitin-proteasome system impairment and inversely correlates with the degree of nuclear inclusion formation. Hum Mol Genet. 2005 Mar 1;14(5):679–91.

61. Reiner A, del Mar N, Deng Y-P, Meade CA, Sun Z, Goldowitz D. R6/2 neurons with intranuclear inclusions survive for prolonged periods in the brains of chimeric mice. J. Comp. Neurol. 2007 Dec 20;505(6):603–29.

62. Yoshizawa T, Yoshida H, Shoji S. Differential susceptibility of cultured cell lines to aggregate formation and cell death produced by the truncated Machado-Joseph disease gene product with an expanded polyglutamine stretch. Brain Res Bull. 2001 Oct;56(3-4):349–52.

63. Slow EJ, Graham RK, Osmand AP, Devon RS, Lu G, Deng Y, et al. Absence of behavioral abnormalities and neurodegeneration in vivo despite widespread neuronal huntingtin inclusions. Proc Natl Acad Sci USA. 2005 Aug 9;102(32):11402–7.

64. Nucifora LG, Burke KA, Feng X, Arbez N, Zhu S, Miller J, et al. Identification of novel potentially toxic oligomers formed in vitro from mammalian-derived expanded huntingtin exon-1 protein. Journal of Biological Chemistry. 2012 Mar 20.

65. Manogaran AL, Hong JY, Hufana J, Tyedmers J, Lindquist S, Liebman SW. Prion formation and polyglutamine aggregation are controlled by two classes of genes. PLoS Genet. 2011 May;7(5):e1001386.

66. Bemporad F, Chiti F. Protein misfolded oligomers: experimental approaches, mechanism of formation, and structure-toxicity relationships. Chem Biol. 2012 Mar 23;19(3):315–27.

67. Koffie RM, Meyer-Luehmann M, Hashimoto T, Adams KW, Mielke ML, Garcia-Alloza M, et al. Oligomeric amyloid beta associates with postsynaptic densities and correlates with excitatory synapse loss near senile plaques. Proc Natl Acad Sci USA. 2009 Mar 10;106(10):4012–7.

68. Bitan G, Kirkitadze MD, Lomakin A, Vollers SS, Benedek GB, Teplow DB. Amyloid beta -protein (Abeta) assembly: Abeta 40 and Abeta 42 oligomerize through distinct pathways. Proc Natl Acad Sci USA. 2003 Jan 7;100(1):330–5.

69. Calamai M, Canale C, Relini A, Stefani M, Chiti F, Dobson CM. Reversal of protein aggregation provides evidence for multiple aggregated States. J. Mol. Biol. 2005 Feb 18;346(2):603–16.

70. Ladiwala ARA, Dordick JS, Tessier PM. Aromatic small molecules remodel toxic soluble oligomers of amyloid beta through three independent pathways. Journal of Biological Chemistry. 2011 Feb 4;286(5):3209–18.

71. Bucciantini M, Giannoni E, Chiti F, Baroni F, Formigli L, Zurdo J, et al. Inherent toxicity of aggregates implies a common mechanism for protein misfolding diseases. Nature. 2002 Apr 4;416(6880):507–11.

72. Campioni S, Mannini B, Zampagni M, Pensalfini A, Parrini C, Evangelisti E, et al. A causative link between the structure of aberrant protein oligomers and their toxicity. Nat Chem Biol. 2010 Feb;6(2):140–7.

73. Lotz GP, Legleiter J, Aron R, Mitchell EJ, Huang S-Y, Ng C, et al. Hsp70 and Hsp40 functionally interact with soluble mutant huntingtin oligomers in a classic ATP-dependent reaction cycle. Journal of Biological Chemistry. 2010 Dec 3;285(49):38183–93.

74. Cleary JP, Walsh DM, Hofmeister JJ, Shankar GM, Kuskowski MA, Selkoe DJ, et al. Natural oligomers of the amyloid-beta protein specifically disrupt cognitive function. Nat Neurosci. 2005 Jan;8(1):79–84.

75. Winner B, Jappelli R, Maji SK, Desplats PA, Boyer L, Aigner S, et al. In vivo demonstration that alpha-synuclein oligomers are toxic. Proc Natl Acad Sci USA. 2011 Mar 8;108(10):4194–9.

76. Billings LM, Oddo S, Green KN, McGaugh JL, LaFerla FM. Intraneuronal Abeta causes the onset of early Alzheimer's disease-related cognitive deficits in transgenic mice. Neuron. 2005 Mar 3;45(5):675–88.

77. Lesné S, Koh MT, Kotilinek L, Kayed R, Glabe CG, Yang A, et al. A specific amyloid-beta protein assembly in the brain impairs memory. Nature. 2006 Mar 16;440(7082):352–7.

78. Nekooki-Machida Y, Kurosawa M, Nukina N, Ito K, Oda T, Tanaka M. Distinct conformations of in vitro and in vivo amyloids of huntingtin-exon1 show different cytotoxicity. Proc Natl Acad Sci USA. 2009 Jun 16;106(24):9679–84.

79. Qin Z-H, Wang Y, Sapp E, Cuiffo B, Wanker E, Hayden MR, et al. Huntingtin bodies sequester vesicle-associated proteins by a polyproline-dependent interaction. J Neurosci. 2004 Jan 7;24(1):269–81.

80. Smith DL, Portier R, Woodman B, Hockly E, Mahal A, Klunk WE, et al. Inhibition of polyglutamine aggregation in R6/2 HD brain slices-complex dose-response profiles. Neurobiology of Disease. 2001 Dec;8(6):1017–26.

81. Stack EC, Kubilus JK, Smith K, Cormier K, del Signore SJ, Guelin E, et al. Chronology of behavioral symptoms and neuropathological sequela in R6/2 Huntington's disease transgenic mice. J. Comp. Neurol. 2005 Oct 3;490(4):354–70.

82. Suhr ST, Senut MC, Whitelegge JP, Faull KF, Cuizon DB, Gage FH. Identities of sequestered proteins in aggregates from cells with induced polyglutamine expression. The Journal of Cell Biology. 2001 Apr 16;153(2):283–94.

83. Ravikumar B, Vacher C, Berger Z, Davies JE, Luo S, Oroz LG, et al. Inhibition of mTOR induces autophagy and reduces toxicity of polyglutamine expansions in fly and mouse models of Huntington disease. Nat Genet. 2004 Jun;36(6):585–95.

84. Cha J-HJ. Transcriptional signatures in Huntington's disease. Prog Neurobiol. 2007 Nov;83(4):228–48.

85. Yu Z-X, Li S-H, Nguyen HP, Li X-J. Huntingtin inclusions do not deplete polyglutamine-containing transcription factors in HD mice. Hum Mol Genet. 2002 Apr 15;11(8):905–14.

86. Schaffar G, Breuer P, Boteva R, Behrends C, Tzvetkov N, Strippel N, et al. Cellular toxicity of polyglutamine expansion proteins: mechanism of transcription factor deactivation. Mol Cell. 2004 Jul 2;15(1):95–105.

87. Wyttenbach A, Carmichael J, Swartz J, Furlong RA, Narain Y, Rankin J, et al. Effects of heat shock, heat shock protein 40 (HDJ-2), and proteasome inhibition on protein aggregation in cellular models of Huntington's disease. Proc Natl Acad Sci USA. 2000 Mar 14;97(6):2898–903.

88. Jana NR, Tanaka M, Wang GH, Nukina N. Polyglutamine length-dependent interaction of Hsp40 and Hsp70 family chaperones with truncated N-terminal huntingtin: their role in suppression of aggregation and cellular toxicity. Hum Mol Genet. 2000 Aug 12;9(13):2009–18.

89. Wacker JL, Huang S-Y, Steele AD, Aron R, Lotz GP, Nguyen Q, et al. Loss of Hsp70 exacerbates pathogenesis but not levels of fibrillar aggregates in a mouse model of Huntington's disease. J Neurosci. 2009 Jul 15;29(28):9104–14.

90. Baldo B, Weiss A, Parker CN, Bibel M, Paganetti P, Kaupmann K. A screen for enhancers of clearance identifies huntingtin as an heat shock protein 90 (Hsp90) client protein. Journal of Biological Chemistry. 2011 Nov 28.

91. Tagawa K, Marubuchi S, Qi M-L, Enokido Y, Tamura T, Inagaki R, et al. The induction levels of heat shock protein 70 differentiate the vulnerabilities to mutant huntingtin among neuronal subtypes. J Neurosci. 2007 Jan 24;27(4):868–80.

92. Warrick JM, Chan HY, Gray-Board GL, Chai Y, Paulson HL, Bonini NM. Suppression of polyglutamine-mediated neurodegeneration in Drosophila by the molecular chaperone HSP70. Nat Genet. 1999 Dec;23(4):425–8.

93. Chan HYE, Warrick JM, Andriola I, Merry D, Bonini NM. Genetic modulation of polyglutamine toxicity by protein conjugation pathways in Drosophila. Hum Mol Genet. 2002 Nov 1;11(23):2895–904.

94. Al-Ramahi I, Lam YC, Chen H-K, de Gouyon B, Zhang M, Pérez AM, et al. CHIP protects from the neurotoxicity of expanded and wild-type ataxin-1 and promotes their ubiquitination and degradation. J Biol Chem. 2006 Sep 8;281(36):26714–24.

95. Wang AM, Miyata Y, Klinedinst S, Peng H-M, Chua JP, Komiyama T, et al. Activation of Hsp70 reduces neurotoxicity by promoting polyglutamine protein degradation. Nat Chem Biol. 2012 Dec 9;:–.

96. Subramaniam S, Sixt KM, Barrow R, Snyder SH. Rhes, a striatal specific protein, mediates mutant-huntingtin cytotoxicity. Science. 2009 Jun 5;324(5932):1327–30.

97. Mitsui K, Nakayama H, Akagi T, Nekooki M, Ohtawa K, Takio K, et al. Purification of polyglutamine aggregates and identification of elongation factor-1alpha and heat shock protein 84 as aggregate-interacting proteins. J Neurosci. 2002 Nov 1;22(21):9267–77.

98. Hansson O, Nylandsted J, Castilho RF, Leist M, Jäättelä M, Brundin P. Overexpression of heat shock protein 70 in R6/2 Huntington's disease mice has only modest effects on disease progression. Brain Res. 2003 Apr 25;970(1-2):47–57.

99. Hay DG, Sathasivam K, Tobaben S, Stahl B, Marber M, Mestril R, et al. Progressive decrease in chaperone protein levels in a mouse model of Huntington's disease and induction of stress proteins as a therapeutic approach. Hum Mol Genet. 2004 Jul 1;13(13):1389–405.

100. Fujimoto M, Takaki E, Hayashi T, Kitaura Y, Tanaka Y, Inouye S, et al. Active HSF1 significantly suppresses polyglutamine aggregate formation in cellular and mouse models. J Biol Chem. 2005 Oct 14;280(41):34908–16.

101. Hong DS, Banerji U, Tavana B, George GC, Aaron J, Kurzrock R. Targeting the molecular chaperone heat shock protein 90 (HSP90): Lessons learned and future directions. Cancer Treat. Rev. 2013 Jun;39(4):375–87.

102. Ji J, Sundquist K, Sundquist J. Cancer incidence in patients with polyglutamine diseases: a population-based study in Sweden. Lancet Oncol. 2012 Apr 11.

103. Spiess C, Meyer AS, Reissmann S, Frydman J. Mechanism of the eukaryotic

chaperonin: protein folding in the chamber of secrets. Trends Cell Biol. 2004 Nov;14(11):598–604.

104. Behrends C, Langer CA, Boteva R, Böttcher UM, Stemp MJ, Schaffar G, et al. Chaperonin TRiC promotes the assembly of polyQ expansion proteins into nontoxic oligomers. Mol Cell. 2006 Sep 15;23(6):887–97.

105. Tam S, Spiess C, Auyeung W, Joachimiak L, Chen B, Poirier MA, et al. The chaperonin TRiC blocks a huntingtin sequence element that promotes the conformational switch to aggregation. Nat. Struct. Mol. Biol. 2009 Dec;16(12):1279–85.

106. Sontag EM, Joachimiak LA, Tan Z, Tomlinson A, Housman DE, Glabe CG, et al. Exogenous delivery of chaperonin subunit fragment ApiCCT1 modulates mutant Huntingtin cellular phenotypes. Proc Natl Acad Sci USA. 2013 Jan 30.

107. Weeks RA, Piccini P, Harding AE, Brooks DJ. Striatal D1 and D2 dopamine receptor loss in asymptomatic mutation carriers of Huntington's disease. Ann Neurol. 1996 Jul 1;40(1):49–54.

108. Augood SJ, Faull RL, Emson PC. Dopamine D1 and D2 receptor gene expression in the striatum in Huntington's disease. Ann Neurol. 1997 Aug 1;42(2):215–21.

109. Augood SJ, Faull RL, Love DR, Emson PC. Reduction in enkephalin and substance P messenger RNA in the striatum of early grade Huntington's disease: a detailed cellular in situ hybridization study. NSC. 1996 Jun;72(4):1023–36.

110. Norris PJ, Waldvogel HJ, Faull RL, Love DR, Emson PC. Decreased neuronal nitric oxide synthase messenger RNA and somatostatin messenger RNA in the striatum of Huntington's disease. NSC. 1996 Jun;72(4):1037–47.

111. Cornett J, Smith L, Friedman M, Shin J-Y, Li X-J, Li S-H. Context-dependent dysregulation of transcription by mutant huntingtin. J Biol Chem. 2006 Nov 24;281(47):36198–204.

112. Zuccato C, Tartari M, Crotti A, Goffredo D, Valenza M, Conti L, et al. Huntingtin interacts with REST/NRSF to modulate the transcription of NRSE-controlled neuronal genes. Nat Genet. 2003 Sep;35(1):76–83.

113. Shimojo M. Huntingtin regulates RE1-silencing transcription factor/neuron-restrictive silencer factor (REST/NRSF) nuclear trafficking indirectly through a complex with REST/NRSF-interacting LIM domain protein (RILP) and dynactin p150 Glued. J Biol Chem. 2008 Dec 12;283(50):34880–6.

114. Hodges A, Strand AD, Aragaki AK, Kuhn A, Sengstag T, Hughes G, et al. Regional and cellular gene expression changes in human Huntington's disease

brain. Hum Mol Genet. 2006 Mar 15;15(6):965–77.

115. Borovecki F, Lovrecic L, Zhou J, Jeong H, Then F, Rosas HD, et al. Genome-wide expression profiling of human blood reveals biomarkers for Huntington's disease. Proc Natl Acad Sci USA. 2005 Aug 2;102(31):11023–8.

116. Strand AD, Aragaki AK, Shaw D, Bird T, Holton J, Turner C, et al. Gene expression in Huntington's disease skeletal muscle: a potential biomarker. Hum Mol Genet. 2005 Jul 1;14(13):1863–76.

117. Luthi-Carter R, Strand A, Peters NL, Solano SM, Hollingsworth ZR, Menon AS, et al. Decreased expression of striatal signaling genes in a mouse model of Huntington's disease. Hum Mol Genet. 2000 May 22;9(9):1259–71.

118. Hodges A, Hughes G, Brooks S, Elliston L, Holmans P, Dunnett SB, et al. Brain gene expression correlates with changes in behavior in the R6/1 mouse model of Huntington's disease. Genes Brain Behav. 2008 Apr 1;7(3):288–99.

119. Strand AD, Baquet ZC, Aragaki AK, Holmans P, Yang L, Cleren C, et al. Expression profiling of Huntington's disease models suggests that brain-derived neurotrophic factor depletion plays a major role in striatal degeneration. J Neurosci. 2007 Oct 24;27(43):11758–68.

120. Johnson R, Buckley NJ. Gene dysregulation in Huntington's disease: REST, microRNAs and beyond. Neuromol Med. 2009 Jan 1;11(3):183–99.

121. Altar CA, Cai N, Bliven T, Juhasz M, Conner JM, Acheson AL, et al. Anterograde transport of brain-derived neurotrophic factor and its role in the brain. Nature. 1997 Oct 23;389(6653):856–60.

122. Zuccato C, Cattaneo E. Role of brain-derived neurotrophic factor in Huntington's disease. Prog Neurobiol. 2007 Apr;81(5-6):294–330.

123. Cui L, Jeong H, Borovecki F, Parkhurst CN, Tanese N, Krainc D. Transcriptional repression of PGC-1alpha by mutant huntingtin leads to mitochondrial dysfunction and neurodegeneration. Cell. 2006 Oct 6;127(1):59–69.

124. Chaturvedi RK, Calingasan NY, Yang L, Hennessey T, Johri A, Beal MF. Impairment of PGC-1alpha expression, neuropathology and hepatic steatosis in a transgenic mouse model of Huntington's disease following chronic energy deprivation. Hum Mol Genet. 2010 Aug 15;19(16):3190–205.

125. Lin J, Wu P-H, Tarr PT, Lindenberg KS, St-Pierre J, Zhang C-Y, et al. Defects in adaptive energy metabolism with CNS-linked hyperactivity in PGC-1alpha null mice. Cell. 2004 Oct 1;119(1):121–35.

126. Mitra S, Tsvetkov AS, Finkbeiner S. Protein turnover and inclusion body formation. Autophagy. 2009 Oct;5(7):1037–8.

127. Waelter S, Boeddrich A, Lurz R, Scherzinger E, Lueder G, Lehrach H, et al. Accumulation of mutant huntingtin fragments in aggresome-like inclusion bodies as a result of insufficient protein degradation. Mol Biol Cell. 2001 May;12(5):1393–407.

128. Venkatraman P, Wetzel R, Tanaka M, Nukina N, Goldberg AL. Eukaryotic proteasomes cannot digest polyglutamine sequences and release them during degradation of polyglutamine-containing proteins. Mol Cell. 2004 Apr 9;14(1):95–104.

129. Qin Z-H, Wang Y, Kegel KB, Kazantsev A, Apostol BL, Thompson LM, et al. Autophagy regulates the processing of amino terminal huntingtin fragments. Hum Mol Genet. 2003 Dec 15;12(24):3231–44.

130. Roscic A, Baldo B, Crochemore C, Marcellin D, Paganetti P. Induction of autophagy with catalytic mTOR inhibitors reduces huntingtin aggregates in a neuronal cell model. J Neurochem. 2011 Oct;119(2):398–407.

131. Duan W, Guo Z, Jiang H, Ware M, Li X-J, Mattson MP. Dietary restriction normalizes glucose metabolism and BDNF levels, slows disease progression, and increases survival in huntingtin mutant mice. Proc Natl Acad Sci USA. 2003 Mar 4;100(5):2911–6.

132. Kegel KB, Kim M, Sapp E, McIntyre C, Castaño JG, Aronin N, et al. Huntingtin expression stimulates endosomal-lysosomal activity, endosome tubulation, and autophagy. J Neurosci. 2000 Oct 1;20(19):7268–78.

133. Jeong H, Then F, Melia TJ, Mazzulli JR, Cui L, Savas JN, et al. Acetylation targets mutant huntingtin to autophagosomes for degradation. Cell. 2009 Apr 3;137(1):60–72.

134. Koga H, Martinez-Vicente M, Arias E, Kaushik S, Sulzer D, Cuervo AM. Constitutive upregulation of chaperone-mediated autophagy in Huntington's disease. J Neurosci. 2011 Dec 14;31(50):18492–505.

135. Metzger S, Saukko M, Van Che H, Tong L, Puder Y, Riess O, et al. Age at onset in Huntington's disease is modified by the autophagy pathway: implication of the V471A polymorphism in Atg7. Hum Genet. 2010 Oct;128(4):453–9.

136. Beal MF, Brouillet E, Jenkins BG, Ferrante RJ, Kowall NW, Miller JM, et al. Neurochemical and histologic characterization of striatal excitotoxic lesions produced by the mitochondrial toxin 3-nitropropionic acid. J Neurosci. 1993 Oct 1;13(10):4181–92.

137. Saulle E, Gubellini P, Picconi B, Centonze D, Tropepi D, Pisani A, et al. Neuronal vulnerability following inhibition of mitochondrial complex II: a possible ionic mechanism for Huntington's disease. Mol Cell Neurosci. 2004 Jan 1;25(1):9–20.

138. Acevedo-Torres K, Berríos L, Rosario N, Dufault V, Skatchkov S, Eaton MJ, et al. Mitochondrial DNA damage is a hallmark of chemically induced and the R6/2 transgenic model of Huntington's disease. DNA Repair (Amst.). 2009 Jan 1;8(1):126–36.

139. Fontaine MA, Geddes JW, Banks A, Butterfield DA. Effect of exogenous and endogenous antioxidants on 3-nitropionic acid-induced in vivo oxidative stress and striatal lesions: insights into Huntington's disease. J Neurochem. 2000 Oct;75(4):1709–15.

140. Solesio ME, Saez-Atienzar S, Jordan J, Galindo MF. 3-Nitropropionioc acid induces autophagy by mitochondrial permeability transition pore formation rather than activation of the mitochondrial fission pathway. Br J Pharmacol. 2012 Apr 18.

141. Rosenstock TR, Carvalho ACP, Jurkiewicz A, Frussa-Filho R, Smaili SS. Mitochondrial calcium, oxidative stress and apoptosis in a neurodegenerative disease model induced by 3-nitropropionic acid. J Neurochem. 2004 Mar 1;88(5):1220–8.

142. Pickrell AM, Fukui H, Wang X, Pinto M, Moraes CT. The striatum is highly susceptible to mitochondrial oxidative phosphorylation dysfunctions. J Neurosci. 2011 Jul 6;31(27):9895–904.

143. Gu M, Gash MT, Mann VM, Javoy-Agid F, Cooper JM, Schapira AH. Mitochondrial defect in Huntington's disease caudate nucleus. Ann Neurol. 1996 Mar;39(3):385–9.

144. Guidetti P, Charles V, Chen EY, Reddy PH, Kordower JH, Whetsell WO, et al. Early degenerative changes in transgenic mice expressing mutant huntingtin involve dendritic abnormalities but no impairment of mitochondrial energy production. Experimental Neurology. 2001 Jun;169(2):340–50.

145. Browne SE, Bowling AC, MacGarvey U, Baik MJ, Berger SC, Muqit MM, et al. Oxidative damage and metabolic dysfunction in Huntington's disease: selective vulnerability of the basal ganglia. Ann Neurol. 1997 May;41(5):646–53.

146. Seong IS, Ivanova E, Lee J-M, Choo YS, Fossale E, Anderson M, et al. HD CAG repeat implicates a dominant property of huntingtin in mitochondrial energy metabolism. Hum Mol Genet. 2005 Oct 1;14(19):2871–80.

147. Weydt P, Pineda VV, Torrence AE, Libby RT, Satterfield TF, Lazarowski ER, et al. Thermoregulatory and metabolic defects in Huntington“s disease transgenic mice implicate PGC-1alpha in Huntington”s disease neurodegeneration. Cell Metab. 2006 Nov;4(5):349–62.

148. Bogdanov MB, Andreassen OA, Dedeoglu A, Ferrante RJ, Beal MF. Increased oxidative damage to DNA in a transgenic mouse model of Huntington's disease.

J Neurochem. 2001 Dec 1;79(6):1246–9.

149. Choo YS, Mao Z, Johnson GVW, Lesort M. Increased glutathione levels in cortical and striatal mitochondria of the R6/2 Huntington's disease mouse model. Neurosci Lett. 2005 Sep 23;386(1):63–8.

150. Bogdanov MB, Ferrante RJ, Kuemmerle S, Klivenyi P, Beal MF. Increased vulnerability to 3-nitropropionic acid in an animal model of Huntington's disease. J Neurochem. 1998 Dec;71(6):2642–4.

151. Gines S, Seong IS, Fossale E, Ivanova E, Trettel F, Gusella JF, et al. Specific progressive cAMP reduction implicates energy deficit in presymptomatic Huntington's disease knock-in mice. Hum Mol Genet. 2003 Mar 1;12(5):497–508.

152. Trushina E, Dyer RB, Badger JD, Ure D, Eide L, Tran DD, et al. Mutant huntingtin impairs axonal trafficking in mammalian neurons in vivo and in vitro. Mol Cell Biol. 2004 Sep;24(18):8195–209.

153. Orr AL, Li S, Wang C-E, Li H, Wang J, Rong J, et al. N-terminal mutant huntingtin associates with mitochondria and impairs mitochondrial trafficking. J Neurosci. 2008 Mar 12;28(11):2783–92.

154. Squitieri F, Cannella M, Sgarbi G, Maglione V, Falleni A, Lenzi P, et al. Severe ultrastructural mitochondrial changes in lymphoblasts homozygous for Huntington disease mutation. Mech. Ageing Dev. 2006 Feb;127(2):217–20.

155. Squitieri F, Falleni A, Cannella M, Orobello S, Fulceri F, Lenzi P, et al. Abnormal morphology of peripheral cell tissues from patients with Huntington disease. J Neural Transm. 2010 Jan;117(1):77–83.

156. Smirnova E, Griparic L, Shurland DL, van der Bliek AM. Dynamin-related protein Drp1 is required for mitochondrial division in mammalian cells. Mol Biol Cell. 2001 Aug;12(8):2245–56.

157. Kim J, Moody JP, Edgerly CK, Bordiuk OL, Cormier K, Smith K, et al. Mitochondrial loss, dysfunction and altered dynamics in Huntington's disease. Hum Mol Genet. 2010 Oct 15;19(20):3919–35.

158. Shirendeb U, Reddy AP, Manczak M, Calkins MJ, Mao P, Tagle DA, et al. Abnormal mitochondrial dynamics, mitochondrial loss and mutant huntingtin oligomers in Huntington's disease: implications for selective neuronal damage. Hum Mol Genet. 2011 Apr 1;20(7):1438–55.

159. Shirendeb UP, Calkins MJ, Manczak M, Anekonda V, Dufour B, McBride JL, et al. Mutant huntingtin“s interaction with mitochondrial protein Drp1 impairs mitochondrial biogenesis and causes defective axonal transport and synaptic degeneration in Huntington”s disease. Hum Mol Genet. 2012 Jan 15;21(2):406–

20.

160. Song W, Chen J, Petrilli A, Liot G, Klinglmayr E, Zhou Y, et al. Mutant huntingtin binds the mitochondrial fission GTPase dynamin-related protein-1 and increases its enzymatic activity. Nat Med. 2011 Mar;17(3):377–82.

161. Costa V, Giacomello M, Hudec R, Lopreiato R, Ermak G, Lim D, et al. Mitochondrial fission and cristae disruption increase the response of cell models of Huntington's disease to apoptotic stimuli. EMBO Mol Med. 2010 Dec;2(12):490–503.

162. Wang H, Lim PJ, Karbowski M, Monteiro MJ. Effects of overexpression of huntingtin proteins on mitochondrial integrity. Hum Mol Genet. 2009 Feb 15;18(4):737–52.

163. Mattson MP. Calcium and neurodegeneration. Aging Cell. 2007 Jun;6(3):337–50.

164. Gizatullina ZZ, Lindenberg KS, Harjes P, Chen Y, Kosinski CM, Landwehrmeyer BG, et al. Low stability of Huntington muscle mitochondria against Ca2+ in R6/2 mice. Ann Neurol. 2006 Feb;59(2):407–11.

165. Fernandes HB, Baimbridge KG, Church J, Hayden MR, Raymond LA. Mitochondrial sensitivity and altered calcium handling underlie enhanced NMDA-induced apoptosis in YAC128 model of Huntington's disease. J Neurosci. 2007 Dec 12;27(50):13614–23.

166. Panov A, Obertone T, Bennett-Desmelik J, Greenamyre JT. Ca(2+)-dependent permeability transition and complex I activity in lymphoblast mitochondria from normal individuals and patients with Huntington“s or Alzheimer”s disease. Ann N Y Acad Sci. 1999;893:365–8.

167. Choo YS, Johnson GVW, MacDonald M, Detloff PJ, Lesort M. Mutant huntingtin directly increases susceptibility of mitochondria to the calcium-induced permeability transition and cytochrome c release. Hum Mol Genet. 2004 Jul 15;13(14):1407–20.

168. Olney JW, Rhee V, Ho OL. Kainic acid: a powerful neurotoxic analogue of glutamate. Brain Res. 1974 Sep 13;77(3):507–12.

169. Coyle JT, Schwarcz R. Lesion of striatal neurones with kainic acid provides a model for Huntington's chorea. Nature. 1976 Sep 16;263(5574):244–6.

170. Beal MF, Kowall NW, Ellison DW, Mazurek MF, Swartz KJ, Martin JB. Replication of the neurochemical characteristics of Huntington's disease by quinolinic acid. Nature. 1986 Jan 1;321(6066):168–71.

171. Beal MF, Ferrante RJ, Swartz KJ, Kowall NW. Chronic quinolinic acid lesions in

rats closely resemble Huntington's disease. J Neurosci. 1991 Jun 1;11(6):1649–59.

172. Ferrante RJ, Kowall NW, Cipolloni PB, Storey E, Beal MF. Excitotoxin lesions in primates as a model for Huntington's disease: histopathologic and neurochemical characterization. Experimental Neurology. 1993 Jan 1;119(1):46–71.

173. Campesan S, Green EW, Breda C, Sathyasaikumar KV, Muchowski PJ, Schwarcz R, et al. The kynurenine pathway modulates neurodegeneration in a Drosophila model of Huntington's disease. Curr. Biol. 2011 Jun 7;21(11):961–6.

174. Zwilling D, Huang S-Y, Sathyasaikumar KV, Notarangelo FM, Guidetti P, Wu H-Q, et al. Kynurenine 3-monooxygenase inhibition in blood ameliorates neurodegeneration. Cell. 2011 Jun 10;145(6):863–74.

175. Wahl A-S, Buchthal B, Rode F, Bomholt SF, Freitag HE, Hardingham GE, et al. Hypoxic/ischemic conditions induce expression of the putative pro-death gene Clca1 via activation of extrasynaptic N-methyl-D-aspartate receptors. NSC. 2009 Jan 12;158(1):344–52.

176. Li L, Murphy TH, Hayden MR, Raymond LA. Enhanced striatal NR2B-containing N-methyl-D-aspartate receptor-mediated synaptic currents in a mouse model of Huntington disease. J Neurophysiol. 2004 Nov 1;92(5):2738–46.

177. Li L, Fan M, Icton CD, Chen N, Leavitt BR, Hayden MR, et al. Role of NR2B-type NMDA receptors in selective neurodegeneration in Huntington disease. Neurobiol Aging. 2003 Dec 1;24(8):1113–21.

178. Tang T-S, Slow E, Lupu V, Stavrovskaya IG, Sugimori M, Llinás R, et al. Disturbed Ca2+ signaling and apoptosis of medium spiny neurons in Huntington's disease. Proc Natl Acad Sci USA. 2005 Feb 15;102(7):2602–7.

179. Heng MY, Detloff PJ, Wang PL, Tsien JZ, Albin RL. In vivo evidence for NMDA receptor-mediated excitotoxicity in a murine genetic model of Huntington disease. J Neurosci. 2009 Mar 11;29(10):3200–5.

180. Gladding CM, Sepers MD, Xu J, Zhang LYJ, Milnerwood AJ, Lombroso PJ, et al. Calpain and STriatal-Enriched protein tyrosine phosphatase (STEP) activation contribute to extrasynaptic NMDA receptor localization in a Huntington's disease mouse model. Hum Mol Genet. 2012 Sep 1;21(17):3739–52.

181. Kaufman AM, Milnerwood AJ, Sepers MD, Coquinco A, She K, Wang L, et al. Opposing Roles of Synaptic and Extrasynaptic NMDA Receptor Signaling in Cocultured Striatal and Cortical Neurons. J Neurosci. 2012 Mar 21;32(12):3992–4003.

182. Cowan CM, Fan MMY, Fan J, Shehadeh J, Zhang LYJ, Graham RK, et al.

Polyglutamine-Modulated Striatal Calpain Activity in YAC Transgenic Huntington Disease Mouse Model: Impact on NMDA Receptor Function and Toxicity. J Neurosci. 2008 Nov 26;28(48):12725–35.

183. Graham RK, Pouladi MA, Joshi P, Lu G, Deng Y, Wu N-P, et al. Differential Susceptibility to Excitotoxic Stress in YAC128 Mouse Models of Huntington Disease between Initiation and Progression of Disease. J Neurosci. 2009 Feb 18;29(7):2193–204.

184. Dedeoglu A, Ferrante RJ, Andreassen OA, Dillmann WH, Beal MF. Mice overexpressing 70-kDa heat shock protein show increased resistance to malonate and 3-nitropropionic acid. Experimental Neurology. 2002 Jul 1;176(1):262–5.

185. Sorolla MA, Rodríguez-Colman MJ, Tamarit J, Ortega Z, Lucas JJ, Ferrer I, et al. Protein oxidation in Huntington disease affects energy production and vitamin B6 metabolism. Free Radic. Biol. Med. 2010 Aug 15;49(4):612–21.

186. Chatterjee M, Andrulis M, Stühmer T, Müller E, Hofmann C, Steinbrunn T, et al. The PI3K/Akt signalling pathway regulates the expression of Hsp70, which critically contributes to Hsp90-chaperone function and tumor cell survival in multiple myeloma. Haematologica. 2012 Oct 12.

187. Gines S, Ivanova E, Seong IS, Saura CA, Macdonald ME. Enhanced Akt signaling is an early pro-survival response that reflects N-methyl-D-aspartate receptor activation in Huntington's disease knock-in striatal cells. J Biol Chem. 2003 Dec 12;278(50):50514–22.

188. Graham RK, Deng Y, Slow EJ, Haigh B, Bissada N, Lu G, et al. Cleavage at the caspase-6 site is required for neuronal dysfunction and degeneration due to mutant huntingtin. Cell. 2006 Jun 16;125(6):1179–91.

189. Zhang H, Li Q, Graham RK, Slow E, Hayden MR, Bezprozvanny I. Full length mutant huntingtin is required for altered Ca2+ signaling and apoptosis of striatal neurons in the YAC mouse model of Huntington's disease. Neurobiology of Disease. 2008 Jul;31(1):80–8.

190. Stack EC, Dedeoglu A, Smith KM, Cormier K, Kubilus JK, Bogdanov M, et al. Neuroprotective effects of synaptic modulation in Huntington's disease R6/2 mice. J Neurosci. 2007 Nov 21;27(47):12908–15.

191. Metzler M, Gan L, Wong TP, Liu L, Helm J, Liu L, et al. NMDA receptor function and NMDA receptor-dependent phosphorylation of huntingtin is altered by the endocytic protein HIP1. J Neurosci. 2007 Feb 28;27(9):2298–308.

192. Metzler M, Gan L, Mazarei G, Graham RK, Liu L, Bissada N, et al. Phosphorylation of huntingtin at Ser421 in YAC128 neurons is associated with protection of YAC128 neurons from NMDA-mediated excitotoxicity and is

modulated by PP1 and PP2A. J Neurosci. 2010 Oct 27;30(43):14318–29.

193. Xifró X, García-Martínez JM, del Toro D, Alberch J, Pérez-Navarro E. Calcineurin is involved in the early activation of NMDA-mediated cell death in mutant huntingtin knock-in striatal cells. J Neurochem. 2008 Jun;105(5):1596–612.

194. Warby SC, Doty CN, Graham RK, Shively J, Singaraja RR, Hayden MR. Phosphorylation of huntingtin reduces the accumulation of its nuclear fragments. Mol Cell Neurosci. 2009 Feb;40(2):121–7.

195. Colin E, Zala D, Liot G, Rangone H, Borrell-Pagès M, Li X-J, et al. Huntingtin phosphorylation acts as a molecular switch for anterograde/retrograde transport in neurons. EMBO J. 2008 Aug 6;27(15):2124–34.

196. Pardo R, Colin E, Régulier E, Aebischer P, Déglon N, Humbert S, et al. Inhibition of calcineurin by FK506 protects against polyglutamine-huntingtin toxicity through an increase of huntingtin phosphorylation at S421. J Neurosci. 2006 Feb 1;26(5):1635–45.

197. Xie Y, Hayden MR, Xu B. BDNF overexpression in the forebrain rescues Huntington's disease phenotypes in YAC128 mice. J Neurosci. 2010 Nov 3;30(44):14708–18.

198. Pineda JR, Pardo R, Zala D, Yu H, Humbert S, Saudou F. Genetic and pharmacological inhibition of calcineurin corrects the BDNF transport defect in Huntington's disease. Mol Brain. 2009 Jan 1;2(1):33.

199. Canals JM, Pineda JR, Torres-Peraza JF, Bosch M, Martín-Ibañez R, Muñoz MT, et al. Brain-derived neurotrophic factor regulates the onset and severity of motor dysfunction associated with enkephalinergic neuronal degeneration in Huntington's disease. J Neurosci. 2004 Sep 1;24(35):7727–39.

200. Cho S-R, Benraiss A, Chmielnicki E, Samdani A, Economides A, Goldman SA. Induction of neostriatal neurogenesis slows disease progression in a transgenic murine model of Huntington disease. J Clin Invest. 2007 Oct;117(10):2889–902.

201. Gharami K, Xie Y, An JJ, Tonegawa S, Xu B. Brain-derived neurotrophic factor over-expression in the forebrain ameliorates Huntington's disease phenotypes in mice. J Neurochem. 2008 Apr;105(2):369–79.

CHAPTER 2 – ASSESSING HD PROGRESS AND CANDIDATE THERAPIES

Introduction

There are no validated neuroprotective therapies for Huntington's Disease, but if the previous chapter is any indication, we understand a great deal about the pathways leading to neuropathology. For the last 10 years, it has been fairly well known that rescuing mitochondrial energetics, reducing corticostriatal glutamate signaling, scavenging free radicals, normalizing protein homeostasis, or reversing transcriptional dysregulation at a single-transcript (e.g. *BDNF*) or global level could eventually be viable options for therapeutic intervention. The crux of the issue, now, is not just continuing to identify new targets, but also sifting through the potential interventions, whether drug or otherwise, and evaluating their efficacy in patients. The slow course of the disease may be preferable for patients when contrasted with a rapid, deadly neurodegenerative disorder like Amyotrophic Lateral Sclerosis. However, the slow and steady nature of HD also makes conclusive determination of a candidate therapeutic's ability to alter disease progression very difficult. In this chapter, I will discuss therapeutic development for HD. This will include a review of how disease progression is tracked in patients, what interventions have been attempted (and suggestions for why most have failed), and what novel therapeutics may be around the corner.

Diagnosing HD and Measuring its Progress

HD patients present a classical set of symptoms, the combination of which is not often confused with other disorders, particularly when a parent or grandparent has

diagnosed HD (with some exceptions). HD's progressive nature also makes it possible to quantify the degree to which the disease is impairing neural pathways or social functions. The Unified Huntington's Disease Rating Scale (UHDRS) was developed in the mid 1990's to attempt to standardize diagnostic parameters across many sites and as performed by different investigators (1). With an eye on clinical trial facilitation, it places an emphasis on those symptoms which advance most rapidly but all of which can ideally be evaluated within a 30 minute period. The UHDRS divides symptoms into four categories:

1) Motor symptoms, including oculomotor, dysarthria, chorea, dystonia, gait, and posture. Among the dystonia motor tests, timed finger tapping has become a popular evaluation for both its quantitative nature and the fact that it is often observed as mildly altered in premanifest patients.
2) Cognitive symptoms, including phonetic verbal fluency, symbol digit modalities, and the Stroop word test. Facial emotion recognition is not classically included in the UHDRS, but it is also commonly tested (2).
3) Behavioral Assessment, organized into subscales of mood (Does the subject often feel sad?), behavior (Is the subject often impatient or demanding?), psychosis (Has the subject been experiencing delusions or hallucinations?), and obsessiveness (Does the subject have recurrent and persistent ideas or images?).
4) Functional capacity, asked largely in the form of a yes/no questionnaire and including questions that cover a wide range of functional impediment, from the subtle ("Could the subject supervise children without help?") to the highly

disruptive (“Could the subject use the toilet without help?”).

Nearly every HD Phase II or III clinical trial since the mid-1990’s has used this or a subsection of this as a primary endpoint, often Motor Score or Total Functional Capacity, as worsening in these categories is highly associated with patients’ quality of life decline. While it is clear that improvement in these real-life behavioral derangements is the overall goal for patients, many of these are by their very nature subjective and variable. A patient may be more likely to be depressed if a family member died, or more irritable after an argument with his or her spouse, or have better chorea depending on the time of day. Efforts can be made to normalize and reduce variability in these, but it is well appreciated that other measurement tools, not subject to day-to-day randomness or bias, can augment the evaluation of disease progression. This is not just essential for drug rescue measurements, but for giving accurate assessments of whether a patient’s acute worsening is likely a “bad day” at the test, or a sign that a change in his or her medical care is in order.

The field has made advancements in disease progress measurement in two main areas: brain volumetric or activity imaging, and peripheral biomarker discovery. Imaging is the area with the most precision at the moment, though its high cost and the challenges of standardizing techniques center-to-center remain to be solved. Soon after postmortem tissue evaluation detected loss in neurotransmitter receptor levels, Positron Emission Tomography (PET) was used in living patients. Using specific ligands for dopamine D1 and D2 receptors, it was determined that binding of these ligands sharply decreases in patients (3). Furthermore, D2 receptor signal loss was found to agree almost perfectly with postmortem tissue analysis in a specific way: 35.5 CAG repeats

represent a clinical threshold of sorts, wherein any increase of repeats past 35.5 presents a proportionally increased rate of cell loss, pathological grade advancement, and D2 receptor binding loss (4,5). In other words, a patient with 48 repeats (12.5 over the threshold) at age 60 will have lost roughly twice as many neurons and twice as much D2 binding as a 60 year old patient with 42 repeats (6.5 over the threshold).

Given what we know about the specificity of degeneration, it is no surprise that progression can be followed by MRI volumetric measurements. There is a wealth of knowledge in this regard, and many studies have been focused on presymptomatic individuals (to be discussed in more detail later), but in general, the common sites for measureable changes are the striatum (both caudate nucleus and putamen), globus pallidus, nucleus accumbens, and cortical white matter (6,7). This regional degeneration is not uniform patient-to-patient, particularly in the cortex, and this regional variation is likely to underlie and explain at least a proportion of symptom variability from patient to patient. Through careful postmortem stereology, it was determined that patients with strong motor symptoms consistently demonstrate more cell loss in the primary motor cortex, whereas cell loss in the anterior cingulate cortex was strongly associated with mood dysfunction (8). Such information could help stratify patients in clinical trials to improve the power of trials that use volumetric MRI as an endpoint. Volumetric analysis is not the only use of MRI technology with practical applications to HD. Another useful technology is functional MRI, which measures the uptake of glucose molecules radiolabeled to emit positrons, which are visible to MRI. As neurons take up glucose in proportion to their rate of action potential firing, such images can be taken during tasks to measure brain activity (or lack thereof). In one such study, caudate and putamen

activities were seen to rapidly decline in HD patients, with slower declines seen in many cortical structures (9).

MRI is powerful, but due to its high cost and the necessity of bringing patients to the testing centers, peripheral biomarkers of disease progression are sorely needed. There is some progress in this regard, as blood can be collected easily and HD patient samples have already demonstrated differences in a subset of transcripts (10) as well as creatine kinase levels (11). Gene-positive individuals have also demonstrated increases in oxidative damage markers, namely 8-OHdG DNA (12) and lipid peroxidation (13). The former may not have robust utility (14), but lipid peroxidation correlated well with patients' UHDRS motor scores and independence scales. Remarkably, mHTT itself can be measured in patient leukocytes, using a highly quantitative fluorescence assay (15). This may be particularly useful if an attempt is made to knock down *HTT* levels systemically using oligonucleotide therapeutic approaches. Muscle biopsies have also been analyzed by transcriptomics, and there are at least 100 transcripts showing strong changes between patients and controls (16). More studies are needed to arrive at a workable group of tests to assess progression with minimal invasiveness, but the progress so far is encouraging.

Pathology Before Phenoconversion: Premanifest HD

As demonstrated by MRI and postmortem studies, significant tissue damage and neuronal loss is apparent even early in manifest disease. However, the HD community is in the unique position of being able to conclusively identify individuals who, assuming no accidents occur, will eventually get the disease. Of course, many individuals at risk

for HD (those with an affected parent) choose not to be genotyped, an understandable decision given the future implications that such a genetic diagnosis carries. Nevertheless, populations of such genotyped individuals allow for a wealth of research into the dysfunctions prior to visible symptoms. Just as importantly, clinicians can use premanifest populations for the development of neuroprotective therapeutics with the hope of forestalling or preventing pathology altogether. As an aside, nomenclature in these studies is not uniform when referring to individuals with the mutation but who do not yet have conclusively-diagnosed HD. So, despite their subtle differences in the medical literature, for clarity, “presymptomatic”, “asymptomatic”, “prodromal”, and “premanifest” will all be referred to as premanifest when discussing the below studies.

All of the above diagnostic tools have been brought to bear to monitor the progression of neuropathology in premanifest populations, revealing some interesting clues to the disease process. Several early studies using PET ligands for dopamine receptor D2 demonstrate loss of signal in premanifest patients (5,17-19). This loss of signal may be attributable to the loss of caudate and putamen volume in premanifest patients (20), but it likely isn’t that simple. The transcription factor Sp1 is partly responsible for control of dopamine receptor D2 (*DRD2*) transcription, and its binding to the transcriptional coactivator TAFII130 is weaker in both manifest and premanifest brain tissue samples (21), so transcriptional dysregulation is likely also occurring very early in pathology. The presence of blood mRNA biomarker elevations in premanifest patient samples supports this (10).

Structurally, many of the alterations observed in manifest HD are present in a lesser form in premanifest HD. Studies have demonstrated reductions in the volumes of

the whole brain, striatum, cortical white matter, and globus pallidus, with an expected increase in the size of lateral ventricles (20,22-26). Most of these changes are progressive, and tracking these changes longitudinally within a patient will allow clinicians to have a better idea of whether their interventions are having a beneficial effect on halting pathology. However, even measurements taken in single visits for premanifest patients are informative. It was demonstrated that both ^{18}F-FDG uptake and the ratio of striatal to total brain volume can be used to augment standard predictive measures (CAG repeat length and age) to more accurately predict the age of onset for patients (25,27). This may allow patients to better plan for future medical care. Additionally, it can help clinicians to further stratify premanifest patients in clinical trials into those who are, or are not, expected to phenoconvert (progress from premanifest to manifest) during the trial or follow up period.

Brain activity and structural alterations in the premanifest period may come as no surprise, as a late onset, slowly-progressive disease like HD is not going to demonstrate its characteristic degenerative pattern overnight. However, there are also many behavioral symptoms that appear in patients not yet diagnosed with HD. This may seem counterintuitive, but it's worth remembering that an HD diagnosis does not necessitate just any neurological or neuropsychological impairment often present in HD patients. It requires that the neurologist can be certain that this patient has HD, based on the presence of many HD-like behavioral, psychological, and motor manifestations (as laid out in the UHDRS). This array of symptoms is clearly not going to appear all at once. With this in mind, the behavioral alterations present in premanifest individuals have some patterns. Almost by definition, total functional capacity scores are rarely worsened

in premanifest patients, but motor, cognitive, and behavioral alterations are commonly observed and worsen as patients approach the expected age of onset (20,28). These commonly include bradykinesia (specifically, finger tapping impairment), impaired circle drawing, poor performance at smell tests, and failures of emotion recognition (22,26,29-31). Detailed analyses demonstrate that word learning and smell tests begin to decline ~15 years before diagnosis, while motor scores like tapping don't decline until ~10 years before diagnosis (32). This seems to add detail to the pattern of cortical white matter degeneration apparent in premanifest patients. Not surprisingly, these behavioral changes are often subtle, yet it still appears that volumetric changes of premanifest patients are more quantitative and statistically significant than most UHDRS tests (22). Some metrics may be more useful than others, though, and tapping, being highly quantitative in nature, might be the best candidate, as it correlates well with striatal and cortical volumetric changes (30).

Such tools to measure premanifest disease progression are of great use to clinicians in trials, but they are still highly variable in this population. This is hardly a criticism, as clinicians don't have the advantage of age-matched, inbred populations used in preclinical trials. Nevertheless, many clinical trials likely fail simply due to small sample size, and this is an even greater issue when assessing the power of the subtle premanifest changes. Various studies using volumetric imaging or behavioral alterations, even those of a highly quantitative nature, still estimate sample sizes of approximately 100-350 premanifest individuals would be needed to reliably detect a disease-altering effect of 20-50%, which would be a substantial alteration (23,26,33). Such clinical trials are often difficult to organize for a rare disorder, particularly one

whose premanifest population often chooses not to be tested. Therefore, this places particular emphasis on the efficient culling of ineffective candidate therapeutics in the preclinical setting.

There is good news, though. In spite of the difficulties in organizing and funding trials that often take a minimum of 1-2 years for confident “go / no go” assessment, there is a tremendous potential market for an HD treatment. Estimates for the market for such a treatment (34), in the US alone, may conservatively assume a patient population of 30,000 with diagnosed HD, and another 170,000 individuals who may elect to take the drug because they are at risk or have a related disorder. In the case of this population, and assuming a conservative estimate of $15 per day for drug costs, the potential market exceeds $1 billion per year even before accounting for increased survival, such as was seen for patients with chronic myelogenous leukemia taking Gleevec. Combined with the similarities between the cellular and molecular pathogenesis of HD and many more common neurodegenerative diseases, it is easy to see why there is not only a medical need for a treatment, but a commercial motivation for one as well.

The Current Therapeutic Landscape: Small Molecules, Small Effects

Therapeutics for HD (and for neurodegenerative diseases in general) are generally classified into either symptom management or disease modifying drugs, the latter of which can be further differentiated into neuroprotective (preventing neurons from being damaged) or neurorestorative (either promoting the regrowth of neurons or strengthening the pathways crippled by the absence of the degenerated connections).

The neuroprotective vs. neurorestorative distinctions are important in the context of patient populations. Premanifest indivituals can benefit from both neuroprotection and neurorestoration, but manifest HD patients have already suffered enough degeneration that behavioral impairment is present. This makes neuroprotection somewhat irrelevant and prone to failure. At this point, there are no approved disease-modifying therapeutics for patients. Symptom management has improved, but thus far, no drugs given to patients extend life expectancy.

After diagnosis, patient therapies are highly individualized. They often include antichoreics, of which tetrabenazine (TBZ) has become the most popular choice and is the only FDA approved drug for HD chorea. However, it has some unfortunate side effects, commonly including depression, drowsiness, fatigue, and parkinsonism (35-37). A depressive effect is not surprising from a drug with a dopamine depleting function (TBZ inhibits VMAT2, the transporter that loads dopamine into presynaptic vesicles) (38,39), but given that depression is already a common psychiatric symptom for HD patients, an alternative antichoreic without these side effects would be preferred. Pridopidine is a putative dopamine stabilizer that may serve such a purpose, as a relatively small clinical trial in HD patients demonstrated trends toward improvement of both voluntary and involuntary movement (40). Importantly, it had no significant side effects, and larger clinical trials are onging. Other symptom management interventions include SSRIs for depression, atypical neuroleptics for psychosis, and benzodiazepines for anxiety (41,42). Non-pharmaceutical therapies are also crucial for patient care, particularly as patients lose independence in late stage disease (43). This includes physical therapy, occupational therapy, speech therapy (including swallowing training),

and even simple exercise, all of which can improve quality of life in all of the disease stages.

Symptom management is necessary and helpful, but there are also many potential disease-modifying therapeutics already in the clinical pipeline. Those that have made the most progress concern the pathway that was perhaps earliest connected to HD, that of mitochondrial dysfunction. Creatine and coenzyme Q10 (CoQ10) both restore mitochondrial function as antioxidants and also aid energy production through oxidative phosphorylation, and are furthest along in clinical trials. Creatine is well tolerated in doses up to 10 g/day but showed no benefit to symptoms after up to 2 years of treatment (44-46) other than a reduction of serum 8-OHdG levels (47). However, there is reason to believe that higher dosing may be required, as the mouse trials on which these were founded supplemented the mouse chow with as much as 2% creatine. This would correspond to ~25 g for a patient that eats 1.25 kg/day. Hence, there are two ongoing large clinical trials with higher doses of creatine, one in manifest HD (CREST-E), and another in premanifest HD (Pre-CREST) both of which dose up to 30 or 40 g/day of creatine.

CoQ10 has a similar history. Early clinical trials demonstrated no benefit (48,49), but the dose was on the low side (600 mg/day). Upon successful dose escalation trials to demonstrate peak tolerability at 2400 mg/day without adverse events (50), two trials are ongoing at this higher dose. As with creatine, one targets manifest HD (2CARE) and another premanifest HD (PREQUEL), the latter of which is mainly assessing safety and tolerability at this point. Creatine and CoQ10 are also among the few items in clinical trials available as over the counter supplements, another being highly unsaturated fatty

acids. A clinical trial has been completed with only a trend towards benefit in the UHDRS motor scale and total functional capacity (P=0.08 for each), but most interestingly, there seemed to be not just a halting of progression but an improvement (51). This may warrant more testing as a potential neurorestorative therapy.

Cystamine and its redox partner cysteamine (upon administration, they rapidly interconvert) are another pair of antioxidants with strong interest from the HD clinical community. Like creatine and CoQ10, they are present in tissues already and represent little risk in high doses, having been given at up to 20 g/day (52). Originally thought to function through transglutaminase inhibition but now found to primarily protect neurons as an antioxidant, cysteamine is fairly effective in mouse trials (10-20% enhanced lifespan, reduced weight loss and motor phenotypes, and less striatal degeneration) (53-55), and a Phase II clinical trial is ongoing in France (CYST-HD).

Given that mHTT's toxicity is mediated at least partially (if not entirely) by altered protein folding, efforts to facilitate its refolding or degradation are ongoing. As discussed in Chapter 1, the upregulation of heat shock proteins has therapeutic potential. While no specific HD trials have been completed, low doses of the Hsp90 inhibitors geldanamycin or 17-AAG have been tested in many cell and animal models of polyQ diseases with promising results (56,57). They have been shown to both alter Hsp90 client protein proteasomal targeting and to disrupt Hsp90 / HSF1 binding, which releases HSF1 to the nucleus for induction of Hsps like Hsp70 and Hsp40 (58-60). 17-AAG doesn't cross the blood brain barrier efficiently, but other Hsp90 inhibitors with similar mechanisms of action are in the pipeline. Ganetespib, currently in clinical trials for some cancers, is more lipophilic and less toxic than 17-AAG (61). Additionally, a novel Hsp90-inhibiting

compound called AT13387 has very long lasting effects, and an interesting (if somewhat disconcerting) side effect of blurred vision with light flashes may be indicative of CNS penetrance (62,63).

Other disease-modifying therapeutics are not as far along or have been demonstrated ineffective. Autophagy augmentation through mTOR inhibition has promise, but may require more specificity of action. For example, a rapamycin analog everolimus has good pharmacokinetics, but was ineffective in R6/2 mice (64). This may be because mTOR has two main downstream pathways, and rapamycin analogs target mTORC1 but not mTORC2, the latter of which has more efficacy at reducing aggregated mHTT proteins in cells (65). Minocycline was enthusiastically studied 10 years ago and reduces cytochrome C release from mitochondria in HD models (66,67). In mice, the results were conflicting (68-70), and a futility trial in HD patients demonstrated no efficacy and suggested halting its study for HD (71). A DNA-binding compound mithramycin seems to rescue histone H3K9 hypermethylation and rescues pathology in R6/2 mice (72), but has not made it to clinical trials, possibly because it has demonstrated transcription factor Sp1 inhibition (73), so there may be worry of worsening an already present phenotype.

The pleiotropic effects of mHTT on transcriptional profiles, primarily downregulation of neuroprotective genes, have led to investigation of histone deacetylase (HDAC) inhibitors, which might globally relieve this transcriptional repression. Many have therapeutic potential in mouse models (Reviewed in (74)). Sodium phenylbutyrate is one such HDAC inhibitor of interest in HD. It has minimal adverse effects, and a 16-week safety and tolerability trial in HD has been completed,

with the results yet to be published (PHEND-HD). The potential of HDAC inhibitors to reverse the global transcriptional dysregulation seen in HD is tempered by the fact that they would be quite likely to have significant adverse effects in patients if treated at high doses, as has been demonstrated in mice alongside neuroprotective benefit (75-77). Because there are many different histone deacetylases, a targeted pharmaceutical approach may be warranted. With that in mind, Gillian Bates' group is making strides to identify the particular HDACs whose modulation is most likely to have therapeutic impact (78-80), with the hope that specific inhibitors to those HDACs could be developed with reduced adverse effects and improved efficacy.

Neurotransmitter modulation aimed at neuroprotection has also been attempted, with little success so far. Memantine, an NMDAR antagonist, demonstrated a trend towards motor rescue, but the trial was small (81). Riluzole, a glutamate antagonist with a somewhat unknown mechanism of action, has been tested numerous times in animals, with demonstrated protection against mitochondrial toxins and excitotoxicity (82-84). However, its trial was halted in patients due to liver enzyme elevation, despite a benefit for patients in total chorea score and UHDRS motor score (85).

Based on these and other clinical and preclinical studies, there is clearly no shortage of targets in deranged HD pathways for small molecule therapeutics. At this point, the motivation at the bench needs to be generating compounds with safe toxicity profiles that effectively target these pathways, and using available models to more efficiently weed out ineffective drugs or subtherapeutic dosing regimes. The latter is perhaps hardest to predict from preclinical trials, given the differences in pharmacokinetic properties between rodents and humans (and primates are simply too

expensive to be a standard in-between step). Alternative strategies using cell, gene, or oligonucleotide therapeutics are younger in their development, but as they are more targeted than most small molecules (e.g. delivery of a growth factor rather than a drug that could upregulate many genes, including the desired growth factor), they may provide better predictability in the transition from bench to bedside.

Cell Grafting for Tissue Replacement or Trophic Factor Supplementation

One of the main impediments of small molecule therapeutics is the blood brain barrier (BBB), a specialized membrane surrounding blood vessels in the CNS that gives an extra layer of protection from the likes of blood borne pathogens and hyperactive immune insults, among others. However, this also limits the passage of potential therapeutic small molecules. Without a doubt, patients would tolerate continuous intracranial dosage if such an intervention promised significant improvements in longevity and quality of life compared to current treatment options. Nevertheless, cerebral pump implantation and maintenance is fraught with risks of infection. To avoid this problem, cell and gene therapies that only require single dose implantations to bypass the BBB are being rigorously investigated.

Cell implantation first began as a simple neuronal replacement strategy with the hope that implanted fetal neuronal precursor cells would differentiate into neurons and become useful parts of the corticostriatal network, restoring motor control to patients. Several small patient cohorts have been tested, with varying degrees of success (86-91). While cell growth is often shown and proper nigrostriatal dopaminergic connections can occasionally be seen, in general the results are only an occasional benefit to the

patients' motor scores or total functional capacity. Immunosuppression is often needed, which can lead to infections. It may be possible to get around this using modern induced pluripotent stem cell (iPSC) technology, where it has been demonstrated that patient fibroblasts can not only be reprogrammed into transplantable MSN-like cells (92), but that the cells can be genetically corrected beforehand (93). In such grafts in patients, though, rejection is likely not the cause for failure. As reviewed in Cicchetti et al., 2011 (94), which discusses the fetal grafting clinical history in HD and Parkinson's Disease, the likely result of such failures is the death of the engrafted cells, probably as a result of poor trophic support. This makes sense in the context of the hampered delivery of neurotrophic factors from cortex to striatum that plays a well-established role in HD neuropathology.

Hence, for HD and other neurodegenerative diseases, the delivery of such growth factors by way of transduced cells has been rigorously investigated. Many such growth factors may be therapeutic in HD; in 3-NP-treated rats, fibroblasts expressing the factors *BDNF*, neurotrophin-3 (*NT-3*), neurturin (*NTN*), or *GDNF* all suppressed neurotoxicity (95). BDNF has perhaps been the best studied in this context, as it has demonstrated protective efficacy in toxin and genetic models, and using cell delivery methods including mesenchymal stem cells, fibroblasts, and bone-marrow stem cells (96-103). Among these varied studies, two are of particular interest. Astrocytes often become activated in HD patients and animal models, as demonstrated by increased presence in the tissue and elevated *GFAP* expression. These astrocytes, when altered to express *BDNF* under the control of the *GFAP* promoter, can be cultured and transplanted, and there is evidence suggesting that *BDNF* expression from these cells

may selectively increase when neurotoxic stress is present (98,99).

BDNF has incontrovertible therapeutic potential, primarily by activating several pro-survival kinase pathways (including Akt and MAPK), and has relevance in many neurodegenerative diseases (104). However, despite the recent development of effective small molecule agonists for the BDNF receptor (105), the directed implantation of BDNF-secreting cells into a confined area may be safer in the long run. This is due to evidence that brain-wide hyperactivity of BDNF activity has been associated with a number of disorders including epilepsy, addiction, chronic pain, and depression (106).

Other neurotrophic factors have been delivered by transduced secreting cell implantation, including GDNF (107-109), Neurturin (110), and CNTF (111-113). The CNTF studies are particularly interesting in that they were xenografts, but the cells survived *in vivo* by being encapsulated in a semipermeable membrane that renders them immunoisolated. However, this also prevents the cells from growing, which is safe in the context of undesirable hypertrophy but also necessitates a large amount of engrafted material for sufficient dosage. In the Phase I clinical trial (113), some electrophysiological improvements were seen in patients for whom the implanted capsules released the largest amount of CNTF, but cell survival was poor in more than half of the patients' capsules, stressing the need for improving both implanted cell survival and neurotrophic factor production.

Gene Therapy Delivery of Growth Factors

Implantation of transduced, engrafted cells is not necessary for long-lasting growth factor supplementation. Gene therapy approaches (transduction of patient cells

in vivo) are also beginning to be investigated for neurodegenerative diseases. Viral vectors for accomplishing this task are varied, but mainly are limited to vectors based on adenovirus, lentivirus, or adeno-associated virus (AAV), as these three can transduce postmitotic neurons. Adenovirus has fallen out of fashion due to high immunogenicity, but preclinical studies for all three have been effective. AAV and adenovirus have delivered a combination of *Bdnf* and noggin (*Nog*) in R6/2 transgenic mice and rat toxin models (114,115). These studies were notable because the combination of neurotrophic factors actually induced neurogenesis. While this carries with it the risk for uncontrolled cell growth, it also offers the potential for neurorestoration in manifest patients whose striata have already suffered significant deterioration. AAV-delivered *Gdnf* is also therapeutic in 3-NP-treated rats and N171-82Q transgenic mice (116,117), but neurturin (*Nrtn*) has perhaps the most immediate potential due to the clinical trial safety data in the PD field. AAV-delivered neurturin therapy, known as CERE-120, was tested in 6-OHDA treated rats (6-OHDA destroys dopaminergic nigrostriatal neurons, causing PD-like symptoms) and produced substantial therapeutic rescue with evidence of *Nrtn* expression out to at least 1 year post-transduction (118). Clinical trials were initiated, with enough modest success to warrant protocol alterations and further clinical investigation (119-121). Given the protective evidence of neurturin-secreting engrafted fibroblasts (95,110) and demonstrated protection for AAV-*Nrtn* in toxin rat models of HD (122), the HD field will be anxiously watching CERE-120 progress, and if promising, its evaluation in HD could initiate before the end of the decade.

HD gene therapy treatment need not be limited to endogenous growth factors, and the immune privileged state of the CNS may in fact be the perfect place for

expression of novel molecular therapeutics with minimal risk of inflammation due to the presence of foreign epitopes. Intracellular antibodies, single-chain non-secreted antibody fragments known as intrabodies, have significant potential. They can be directed to specific portions of the mHTT protein (123), and after delivery by AAV or lentivirus, have demonstrated significant neuroprotective potential (124,125) likely by hastening mHTT turnover. In the context of mHTT's toxic oligomers but likely benign inclusions, demonstration that mHTT is actually degraded after intrabody treatment rather than simply showing reduction of inclusion size is the most promising part of this avenue. In that vein, using polyQ-binding peptides with Hsc70-recognition domains to directly drag mHTT to autophagosomes for chaperone-mediated autophagy is also promising, and reduces pathology in transgenic mice (126).

Prevention Rather than Rescue: Knockdown Approaches for HD

Growth factors, intrabodies, and peptides may have therapeutic potential by aiding the degradation of mHTT or reversing some of its downstream toxic pathways, but recent advances in RNAi therapeutics may soon make it possible to prevent mHTT's production in the first place. Making use of endogenous microRNA (miRNA) transcriptional regulation pathways, artificial short hairpin RNAs (shRNAs) or genetically modified miRNAs altered to target different sites have been investigated for safety and efficacy. Safety has a specific focus for such approaches in HD. The mutation in *mHTT* is relatively subtle, so RNAi-based therapeutics against the HTT transcript don't always differentiate between mutant and wild type alleles, depending on the target site. We know that *wtHTT* is essential, but heterozygous knockout mice have only subtle

phenotypes (127). Thus, it may be necessary to only transiently reduce *mHTT* transcript levels and allow neurons the chance to “hit the reset button” on proteotoxic stress (128). Limiting the effects on *wtHTT* and evaluating the safety of partial *wtHTT* knockdown have been just as much a focus of the HD RNAi therapeutic field as demonstrating therapeutic efficacy.

AAV-delivered shRNA constructs have been evaluated in transgenic murine HD models. The first such published study showed a strong ability to reduce *mHTT* RNA, protein, and inclusion levels, and to improve transcriptional dysregulation and behavioral dysfunction (129). However, of the two constructs tested, both were equally effective at reducing *mHTT* RNA and proteins, but one of the two was highly toxic and actually exacerbated transcriptional profile alterations. This was likely the result of off target effects, a risk for any RNAi therapeutic as they often depend on the 6-base seed sequence to mediate most of their target specificity, and such 6-base sequences in shRNAs can be toxic if promiscuous (130). Nevertheless, careful evaluation of off target risks can yield safe knockdown vectors, which have been evaluated and proven tolerable in primates (131,132) and effective in murine HD models (133-135).

Harnessing the miRNA pathway is only one way nucleic acids can suppress mHTT levels, the other being chemically-modified oligonucleotides (oligos). Most promising is a chemically-modified oligo versus human HTT that specifically reduces human mHTT levels by >50% in transgenic mouse models, and was somewhat effective in rhesus after intrathecal injection. Most remarkably, the protein reduction was maintained for up to 3 months in mice from a single 2-week-long intracranial infusion (136). This surprising longevity is the result of the modified nucleic acid chemistry. Its

cell penetrance was sufficient when the oligo was simply provided in a saline suspension. Additionally, altered oligonucleotide chemistry facilitated binding, cellular uptake, and nuclease resistance. This was achieved by using phosphorothioate rather than phosphodiester bonds between bases, as well as a base structure including 2'-O-methoxyethyl nucleosides on the outermost 5 bases rather than standard deoxynucleotides. Unlike small RNAs that use the RNAi pathway to reduce transcript levels, it requires no interaction with the RISC complex, instead relying on RNase H degrading the RNA portion of the RNA-DNA hybrid. That the modified DNA oligo is not degraded in the process allows it to be recycled, enhances longevity without diluting its knockdown capabilities, and avoids potential unintended modulation of the RNAi pathway by not serving as a substrate.

The above study was allele-specific only insofar as it was species specific. For true allele-specificity, one can potentially take advantage of common patient single nucleotide polymorphisms (SNPs). There is evidence that only 2 SNP-targeting oligos are needed to differentially target *mHTT* in 2/3 of patients (137). Potent oligos have been targeted to SNP-bearing sequences in *HTT* (138), and humanized mouse models are being used to test them in a preclinical setting (139). Nevertheless, it is worth noting that the presence of a SNP in a transcript does not necessarily mean that location would make a good target site for an oligo, as local secondary structure and RNA binding proteins in the region might modify an oligo's binding strength. Indeed, in the above studies, only four such SNP targets were found to provide both significant allele specificity and sufficient knockdown strength. The CAG repeat itself may also serve as an effective target for RNaseH mediated degradation of *mHTT* transcripts, which would

by definition be allele-specific (140). However, there are many other mRNAs that include CAG repeats of significant length. This makes the evaluation of potential off target effects particularly important for this approach.

Summary

As a field, there is much known about the pathogenic processes in HD and the possible treatments for them. The clinical and preclinical research communities have tremendous tools for both administering these potential treatments and, more importantly, assessing their efficacy with minimal invasiveness. Nevertheless, the lack of an effective disease modifying therapeutic for HD in spite of the hundreds of drugs tested in models by this point tells us two things. Firstly, the clinical trials likely need to be longer with better sensitivity and power to detect a reduction in symptoms, both behavioral and neuropathological. Secondly, preclinical models must improve in identifying when a therapeutic intervention has little to no potential in the clinic. The next chapter will discuss mouse models of HD, the symptoms that can be measured in these models, and how they can be better leveraged for determination of a candidate therapeutic intervention's potential to treat HD.

Bibliography

1. The Huntington's Study Group. Unified Huntington's Disease Rating Scale: reliability and consistency. Huntington Study Group. Mov Disord. 1996 Mar;11(2):136–42.

2. Ille R, Schäfer A, Scharmüller W, Enzinger C, Schöggl H, Kapfhammer H-P, et al. Emotion recognition and experience in Huntington disease: a voxel-based morphometry study. J Psychiatry Neurosci. 2011 Nov;36(6):383–90.

3. Bäckman L, Robins-Wahlin TB, Lundin A, Ginovart N, Farde L. Cognitive deficits in Huntington's disease are predicted by dopaminergic PET markers and brain volumes. Brain. 1997 Dec 1;120 (Pt 12):2207–17.

4. Penney JB, Vonsattel JP, MacDonald ME, Gusella JF, Myers RH. CAG repeat number governs the development rate of pathology in Huntington's disease. Ann Neurol. 1997 May;41(5):689–92.

5. Antonini A, Leenders KL, Eidelberg D. [11C]raclopride-PET studies of the Huntington's disease rate of progression: relevance of the trinucleotide repeat length. Ann Neurol. 1998 Feb 1;43(2):253–5.

6. Rosas HD, Koroshetz WJ, Chen YI, Skeuse C, Vangel M, Cudkowicz ME, et al. Evidence for more widespread cerebral pathology in early HD: an MRI-based morphometric analysis. Neurology. 2003 May 27;60(10):1615–20.

7. Fennema-Notestine C, Archibald SL, Jacobson MW, Corey-Bloom J, Paulsen JS, Peavy GM, et al. In vivo evidence of cerebellar atrophy and cerebral white matter loss in Huntington disease. Neurology. 2004 Sep 28;63(6):989–95.

8. Thu DCV, Oorschot DE, Tippett LJ, Nana AL, Hogg VM, Synek BJ, et al. Cell loss in the motor and cingulate cortex correlates with symptomatology in Huntington's disease. Brain. 2010 Apr;133(Pt 4):1094–110.

9. Ciarmiello A, Cannella M, Lastoria S, Simonelli M, Frati L, Rubinsztein DC, et al. Brain white-matter volume loss and glucose hypometabolism precede the clinical symptoms of Huntington's disease. J Nucl Med. 2006 Feb 1;47(2):215–22.

10. Borovecki F, Lovrecic L, Zhou J, Jeong H, Then F, Rosas HD, et al. Genome-wide expression profiling of human blood reveals biomarkers for Huntington's disease. Proc Natl Acad Sci USA. 2005 Aug 2;102(31):11023–8.

11. Kim J, Amante DJ, Moody JP, Edgerly CK, Bordiuk OL, Smith K, et al. Reduced creatine kinase as a central and peripheral biomarker in Huntington's disease. Biochim Biophys Acta. 2010 Jul;1802(7-8):673–81.

12. Long JD, Matson WR, Juhl AR, Leavitt BR, Paulsen JS, the PREDICT-HD

Investigators and Coordinators of the Huntington Study Group. 8OHdG as a marker for Huntington disease progression. Neurobiology of Disease. 2012 Mar 5.

13. Chen C-M, Wu Y-R, Cheng M-L, Liu J-L, Lee Y-M, Lee P-W, et al. Increased oxidative damage and mitochondrial abnormalities in the peripheral blood of Huntington's disease patients. Biochem Biophys Res Commun. 2007 Jul 27;359(2):335–40.

14. Borowsky B, Warner J, Leavitt BR, Tabrizi SJ, Roos RAC, Dürr A, et al. 8OHdG is not a biomarker for Huntington disease state or progression. Neurology. 2013 Apr 24.

15. Moscovitch-Lopatin M, Weiss A, Rosas HD, Ritch J, Doros G, Kegel KB, et al. Optimization of an HTRF Assay for the Detection of Soluble Mutant Huntingtin in Human Buffy Coats: A Potential Biomarker in Blood for Huntington Disease. PLoS Curr. 2010;2:RRN1205.

16. Strand AD, Aragaki AK, Shaw D, Bird T, Holton J, Turner C, et al. Gene expression in Huntington's disease skeletal muscle: a potential biomarker. Hum Mol Genet. 2005 Jul 1;14(13):1863–76.

17. Weeks RA, Piccini P, Harding AE, Brooks DJ. Striatal D1 and D2 dopamine receptor loss in asymptomatic mutation carriers of Huntington's disease. Ann Neurol. 1996 Jul 1;40(1):49–54.

18. van Oostrom JCH, Maguire RP, Verschuuren-Bemelmans CC, Veenma-van der Duin L, Pruim J, Roos RAC, et al. Striatal dopamine D2 receptors, metabolism, and volume in preclinical Huntington disease. Neurology. 2005 Sep 27;65(6):941–3.

19. Andrews TC, Weeks RA, Turjanski N, Gunn RN, Watkins LH, Sahakian B, et al. Huntington's disease progression. PET and clinical observations. Brain. 1999 Dec 1;122 (Pt 12):2353–63.

20. Paulsen JS, Hayden M, Stout JC, Langbehn DR, Aylward E, Ross CA, et al. Preparing for preventive clinical trials: the Predict-HD study. Arch Neurol. 2006 Jun;63(6):883–90.

21. Dunah AW, Jeong H, Griffin A, Kim Y-M, Standaert DG, Hersch SM, et al. Sp1 and TAFII130 transcriptional activity disrupted in early Huntington's disease. Science. 2002 Jun 21;296(5576):2238–43.

22. Tabrizi SJ, Scahill RI, Dürr A, Roos RA, Leavitt BR, Jones R, et al. Biological and clinical changes in premanifest and early stage Huntington's disease in the TRACK-HD study: the 12-month longitudinal analysis. Lancet Neurology. 2011 Jan;10(1):31–42.

23. Aylward EH, Nopoulos PC, Ross CA, Langbehn DR, Pierson RK, Mills JA, et al. Longitudinal change in regional brain volumes in prodromal Huntington disease. J Neurol Neurosurg Psychiatr. 2011 Apr;82(4):405–10.

24. van den Bogaard SJA, Dumas EM, Ferrarini L, Milles J, van Buchem MA, van der Grond J, et al. Shape analysis of subcortical nuclei in Huntington's disease, global versus local atrophy--results from the TRACK-HD study. J Neurol Sci. 2011 Aug 15;307(1-2):60–8.

25. Aylward EH, Liu D, Nopoulos PC, Ross CA, Pierson RK, Mills JA, et al. Striatal volume contributes to the prediction of onset of Huntington disease in incident cases. Biol Psychiatry. 2012 May 1;71(9):822–8.

26. Tabrizi SJ, Reilmann R, Roos RAC, Dürr A, Leavitt B, Owen G, et al. Potential endpoints for clinical trials in premanifest and early Huntington's disease in the TRACK-HD study: analysis of 24 month observational data. Lancet Neurology. 2012 Jan;11(1):42–53.

27. Ciarmiello A, Giovacchini G, Orobello S, Bruselli L, Elifani F, Squitieri F. (18)F-FDG PET uptake in the pre-Huntington disease caudate affects the time-to-onset independently of CAG expansion size. Eur J Nucl Med Mol Imaging. 2012 Apr 12.

28. Duff K, Paulsen JS, Beglinger LJ, Langbehn DR, Stout JC, PREDICT-HD Investigators of the Huntington Study Group. Psychiatric symptoms in Huntington's disease before diagnosis: the predict-HD study. Biol Psychiatry. 2007 Dec 15;62(12):1341–6.

29. Biglan KM, Ross CA, Langbehn DR, Aylward EH, Stout JC, Queller S, et al. Motor abnormalities in premanifest persons with Huntington's disease: the PREDICT-HD study. Mov Disord. 2009 Sep 15;24(12):1763–72.

30. Bechtel N, Scahill RI, Rosas HD, Acharya T, van den Bogaard SJA, Jauffret C, et al. Tapping linked to function and structure in premanifest and symptomatic Huntington disease. Neurology. 2010 Dec 14;75(24):2150–60.

31. Harrington DL, Smith MM, Zhang Y, Carlozzi NE, Paulsen JS, the PREDICT-HD Investigators of the Huntington Study Group. Cognitive domains that predict time to diagnosis in prodromal Huntington disease. J Neurol Neurosurg Psychiatr. 2012 Mar 26.

32. Paulsen JS, Langbehn DR, Stout JC, Aylward E, Ross CA, Nance M, et al. Detection of Huntington's disease decades before diagnosis: the Predict-HD study. J Neurol Neurosurg Psychiatr. 2008 Aug 1;79(8):874–80.

33. Stout JC, Jones R, Labuschagne I, O'Regan AM, Say MJ, Dumas EM, et al. Evaluation of longitudinal 12 and 24 month cognitive outcomes in premanifest and early Huntington's disease. J Neurol Neurosurg Psychiatr. 2012 May 7.

34. Hersch SM, Rosas HD. Neuroprotective therapy for Huntington's disease: new prospects and challenges. Expert review of neurotherapeutics. 2001 Sep 1;1(1):111–8.

35. Huntington Study Group. Tetrabenazine as antichorea therapy in Huntington disease: a randomized controlled trial. Neurology. 2006 Feb 14;66(3):366–72.

36. Frank S. Tetrabenazine as anti-chorea therapy in Huntington disease: an open-label continuation study. Huntington Study Group/TETRA-HD Investigators. BMC Neurol. 2009 Jan 1;9:62.

37. Kenney C, Jankovic J. Tetrabenazine in the treatment of hyperkinetic movement disorders. Expert review of neurotherapeutics. 2006 Jan;6(1):7–17.

38. Login IS, Cronin MJ, MacLeod RM. Tetrabenazine has properties of a dopamine receptor antagonist. Ann Neurol. 1982 Sep;12(3):257–62.

39. Pettibone DJ, Totaro JA, Pflueger AB. Tetrabenazine-induced depletion of brain monoamines: characterization and interaction with selected antidepressants. Eur. J. Pharmacol. 1984 Jul 20;102(3-4):425–30.

40. The Huntington Study Group HART Investigators. A randomized, double-blind, placebo-controlled trial of pridopidine in Huntington's disease. Mov Disord. 2013 Feb 28.

41. Venuto CS, McGarry A, Ma Q, Kieburtz K. Pharmacologic approaches to the treatment of Huntington's disease. Mov Disord. 2012 Jan;27(1):31–41.

42. Mestre TA, Ferreira JJ. An evidence-based approach in the treatment of Huntington's disease. Parkinsonism Relat Disord. 2012 May;18(4):316–20.

43. Killoran A, Biglan KM. Therapeutics in Huntington's Disease. Curr Treat Options Neurol. 2012 Feb 8.

44. Tabrizi SJ, Blamire AM, Manners DN, Rajagopalan B, Styles P, Schapira AHV, et al. Creatine therapy for Huntington's disease: clinical and MRS findings in a 1-year pilot study. Neurology. 2003 Jul 8;61(1):141–2.

45. Tabrizi SJ, Blamire AM, Manners DN, Rajagopalan B, Styles P, Schapira AHV, et al. High-dose creatine therapy for Huntington disease: a 2-year clinical and MRS study. Neurology. 2005 May 10;64(9):1655–6.

46. Verbessem P, Lemiere J, Eijnde BO, Swinnen S, Vanhees L, van Leemputte M, et al. Creatine supplementation in Huntington's disease: a placebo-controlled pilot trial. Neurology. 2003 Oct 14;61(7):925–30.

47. Hersch SM, Gevorkian S, Marder K, Moskowitz C, Feigin A, Cox M, et al. Creatine in Huntington disease is safe, tolerable, bioavailable in brain and

reduces serum 8OH2'dG. Neurology. 2006 Jan 24;66(2):250–2.

48. Huntington Study Group. A randomized, placebo-controlled trial of coenzyme Q10 and remacemide in Huntington's disease. Neurology. 2001 Aug 14;57(3):397–404.

49. Feigin A, Kieburtz K, Como P, Hickey C, Claude K, Abwender D, et al. Assessment of coenzyme Q10 tolerability in Huntington's disease. Mov Disord. 1996 May;11(3):321–3.

50. Huntington Study Group Pre2CARE Investigators, Hyson HC, Kieburtz K, Shoulson I, McDermott M, Ravina B, et al. Safety and tolerability of high-dosage coenzyme Q10 in Huntington's disease and healthy subjects. Mov Disord. 2010 Sep 15;25(12):1924–8.

51. Vaddadi KS, Soosai E, Chiu E, Dingjan P. A randomised, placebo-controlled, double blind study of treatment of Huntington's disease with unsaturated fatty acids. NeuroReport. 2002 Jan 21;13(1):29–33.

52. Dubinsky R, Gray C. CYTE-I-HD: phase I dose finding and tolerability study of cysteamine (Cystagon) in Huntington's disease. Mov Disord. 2006 Apr;21(4):530–3.

53. Karpuj MV, Becher MW, Springer JE, Chabas D, Youssef S, Pedotti R, et al. Prolonged survival and decreased abnormal movements in transgenic model of Huntington disease, with administration of the transglutaminase inhibitor cystamine. Nat Med. 2002 Feb;8(2):143–9.

54. Dedeoglu A, Kubilus JK, Jeitner TM, Matson SA, Bogdanov M, Kowall NW, et al. Therapeutic effects of cystamine in a murine model of Huntington's disease. J Neurosci. 2002 Oct 15;22(20):8942–50.

55. van Raamsdonk JM, Pearson J, Bailey CDC, Rogers DA, Johnson GVW, Hayden MR, et al. Cystamine treatment is neuroprotective in the YAC128 mouse model of Huntington disease. J Neurochem. 2005 Oct;95(1):210–20.

56. Sittler A, Lurz R, Lueder G, Priller J, Lehrach H, Hayer-Hartl MK, et al. Geldanamycin activates a heat shock response and inhibits huntingtin aggregation in a cell culture model of Huntington's disease. Hum Mol Genet. 2001 Jun 1;10(12):1307–15.

57. Waza M, Adachi H, Katsuno M, Minamiyama M, Sang C, Tanaka F, et al. 17-AAG, an Hsp90 inhibitor, ameliorates polyglutamine-mediated motor neuron degeneration. Nat Med. 2005 Oct;11(10):1088–95.

58. Mimnaugh EG, Chavany C, Neckers L. Polyubiquitination and proteasomal degradation of the p185c-erbB-2 receptor protein-tyrosine kinase induced by geldanamycin. J Biol Chem. 1996 Sep 13;271(37):22796–801.

59. Bonvini P, Dalla Rosa H, Vignes N, Rosolen A. Ubiquitination and proteasomal degradation of nucleophosmin-anaplastic lymphoma kinase induced by 17-allylamino-demethoxygeldanamycin: role of the co-chaperone carboxyl heat shock protein 70-interacting protein. Cancer Res. 2004 May 1;64(9):3256–64.

60. Fujikake N, Nagai Y, Popiel HA, Okamoto Y, Yamaguchi M, Toda T. Heat shock transcription factor 1-activating compounds suppress polyglutamine-induced neurodegeneration through induction of multiple molecular chaperones. J Biol Chem. 2008 Sep 19;283(38):26188–97.

61. Ying W, Du Z, Sun L, Foley KP, Proia DA, Blackman RK, et al. Ganetespib, a unique triazolone-containing Hsp90 inhibitor, exhibits potent antitumor activity and a superior safety profile for cancer therapy. Mol. Cancer Ther. 2012 Feb;11(2):475–84.

62. Graham B, Curry J, Smyth T, Fazal L, Feltell R, Harada I, et al. The heat shock protein 90 inhibitor, AT13387, displays a long duration of action in vitro and in vivo in non-small cell lung cancer. Cancer Sci. 2012 Mar;103(3):522–7.

63. Hong DS, Banerji U, Tavana B, George GC, Aaron J, Kurzrock R. Targeting the molecular chaperone heat shock protein 90 (HSP90): Lessons learned and future directions. Cancer Treat. Rev. 2013 Jun;39(4):375–87.

64. Fox JH, Connor T, Chopra V, Dorsey K, Kama JA, Bleckmann D, et al. The mTOR kinase inhibitor Everolimus decreases S6 kinase phosphorylation but fails to reduce mutant huntingtin levels in brain and is not neuroprotective in the R6/2 mouse model of Huntington's disease. Mol Neurodegener. 2010;5:26.

65. Roscic A, Baldo B, Crochemore C, Marcellin D, Paganetti P. Induction of autophagy with catalytic mTOR inhibitors reduces huntingtin aggregates in a neuronal cell model. J Neurochem. 2011 Oct;119(2):398–407.

66. Wang X, Zhu S, Drozda M, Zhang W, Stavrovskaya IG, Cattaneo E, et al. Minocycline inhibits caspase-independent and -dependent mitochondrial cell death pathways in models of Huntington's disease. Proc Natl Acad Sci USA. 2003 Sep 2;100(18):10483–7.

67. Chen M, Ona VO, Li M, Ferrante RJ, Fink KB, Zhu S, et al. Minocycline inhibits caspase-1 and caspase-3 expression and delays mortality in a transgenic mouse model of Huntington disease. Nat Med. 2000 Jul;6(7):797–801.

68. Smith DL, Woodman B, Mahal A, Sathasivam K, Ghazi-Noori S, Lowden PAS, et al. Minocycline and doxycycline are not beneficial in a model of Huntington's disease. Ann Neurol. 2003 Aug;54(2):186–96.

69. Diguet E, Fernagut P-O, Wei X, Du Y, Rouland R, Gross C, et al. Deleterious effects of minocycline in animal models of Parkinson“s disease and Huntington”s disease. Eur J Neurosci. 2004 Jun;19(12):3266–76.

70. Hersch S, Fink K, Vonsattel J-P, Friedlander RM. Minocycline is protective in a mouse model of Huntington's disease. Ann Neurol. 2003 Dec;54(6):841–authorreply842–3.

71. Huntington Study Group DOMINO Investigators. A futility study of minocycline in Huntington's disease. Mov Disord. 2010 Oct 15;25(13):2219–24.

72. Ferrante RJ, Ryu H, Kubilus JK, D'Mello S, Sugars KL, Lee J, et al. Chemotherapy for the brain: the antitumor antibiotic mithramycin prolongs survival in a mouse model of Huntington's disease. J Neurosci. 2004 Nov 17;24(46):10335–42.

73. Sleiman SF, Langley BC, Basso M, Berlin J, Xia L, Payappilly JB, et al. Mithramycin is a gene-selective Sp1 inhibitor that identifies a biological intersection between cancer and neurodegeneration. J Neurosci. 2011 May 4;31(18):6858–70.

74. Zuccato C, Valenza M, Cattaneo E. Molecular mechanisms and potential therapeutical targets in Huntington's disease. Physiol. Rev. 2010 Jul;90(3):905–81.

75. Hockly E, Richon VM, Woodman B, Smith DL, Zhou X, Rosa E, et al. Suberoylanilide hydroxamic acid, a histone deacetylase inhibitor, ameliorates motor deficits in a mouse model of Huntington's disease. Proc Natl Acad Sci USA. 2003 Feb 18;100(4):2041–6.

76. Ferrante RJ, Kubilus JK, Lee J, Ryu H, Beesen A, Zucker B, et al. Histone deacetylase inhibition by sodium butyrate chemotherapy ameliorates the neurodegenerative phenotype in Huntington's disease mice. J Neurosci. 2003 Oct 15;23(28):9418–27.

77. Gardian G, Browne SE, Choi D-K, Klivenyi P, Gregorio J, Kubilus JK, et al. Neuroprotective effects of phenylbutyrate in the N171-82Q transgenic mouse model of Huntington's disease. J Biol Chem. 2005 Jan 7;280(1):556–63.

78. Benn CL, Butler R, Mariner L, Nixon J, Moffitt H, Mielcarek M, et al. Genetic knock-down of HDAC7 does not ameliorate disease pathogenesis in the R6/2 mouse model of Huntington's disease. PLoS ONE. 2009 Jan 1;4(6):e5747.

79. Bobrowska A, Paganetti P, Matthias P, Bates GP. Hdac6 knock-out increases tubulin acetylation but does not modify disease progression in the R6/2 mouse model of Huntington's disease. PLoS ONE. 2011;6(6):e20696.

80. Moumné L, Campbell K, Howland D, Ouyang Y, Bates GP. Genetic knock-down of HDAC3 does not modify disease-related phenotypes in a mouse model of Huntington's disease. PLoS ONE. 2012;7(2):e31080.

81. Ondo WG, Mejia NI, Hunter CB. A pilot study of the clinical efficacy and safety of

memantine for Huntington's disease. Parkinsonism Relat Disord. 2007 Oct;13(7):453–4.

82. Guyot MC, Palfi S, Stutzmann JM, Mazière M, Hantraye P, Brouillet E. Riluzole protects from motor deficits and striatal degeneration produced by systemic 3-nitropropionic acid intoxication in rats. NSC. 1997 Nov;81(1):141–9.

83. Palfi S, Riche D, Brouillet E, Guyot MC, Mary V, Wahl F, et al. Riluzole reduces incidence of abnormal movements but not striatal cell death in a primate model of progressive striatal degeneration. Experimental Neurology. 1997 Jul;146(1):135–41.

84. Mary V, Wahl F, Stutzmann JM. Effect of riluzole on quinolinate-induced neuronal damage in rats: comparison with blockers of glutamatergic neurotransmission. Neurosci Lett. 1995 Dec 1;201(1):92–6.

85. Huntington Study Group. Dosage effects of riluzole in Huntington's disease: a multicenter placebo-controlled study. Neurology. 2003 Dec 9;61(11):1551–6.

86. Furtado S, Sossi V, Hauser RA, Samii A, Schulzer M, Murphy CB, et al. Positron emission tomography after fetal transplantation in Huntington's disease. Ann Neurol. 2005 Aug;58(2):331–7.

87. Gallina P, Paganini M, Lombardini L, Mascalchi M, Porfirio B, Gadda D, et al. Human striatal neuroblasts develop and build a striatal-like structure into the brain of Huntington's disease patients after transplantation. Experimental Neurology. 2010 Mar;222(1):30–41.

88. Reuter I, Tai YF, Pavese N, Chaudhuri KR, Mason S, Polkey CE, et al. Long-term clinical and positron emission tomography outcome of fetal striatal transplantation in Huntington's disease. J Neurol Neurosurg Psychiatr. 2008 Aug;79(8):948–51.

89. Cicchetti F, Saporta S, Hauser RA, Parent M, Saint-Pierre M, Sanberg PR, et al. Neural transplants in patients with Huntington's disease undergo disease-like neuronal degeneration. Proc Natl Acad Sci USA. 2009 Jul 28;106(30):12483–8.

90. Keene CD, Sonnen JA, Swanson PD, Kopyov O, Leverenz JB, Bird TD, et al. Neural transplantation in Huntington disease: long-term grafts in two patients. Neurology. 2007 Jun 12;68(24):2093–8.

91. Capetian P, Knoth R, Maciaczyk J, Pantazis G, Ditter M, Bokla L, et al. Histological findings on fetal striatal grafts in a Huntington's disease patient early after transplantation. Neuroscience. 2009 May 19;160(3):661–75.

92. The Hd Ipsc Consortium. Induced Pluripotent Stem Cells from Patients with Huntington's Disease Show CAG-Repeat-Expansion-Associated Phenotypes. Cell Stem Cell. 2012 Jun 28.

93. An MC, Zhang N, Scott G, Montoro D, Wittkop T, Mooney S, et al. Genetic Correction of Huntington's Disease Phenotypes in Induced Pluripotent Stem Cells. Cell Stem Cell. 2012 Jun 26.

94. Cicchetti F, Soulet D, Freeman TB. Neuronal degeneration in striatal transplants and Huntington's disease: potential mechanisms and clinical implications. Brain. 2011 Mar;134(Pt 3):641–52.

95. Gratacòs E, Pérez-Navarro E, Tolosa E, Arenas E, Alberch J. Neuroprotection of striatal neurons against kainate excitotoxicity by neurotrophins and GDNF family members. J. Neurochem. 2001. pp. 1287–96.

96. Dey ND, Bombard MC, Roland BP, Davidson S, Lu M, Rossignol J, et al. Genetically engineered mesenchymal stem cells reduce behavioral deficits in the YAC 128 mouse model of Huntington's disease. Behav Brain Res. 2010 Dec 25;214(2):193–200.

97. Lucidi-Phillipi CA, Gage FH, Shults CW, Jones KR, Reichardt LF, Kang UJ. Brain-derived neurotrophic factor-transduced fibroblasts: production of BDNF and effects of grafting to the adult rat brain. J. Comp. Neurol. 1995 Apr 10;354(3):361–76.

98. Pérez-Navarro E, Canudas AM, Akerund P, Alberch J, Arenas E. Brain-derived neurotrophic factor, neurotrophin-3, and neurotrophin-4/5 prevent the death of striatal projection neurons in a rodent model of Huntington's disease. J Neurochem. 2000 Nov;75(5):2190–9.

99. Canals JM, Checa N, Marco S, Akerud P, Michels A, Pérez-Navarro E, et al. Expression of brain-derived neurotrophic factor in cortical neurons is regulated by striatal target area. J Neurosci. 2001 Jan 1;21(1):117–24.

100. Makar TK, Trisler D, Eglitis MA, Mouradian MM, Dhib-Jalbut S. Brain-derived neurotrophic factor (BDNF) gene delivery into the CNS using bone marrow cells as vehicles in mice. Neurosci Lett. 2004 Feb 19;356(3):215–9.

101. Giralt A, Friedman HC, Caneda-Ferrón B, Urbán N, Moreno E, Rubio N, et al. BDNF regulation under GFAP promoter provides engineered astrocytes as a new approach for long-term protection in Huntington's disease. Gene Ther. 2010 Oct;17(10):1294–308.

102. Tóth ZE, Leker RR, Shahar T, Bratincsak A, Szalayova I, Key S, et al. Bone marrow-derived nonreactive astrocytes in the mouse brain after permanent middle cerebral artery occlusion. Stem Cells Dev. 2011 Mar;20(3):539–46.

103. Rossignol J, Boyer C, Lévèque X, Fink KD, Thinard R, Blanchard F, et al. Mesenchymal stem cell transplantation and DMEM administration in a 3NP rat model of Huntington's disease: morphological and behavioral outcomes. Behav Brain Res. 2011 Mar 1;217(2):369–78.

104. Nagahara AH, Tuszynski MH. Potential therapeutic uses of BDNF in neurological and psychiatric disorders. Nat Rev Drug Discov. 2011 Mar;10(3):209–19.

105. Jiang M, Peng Q, Liu X, Jin J, Hou Z, Zhang J, et al. Small-molecule TrkB receptor agonists improve motor function and extend survival in a mouse model of Huntington's disease. Hum Mol Genet. 2013 Mar 6.

106. Boulle F, Kenis G, Cazorla M, Hamon M, Steinbusch HWM, Lanfumey L, et al. TrkB inhibition as a therapeutic target for CNS-related disorders. Prog Neurobiol. 2012 Aug;98(2):197–206.

107. Ebert AD, Barber AE, Heins BM, Svendsen CN. Ex vivo delivery of GDNF maintains motor function and prevents neuronal loss in a transgenic mouse model of Huntington's disease. Experimental Neurology. 2010 Jul;224(1):155–62.

108. Pérez-Navarro E, Arenas E, Reiriz J, Calvo N, Alberch J. Glial cell line-derived neurotrophic factor protects striatal calbindin-immunoreactive neurons from excitotoxic damage. NSC. 1996 Nov;75(2):345–52.

109. Pérez-Navarro E, Arenas E, Marco S, Alberch J. Intrastriatal grafting of a GDNF-producing cell line protects striatonigral neurons from quinolinic acid excitotoxicity in vivo. Eur J Neurosci. 1999 Jan;11(1):241–9.

110. Pérez-Navarro E, Akerud P, Marco S, Canals JM, Tolosa E, Arenas E, et al. Neurturin protects striatal projection neurons but not interneurons in a rat model of Huntington's disease. NSC. 2000;98(1):89–96.

111. Emerich DF, Lindner MD, Winn SR, Chen EY, Frydel BR, Kordower JH. Implants of encapsulated human CNTF-producing fibroblasts prevent behavioral deficits and striatal degeneration in a rodent model of Huntington's disease. J Neurosci. 1996 Aug 15;16(16):5168–81.

112. Bachoud-Lévi A-C, Deglon N, Nguyen JP, Bloch J, Bourdet C, Winkel L, et al. Neuroprotective gene therapy for Huntington's disease using a polymer encapsulated BHK cell line engineered to secrete human CNTF. Human Gene Therapy. 2000 Aug 10;11(12):1723–9.

113. Bloch J, Bachoud-Lévi A-C, Deglon N, Lefaucheur JP, Winkel L, Palfi S, et al. Neuroprotective gene therapy for Huntington's disease, using polymer-encapsulated cells engineered to secrete human ciliary neurotrophic factor: results of a phase I study. Human Gene Therapy. 2004 Oct;15(10):968–75.

114. Cho S-R, Benraiss A, Chmielnicki E, Samdani A, Economides A, Goldman SA. Induction of neostriatal neurogenesis slows disease progression in a transgenic murine model of Huntington disease. J Clin Invest. 2007 Oct;117(10):2889–902.

115. Benraiss A, Bruel-Jungerman E, Lu G, Economides AN, Davidson B, Goldman SA. Sustained induction of neuronal addition to the adult rat neostriatum by AAV4-delivered noggin and BDNF. Gene Ther. 2011 Sep 15;19(5):483–93.

116. McBride JL, During MJ, Wuu J, Chen EY, Leurgans SE, Kordower JH. Structural and functional neuroprotection in a rat model of Huntington's disease by viral gene transfer of GDNF. Experimental Neurology. 2003 Jun;181(2):213–23.

117. McBride JL, Ramaswamy S, Gasmi M, Bartus RT, Herzog CD, Brandon EP, et al. Viral delivery of glial cell line-derived neurotrophic factor improves behavior and protects striatal neurons in a mouse model of Huntington's disease. Proc Natl Acad Sci USA. 2006 Jun 13;103(24):9345–50.

118. Gasmi M, Brandon EP, Herzog CD, Wilson A, Bishop KM, Hofer EK, et al. AAV2-mediated delivery of human neurturin to the rat nigrostriatal system: long-term efficacy and tolerability of CERE-120 for Parkinson's disease. Neurobiology of Disease. 2007 Jul;27(1):67–76.

119. Marks WJ, Bartus RT, Siffert J, Davis CS, Lozano A, Boulis N, et al. Gene delivery of AAV2-neurturin for Parkinson's disease: a double-blind, randomised, controlled trial. Lancet Neurology. 2010 Dec;9(12):1164–72.

120. Hickey P, Stacy M. AAV2-neurturin (CERE-120) for Parkinson's disease. Expert Opin Biol Ther. 2013 Jan;13(1):137–45.

121. Bartus RT, Baumann TL, Siffert J, Herzog CD, Alterman R, Boulis N, et al. Safety/feasibility of targeting the substantia nigra with AAV2-neurturin in Parkinson patients. Neurology. 2013 Apr 10.

122. Ramaswamy S, McBride JL, Herzog CD, Brandon E, Gasmi M, Bartus RT, et al. Neurturin gene therapy improves motor function and prevents death of striatal neurons in a 3-nitropropionic acid rat model of Huntington's disease. Neurobiology of Disease. 2007 May;26(2):375–84.

123. Southwell AL, Khoshnan A, Dunn DE, Bugg CW, Lo DC, Patterson PH. Intrabodies binding the proline-rich domains of mutant huntingtin increase its turnover and reduce neurotoxicity. J Neurosci. 2008 Sep 3;28(36):9013–20.

124. Southwell AL, Ko J, Patterson PH. Intrabody gene therapy ameliorates motor, cognitive, and neuropathological symptoms in multiple mouse models of Huntington's disease. J Neurosci. 2009 Oct 28;29(43):13589–602.

125. Wang C-E, Zhou H, McGuire JR, Cerullo V, Lee B, Li S-H, et al. Suppression of neuropil aggregates and neurological symptoms by an intracellular antibody implicates the cytoplasmic toxicity of mutant huntingtin. The Journal of Cell Biology. 2008 Jun 2;181(5):803–16.

126. Bauer PO, Goswami A, Wong HK, Okuno M, Kurosawa M, Yamada M, et al.

Harnessing chaperone-mediated autophagy for the selective degradation of mutant huntingtin protein. Nat Biotechnol. 2010 Mar;28(3):256–63.

127. Zeitlin S, Liu JP, Chapman DL, Papaioannou VE, Efstratiadis A. Increased apoptosis and early embryonic lethality in mice nullizygous for the Huntington's disease gene homologue. Nat Genet. 1995 Oct;11(2):155–63.

128. Lu X-H, Yang XW. “Huntingtin holiday”: progress toward an antisense therapy for Huntington's disease. Neuron. 2012 Jun 21;74(6):964–6.

129. Rodriguez-Lebron E, Denovan-Wright EM, Nash K, Lewin AS, Mandel RJ. Intrastriatal rAAV-mediated delivery of anti-huntingtin shRNAs induces partial reversal of disease progression in R6/1 Huntington's disease transgenic mice. Mol Ther. 2005 Oct;12(4):618–33.

130. Boudreau RL, Spengler RM, Davidson BL. Rational Design of Therapeutic siRNAs: Minimizing Off-targeting Potential to Improve the Safety of RNAi Therapy for Huntington's Disease. Mol Ther. 2011 Sep 27.

131. McBride JL, Pitzer MR, Boudreau RL, Dufour B, Hobbs T, Ojeda SR, et al. Preclinical Safety of RNAi-Mediated HTT Suppression in the Rhesus Macaque as a Potential Therapy for Huntington's Disease. Mol Ther. 2011 Dec;19(12):2152–62.

132. Grondin R, Kaytor MD, Ai Y, Nelson PT, Thakker DR, Heisel J, et al. Six-month partial suppression of Huntingtin is well tolerated in the adult rhesus striatum. Brain. 2012 Apr;135(Pt 4):1197–209.

133. McBride JL, Boudreau RL, Harper SQ, Staber PD, Monteys AM, Martins I, et al. Artificial miRNAs mitigate shRNA-mediated toxicity in the brain: Implications for the therapeutic development of RNAi. Proc Natl Acad Sci USA. 2008 Apr 15;105(15):5868–73.

134. Franich NR, Fitzsimons HL, Fong DM, Klugmann M, During MJ, Young D. AAV vector-mediated RNAi of mutant huntingtin expression is neuroprotective in a novel genetic rat model of Huntington's disease. Mol Ther. 2008 May 1;16(5):947–56.

135. Boudreau RL, McBride JL, Martins I, Shen S, Xing Y, Carter BJ, et al. Nonallele-specific silencing of mutant and wild-type huntingtin demonstrates therapeutic efficacy in Huntington's disease mice. Mol Ther. 2009 Jun;17(6):1053–63.

136. Kordasiewicz HB, Stanek LM, Wancewicz EV, Mazur C, McAlonis MM, Pytel KA, et al. Sustained therapeutic reversal of Huntington's disease by transient repression of huntingtin synthesis. Neuron. 2012 Jun 21;74(6):1031–44.

137. Lombardi MS, Jaspers L, Spronkmans C, Gellera C, Taroni F, Di Maria E, et al. A majority of Huntington's disease patients may be treatable by individualized

allele-specific RNA interference. Experimental Neurology. 2009 Jun;217(2):312–9.

138. Carroll JB, Warby SC, Southwell AL, Doty CN, Greenlee S, Skotte N, et al. Potent and selective antisense oligonucleotides targeting single-nucleotide polymorphisms in the Huntington disease gene / allele-specific silencing of mutant huntingtin. Mol Ther. 2011 Dec;19(12):2178–85.

139. Southwell AL, Warby SC, Carroll JB, Doty CN, Skotte NH, Zhang W, et al. A fully humanized transgenic mouse model of Huntington disease. Hum Mol Genet. 2012 Oct 5.

140. Gagnon KT, Pendergraff HM, Deleavey GF, Swayze EE, Potier P, Randolph J, et al. Allele-selective inhibition of mutant huntingtin expression with antisense oligonucleotides targeting the expanded CAG repeat. Biochemistry. 2010 Nov 30;49(47):10166–78.

CHAPTER 3 – MOUSE MODELS OF HUNTINGTON'S DISEASE

Introduction

All of the therapeutic options discussed in Chapter 2 have made the most progress towards the clinic by demonstrating neuroprotection and behavioral rescue in mouse models of HD. However, not all models are created equal, and it is important to realize the differences between the models and their expected phenotypes before attempting to demonstrate that a given intervention will show therapeutic benefit. Some strains display neuropathology from birth and early mortality, while others progress so slowly that visible phenotypes are not seen until the mice are very old, and do not present with morbidity. The age of onset of a number of frequently utilized behavioral and biological measures of pathology for HD mouse models are summarized in Figure 1.

The first transgenic models of HD in mice were developed in 1996 (1) by introducing a fragment of a juvenile HD patient's *HTT* gene into the mouse genome. Although these strains (R6/2 and R6/1) were initially designed to study repeat expansion, these strains displayed motor and metabolic symptoms, including tremors, lack of coordination (rotarod balance difficulty), and excessive weight loss, leading to death at a very early age (~12-14 weeks in the R6/2 line). The rapid and reproducible progression of HD-like symptomology in R6/2 mice has made this line a mainstay of HD research. However, the limitations of R6/2, the absence of a full length mutant HTT protein and the extremely rapid progression of disease, led to the development of quite a number of other animal models, each with their own unique genetic and phenotypic

characteristics summarized in Table 2.

Mouse models of HD can be grouped into three categories, based on the genetic basis of their creation. N-terminal transgenic animals are those carrying a small 5' portion of huntingtin, either human or chimeric human/mouse, at random in their genome. These animals tend to have the earliest onset of motor symptoms and diminished lifespan (1-5), thought to be because mHTT pathology is greatly enhanced by its proteolytic processing into N-terminal fragments (6,7); these mouse models are probably a short cut to this particularly toxic state.

Transgenic models expressing full-length *mHTT* mice also exist, containing random insertions of the full-length human *HTT* gene with an expanded CAG repeat in the form of either YAC or BAC DNA (8-10). One interesting observation of the two most commonly used models in this category is the unexpected age of onset difference (~6 months in YAC128 mice and as early as 8 weeks in BACHD mice) despite the shorter repeat length of BACHD mice (97 vs. 128).

Several strains in which a pathological length CAG repeat is introduced into the mouse huntingtin (*Htt*) gene have also been created (so called knock-in strains) (11-17). The best studied long repeat models (140 and 150 repeats) have motor symptom onset within 6 months, but the shorter models have little or no observable motor dysfunction for the first year of life, and no decrease in lifespan has been reported in any knock-in models. This may properly model the late adult onset of human HD but does not replicate the impaired quality of life and inevitable mortality.

As many models have been brought into use, significant differences among the models have emerged. It is important to note, however, that many cross-model studies

underline significant pathological and molecular similarities in the different genetic models in spite of their inevitable differences (18-28).

Behavioral Symptoms in HD Model Mice

HD in patients is characterized by motor, cognitive and behavioral symptoms, and assays testing these broad categories are used to measure progression of pathology in HD mice. Motor phenotypes have been tested in a number of HD model mice, including limb clasping upon tail suspension, basal activity level, gait abnormalities, balance beam traversing time, swimming speed, suspended horizontal beam turning, and latency to remain on a fixed-speed or accelerating rotarod. The rotarod, in particular, has proven to be a robust measurement of balance and coordination deficits for which nearly every HD model mouse has demonstrated a deficiency, and is the metric for which the most data exists on motor dysfunction. N-terminal transgenic mice consistently display an early onset of severe motor symptoms. R6/2 mice swim poorly by 5 weeks of age, and show beam walking and rotarod deficiencies by 6 weeks, both of which progressively worsen with age (1,2). R6/1 mice experience clear rotarod deficiency at 18 weeks (1-5) with an earlier (13 week) onset of failure to turn around on a suspended horizontal rod (6,7,29), while N171-82Q mice display a subtle but progressive rotarod phenotype at 3 months (4,8-10).

Full-length transgenic models display delayed motor symptoms compared to N-terminal transgenics; YAC72 mice do not display a significant rotarod phenotype until 16 months (11-17,30), while YAC128 mice decline starting at 6-7 months (10,18-28,31). BACHD transgenics do show a significant reduction in rotarod latency as early as 4

weeks of age, but they do not precipitously decline in performance until 28 weeks; this is in contrast to R6/2 rotarod performance, which rapidly declines once a difference is measured (2,32).

Knockin mice do not always display the characteristic motor phenotype seen in transgenic models, despite some strains carrying as many CAG repeats as R6/2 mice (~150) and having twice the gene dose as most transgenic strains (behavioral experiments carried out in knockin mice typically use homozygotes). This could reflect differences in chromosomal context, transgene expression, the chimeric nature of knockin *Htt* inserts, or strain background. HdhQ140 rotarod latency appears at 4 months at 30 rpm on a fixed-speed rotarod (3,33), but another group reported no accelerating rotarod phenotype through 6 months (29,34), while rotarod deficits are not seen in HdhQ92, HdhQ111, and HdhQ150 mice until about 2 years of age (4,11,32,35).

Cognitive phenotypes can again be measured in many ways, but tasks based on spatial learning and memory such as the Morris water maze or T maze (swimming or elevated) have been used to reveal deficits in initial task learning and re-learning upon parameter changes. 4-5 week old R6/2 mice learn the Morris water maze as well as wild types when the platform is visible, but display spatial memory deficits when the platform is hidden, and cannot re-learn upon platform movement as well as wild type mice. Two-choice swim testing revealed an earlier deficit in task reversal (6.5 weeks) than for initial visual learning of the task (10-11 weeks) (1,36). Initial visual learning deficiency of the two-choice swim test was also found in YAC128 mice (1-5,31), but HdhQ150 knockins displayed no learning deficits on the Morris water maze (6,7,11).

Cognitive tests are challenging to standardize, as environmental conditions and

spatial cues are difficult to replicate from lab-to-lab and can influence animals' performance in behavioral tests. Despite these challenges, these consistent observations from many different labs demonstrating a clear effect on cognitive performance in HD model mice suggests that the cognitive decline commonly observed in HD patients is well represented by HD model mice.

Neuropathology of Murine Models

Human neuropathology is characterized by a severe loss of striatal volume (in particular the caudate nucleus). Medium spiny neurons but not interneurons are lost, and reactive gliosis is apparent (8-10,37). Cortical degeneration is also prominent in late stages. HTT inclusions in patients are only found in a small fraction of cells (11-17,38), though they are visible in almost all HD patient brains with a clinical grade of at least 2 (18-28,39). Within HD model mice, the progressive neuropathology is unique for each strain, but they share some commonalities.

N-terminal transgene strains display neuropathology at or prior to symptom onset. In contrast to patients, neuron loss is somewhat minimal, but R6/2 brains decrease in weight as much as 20% with enlargement of the lateral ventricles (1,2). They demonstrate neuronal intranuclear inclusions (NIIs) as early as at birth (3,40), though NII's are typically reported in this strain around 3-4.5 weeks (29,41-43), significantly prior to onset of easily observed symptoms. Inclusions were found in the cortex, striatum, cerebellum, spinal cord, and hippocampus, and progressively increase in prevalence and size (4,42). Despite this, chimera studies suggest that medium spiny neurons (MSNs) bearing large inclusions can survive for almost a year (30,44) when

surrounded by wild type cells. R6/2 MSN dendritic diameters and spine density also decrease with age (10,31,45).

R6/1 mice share most of the R6/2 pathology, but at a later age. NII's appear by 9 weeks (32,46) and also show minimal gliosis (33,47) and similar dendritic spine atrophy by 8 months (34,48). Apoptotic and necrotic cells are rarely seen in the striatum of R6/2 and R6/1 mice, despite significant atrophy and ventricular enlargement; instead, electron micrographs contain so called dark neurons, displaying condensation of the cytoplasm and nucleus without the chromatin fragmentation and nuclear blebbing characteristic of apoptosis (11,32,35,47). In contrast, 3 month old N171-82Q mice do demonstrate cortical and striatal apoptotic neurons, with reactive gliosis by 4 months. Note that in old (22-30 week) R6/2 chimeras, gliosis is apparent in regions densely populated in transgenic neurons (44), and particularly old R6/2 animals (17 weeks) show astrocytes with processes enveloping degenerating neurons (49). Therefore, the signals necessary to develop gliosis in R6/2 mice may be present, but the mice may die before glial recruitment and activation. N171-82Q mice also presented with striatal degeneration and ventricular enlargement by 17 weeks (50) and NII's in many brain regions (cortex, hippocampus, cerebellum, and striatum among others) by late endstage of 6.5 months.

NII's are not seen until far after symptom onset in full-length transgenic HD lines. YAC128 mice display behavioral symptoms at 12 months, and striatal neuron loss of ~15% is seen by this time (10) along with increased intranuclear HTT staining of certain brain structures (51). However, NII's did not show up until 18 months of age, and only populated ~30% of striatal neurons and ~5% of cortical neurons. NII's were absent in

the YAC128 hippocampus, a site of NII staining in endstage R6/2's (43). In the other distinct full-length transgenic strain, BACHD mice also display atrophy of the cortex and striatum by as much as 30% at 12 months (8), with 14% of striatal neurons with the aforementioned "dark" morphology. Interestingly and as opposed to R6 mice, inclusions (over 90%) were extranuclear and were more common in the cortex than striatum, a feature reminiscent of adult onset HD.

R6/2 chimaeras suggest that inclusions themselves may be neither toxic nor markers of cells about to die, and a strain arising with a spontaneous mutation in the YAC128 transgene (termed Shortstop or Ss for its early termination) provides further evidence to this end (52). The mutation truncated the transgene after exon 2, providing a product with 128 glutamines and an expected and observed protein size similar to that encoded by the R6/2 transgene. NII's are particularly common (90% of striatal, cortical, and hippocampal cells) and appear earlier in Ss mice versus YAC128s; however, Ss mice had no obvious phenotype at all ages examined. Why this strain is free from the early onset behavioral symptoms one would expect in what is essentially an N-terminal transgene HD model is still under investigation, but as explained in Chapter 1, it may represent a unique kinetic balance favoring aggregation over toxic oligomer formation.

Knockin mouse neuropathology, as with their symptoms, usually occurs very late in life and is minor in comparison to transgenic strains. HdhQ72-80 mice demonstrate loss of brain weight by 16 months (15), while NII's are primarily seen in striatal MSNs. Knockins with 94 repeats demonstrate striatal NII's by 18 months (53) while HdhQ111 mice show NII appearance at an earlier age (10 months), and mHtt nuclear accumulation is evident at a very early (6 weeks) age (54). HdhQ150 knockins lose as

much as 40% of striatal volume and neurons by 23 months, but significant gliosis and NII's appear by 10-14 months (11,13,47,55). Degenerating neurons are not apoptotic in this strain, though occasional dark neurons are encountered. Knockin mice with 140 CAG repeats display relatively early onset striatal NII's and neuropil aggregates (4 months) becoming progressively stronger in other brain regions as well by 6 months (14). These data do not imply that knockin brains only present with abnormality in old age, as HdhQ111 embryos demonstrate impaired neurogenesis as early as embryonic day 13.5 (56).

As discussed in Chapter 1, inclusions are a historic histological hallmark of HD, though evidence continues to mount that their presence does not correlate with toxicity, as seen in chimaeric R6/2 or in Ss mice. Nevertheless, compounds that reduce levels of mHTT consistently reduce visible aggregates, so quantifying their presence in treated versus untreated samples continues to be a common assay for such approaches. While useful and relevant in certain settings, this approach (documenting a reduction in aggregate appearance) cannot be directly correlated to a reversal of toxicity.

Cell Autonomous vs. Non-autonomous Pathology

Neurodegeneration in HD affects multiple brain regions, but striatal degeneration has been the focus of much of the research field, for two reasons: the massive loss of neurons suggests a particular vulnerability of striatal MSN's, and more specifically, the characteristic motor phenotype is classically attributed to the early loss of one of two nearly identical arms of the corticostriatal loop, the indirect (striatopalladial) pathway. Nevertheless, recent research suggests that multiple cell types in the brain contribute to

pathology. Driving an expanded poly(CAG) *HTT* fragment in glial (GFAP+) cells also induces many features in common with other mouse models of HD (clasping, failure to keep on weight, rotarod phenotype, and premature death), albiet at a later time than is common for models expressing N-terminal transgenes in neurons (57). This is interesting when one considers the stark phenotype of the N171-82Q mice, whose N-terminal transgene is driven primarily in neurons by the prion promoter (4). However, a conditional model of HD suggests that expression of mutant *HTT* in multiple cell types is required for motor symptoms. A lox-STOP-lox poly(CAG) *HTT* exon 1 strain mated to Nestin-Cre mice (pan-neuronal expression) induced a behavioral phenotype at 6 months of age, but mating it to Emx1-Cre (cortical pyramidal cell expression) (58) or Dlx5/6-Cre mice (striatal MSN expression) produced EM48+ aggregates in the expected brain regions but no observed motor phenotype; the animal's short lifespan may limit phenotypic progression in these models. Taken as a whole, we can see that *mHTT* can cause neuropathology (aggregate formation at the least) in nearly every neuronal or glial cell in which it is expressed, and while MSN expression plays a large role, cells other than MSNs can contribute to manifest disease in mice. This has particular importance from a therapeutic perspective, as it suggests that drugs which by default cannot affect neurons (e.g. the target enzyme is not expressed in neurons) should not a priori be set aside.

Specific Excitotoxicity Responses in Various Models

The cellular and molecular causes of excitotoxicity (glutamate receptor hyperactivation with resulting Ca^{2+}-mediated mitochondrial toxicity, normally induced by

NMDA-receptor ligand analogs quinolinic acid or kainic acid) were discussed at length in Chapter 1, but many of the HD model mice react quite differently to the insult. R6/1 and R6/2 mice injected presymptomatically (18 weeks and 6 weeks, respectively) displayed marked resistance to excitotoxic lesions compared to wild type littermates (59); this resistance was progressive with age. N171-82Q mice displayed resistance to intrastriatal quinolinic acid (QA) administered at 15 weeks (60), and asymptomatic shortstop mice are also QA resistant (52), but this phenotype is not ubiquitous among the N-terminal transgene strains. Older R6 mice have five-fold higher basal levels of Ca^{2+}, suggesting that resistance might be the result of compensatory mechanisms (61). Modest protection from mHTT is observed upon decortication or administration of glutamate release inhibitors, glutamate transporter upregulators, mGluR5 antagonists, and mGluR2/3 agonists (62-65). YAC mice display early QA sensitivity but a progressive loss of sensitivity, becoming resistance to QA in 10 month YAC128 mice (66).

While the above studies document changes in excitotoxicity resistance as molecular pathology sets in, it should be noted that different strains of mice demonstrate different basal susceptibilities to kainic acid (KA) or QA (61,67). Furthermore, F1 hybrids demonstrate different inheritance of susceptibility depending on the tissue. This tells us that vulnerability to these toxins is mHTT expression, age, and also strain dependent. Most interestingly, though, it also suggests that excitotoxicity vulnerability may be altered based on natural genetic variants, which could plausibly contribute to some of the residual age of onset variance in HD patients after accounting for CAG repeat size.

In at least four HD mouse models, there is consistent resistance to excitotoxic

stress, either pre-symptomatic (R6/1, R6/2, and N171-82Q) or after symptom onset (YAC128). The nature of the resistance phenotype is still under investigation, but as laid out in Chapter 1, may be mediated by compensatory adjustments to higher basal Ca^{2+} levels (61) and could be aided by observed decreases in dendritic spine density and length (45,48). Despite compensatory pathways, even the loss of normal glutamatergic afferents increases neuronal survival, suggesting that despite tolerance to acute excitotoxic insult, corticostriatal glutamate signaling still contributes to neuropathology in HD.

Murine Mitochondria and Energy Imbalance

As discussed in Chapter 1, neurons are sensitive to perturbations of mitochondrial activity (such as the succinate dehydrogenase inhibitor 3-NP) (68), particularly striatal MSNs. Reducing oxidative damage helps, as the toxicity of 3-NP in rats is significantly ameliorated by dietary creatine supplements (69), a compound that also improved survival, rotarod latency, weight, and neuronal atrophy in R6/2 (70) and N171-82Q mice (71) in the absence of an exogenous mitochondrial poison. In addition, studies of HD mouse model mitochondria demonstrate resistance to Ca^{2+}. R6/2, HdhQ92 and HdhQ111 striatal mitochondria become progressively desensitized to Ca^{2+} depolarization over time by 3, 12, and 3 months of age, respectively (72). Total forebrain mitochondria also show increase in Ca^{2+} buffering capacity in 12 week R6/2 and 12 month YAC128 mice prior to permeabilization, though no difference was seen in 16 week HdhQ150 mice (73), at an age when subtle gait abnormalities are visible (13). These observations may be indicative of progressive compensation to heightened basal

Ca^{2+} levels in aged HD mouse striatal neurons, perhaps explaining QA resistance. In all, mitochondria from mouse models of HD consistently demonstrate attempts to compensate for basal Ca^{2+} perturbations, a well-established neurotoxic byproduct of mHTT.

Electrophysiology

Many motor and behavioral symptoms in HD arise from the massive loss of MSNs, and the motor symptoms that acute 3-NP and QA toxicity produce are reminiscent of advanced Huntington's Disease. However, many mouse models of HD demonstrate almost no neuronal death. That neurons can be intact but still clearly malfunctioning, combined with the cognitive and memory deficits seen in most patients, suggest that synaptic abnormalities may be significant in HD pathology.

Disturbances in long term potentiation (LTP) and long term depression (LTD) are presented as evidence of a synaptic plasticity dysfunction, and such abnormal responses to LTP and LTD are seen in almost all mouse HD models. Such defects are seen in R6/1, R6/2, and HdhQ140 mice, which are known to display obvious motor symptoms (74-77), but are also seen in several full length transgenic and knockin mice with shorter alleles that display only subtle behavioral phenotypes (9,75,78). LTP or LTD deficits have not been reported in BACHD mice, but reduction in high amplitude miniature excitatory postsynaptic currents (a measure of steady state synaptic activity) of MSNs at 6 months (8), as well as cortical synaptic alterations at the same age (79) demonstrate some corticostriatal circuitry impairment in this strain as well. As impaired performance at cognitive tasks such as the Morris water maze or T maze is seen in

R6/2s (36) and YAC128 (31) animals, as well as somatosensory associative memory problems in R6/1s (80), the LTP and LTD impairments likely represent behaviorally relevant plasticity deficits. Because these phenotypes exist in mice that recapitulate many HD pathologic features but without massive neuronal loss, these studies suggest that defects within existing neuronal circuits contribute to early behavioral symptoms.

CAG Expansion

The CAG repeats within human HD and mouse HD models are prone to mutation, both in the germline and in somatic tissue. Germline expansions are more common in males (81), correlating with baseline mutant repeat length, and are thought to occur during mitosis, based on the very high percentage of sperm found with mutated alleles (averaging over 80%) in HD patient samples (82).

R6/2 mice are notoriously prone to intergenerational CAG repeat expansion (83). This has prompted many labs studying this strain to adopt a selective breeding strategy using only breeders with the desired number of repeats. R6/1 mice are almost as prone to expansions as R6/2s (84), but contractions are also seen, notably an R6/1 substrain with 89 CAG repeats that demonstrates a later onset of neuropathology and motor symptoms than standard R6/1s (85). Interestingly, in spite of the fact that CAG repeat length is the strongest correlate for age of onset in HD, R6/2 substrains carrying anywhere from 150 to over 400 repeats have demonstrated that in this transgene and background, higher CAG lengths strongly correlate with a later age of onset (83), perhaps due to changes in mHTT subcellular localization. Knockin mice also demonstrate intergenerational CAG repeat length instability, with more mutations seen

in mice with higher repeat lengths (HdhQ92, HdhQ111) and higher rates in males (15,16,86). I am not aware of germline instability in YAC HD model mice, but BACHD mice do not expand due to the alternating CAA-CAG repeats of the transgene (8).

Somatic poly(CAG) instability is also observed in most HD model mice; that BACHD mice display symptoms despite the absence of CAG instability demonstrates that somatic expansions are not required for neuropathology. However, knockins (HdhQ111) lacking DNA mismatch repair enzyme Msh2 have delayed intranuclear mHtt accumulation with absence of somatic CAG repeat expansion (87). *Msh2* knockout R6/1 mice also lacked somatic expansion (88). HdhQ72-80 knockins also display prominent striatal, cortical and cerebellar expansions, and HdhQ150 animals show somatic expansions as early as at 4 months of age (89,90).

The phenotype of BACHD mice clearly demonstrates that somatic CAG expansion is unlikely to be a major driving force in early disease onset. A possible propensity to cancer that could arise from reducing the activity of mismatch repair proteins also demands caution in exploring this specific pathway for HD therapy. Nevertheless, the mouse *Msh2* ablation studies and correlation of expansions to patient samples demonstrate that somatic expansion may contribute to HD.

Transcriptional Dysregulation: Striking Similarities Among Models

Abnormal interactions between mHTT and transcription factors may play a prominent role in neuropathology, and as they are expected to be quite pleiotropic, it suggests both an intriguing explanation for the wide-ranging systems disrupted in HD neurons as well as a promising target for therapy. The reduction of neurotransmitter

receptors in the HD striatum (91-93) is one of the earliest observed symptoms, and mHTT is known to interact with or sequester numerous transcription factors (94-98). The advent of more advanced transcriptional profiling in the last 10 years along with a bevy of mouse models of HD have provided ample opportunity for assaying this dysregulation and attempting therapies.

Microarray transcriptional profiles were compiled for R6/2 mice both before (6 weeks) and after (12 weeks) onset of overt motor symptoms. ~1.5% of transcripts displayed altered levels at each age, with a majority (75%) displaying decreased expression (99). Many of these transcriptional changes were verified in N171-82Q mice, though they were not shared by YAC72 mice (100). Further analysis from this group demonstrated that 12 week old R6/2, 16 week old N171-82Q, and 12 month old animals modeling DRPLA (a disorder resulting from polyglutamine expansion in the Atrophin-1 gene) all show significant overlap of cerebellar profiles (23). That cerebellar tissue and also laser-capture microdissected interneurons (101) of R6/2 mice demonstrate transcriptional dysregulation suggest that this phenomenon is not unique to the cells most vulnerable to degeneration, nor are inclusion-bearing cells more prone to transcriptionally-altered neurotransmitter receptor levels (102). What has been particularly striking is the significant similarities in transcriptional profiles of most genetic HD mouse models tested, both among each other and with human HD. Simultaneous profiling of R6/1, R6/2, HdhQ150, HdhQ92, and YAC128 mice demonstrated that every model correlated significantly with every other model and with human HD, with the caveat that the strains had to be aged appropriately (22). Other studies have reached similar conclusions (3,26).

Given that the global transcriptional changes are more commonly downregulations than upregulations in HD model mice (99), and that there are altered chromatin dynamics associated with repressed transcription (increased histone methylation, decreased acetylation) (103), it has been investigated whether general modifications to histone dynamics in the form of histone deacetylase (HDAC) modulation could be therapeutic. Suberoylanilide hydroxamic acid (SAHA) and sodium butyrate, two HDAC inhibitors, both caused a delay in motor symptom onset in R6/2 animals, though SAHA was toxic. (104,105). HDAC inhibitors 4b and valproate alleviated locomotor deficits in R6/2 and N171-82Q mice, respectively (106,107). N171-82Q mice demonstrated marked improvement in lifespan, striatal atrophy, and histone methylation:acetylation ratio upon administration of HDAC inhibitor phenylbutyrate after symptom onset, an important result for a disease in which not every carrier chooses to know their gene status and may only initiate treatment after overt symptoms are detected (50). In order to limit the off target effects of a general HDAC inhibitor, drugs with tighter specificity are needed as well as more focused targets. Recently, R6/2 mice have been bred to strains carrying either homozygous (if not lethal) or heterozygous deletions in HDACs to parse out which HDACs are the best modifiers of pathology. So far *Hdac7* has been discounted as a potential modifier (108), but *Hdac4* does show some promise (Gillian Bates, personal communication).

The similarity in transcriptional profiles between many aged HD model mice and patient samples suggests a fundamental consequence of mHTT on basal levels of transcription, either by direct interaction with transcription factors, attempts at compensatory changes, or both. That this phenotype is directly quantifiable in mice and

correlates so strongly with patient samples supports its utility as a biological measure for pathology.

From Preclinical to Clinical Treatment of HD

Candidate based approaches and success in mouse models have resulted in many drug trials progressing from preclinical mouse work to patients. Two excellent reviews (109,110) enumerate the trials conducted in the R6 lines, and Mestre et al. (111) provide a detailed summary and discussion of published HD clinical trials. Of those treatments tested in rodents, many have made it to clinical trials; nine trials passing the Mestre et al. criteria (randomized, placebo-controlled, symptomatic therapy with at least 10 participants), plus the combination remacemide / Coenzyme Q10 trials, are listed in Table 3. The majority of these selected clinical trials were aimed at safety and tolerability, rather than efficacy, so it comes as little surprise that no improvement in clinical outcome was seen for most. However, to date, only tetrabenazine (TBZ) has demonstrated a reduction of motor symptoms in both mice and patients (112-114), and though the mouse studies showed a reduction in striatal atrophy and motor symptoms, reduced neurodegeneration has not been documented in human patients on TBZ. Mice have also served as a proving ground for more cutting-edge therapeutic strategies like gene and oligonucleotide therapies (discussed earlier in the chapter). None have made it to clinical trial in HD patients, so evaluation of the HD mouse models' predictive value cannot be made.

Summary

The commonplace clinical failure of drugs that appear to benefit murine models makes clear the need for refinements in the measurements of pathology in these mice. In the last few years, imaging modalities such as MRI have been minaturized for use in HD model mice (115,116), and show promise. Nevertheless, it may be that behavioral alterations and volumetric imaging in mice have only limited correspondence, and better predictive value could require measuring phenotypes at a cellular level, representing the earliest stages in pathology. One such well-studied phenotype, present early in pathology in mouse models and patients and with unparalleled similarity between patients and mice, is transcriptional dysregulation of neurotransmitter receptors. Hence, for my graduate studies, I chose to address the need for efficient evaluation of candidate therapeutic efficacy in mouse models of HD by first exploring this well established phenotype (transcriptional dysregulation of the gene *Drd2*) in many mouse models, then developing a technique for rapid and highly accurate analysis of the progression of this phenotype, and finally demonstrating the ability to both induce and correct this phenotype using viral vector-delivered constructs, singly and in pools.

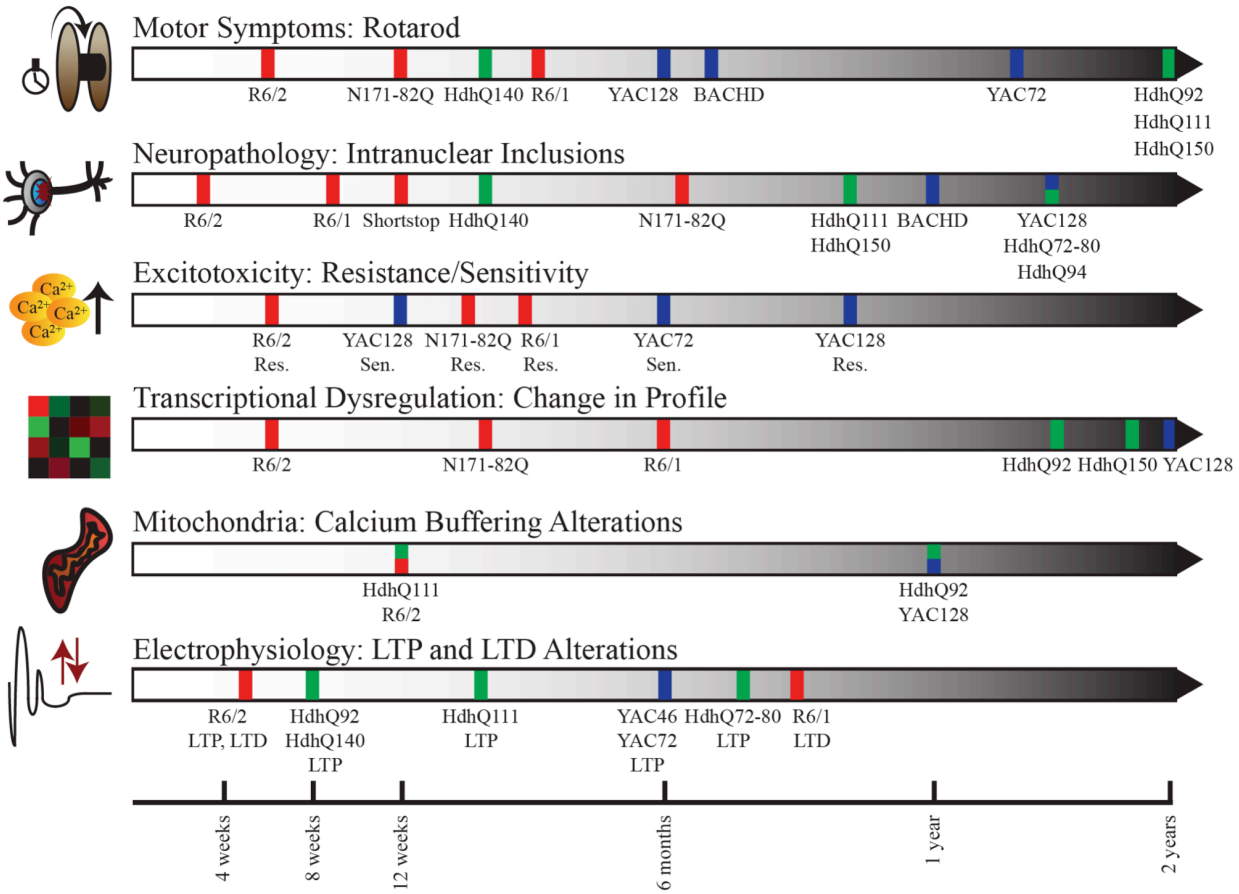

Figure 1. Timeline of behavioral and neuropathological symptoms in selected HD model mice. Strains are categorized by color: red indicates N-terminal transgenic, blue indicates full-length transgenic, and green indicates knockin. Approximate age of onset is given by the scale at the bottom.

Strain Name	Category	Gene Characteristics	Promoter	CAG size	Motor onset	Lifespan	Background Strain(s)	References
R6/2	Tg NTF	Exon 1 of human HTT gene	1 kb of Human HTT	~150	6 wks	10-13 wks	C57BL/6xCBA	Mangiarini et al., 1996 , Carter et al., 1999
R6/1	Tg NTF	Exon 1 of human HTT gene	1 kb of Human HTT	116	18 wks	32-40 wks	C57BL/6xCBA or C57BL/6	Mangiarini et al., 1996 , Hodges et al., 2008
N171-82Q	Tg NTF	First 171 AA of human HTT (exons 1, 2, part of 30	Prnp	82	3 mo	16-22 wks	C57BL/6xC3H/He	Schilling et al., 1999 , Schilling et al., 2004
Tg100	Tg NTF	First ~3 kb of human HTT cDNA	Rat NSE	100	3 mo (nonspecific)	Normal	C57BL/6xSJL	Laforet et al., 2001
HD94	Tg NTF	Chimeric human/mouse HTT exon 1	TetO + tTA	94	4-8 wks (clasping)	Normal	C57BL/6xCBA	Yamamoto et al., 2000
YAC72	Tg FL	Full length human HTT gene	Human HTT	72	16 mo	Normal	FVB/N	Hodgson et al., 1999 , Seo et al., 2008
YAC128	Tg FL	Full length human HTT gene	Human HTT	120	6 mo	Normal	FVB/N	Slow et al., 2003
BACHD	Tg FL	Full length human HTT gene (floxed exon 1)	Human HTT	97 (Mixed)	2 mo	Normal	FVB/N	Gray et al., 2008
HdhQ72,Q80	KI	Endogenous murine Htt gene, expanded CAG inserted	Mouse Htt	72,80	12 mo	Normal	Mixed 129Sv, C57BL/6	Shelbourne et al., 1999 , Kennedy et al., 2003
HdhQ111	KI	Endogenous murine Htt gene, chimeric human/mouse exon 1	Mouse Htt	109	24 mo (gait)	Normal	Mixed 129Sv, CD1	Wheeler et al., 1999 , Wheeler et al., 2002
HdhQ94	KI	Endogenous murine Htt gene, chimeric human/mouse exon 1	Mouse Htt	94	2 mo (rearing)	Normal	Mixed 129Sv, C57BL/6	Levine et al., 1999 , Menalled et al., 2002
HdhQ140	KI	Endogenous murine Htt gene, chimeric human/mouse exon 1	Mouse Htt	140	12 mo (gait)	Normal	Mixed 129Sv, C57BL/6	Menalled et al., 2003
HdhQ150	KI	Endogenous murine Htt gene, expanded CAG inserted	Mouse Htt	150	100 wks	Normal	Mixed 129Ola, C57BL/6	Lin et al., 2001 , Heng et al., 2007

Table 1: Commonly used mouse models of HD. Tg NTF = Transgenic N-terminal fragment of human *mHTT*; Tg FL = Transgenic full-length human *mHTT*; KI = Knockin.

Drug	Animal model	Animal dosage	Animal duration	Animal effect
Cannabidiol	3-NP Rat	5 mg/kg daily	From 12 weeks for 5 days	*
Creatine	R6/2	2% in chow ad lib	From 21 days	18% improved survival
Ethyl-EPA	YAC128	1% in chow ad lib	From 7 months	44% improved rotarod
Fluoxetine	R6/1	20 mg/kg daily	10 to 20 weeks	#
L-carnitine	N171-82Q	250 mg/kg, 5x/week	From 6 weeks	15% improved survival
Minocycline	R6/2	5 mg/kg daily	From 6 weeks	13% improved survival
Remacemide	R6/2	0.007% in chow ad lib	From 21 days	16% improved survival
Remacemide + CoQ10	R6/2	0.007% Rem, 0.2% CoQ10 in chow ad lib	From 21 days	32% improved survival
Riluzole	R6/2	10 mg/kg daily	From 21 days	10% improved survival
Tetrabenazine	YAC128	5 mg/kg, 3x/week	From 2 months	~60% improved rotarod

Drug	Patient dosage	Patient duration	Patient effect	References
Cannabidiol	10 mg/kg daily	6 weeks drug, 15 weeks obs.	n.s.	Sagredo et al., 2007 , Consroe et al., 1991
Creatine	8 g daily	16 weeks drug, 24 weeks obs.	n.s.	Ferrante et al., 2000 , Hersch et al., 2006
Ethyl-EPA	2 g daily	6 or 12 months drug	n.s.	Van Raamsdonk et al., 2005 b, TREND-HD, 2008
Fluoxetine	20 mg daily	4 months drug	n.s.	Grote et al., 2005 , Como et al., 1997
L-carnitine	45 mg/kg daily	1 week drug, 4 weeks obs.	n.s.	Vamos et al., 2010 , Goetz et al., 1990
Minocycline	200 mg daily	8 weeks drug	n.s.	Chen et al., 2000 , The Huntington Study Group 2004
Remacemide	200 or 600 mg daily	6 weeks drug	n.s.	Ferrante et al., 2002 , Kieburtz et al., 1996
Remacemide + CoQ10	600 mg each daily	30 months drug	n.s.	Ferrante et al., 2002 , The Huntington Study Group, 2001
Riluzole	200 mg daily	8 weeks drug	n.s.	Schiefer 2002 , The Huntington Study Group, 2003
Tetrabenazine	Up to 100 mg daily	12 weeks drug	3.5 UHDRS units improvement	Wang et al., 2010 , The Huntington Study Group 2006

* No behavior tested; reduced striatal lesion size and some transcript reduction

n.s. on rotarod; protected against degeneration in dentate gyrus

Table 2. Selection of Drugs Tested in Both HD Model Mice and in Clinical Trials with HD Patients

Bibliography

1. Mangiarini L, Sathasivam K, Seller M, Cozens B, Harper A, Hetherington C, et al. Exon 1 of the HD gene with an expanded CAG repeat is sufficient to cause a progressive neurological phenotype in transgenic mice. Cell. 1996 Nov 1;87(3):493–506.

2. Carter RJ, Lione LA, Humby T, Mangiarini L, Mahal A, Bates GP, et al. Characterization of progressive motor deficits in mice transgenic for the human Huntington's disease mutation. J Neurosci. 1999 Apr 15;19(8):3248–57.

3. Hodges A, Hughes G, Brooks S, Elliston L, Holmans P, Dunnett SB, et al. Brain gene expression correlates with changes in behavior in the R6/1 mouse model of Huntington's disease. Genes Brain Behav. 2008 Apr 1;7(3):288–99.

4. Schilling G, Becher MW, Sharp AH, Jinnah HA, Duan K, Kotzuk JA, et al. Intranuclear inclusions and neuritic aggregates in transgenic mice expressing a mutant N-terminal fragment of huntingtin. Hum Mol Genet. 1999 Mar 1;8(3):397–407.

5. Schilling G, Savonenko AV, Coonfield ML, Morton JL, Vorovich E, Gale A, et al. Environmental, pharmacological, and genetic modulation of the HD phenotype in transgenic mice. Experimental Neurology. 2004 May;187(1):137–49.

6. Graham RK, Deng Y, Slow EJ, Haigh B, Bissada N, Lu G, et al. Cleavage at the caspase-6 site is required for neuronal dysfunction and degeneration due to mutant huntingtin. Cell. 2006 Jun 16;125(6):1179–91.

7. Li S-H, Lam S, Cheng AL, Li X-J. Intranuclear huntingtin increases the expression of caspase-1 and induces apoptosis. Hum Mol Genet. 2000 Nov 22;9(19):2859–67.

8. Gray M, Shirasaki DI, Cepeda C, André VM, Wilburn B, Lu X-H, et al. Full-length human mutant huntingtin with a stable polyglutamine repeat can elicit progressive and selective neuropathogenesis in BACHD mice. J Neurosci. 2008 Jun 11;28(24):6182–95.

9. Hodgson JG, Agopyan N, Gutekunst CA, Leavitt BR, LePiane F, Singaraja R, et al. A YAC mouse model for Huntington's disease with full-length mutant huntingtin, cytoplasmic toxicity, and selective striatal neurodegeneration. Neuron. 1999 May 1;23(1):181–92.

10. Slow EJ. Selective striatal neuronal loss in a YAC128 mouse model of Huntington disease. Hum Mol Genet. 2003 Jul 1;12(13):1555–67.

11. Heng MY, Tallaksen-Greene SJ, Detloff PJ, Albin RL. Longitudinal Evaluation of the Hdh(CAG)150 Knock-In Murine Model of Huntington's Disease. J Neurosci. 2007 Aug 22;27(34):8989–98.

12. Levine MS, Klapstein GJ, Koppel A, Gruen E, Cepeda C, Vargas ME, et al. Enhanced sensitivity to N-methyl-D-aspartate receptor activation in transgenic and knockin mouse models of Huntington's disease. J Neurosci Res. 1999 Nov 15;58(4):515–32.

13. Lin CH, Tallaksen-Greene S, Chien WM, Cearley JA, Jackson WS, Crouse AB, et al. Neurological abnormalities in a knock-in mouse model of Huntington's disease. Hum Mol Genet. 2001 Jan 15;10(2):137–44.

14. Menalled LB, Sison JD, Dragatsis I, Zeitlin S, Chesselet M-F. Time course of early motor and neuropathological anomalies in a knock-in mouse model of Huntington's disease with 140 CAG repeats. J. Comp. Neurol. 2003 Oct 6;465(1):11–26.

15. Shelbourne PF, Killeen N, Hevner RF, Johnston HM, Tecott L, Lewandoski M, et al. A Huntington's disease CAG expansion at the murine Hdh locus is unstable and associated with behavioural abnormalities in mice. Hum Mol Genet. 1999 May 1;8(5):763–74.

16. Wheeler VC, Auerbach W, White JK, Srinidhi J, Auerbach A, Ryan A, et al. Length-dependent gametic CAG repeat instability in the Huntington's disease knock-in mouse. Hum Mol Genet. 1999 Jan;8(1):115–22.

17. Wheeler VC, Gutekunst C-A, Vrbanac V, Lebel L-A, Schilling G, Hersch S, et al. Early phenotypes that presage late-onset neurodegenerative disease allow testing of modifiers in Hdh CAG knock-in mice. Hum Mol Genet. 2002 Mar 15;11(6):633–40.

18. Bennett EJ, Shaler TA, Woodman B, Ryu K-Y, Zaitseva TS, Becker CH, et al. Global changes to the ubiquitin system in Huntington's disease. Nature. 2007 Aug 9;448(7154):704–8.

19. Björkqvist M, Wild EJ, Thiele J, Silvestroni A, Andre R, Lahiri N, et al. A novel pathogenic pathway of immune activation detectable before clinical onset in Huntington's disease. J Exp Med. 2008 Aug 4;205(8):1869–77.

20. Ginés S, Bosch M, Marco S, Gavaldà N, Díaz-Hernández M, Lucas JJ, et al. Reduced expression of the TrkB receptor in Huntington's disease mouse models and in human brain. Eur J Neurosci. 2006 Feb 1;23(3):649–58.

21. Jenkins BG, Andreassen OA, Dedeoglu A, Leavitt B, Hayden M, Borchelt D, et al. Effects of CAG repeat length, HTT protein length and protein context on cerebral metabolism measured using magnetic resonance spectroscopy in transgenic mouse models of Huntington's disease. J Neurochem. 2005 Oct 1;95(2):553–62.

22. Kuhn A, Goldstein DR, Hodges A, Strand AD, Sengstag T, Kooperberg C, et al. Mutant huntingtin“s effects on striatal gene expression in mice recapitulate

changes observed in human Huntington”s disease brain and do not differ with mutant huntingtin length or wild-type huntingtin dosage. Hum Mol Genet. 2007 May 20;16(15):1845–61.

23. Luthi-Carter R, Strand AD, Hanson SA, Kooperberg C, Schilling G, La Spada AR, et al. Polyglutamine and transcription: gene expression changes shared by DRPLA and Huntington's disease mouse models reveal context-independent effects. Hum Mol Genet. 2002 Aug 15;11(17):1927–37.

24. Menalled L, Zanjani H, MacKenzie L, Koppel A, Carpenter E, Zeitlin S, et al. Decrease in striatal enkephalin mRNA in mouse models of Huntington's disease. Experimental Neurology. 2000 Apr;162(2):328–42.

25. Southwell AL, Ko J, Patterson PH. Intrabody gene therapy ameliorates motor, cognitive, and neuropathological symptoms in multiple mouse models of Huntington's disease. J Neurosci. 2009 Oct 28;29(43):13589–602.

26. Strand AD, Baquet ZC, Aragaki AK, Holmans P, Yang L, Cleren C, et al. Expression profiling of Huntington's disease models suggests that brain-derived neurotrophic factor depletion plays a major role in striatal degeneration. J Neurosci. 2007 Oct 24;27(43):11758–68.

27. Walker AG, Miller BR, Fritsch JN, Barton SJ, Rebec GV. Altered information processing in the prefrontal cortex of Huntington's disease mouse models. J Neurosci. 2008 Sep 3;28(36):8973–82.

28. Woodman B, Butler R, Landles C, Lupton MK, Tse J, Hockly E, et al. The Hdh(Q150/Q150) knock-in mouse model of HD and the R6/2 exon 1 model develop comparable and widespread molecular phenotypes. Brain Res Bull. 2007 Apr 30;72(2-3):83–97.

29. van Dellen A, Blakemore C, Deacon R, York D, Hannan AJ. Delaying the onset of Huntington's in mice. Nature. 2000 Apr 13;404(6779):721–2.

30. Seo H, Kim W, Isacson O. Compensatory changes in the ubiquitin-proteasome system, brain-derived neurotrophic factor and mitochondrial complex II/III in YAC72 and R6/2 transgenic mice partially model Huntington's disease patients. Hum Mol Genet. 2008 Oct 15;17(20):3144–53.

31. van Raamsdonk JM, Pearson J, Slow EJ, Hossain SM, Leavitt BR, Hayden MR. Cognitive dysfunction precedes neuropathology and motor abnormalities in the YAC128 mouse model of Huntington's disease. J Neurosci. 2005 Apr 20;25(16):4169–80.

32. Menalled L, El-Khodor BF, Patry M, Suárez-Fariñas M, Orenstein SJ, Zahasky B, et al. Systematic behavioral evaluation of Huntington's disease transgenic and knock-in mouse models. Neurobiology of Disease. 2009 Sep;35(3):319–36.

33. Hickey MA, Kosmalska A, Enayati J, Cohen R, Zeitlin S, Levine MS, et al. Extensive early motor and non-motor behavioral deficits are followed by striatal neuronal loss in knock-in Huntington's disease mice. NSC. 2008 Nov 11;157(1):280–95.

34. Dorner JL, Miller BR, Barton SJ, Brock TJ, Rebec GV. Sex differences in behavior and striatal ascorbate release in the 140 CAG knock-in mouse model of Huntington's disease. Behav Brain Res. 2007 Mar 12;178(1):90–7.

35. Trueman RC, Brooks SP, Jones L, Dunnett SB. Rule learning, visuospatial function and motor performance in the Hdh(Q92) knock-in mouse model of Huntington's disease. Behav Brain Res. 2009 Nov 5;203(2):215–22.

36. Lione LA, Carter RJ, Hunt MJ, Bates GP, Morton AJ, Dunnett SB. Selective discrimination learning impairments in mice expressing the human Huntington's disease mutation. J Neurosci. 1999 Dec 1;19(23):10428–37.

37. Sharp AH, Ross CA. Neurobiology of Huntington's disease. Neurobiology of Disease. 1996 Feb;3(1):3–15.

38. Gourfinkel-An I, Cancel G, Duyckaerts C, Faucheux B, Hauw JJ, Trottier Y, et al. Neuronal distribution of intranuclear inclusions in Huntington's disease with adult onset. NeuroReport. 1998 Jun 1;9(8):1823–6.

39. Herndon ES, Hladik CL, Shang P, Burns DK, Raisanen J, White CL. Neuroanatomic profile of polyglutamine immunoreactivity in Huntington disease brains. J Neuropathol Exp Neurol. 2009 Mar 1;68(3):250–61.

40. Stack EC, Kubilus JK, Smith K, Cormier K, del Signore SJ, Guelin E, et al. Chronology of behavioral symptoms and neuropathological sequela in R6/2 Huntington's disease transgenic mice. J. Comp. Neurol. 2005 Oct 3;490(4):354–70.

41. Davies SW, Turmaine M, Cozens BA, DiFiglia M, Sharp AH, Ross CA, et al. Formation of neuronal intranuclear inclusions underlies the neurological dysfunction in mice transgenic for the HD mutation. Cell. 1997 Aug 8;90(3):537–48.

42. Meade CA, Deng Y-P, Fusco FR, del Mar N, Hersch S, Goldowitz D, et al. Cellular localization and development of neuronal intranuclear inclusions in striatal and cortical neurons in R6/2 transgenic mice. J. Comp. Neurol. 2002 Jul 29;449(3):241–69.

43. Morton AJ, Lagan MA, Skepper JN, Dunnett SB. Progressive formation of inclusions in the striatum and hippocampus of mice transgenic for the human Huntington's disease mutation. J Neurocytol. 2000 Sep 1;29(9):679–702.

44. Reiner A, del Mar N, Deng Y-P, Meade CA, Sun Z, Goldowitz D. R6/2 neurons

with intranuclear inclusions survive for prolonged periods in the brains of chimeric mice. J. Comp. Neurol. 2007 Dec 20;505(6):603–29.

45. Klapstein GJ, Fisher RS, Zanjani H, Cepeda C, Jokel ES, Chesselet M-F, et al. Electrophysiological and morphological changes in striatal spiny neurons in R6/2 Huntington's disease transgenic mice. J Neurophysiol. 2001 Dec;86(6):2667–77.

46. Naver B, Stub C, Møller M, Fenger K, Hansen AK, Hasholt L, et al. Molecular and behavioral analysis of the R6/1 Huntington's disease transgenic mouse. NSC. 2003 Jan 1;122(4):1049–57.

47. Yu Z-X, Li S-H, Evans J, Pillarisetti A, Li H, Li X-J. Mutant huntingtin causes context-dependent neurodegeneration in mice with Huntington's disease. J Neurosci. 2003 Mar 15;23(6):2193–202.

48. Spires TL, Grote HE, Garry S, Cordery PM, van Dellen A, Blakemore C, et al. Dendritic spine pathology and deficits in experience-dependent dendritic plasticity in R6/1 Huntington's disease transgenic mice. Eur J Neurosci. 2004 May 1;19(10):2799–807.

49. Turmaine M, Raza A, Mahal A, Mangiarini L, Bates GP, Davies SW. Nonapoptotic neurodegeneration in a transgenic mouse model of Huntington's disease. Proc Natl Acad Sci USA. 2000 Jul 5;97(14):8093–7.

50. Gardian G, Browne SE, Choi D-K, Klivenyi P, Gregorio J, Kubilus JK, et al. Neuroprotective effects of phenylbutyrate in the N171-82Q transgenic mouse model of Huntington's disease. J Biol Chem. 2005 Jan 7;280(1):556–63.

51. van Raamsdonk JM, Murphy Z, Slow EJ, Leavitt BR, Hayden MR. Selective degeneration and nuclear localization of mutant huntingtin in the YAC128 mouse model of Huntington disease. Hum Mol Genet. 2005 Dec 15;14(24):3823–35.

52. Slow EJ, Graham RK, Osmand AP, Devon RS, Lu G, Deng Y, et al. Absence of behavioral abnormalities and neurodegeneration in vivo despite widespread neuronal huntingtin inclusions. Proc Natl Acad Sci USA. 2005 Aug 9;102(32):11402–7.

53. Menalled LB, Sison JD, Wu Y, Olivieri M, Li X-J, Li H, et al. Early motor dysfunction and striosomal distribution of huntingtin microaggregates in Huntington's disease knock-in mice. J Neurosci. 2002 Sep 15;22(18):8266–76.

54. Wheeler VC, White JK, Gutekunst CA, Vrbanac V, Weaver M, Li X-J, et al. Long glutamine tracts cause nuclear localization of a novel form of huntingtin in medium spiny striatal neurons in HdhQ92 and HdhQ111 knock-in mice. Hum Mol Genet. 2000 Mar 1;9(4):503–13.

55. Tallaksen-Greene SJ, Crouse AB, Hunter JM, Detloff PJ, Albin RL. Neuronal intranuclear inclusions and neuropil aggregates in HdhCAG(150) knockin mice.

NSC. 2005 Jan 1;131(4):843–52.

56. Molero AE, Gokhan S, Gonzalez S, Feig JL, Alexandre LC, Mehler MF. Impairment of developmental stem cell-mediated striatal neurogenesis and pluripotency genes in a knock-in model of Huntington's disease. Proc Natl Acad Sci USA. 2009 Dec 22;106(51):21900–5.

57. Bradford J, Shin J-Y, Roberts M, Wang C-E, Li X-J, Li S. Expression of mutant huntingtin in mouse brain astrocytes causes age-dependent neurological symptoms. Proc Natl Acad Sci USA. 2009 Dec 29;106(52):22480–5.

58. Gu X, Li C, Wei W, Lo V, Gong S, Li S-H, et al. Pathological cell-cell interactions elicited by a neuropathogenic form of mutant Huntingtin contribute to cortical pathogenesis in HD mice. Neuron. 2005 May 5;46(3):433–44.

59. Hansson O, Petersén A, Leist M, Nicotera P, Castilho RF, Brundin P. Transgenic mice expressing a Huntington's disease mutation are resistant to quinolinic acid-induced striatal excitotoxicity. Proc Natl Acad Sci USA. 1999 Jul 20;96(15):8727–32.

60. Jarabek BR, Yasuda RP, Wolfe BB. Regulation of proteins affecting NMDA receptor-induced excitotoxicity in a Huntington's mouse model. Brain. 2004 Mar;127(Pt 3):505–16.

61. Hansson O, Guatteo E, Mercuri NB, Bernardi G, Li XJ, Castilho RF, et al. Resistance to NMDA toxicity correlates with appearance of nuclear inclusions, behavioural deficits and changes in calcium homeostasis in mice transgenic for exon 1 of the huntington gene. Eur J Neurosci. 2001 Nov 1;14(9):1492–504.

62. Miller BR, Dorner JL, Shou M, Sari Y, Barton SJ, Sengelaub DR, et al. Up-regulation of GLT1 expression increases glutamate uptake and attenuates the Huntington's disease phenotype in the R6/2 mouse. Neuroscience. 2008 Apr 22;153(1):329–37.

63. Schiefer J, Alberty A, Dose T, Oliva S, Noth J, Kosinski CM. Huntington's disease transgenic mice are resistant to global cerebral ischemia. Neurosci Lett. 2002 Dec 13;334(2):99–102.

64. Schiefer J, Sprünken A, Puls C, Lüesse H-G, Milkereit A, Milkereit E, et al. The metabotropic glutamate receptor 5 antagonist MPEP and the mGluR2 agonist LY379268 modify disease progression in a transgenic mouse model of Huntington's disease. Brain Res. 2004 Sep 3;1019(1-2):246–54.

65. Stack EC, Dedeoglu A, Smith KM, Cormier K, Kubilus JK, Bogdanov M, et al. Neuroprotective effects of synaptic modulation in Huntington's disease R6/2 mice. J Neurosci. 2007 Nov 21;27(47):12908–15.

66. Graham RK, Pouladi MA, Joshi P, Lu G, Deng Y, Wu N-P, et al. Differential

Susceptibility to Excitotoxic Stress in YAC128 Mouse Models of Huntington Disease between Initiation and Progression of Disease. J Neurosci. 2009 Feb 18;29(7):2193–204.

67. Mclin JP, Thompson LM, Steward O. Differential susceptibility to striatal neurodegeneration induced by quinolinic acid and kainate in inbred, outbred and hybrid mouse strains. Eur J Neurosci. 2006 Dec;24(11):3134–40.

68. Beal MF, Brouillet E, Jenkins BG, Ferrante RJ, Kowall NW, Miller JM, et al. Neurochemical and histologic characterization of striatal excitotoxic lesions produced by the mitochondrial toxin 3-nitropropionic acid. J Neurosci. 1993 Oct 1;13(10):4181–92.

69. Matthews RT, Yang L, Jenkins BG, Ferrante RJ, Rosen BR, Kaddurah-Daouk R, et al. Neuroprotective effects of creatine and cyclocreatine in animal models of Huntington's disease. J Neurosci. 1998 Jan 1;18(1):156–63.

70. Ferrante RJ, Andreassen OA, Jenkins BG, Dedeoglu A, Kuemmerle S, Kubilus JK, et al. Neuroprotective effects of creatine in a transgenic mouse model of Huntington's disease. J Neurosci. 2000 Jun 15;20(12):4389–97.

71. Andreassen OA, Dedeoglu A, Ferrante RJ, Jenkins BG, Ferrante KL, Thomas M, et al. Creatine increase survival and delays motor symptoms in a transgenic animal model of Huntington's disease. Neurobiology of Disease. 2001 Jun;8(3):479–91.

72. Brustovetsky N, LaFrance R, Purl KJ, Brustovetsky T, Keene CD, Low WC, et al. Age-dependent changes in the calcium sensitivity of striatal mitochondria in mouse models of Huntington's Disease. J Neurochem. 2005 Jun;93(6):1361–70.

73. Oliveira JMA, Jekabsons MB, Chen S, Lin A, Rego AC, Gonçalves J, et al. Mitochondrial dysfunction in Huntington's disease: the bioenergetics of isolated and in situ mitochondria from transgenic mice. J Neurochem. 2007 Apr 1;101(1):241–9.

74. Murphy KP, Carter RJ, Lione LA, Mangiarini L, Mahal A, Bates GP, et al. Abnormal synaptic plasticity and impaired spatial cognition in mice transgenic for exon 1 of the human Huntington's disease mutation. J Neurosci. 2000 Jul 1;20(13):5115–23.

75. Simmons DA, Rex CS, Palmer L, Pandyarajan V, Fedulov V, Gall CM, et al. Up-regulating BDNF with an ampakine rescues synaptic plasticity and memory in Huntington's disease knockin mice. Proc Natl Acad Sci USA. 2009 Mar 24;106(12):4906–11.

76. Cummings DM, Milnerwood AJ, Dallérac GM, Vatsavayai SC, Hirst MC, Murphy KPSJ. Abnormal cortical synaptic plasticity in a mouse model of Huntington's disease. Brain Res Bull. 2007 Apr 30;72(2-3):103–7.

77. Cummings DM, Milnerwood AJ, Dallérac GM, Waights V, Brown JY, Vatsavayai SC, et al. Aberrant cortical synaptic plasticity and dopaminergic dysfunction in a mouse model of Huntington's disease. Hum Mol Genet. 2006 Oct 1;15(19):2856–68.

78. Usdin MT, Shelbourne PF, Myers RM, Madison DV. Impaired synaptic plasticity in mice carrying the Huntington's disease mutation. Hum Mol Genet. 1999 May 1;8(5):839–46.

79. Spampanato J, Gu X, Yang XW, Mody I. Progressive synaptic pathology of motor cortical neurons in a BAC transgenic mouse model of Huntington's disease. NSC. 2008 Dec 2;157(3):606–20.

80. Cybulska-Klosowicz A, Mazarakis NK, van Dellen A, Blakemore C, Hannan AJ, Kossut M. Impaired learning-dependent cortical plasticity in Huntington's disease transgenic mice. Neurobiology of Disease. 2004 Dec 1;17(3):427–34.

81. Wheeler VC, Persichetti F, McNeil SM, Mysore JS, Mysore SS, MacDonald ME, et al. Factors associated with HD CAG repeat instability in Huntington disease. J Med Genet. 2007 Nov;44(11):695–701.

82. Leeflang EP, Tavaré S, Marjoram P, Neal CO, Srinidhi J, MacFarlane H, et al. Analysis of germline mutation spectra at the Huntington's disease locus supports a mitotic mutation mechanism. Hum Mol Genet. 1999 Feb 1;8(2):173–83.

83. Morton AJ, Glynn D, Leavens W, Zheng Z, Faull RLM, Skepper JN, et al. Paradoxical delay in the onset of disease caused by super-long CAG repeat expansions in R6/2 mice. Neurobiology of Disease. 2009 Mar 1;33(3):331–41.

84. Mangiarini L, Sathasivam K, Mahal A, Mott R, Seller M, Bates GP. Instability of highly expanded CAG repeats in mice transgenic for the Huntington's disease mutation. Nat Genet. 1997 Feb 1;15(2):197–200.

85. Vatsavayai SC, Dallérac GM, Milnerwood AJ, Cummings DM, Rezaie P, Murphy KPSJ, et al. Progressive CAG expansion in the brain of a novel R6/1-89Q mouse model of Huntington's disease with delayed phenotypic onset. Brain Res Bull. 2007 Apr 30;72(2-3):98–102.

86. Ishiguro H, Yamada K, Sawada H, Nishii K, Ichino N, Sawada M, et al. Age-dependent and tissue-specific CAG repeat instability occurs in mouse knock-in for a mutant Huntington's disease gene. J Neurosci Res. 2001 Aug 15;65(4):289–97.

87. Wheeler VC, Lebel L-A, Vrbanac V, Teed A, Riele te H, Macdonald ME. Mismatch repair gene Msh2 modifies the timing of early disease in Hdh(Q111) striatum. Hum Mol Genet. 2003 Feb 1;12(3):273–81.

88. Manley K, Shirley TL, Flaherty L, Messer A. Msh2 deficiency prevents in vivo

somatic instability of the CAG repeat in Huntington disease transgenic mice. Nat Genet. 1999 Dec;23(4):471–3.

89. Kennedy L, Evans E, Chen C-M, Craven L, Detloff PJ, Ennis M, et al. Dramatic tissue-specific mutation length increases are an early molecular event in Huntington disease pathogenesis. Hum Mol Genet. 2003 Dec 15;12(24):3359–67.

90. Kennedy L, Shelbourne PF. Dramatic mutation instability in HD mouse striatum: does polyglutamine load contribute to cell-specific vulnerability in Huntington's disease? Hum Mol Genet. 2000 Oct 12;9(17):2539–44.

91. Glass M, Dragunow M, Faull RL. The pattern of neurodegeneration in Huntington“s disease: a comparative study of cannabinoid, dopamine, adenosine and GABA(A) receptor alterations in the human basal ganglia in Huntington”s disease. NSC. 2000;97(3):505–19.

92. Pavese N. Progressive striatal and cortical dopamine receptor dysfunction in Huntington's disease: a PET study. Brain. 2003 May 1;126(5):1127–35.

93. Weeks RA, Piccini P, Harding AE, Brooks DJ. Striatal D1 and D2 dopamine receptor loss in asymptomatic mutation carriers of Huntington's disease. Ann Neurol. 1996 Jul 1;40(1):49–54.

94. Boutell JM, Thomas P, Neal JW, Weston VJ, Duce J, Harper PS, et al. Aberrant interactions of transcriptional repressor proteins with the Huntington's disease gene product, huntingtin. Hum Mol Genet. 1999 Sep 1;8(9):1647–55.

95. Dunah AW, Jeong H, Griffin A, Kim Y-M, Standaert DG, Hersch SM, et al. Sp1 and TAFII130 transcriptional activity disrupted in early Huntington's disease. Science. 2002 Jun 21;296(5576):2238–43.

96. Huang CC, Faber PW, Persichetti F, Mittal V, Vonsattel JP, MacDonald ME, et al. Amyloid formation by mutant huntingtin: threshold, progressivity and recruitment of normal polyglutamine proteins. Somat Cell Mol Genet. 1998 Jul 1;24(4):217–33.

97. Nucifora FC, Sasaki M, Peters MF, Huang H, Cooper JK, Yamada M, et al. Interference by huntingtin and atrophin-1 with cbp-mediated transcription leading to cellular toxicity. Science. 2001 Mar 23;291(5512):2423–8.

98. Steffan JS, Kazantsev A, Spasic-Boskovic O, Greenwald M, Zhu YZ, Gohler H, et al. The Huntington's disease protein interacts with p53 and CREB-binding protein and represses transcription. Proc Natl Acad Sci USA. 2000 Jun 6;97(12):6763–8.

99. Luthi-Carter R, Strand A, Peters NL, Solano SM, Hollingsworth ZR, Menon AS, et al. Decreased expression of striatal signaling genes in a mouse model of

Huntington's disease. Hum Mol Genet. 2000 May 22;9(9):1259–71.

100. Chan EYW, Luthi-Carter R, Strand A, Solano SM, Hanson SA, DeJohn MM, et al. Increased huntingtin protein length reduces the number of polyglutamine-induced gene expression changes in mouse models of Huntington's disease. Hum Mol Genet. 2002 Aug 15;11(17):1939–51.

101. Zucker B, Luthi-Carter R, Kama JA, Dunah AW, Stern EA, Fox JH, et al. Transcriptional dysregulation in striatal projection- and interneurons in a mouse model of Huntington's disease: neuronal selectivity and potential neuroprotective role of HAP1. Hum Mol Genet. 2005 Jan 15;14(2):179–89.

102. Sadri-Vakili G, Menon AS, Farrell LA, Keller-Mcgandy CE, Cantuti-Castelvetri I, Standaert DG, et al. Huntingtin inclusions do not down-regulate specific genes in the R6/2 Huntington's disease mouse. Eur J Neurosci. 2006 Jun;23(12):3171–5.

103. Stack EC, del Signore SJ, Luthi-Carter R, Soh BY, Goldstein DR, Matson S, et al. Modulation of nucleosome dynamics in Huntington's disease. Hum Mol Genet. 2007 May 15;16(10):1164–75.

104. Ferrante RJ, Kubilus JK, Lee J, Ryu H, Beesen A, Zucker B, et al. Histone deacetylase inhibition by sodium butyrate chemotherapy ameliorates the neurodegenerative phenotype in Huntington's disease mice. J Neurosci. 2003 Oct 15;23(28):9418–27.

105. Hockly E, Richon VM, Woodman B, Smith DL, Zhou X, Rosa E, et al. Suberoylanilide hydroxamic acid, a histone deacetylase inhibitor, ameliorates motor deficits in a mouse model of Huntington's disease. Proc Natl Acad Sci USA. 2003 Feb 18;100(4):2041–6.

106. Thomas EA, Coppola G, Desplats PA, Tang B, Soragni E, Burnett R, et al. The HDAC inhibitor 4b ameliorates the disease phenotype and transcriptional abnormalities in Huntington's disease transgenic mice. Proc Natl Acad Sci USA. 2008 Oct 7;105(40):15564–9.

107. Zádori D, Geisz A, Vámos E, Vécsei L, Klivenyi P. Valproate ameliorates the survival and the motor performance in a transgenic mouse model of Huntington's disease. Pharmacol Biochem Behav. 2009 Nov;94(1):148–53.

108. Benn CL, Butler R, Mariner L, Nixon J, Moffitt H, Mielcarek M, et al. Genetic knock-down of HDAC7 does not ameliorate disease pathogenesis in the R6/2 mouse model of Huntington's disease. PLoS ONE. 2009 Jan 1;4(6):e5747.

109. Li JY, Popovic N, Brundin P. The use of the R6 transgenic mouse models of Huntington's disease in attempts to develop novel therapeutic strategies. NeuroRx : the journal of the American Society for Experimental NeuroTherapeutics. 2005 Jul 1;2(3):447–64.

110. Gil JM, Rego AC. The R6 lines of transgenic mice: a model for screening new therapies for Huntington's disease. Brain research reviews. 2009 Mar;59(2):410–31.

111. Mestre T, Ferreira J, Coelho MM, Rosa MR, Sampaio C. Therapeutic interventions for symptomatic treatment in Huntington's disease. Cochrane Database Syst Rev. 2009 Jan 1;(3):CD006456–6.

112. Frank S. Tetrabenazine as anti-chorea therapy in Huntington disease: an open-label continuation study. Huntington Study Group/TETRA-HD Investigators. BMC Neurol. 2009 Jan 1;9:62.

113. Huntington Study Group. Tetrabenazine as antichorea therapy in Huntington disease: a randomized controlled trial. Neurology. 2006 Feb 14;66(3):366–72.

114. Wang H, Chen X, Li Y, Tang T-S, Bezprozvanny I. Tetrabenazine is neuroprotective in Huntington's disease mice. Mol Neurodegener. 2010 Jan 1;5:18.

115. Sawiak SJ, Wood NI, Williams GB, Morton AJ, Carpenter TA. Use of magnetic resonance imaging for anatomical phenotyping of the R6/2 mouse model of Huntington's disease. Neurobiology of Disease. 2009 Jan 1;33(1):12–9.

116. Zhang J, Peng Q, Li Q, Jahanshad N, Hou Z, Jiang M, et al. Longitudinal Characterization of Brain Atrophy of a Huntington Disease Mouse Model by Automated Morphological Analyses of Magnetic Resonance Images. Neuroimage. 2009 Oct 19.

CHAPTER 4 – D2GFP FLOW CYTOMETRY ASSAY DEVELOPMENT

Introduction

As discussed in Chapter 2, effective therapeutic interventions for neurodegenerative diseases such as ALS, Parkinson's Disease, Alzheimer's Disease, and Huntington's Disease (HD) require cell and animal models, many of which have been developed. While cell models allow higher throughput and lower cost, any therapeutic intervention initially evaluated in a cell culture model must subsequently be assessed in an appropriate animal model system before clinical trials in humans can be considered. However, the inherent variance in quantitation of the behavioral or pathological readouts in animals has practical consequences, requiring large cohorts to detect all but the most overt benefits, which limits experimental throughput. I sought to develop and implement an approach to this problem that combines the quantitative accuracy and direct relationship to molecular processes of a cell based assay with the medical relevance of evaluating endogenous neurons in the animal brain.

To develop the quantitative, cell-based preclinical assay system for HD, I focused on a well-characterized early feature of disease pathology in both these animal models and HD patients, transcriptional dysregulation in the medium spiny neurons (MSNs) of the basal ganglion, a phenotype with substantial consistency amongst mouse models and between the models and patients (1-4). One such dysregulated gene, dopamine receptor D2 (*DRD2* or D2), shows high expression levels in MSNs of the indirect pathway (striatopalladial) of the basal ganglion, which are among the earliest to die in HD (Reviewed in (5)). Measuring the binding of the D2 ligand raclopride using PET

scanning demonstrates reduced levels of DRD2 protein in the basal ganglia at, or even prior to, the onset of overt disease (6,7). Many mouse models for HD show a corresponding loss of *Drd2* expression early in the progression of neuronal pathology (1,8,9). Because mouse models of HD do not lose neurons in great numbers until very late in disease progression (10,11), this reduction is likely on a cell-by-cell level.

Dopamine signaling, and hence dopamine receptor alterations, likely plays a significant role in HD pathology. Selected evidence include studies demonstrating that knocking out the dopamine transporter in an HD mouse model accelerates aggregate formation (12), that dopaminergic input depletion by 6-OHDA treatment reduces striatal glutamate levels (13), and the fact that the only current FDA-approved drug for symptom management in HD is an inhibitor of VMAT2 (the main vesiclular dopamine reuptake transporter), tetrabenazine. Downregulation of such receptors may be an indirect byproduct of pathological transcriptional dysregulation, or a specific compensatory response by MSNs undergoing polyglutamine-induced stress.

The NIH-supported GENSAT project proved to be an excellent resource to identify a mouse *Drd2* reporter strain (14). Using BAC transgenic methodologies, this project has created many GFP reporter mouse lines, amongst which is a Drd2-GFP (D2GFP) reporter strain that appeared extremely well suited to my goals. Extensive characterization of this mouse strain by the GENSAT project and others (15) demonstrates a clear correspondence to the expression pattern of the endogenous mouse *Drd2* gene.

HD mouse models carrying the D2GFP reporter transgene were constructed by crossing, with demonstrable pathology typical for HD mouse models. A rapid and

reliable flow cytometry-based protocol for quantitatively assessing the GFP levels of MSNs in these animals was developed. I found that HD mouse models show highly reproducible reductions in GFP levels in the indirect MSNs during the early stages of disease progression, and that per-cell levels of GFP eventually stabilize at reduced levels, even while other pathologic measures are known to continue progressing. Time courses for decline in transcription levels of the reporter for a series of mouse models expressing either full length or N-terminal fragments of mutant huntingtin were evaluated. It is my hope that the availability of an effective, quantitative reporter system in the mouse brain for therapeutic intervention efficacy in HD will improve the rapidity with which therapeutic interventions for HD can be discovered, validated and made ready for human clinical use.

Methods

Mice: All procedures were done in accordance with Massachusetts Institute of Technology Committee on Animal Care guidelines. R6/2 mice (~110 CAG repeats) were maintained on a mixed background, either by crossing a transgenic male each generation to B6CBAF1 females, or using an ovary-transplanted female bred to B6CBAF1 males. N171-82Q mice were maintained on a mixed background, crossing a transgenic male each generation to B6C3F1 females. R6/1 (~140 repeats) and CAG140 male mice were bred congenic to C57BL/6, and HdhQ111/111 homozygotes were originally maintained on an outbred CD1 background before homozygosing and interbreeding within a small colony. BACHD mice were bred congenic to FVB. D2GFP mice were maintained homozygous, congenic to FVB. No differences were observed in

progression of the GFP decline phenotype between males and females, and the data were pooled. Animals were weaned at 3 weeks of age, housed with 1-5 mice per cage on a 12-hour light/dark cycle, and were fed at libitum from a wire cage-top hopper.

Rotarod and weight change: Weight was recorded at the start of every week of rotarod trials. Motor dysfunction on the rotarod was measured on a 4-40 RPM accelerating protocol, taking 10 mins to reach top speed, at which point mice were removed and 600 seconds was recorded (a rare occurrence). Otherwise, a fall was recorded and the time marked when the mouse failed to remain on top of the rod, either by falling off or hanging on while rotating around the bottom. An exception ("re-do") was made for falls within the first minute or falls while the mouse was in the process of turning around; in this circumstance, the time was recorded but the mouse was returned to the rod, and if it did not have a second fall within the next minute, the first fall time was erased. A second re-do was not given. Trials took place 3 days per week, 3 trials per day, with at least 10 mins separating the trials. For a given mouse on a given week, the trials were averaged, eliminating any trials more than 2 standard deviations away from the mean of the remaining trials. That average was assigned as that mouse's rotarod time that week for statistical purposes.

Histology: Mice to be processed for histology were terminally anesthetized with pentobarbital overdose. Mice were transcardially perfused with ~25 mL of 4% paraformaldehyde in PBS. Brains were sectioned (40 μm) on a vibratome and sections were stored in PBS with 0.4% NaAzide before staining. For immunofluorescence

analysis, free floating sections (1 to 4) in Netwell inserts were rinsed 4 times (5 min each) with PBS, and permeabilized with 0.5% Triton X-100 in PBS for 5 mins. Sections were blocked in Blocking Buffer 1 (2% BSA in PBS-T [PBS with 0.1% Triton X-100] and 4 drops of MOM Ig Blocking Reagent [Vector Laboratories] per 5 mL buffer) for 1 hr. Two more PBS rinses (5 min each) preceded additional blocking for 5 mins with Blocking Buffer 2 (2% BSA in PBS-T containing MOM Dilutent [400 μL per 5 mL buffer]), before primary EM48 (1:500, Millipore) antibody was added. Sections were incubated overnight at 4°C and then rinsed 4 x 5 min in PBS. Secondary antibody (Donkey anti-mouse Alexafluor 647, 1:1000, Invitrogen) was used in Blocking Buffer 2 and sections were incubated for 1 hr at RT. Four final 5 min PBS rinses (the second containing 1 μg/mL DAPI) preceded mounting. After mounting, sections were dried overnight and then sealed under coverslips with Vectashield Fluorescent Mounting Media (Vector Laboratories). Images were collected on a Nikon A1R confocal microscope, taking the maximum projection of the section's Z-stack images, then processed and pseudocolored in ImageJ software.

Buffers and reagents for dissociation: HABG: Hibernate-A (Brainbits) with 2% B27 supplement (Invitrogen), 0.25% Glutamax (Invitrogen), and 1% Pen/Strep. Papain buffer: Hibernate-A minus Ca^{2+} (Brainbits) with 0.25% Glutamax. Papain and DNase (Worthington product codes PAP2 and D2, respectively) were distributed as lyophilized aliquots.

Papain dissociation of MSNs for flow cytometry: The following protocol for

dissociation of MSNs for flow cytometry represents the current, highest-yield version. Previous versions produced some of the data presented, but other than a reduced yield of intact neurons, they did not demonstrably affect GFP profiles. Mice were euthanized by CO_2 asphyxiation. Brains were removed and dissected immediately. One or both striata were removed and stored in room temperature HABG for no more than 20 minutes while remaining samples were dissected. Striata were minced in 0.5-1 mL HABG in a petri dish using a razor, producing pieces no thicker than 0.5 mm. During dissection, the papain solution was prepared. Contents of 1 vial of papain were resuspended in each 5 mL papain buffer required, and incubated at 37˚C for 20 mins. Contents were then filtered (0.45 µm), and DNase added (1 vial DNase per 5-10 mL papain solution). Papain solution was aliquotted (1 mL per sample), and minced tissue bits were added using razor-trimmed pipet tips on a P1000, minimizing transfer of HABG (see note 1). Tissue was incubated with gentle rotation at 31-32˚C for 30 mins. After papain incubation, tissue pieces were transferred as above into 1-2 mL room temperature HABG and incubated for at least 5 mins. Fire-polished, silonized Pasteur pipettes (end width narrowed to ~0.8 mm) were used for trituration: material was pipeted up and down 10-20 rounds, ~4 seconds per round, until most tissue was in suspension (see note 2). Afterwards, using razor-blunted pipet tips, dissociated tissue was filtered (70 µm) (see note 3) and either used immediately for flow cytometry (after addition of propidium iodide or DAPI) or subjected to an additional BSA cushion purification step (see note 4). For further purification, dissociated tissue (~2 mL in HABG) was gently placed on top of a 3 mL cushion of HABG plus 2% BSA in a 15 mL conical tube (note 5). The material was centrifuged at 20xg (slow acceleration/deceleration) for 20 mins to

pellet neurons. After centrifugation, the top layer (debris, devoid of neurons) and most of the BSA cushion layer were aspirated, leaving 0.5-1 mL of HABG+BSA and the cell pellet. Pelleted neurons were resuspended in the remaining HABG+BSA, refiltered (70 μm), and used for flow cytometry (propidium iodide or DAPI added).

I found the total time, when performed by someone experienced in the protocol, is approximately 3 hours for 10 samples. It may take as much as twice as long as this for a novice. Because many facilities require advanced scheduling of the flow cytometers, to minimize the time neurons are kept on ice prior to use in the cytometer, this time should be factored in.

Note 1: I found it worked well to bring tissue into the tip, holding the pipette vertically. The tissue pieces settle towards the bottom after a few seconds. When the tip/tissue contacts the papain solution, it will break the surface tension, and the tissue chunks will flow into the papain, minimizing HABG transfer that would happen by simply expelling the tissue into the papain solution. Gently wiggling the pipette sometimes helps. If chunks need to be knocked off the wall, a small air bubble (created by gently releasing the plunger while holding vertically out of solution) will knock the tissue off the inside of the tip, allowing it to settle for transfer as above.

Note 2: The details of the trituration are as follows. Using a pipet-aid, tissue is drawn up; in 2 mL media, it should take ~2 seconds. Tissue is expelled immediately afterwards, taking ~2 seconds. This cycle is repeated 10-20 times. Great care should be taken to prevent bubbles from forming (which limit yield), but the rate of drawing up and

expulsion can be increased if pieces are getting small and still not breaking up. By the end, some pieces will likely remain, but this is often white matter, which is hard to break up and poor in neurons.

Note 3: The filtration was best accomplished using cut P1000 tips (opening ~5 mm), holding the tip in the mesh and slowly forcing ~800 µL through each time. A cut tip is preferable because a substantial amount of material will be caught in the filter, but a wider area of filtration prevents clogging. Care must be taken not to tear the filter membrane when holding pipette tip in it, but it must be held in place firmly enough that material actually passes through the filter membrane rather than collecting above it.

Note 4: Additional purification was usually only done when sorting was performed or time on the required analysis machines was limited, as it removes the majority of debris and concentrates the sample, but it sacrifices some yield, and is unnecessary for simple analysis and GFP quantitation.

Note 5: Layering the filtrate above the BSA cushion is made much more simple using cut P1000 tips. I recommend the following technique. The filtrate is retrieved in a cut tip, and the tip is then gently placed in contact with, but not below, the surface of the BSA cushion. Slow expulsion of the filtrate will allow it to remain above the cushion, while rapid expulsion forces it below the surface, preventing the formation of a clean interface. The above can be repeated until all of the filtrate is in a clean layer above the cushion. It should be noted that, should the samples be disturbed (e.g. dropped accidentally)

before centrifugation, the samples can still be centrifuged as above to prevent loss of the sample. The neurons will still be visible by flow cytometry, but debris events will not be removed.

Flow cytometry data processing: Flow cytometry for D2GFP quantitation took place on FACSCalibur or LSRII cytometers (BD). Data collected on flow cytometers was exported in an appropriate format (.fcs). If compensation was used, care was taken to ensure that all samples in a given dataset are compensated equally to not introduce biases. Exported files were opened in FlowJo analysis software (Treestar). GFP+, DAPI- MSNs can be seen without any gating, but there is a substantial amount of debris in every data set, so clean data was obtained by removing from analysis any events whose forward scatter (FSC) and side scatter (SSC) profiles were inconsistent with that of MSNs. To do so, first, GFP+, low side scatter events were selected to provide the initial gating parameters, as these are chiefly MSNs. These gated events were re-plotted by FSC x SSC and the central population of events was re-gated. The data could be further purified by gating using the Height and Width parameters of FSC and SSC if desired, but this was typically unnecessary. Once the hierarchical gating parameters for MSN-like events were established, the gates were re-assigned to the whole population of events (back-gated), removing events with scatter profiles not resembling MSNs. After this back-gating, GFP+, DAPI- MSNs were now selected for export of GFP (and RFP as appropriate) raw values for further analysis. MATLAB (Mathworks) expectation maximization and Gaussian means regression scripts were used to fit the exported GFP^+, $DAPI^-$ events to a pair of probability distributions. The

mean of the higher GFP distribution was used as the raw GFP value of that sample's MSNs. For mutant mice, this value was normalized to that of one or more simultaneously processed control samples. The script will be provided upon request.

QPCR: For RNA isolation, tissue or cells were added to 1 mL Trizol reagent, homogenized (18G needle or glass bead homogenizer), and extracted with 200 μL chloroform (vortexed for 8 seconds, rested for 2 mins, and then centrifuged at 4°C for 8 mins). The upper aqueous phase was used for standard alcohol precipitation. RNA was further purified using RNeasy columns, including on column DNase digestion (Qiagen). cDNA was synthesized using iScript RT-PCR kits (Bio-Rad), and reaction products either diluted 5x (purified flow sorted cells) or 25x (tissue samples). QPCR was performed using iQ SYBR Green mastermix (Bio-Rad) on a LightCycler 480 System (Roche).

mRNA purification and fragmentation for RNAseq: Total RNA was prepared as for QPCR (tissue) or using Qiashredder columns followed immediately by RNeasy column purification (Qiagen) (flow sorted cells); when sorted cells were destined for RNA purification, they were sorted directly into Qiagen buffer RLT. mRNA was further purified as follows. 2-10 μg purified total RNA (from tissue) or all of the purified RNA (sorted cells) was dissolved in 50 μL H_2O (all H_2O used was RNase-free), and heated to 65°C for 5 mins before placing on ice. 100 μL oligo(dT) magnetic beads (New England Biolabs) were added to an eppendorf and placed on a magnetic rack (Dynal MPC-S or similar), and washed twice with 100 μL Binding Buffer (20 mM Tris-Cl pH 7.5, with 1 M

LiCl and 2 mM EDTA). Beads were resuspended in 50 μL Binding Buffer, combined with the 50 μL RNA, and shaken gently by hand for 5 mins at RT. Tubes were then placed on the magnetic rack, supernatant was removed (bringing with it ribosomal and other non-polyA RNA), and the beads were washed twice with 100 μL Wash Buffer (10 mM Tris-Cl pH 7.5, with 150 mM LiCl and 1 mM EDTA). Beads were then resuspended in 30 μL 10 mM Tris-Cl pH 8.0, and heated for 2 mins at 80°C to remove mRNA from beads. Supernatant was quickly removed using the magnetic rack, temporarily moved to a new tube, and mixed with 70 μL Binding Buffer. The beads were washed twice with 100 μL Wash Buffer while the mRNA was melted for 5 mins at 65°C. After the beads were washed and the mRNA melted, mRNA was added back to the washed beads, shaken again gently for 5 mins at RT, and washed twice more with 100 μL Wash Buffer. Finally, beads were resuspended in 20 μL 10 mM Tris-Cl pH 8.0 and heated for 2 mins at 80°C to elute mRNA from the beads. The tubes were rapidly placed back on the magnetic rack, and the purified polyA+ mRNA was moved to a new tube. mRNA was fragmented (RNA Fragmentation Reagents, from Ambion) at 70°C for exactly 5 mins, before stop solution was added and tubes were placed on ice. mRNA was then purified with sodium acetate, glycogen, and ethanol per standard protocols. After precipitating, centrifuging, and washing the pellet (70% ethanol), the clean, purified, fragmented mRNA was resuspended in 10.5 μL H_2O for cDNA synthesis.

Library prep for Illumina sequencing: Purified, fragmented mRNA was converted into double stranded cDNA using first and second strand synthesis reagents (Invitrogen). In short, for first strand synthesis, random hexamer primers (3 μg/μL, 1 μL) were added to

RNA and heated for 5 mins at 65°C. 5x First Strand Buffer (4 μL), 100 mM DTT (2 μL), dNTPs (10 mM each, 1 μL) and RNase inhibitor (0.5 μL) were added to each reaction, which were then incubated at RT for 5 mins. Afterwards, 1 μL Superscript III reverse transcriptase (Invitrogen) was added, and the reactions were incubated sequentially at 25°C for 10 mins, 42°C for 50 mins, and 70°C for 15 mins. For second strand synthesis, H_2O (51 μL), 5x Second Strand Buffer (20 μL), and dNTPs (10 mM each, 3 μL) were added to each reaction and incubated on ice for 5 mins. Afterwards, RNaseH (2 U/μL, 1 μL) and DNA polymerase 1 (10 U/μL, 5 μL) were added and reactions were incubated at 16°C for 2.5 hrs. Double-stranded cDNA was purified with Qiaquick PCR purification kit columns and reagents (Qiagen), and eluted in 50 μL Tris-Cl pH 8.0. End repair, adaptor ligation, and size selection (200-400 bp) were performed by staff at the MIT BioMicroCenter. Samples were then PCR amplified 12-16 cycles using barcoded primers. Paired end reads were processed on the Illumina HiSeq 2000 platform and reads mapped and analyzed using a combination of in-house pipelines for differential gene expression calling. Data was further processed using Excel (Microsoft) and MATLAB (Mathworks). Heat maps were made using GENE-E Software (The Broad Institute, available at http://www.broadinstitute.org/cancer/software/GENE-E/index.html). Amongst the associated topics (Figure 3) for dysregulated genes, Canonical Pathways and Upstream Regulators were called using Ingenuity Pathway Analysis (Ingenuity Systems), while enriched Components, Functions, and Processes were called using GOrilla (available at http://cbl-gorilla.cs.technion.ac.il/).

Results

Histological and Behavioral Assessment of D2;HD Model Mice of the Strain R6/1.

I wished to assess the potential for the D2GFP transgene to serve as a quantitative marker in the HD model mouse context. After establishing a colony of D2GFP mice (known to demonstrate some behavioral and gene expression alterations that only exist in the homozygous state) (16,17), I began breeding them to various HD model mouse strains. The R6/1 strain demonstrates robust and reproducible behavioral alterations (18) and neuropathology (19). Offspring of D2GFP and R6/1 animals demonstrate minor neuropathology (an enlarged lateral ventricle) at age 12 weeks (Figure 1B), relatively early in pathology and prior to previously published motor symptoms (3,20). The GFP transgene shows the expected striatal enriched expression (15), with axons out of the ventral striatum projecting towards the globus pallidus. Compared to a wild type littermate (Figure 1A), there is a significant reduction in GFP within the striatum. Closer inspection (Figure 1C) demonstrates that, as expected, only ~1/2 of nuclei in the striatum are found within GFP+ cells, the other half presumably within neurons of the direct pathway, known to express dopamine receptor D1 but not D2 (21). Compared to the wild type littermate, the R6/1 animal (Figure 1D) shows a similar pattern of GFP expression but with lower absolute levels of GFP. Additionally, staining with EM48 (recognizing mutant huntingtin exon 1) reveals pervasive neuronal intranuclear inclusions, present in almost every neuron but largely absent from the nuclei in the axon fiber bundles. This suggests that the cells of the axon fibers, largely oligodendrocytes, are less prone to mutant huntingtin (mHTT) aggregation.

A small cohort of animals (N=5 per genotype) were tested for weight loss and performance on the rotarod through 16 weeks of age, approximately half of the upper

limit of the lifespan of these mice in my colony. No statistically significant decline in weight was observed (Figure 2A) in this cohort, but others tested by my lab have demonstrated an eventual reduction in weight in R6/1 mice in the D2GFP background (not shown). However, even in this small cohort, a significant decline in performance on the rotarod was apparent from 12 weeks of age until euthanasia at 16 weeks (Figure 2B).

Transcriptional Profiles of D2;R6/1 Versus D2;WTL Mice Confirm Previous Observations in Non-D2GFP Background

The D2GFP transgene has no effect on the behavioral or neuropathological sequelae common to HD mice, but to confirm that transcriptional dysregulation is uniformly altered beyond the observed loss of GFP signal, RNAseq analaysis was performed on striata from 12 week old D2;R6/1 mice and non-HD littermates (Figure 3). At this age, the mice have either no or mild symptoms. Over 1200 genes, or 8% of genes with mapped reads, had significant dysregulation (fold change $>\log_2(0.5)$, $q < 0.05$), 2/3 of which were downregulations versus upregulations in the HD state. Despite only 8% of the transcriptome being reported as significantly altered, these values were more than adequate to demonstrate hierarchical clustering of samples (Figure 3A) which separated wild type from R6/1 littermates, a clustering that did not change when only those genes with reported dysregulation were subjected to the same algorithm (Figure 3B). Pathway and other functional analysis (Figure 3C) confirmed the alteration of many pathways with previously identified dysregulation in R6/1 mice (3). This includes many pathways and functions associated with G-protein coupled receptor and

cAMP signaling, cation transport, and protein binding. Such in depth transcriptional analyses present a wealth of information and can be used to identify candidate modifiers whose reduction or increases may contribute to pathology (for example, both *Bdnf* and *Hdac4* are significant predicted upstream regulators of downregulated genes). However, for my purposes in this study, it is enough to note that the D2GFP transgene (including the resulting introduction of the FVB strain background) does not appear to influence the transcriptional profile alterations common to this HD mouse model.

Improved Yield for Isolation of MSNs from Adult Mouse Striata.

The decline in GFP seen histologically prompted further study. To best leverage any decline in GFP fluorescence, I wished to develop a way of following this loss on a single-cell level. This would facilitate rapid assessment of alteration of this phenotype, as well as allow for pooled screening in a mixed population expressing a variety of potentially therapeutic constructs.

In order to robustly quantify this *Drd2* dysregulation in *mHTT*-expressing neurons, I optimized a previously reported protocol (22) for dissociation of D2GFP MSNs that originally gave limited yields (~1200 GFP+ cells per striatum), inadequate to carry out the detailed analyses here. My modified protocol increased yield to 15,000-25,000 GFP+ cells per adult striatum, a sufficient number for subsequent experiments. The throughput of this protocol is sufficiently high that one individual can prepare a dozen samples for flow cytometry in roughly three hours. This compares extremely favorably with the other methods commonly used for transcriptional assessment. With the obvious caveat that this analysis is limited to that of one or two transcripts,

strategies like QPCR require at least one day (RNA isolation and purification, cDNA conversion, and QPCR analysis) while *in situ* techniques require multiple days (fixation, sectioning, slide preparation, hybridization, washes and detection). I will elaborate on the specific merits of this analysis, but by adding my novel technique to a conventional repertoire, a rapid and limited interrogation of *Drd2* levels could be used to determine whether further analysis of the remaining tissue is worthwhile. Also of significance is the fact that this technique measures *Drd2* expression accurately on a cell-by-cell basis. This is particularly important when analyzing a sample with a mix of construct-expressing or non-expressing cells (to be discussed in Chapter 5), but it also removes the risk of contamination from nearby non-striatal tissue. Classical transcriptional analysis can be thrown off by the appearance of transcripts from neighboring brain structures, but here, precise dissection is less crucial.

Suspensions of MSNs were subjected to flow cytometry. Event-by-event raw GFP quantities were acquired and further processed to assign a GFP level to the population (and therefore the mouse), using a method to be discussed in the next section. Subjectively, MSN suspensions only demonstrate a GFP+, DAPI- population (presumably that of intact, *Drd2*-expressing MSNs) from animals expressing the D2GFP transgene (Figure 4). To further test this, we bred a small cohort of animals expressing tdTomato under control of the *Drd1a* promoter (D1tdTomato) (15) to D2GFP animals and subjected them to similar flow cytometry analysis (Figure 5). As expected, only animals carrying the D2GFP transgene showed GFP+ events, while mice carrying D1tdTomato had RFP+ events. Also, as expected, double transgenic animals (Figure 5C) have each single-fluorescent population in roughly equal numbers, but very few

double-fluorescent cells. This is consistent with the knowledge that most MSNs express either *Drd1* or *Drd2*, each making up approximately half of the MSN population (15).

This technique is not limited to striatal MSNs, either. A BAC transgenic GFP strain CDG2GFP, driving GFP under the transcriptional control of *Rasgrp1* (also known as CalDAG-GEFII), has proven useful for analysis of both cortical and striatal neurons. The gene is primarily expressed in the striosomes of the striatum, but also is expressed in the motor cortex (23). Hence, when subjecting D2GFP cortex and striata to flow cytometry, GFP+ events are only visible in the striatum (Figure 5D) and are absent in the cortex (Figure 5E). However, from CDG2GFP animals, GFP+ events are visible in suspensions from both the striatum (Figure 5F) and cortex (Figure 5G). This agrees with immunostaining versus GFP available on the GENSAT website (Figure 5H-I) for these two strains, where antigen staining is visible only in the striatum in D2GFP animals, but is visible in both the striatum and in several layers of the overlaying cortex in CDG2GFP brains.

QPCR Validation that GFP+ Events are Indirect MSNs

By analyzing the pre-sorting and post-sorting events (Figure 6), I was able to confirm that debris is pervasive prior to sorting (Figure 6A-C), and within this suspension, there are a few visible GFP+ cells that remain intact (staining negative for DAPI) while un-intact cells (DAPI+) never contain GFP. After sorting (Figure 6D-F) the GFP+, DAPI- population, imaging confirms the absence of both DAPI+ un-intact cells as well as debris. For confirmation that GFP+, DAPI- events were indeed MSNs of the indirect pathway, these events from D2GFP mice were collected and transcript levels

compared to whole striata (Figure 7A, black versus striped bars). The sorted events demonstrated significant enrichment of transcripts known to be characteristic of MSNs of the indirect pathway (*Drd2*, *Adora2a*, and *Penk*) as well as significant reduction of transcripts known to be enriched in direct pathway MSNs (*Drd1a* and *Tac1*) (24,25). The previously reported downregulation (1,9) of *Drd2*, *Adora2a*, and *Penk* in HD models was reproduced in the aged HD model R6/1 striatum (Figure 7A, black versus grey bars), which agrees with my RNAseq data in confirming that the D2GFP background does not significantly alter this phenotype.

Small Numbers of MSNs Can Be Sorted and Analyzed by RNAseq

It has been previously demonstrated that flow sorted D2GFP neurons can be transcriptionally studied (22), and it was worth verifying that those genes demonstrably upregulated in indirect MSNs by previous studies are also altered in my hands. Additionally, it is worthwhile knowing the minimum number of cells required for high quality transcriptomic analysis. Hence, populations of D2GFP+ MSNs (1000, 4000, 16,000, or 64,000) were processed by RNAseq to determine mapped transcripts and, if possible, differential expression versus whole striatum (Figure 8). Overall transcriptional profiles of sorted cells had significant similarity to that of whole striatum (Figure 8A-D), though the most striking similarity was between replicates of whole striatum (Figure 8E) and between libraries from 64,000 and 16,000 sorted D2GFP cells (Figure 8F). Further dilutions, comparing libraries from 16,000 with 4000 cells or 4000 with 1000 cells (Figure 8G-H), demonstrate both less linearity in the correlations, and also a reduction in the presence of transcripts with low FPKM values. Globally (Figure 8I), fewer overall

genes with mapped reads were detected in libraries made from fewer cells, and such libraries also showed an apparent inflation of many FPKM values, particularly on the low-expression end. This was brought on by a specific loss of detection of transcripts whose expression in the whole striatum was weakest (Figure 8J), whereas highly expressed transcripts were present in all sorted cell libraries. As a further confirmation, transcript levels of genes reportedly enriched in direct or indirect MSNs (22) were assessed, and as expected, were either depleted (direct MSN genes: *Lingo2*, *Slc35d3*, *Tac1*, *Zpf521*, *Stmn2*, *Drd1a*, *Nrxn1*, and *Gnb4*) or enriched (indirect MSN genes: *Penk*, *Drd2*, *Adora2a*, *Plxdc1*, *Arpp19*, *Adk*, *Ubp1*) in D2GFP MSNs versus whole striatum. In all, this is confirmation of previous studies that sorted D2GFP cells are a pure population from which RNA can be collected for informative transcriptomic studies. Furthermore, given my improvements to the yields from flow sorted populations, pooling mice may no longer necessary for the collection of sufficient material for such analysis. Certain low abundance transcripts may not be detected, but the quality of such libraries is sufficient for the study of significant transcriptional differences in specific neuronal subpopulations.

Quantitation of GFP Levels in D2GFP MSNs by Flow Cytometry

For use as a preclinical marker of HD pathology, robust and consistent quantitation of D2GFP levels in MSNs required removal of contaminating subpopulations from analysis. Figure 9 represents an example of the quantitation pipeline for a mouse of strain R6/1 at 16 weeks of age and a wild type littermate, processed simultaneously. Initial backgating computationally filtered out events with

forward and side scatter profiles inconsistent with that of GFP^+, $DAPI^-$ events (which contain intact $Drd2^+$ MSNs). In this example, the GFP values of GFP^+, $DAPI^-$ events from a control littermate (Figure 9A, blue gate) and an R6/1 mouse (Figure 9B, red gate) were exported. Overlaying them (Figure 9C) allows one to qualitatively distinguish wild type from HD model samples, but also demonstrates that each contains two sub-populations. This phenomenon was particularly apparent in older R6/1 and R6/2 mice, for which specifically gating the entire GFP+ population was not possible without including a portion of the neighboring debris field. These sub-populations can be separated using Gaussian means regression into two population distributions (Figure 9D). It was determined that the high GFP population demonstrated the lowest variance within cohorts, so for robust quantitation, the mean of the high-GFP distribution is used as the GFP value of each mouse (Figure 9E). Normalizing this R6/1 mouse to the control littermate revealed a reduction to 34.4% of control GFP. The minimal variance of this analysis is demonstrated in Figure 9F for the entire 16-week-old R6/1 cohort (6 R6/1 and 3 control mice were overlayed, producing values of 34.5 ± 1.8% for R6/1 normalized to 100 ± 2.3% in controls).

I normalized each mutant mouse's GFP value to that seen in age-matched control animals processed simultaneously (when more than one control animal was processed on a given day, the average was used). Normalized data of many mutant mice of the same or similar age, processed on the same or different days, were aggregated for study in time courses.

D2GFP Loss is Progressive in Both Fragment and Full-length HD Mouse Models

R6/2 mice: I systematically crossed D2GFP mice to a number of HD model strains and analyzed the time course of decline in GFP expression (Figure 10A). Strain R6/2 is the product of strong expression of a transgene containing human *mHTT* exon 1 and its promoter (26). It has been widely used in the assessment of potential therapeutic interventions for HD (27,28). I found that D2GFP expression in the MSNs of R6/2 showed significant differences from the values for wild type littermates at the earliest age I evaluated, 4.5-5 weeks of age. At this point, R6/2 GFP values were 80% of controls. As R6/2 animals aged, the differences in GFP values between R6/2 and control animals increased. Between 8 and 12 weeks, when R6/2 animals decline precipitously in performance on behavioral tests (29), there was minimal further decline in normalized GFP levels between R6/2 and control, which remained in the range of 30-40%. The low variance of the measurements were demonstrated by power analysis (Table 1, power = 80%, alpha = 0.05), demonstrating that end-stage R6/2 mice (age 10.5-12 weeks) would require only 5 animals to detect a modest 10% rescue of GFP levels.

R6/1 mice: A sister strain to R6/2 that has a similar transgene but delayed pathology, R6/1 mice (26) were also bred and tested at numerous time points. A similar progression to that seen in R6/2 was observed for R6/1 (Figure 10B), with the expected delay of progression. A subtle but statistically significant decline (to 94% of wild type levels) was observed at 4 weeks of age. GFP levels had declined precipitously by 7 weeks of age in R6/1, plateauing at 35% of wild type levels by 16 weeks of age; no further decline was seen in 20-week-old animals, when morbidity precludes further

aging. Variance was even smaller in R6/1 mice than that seen in R6/2, possibly due to the uniform C57BL/6 background of R6/1. Power analysis in this strain (Table 1) suggests a 10% rescue in 7-week-old mice requires only 7 animals. Furthermore, by 16 weeks of age, when D2GFP loss is no longer progressive, only 3 mice could reliably detect a 5% rescue. As estimated by power model curve fitting (Figure 11), R6/1 mice lose D2GFP at half the rate of R6/2 mice upon onset (23% per week in R6/1 versus 54% per week in R6/2), though the age of onset is ~4 weeks for both strains.

CAG140 mice: Knockin models of HD either introduce an expanded CAG repeat into exon 1 of mouse *Htt*, or have the *Htt* gene modified to contain a hybrid human/mouse exon 1 with an expanded CAG repeat. In contrast to the R6 lines, most knockin lines (including CAG140 and HdhQ111) show no reduction in lifespan (30,31), even when bred to homozygosity. However, heterozygous CAG140 (also known as HdhQ140) mice (Figure 10C) demonstrated significant GFP loss as early as 12 weeks of age, to 81% of controls. D2GFP decline progresses through 31 weeks of age before plateauing at ~62% of wild type levels. This D2GFP loss is prior to the reported rotarod latency deficit, and is also prior to the age at which reliable detection of *Drd2* loss by *in situ* hybridization is reported (32). Before plateauing, this strain demonstrates greater variance at the younger ages tested. Normalized GFP values ranged between 92% and 68% of wild type values at 12 weeks of age and between 74% and 59% of wild type levels at 24 weeks of age. However, by 31 weeks of age, when progression had halted, variance was small enough that power analysis (Table 1) suggests only 6 mice would be sufficient for detection of a 10% rescue in GFP loss. Curve fitting (Figure 11)

estimates an age of onset of 7.5 weeks, and an initial rate of 5% per week lost.

HdhQ111 mice: HdhQ111 mice are another knockin HD model, and were also tested in this assay, though I chose to compare HdhQ111 homozygotes to heterozygotes. According to a previous report by the strain's generator, heterozygotes and homozygotes have few reported differences (33), but if this assay is sensitive it should readily distinguish the two genotypes. Comparing homozygotes to heterozygotes (Figure 10D) also demonstrated progressive GFP loss, beginning at 6 months of age. As in the CAG140 mice, the decline was significant early on, to 82% of heterozygote levels, but was more variable, ranging between 94% and 67%. By 12 months of age, homozygote D2GFP had reached 59% of heterozygote levels and variance was minimal in the three mice tested. Power analysis (Table 1) demonstrates a quite robust assay at 12 months of age, requiring only 5 mice for detection of a 10% rescue. Compared to heterozygotes, homozygotes begin their D2GFP decline at ~18 weeks of age with a 3.1% per week initial loss rate (Figure 11).

N171-82Q mice: Like R6/2 and R6/1 mice, the N-terminal transgenic strain N171-82Q has strong neuropathology (34,35) and a diminished lifespan. However, after crossing to D2GFP mice and aging, I was not able to detect a consistent decline in GFP levels (Figure 10E). While some animals showed no detectible decline, others had lost as much as 40% of D2GFP levels (Figure 10F). This is reminiscent of what was seen for young (<20 weeks of age) CAG140 mice, although even in spite of high variance in young mice from that strain, there is a progressive decline in mean levels, where no

progression is present for N171-82Q animals. Unlike R6/2 and R6/1 mice, there is pervasive cell death in N171-82Q MSNs (35), so it is possible that there is selection against cells with strong toxic responses that would otherwise facilitate significant *Drd2* loss in surviving neurons. This seems unlikely, though, simply based on the wildly variant phenotype, which seems to manifest as incomplete penetrance.

BACHD mice: BACHD mice have become a popular strain in the last few years (36) for many reasons, including an interrupted repeat preventing intergenerational or somatic CAG repeat expansion, as well as some neuropathological features that are more reminiscent of human HD than is typical for mouse models. However, it has been previously published in a study comparing the two most commonly used full-length transgenic models, YAC128 and BACHD, that in spite of their numerous similarities, BACHD mice fail to display transcriptional dysregulation as assessed by QPCR (37). Their data were convincing, but I wanted to see whether my particularly sensitive method would be able to detect a difference where previous less-sensitive methods had not. However, after aging BACHD mice for 9 months, the GFP profiles of the transgenic littermates were indistinguishable from that of the wild type animals (Figure 10G). Animals aged further may produce dysregulation, but this strain exhibits significant mortality in my colony when animals reach ~12 months of age, precluding detailed studies in older mice.

D2GFP Levels Decline in Wild Type Animals

The assay I have developed demonstrates remarkable day-to-day and

instrument-to-instrument robustness. This is mainly because each experiment is done with a cohort containing one or more wild type animals, to which all mutant animals are normalized. The absolute GFP values from many cytometers will vary widely, but because flow cytometry accurately quantitates fluorescence over several orders of magnitude, the absolute values are irrelevant after normalization. That being said, this precludes analysis of data between days. Ideally, a given cytometer would produce the same value from an identical sample on any given day (assuming instrument parameters like filter sets and voltages are kept constant). In practice, however, this is often not the case; something as simple as replacing a filter, let alone a laser, will change the absolute values produced, and with an assay as sensitive as this one, even subtle changes would prevent such cross-cohort analysis.

With this in mind, I wanted to assess whether there is any change in D2GFP levels as wild type animals age. For this, I used wild type littermates from R6/1 x D2GFP matings of a variety of ages, and processed them all on one day (Figure 12). There was a significant decline in D2GFP levels as the wild type animals aged from 4 to 21 weeks of age, still very young in the life of these mice (~100 week lifespan). I have not done further analysis to determine whether this change is specific to the GFP transgene or represents decline of *Drd2*, but the minor loss (15% after 21 weeks) pales in comparison to that seen in their R6/1 littermates, whose GFP decline was re-plotted, adjusted for the declined GFP levels present in wild type mice. Hence, while wild type animals lose ~15% of their original (4 week old) GFP levels by 20 weeks of age, R6/1 animals will have lost ~70% of theirs.

Discussion

Quantitative markers for neuropathologic progression in HD mice are few and far between. Standard measures for evaluating phenotypic progression are survival, rotarod, or mHTT aggregation, occasionally including volumetric assessments (36,38-41). In these and many other studies, the power of the assay (i.e. the phenotype's effect size and variance) and the difficulty of assessing it determine the required resource investment. Typically, a rescue on the order of 30% requires 10-20 animals for reliable detection. Because most of these strains have somewhat complicated breeding requirements and, by their nature, need to be aged before sacrifice and tissue investigation, testing even a single compound necessitates a substantial investment. Any method by which ineffective candidates can be efficiently eliminated or recommended for further study is valuable. For therapeutic modalities that have been identified through cell based systems or chemically based screens, the systems described here provide the opportunity to rapidly and systematically measure efficacy *in vivo*, at powers facilitating the evaluation of multiple dosages and time points without becoming a practical burden.

Several promising therapies based on modulation of known disease-related pathways have failed at either the preclinical or clinical stages, and this might be the result of correcting one downstream pathway while leaving the many other disease processes uncorrected. A truly promising therapeutic will likely need to target the core pathogenic mechanisms in HD, of which it is reasonable to believe transcriptional dysregulation to be one. It appears early and influences the levels of many genes involved in the highly pleiotropic response to polyglutamine toxicity, suggesting that

demonstration of transcriptional normalization could signify a fundamental molecular intervention.

The ability to relatively rapidly and quantitatively measure the impact of therapeutic intervention on a full-length model of disease for HD is of particular importance. From a candidate evaluation perspective, N-terminal fragment models have a more rapid and severe pathology in nearly all known tests when compared to full-length models (including CAG140 and HdhQ111), a pattern recapitulated in our assay. The predictability of the D2GFP decline allows one to rapidly pilot potential therapeutics in fragment models and assess efficacy before deciding whether to extend the study to larger cohorts or slower full-length models. These strains are based on the configuration of the HD expanded repeat in its native environment and are critical for most effectively reflecting the situation encountered in the HD patient. The ability to make a go/no-go decision in a small cohort, within a matter of weeks and with great statistical confidence, may significantly improve the rate of progress in assessing potential HD therapies.

The techniques developed are not limited to the study of *Drd2*, or even of HD. *Drd2* was chosen to develop for many reasons, though others were an option. The GENSAT project, for example, contains hundreds of validated strains of mice, making it a good place to search for already-existing strains. However, I wanted a marker whose change occurred early in disease progression. Murine models commonly demonstrate transcriptional profile changes prior to overt symptom onset. This is important from a therapeutic evaluation perspective, because as has been demonstrated in patients, by the time symptoms have set in, there may be little that can be done to improve patient lives other than providing pharmacological symptom management; neurorestorative

tissue transplants are still too ineffective for use. *Drd2* dysregulation is an early and common effect in HD patients and models, consistently occurring before symptom onset, so I reasoned that protection of its dysregulation could indicate a neuroprotective effect, rather than just symptom management.

Another advantage provided by *Drd2* is its cell type specificity. Admittedly, a marker common to all neurons in the striatum whose levels decline would have allowed me to effectively double the number of cells useable in a given piece of tissue. However, the striatum, as with all other brain structures, is not a uniform tissue. In this case, the cells project to either the globus pallidus or the substantia nigra, in roughly equal ratios. While both cell types certainly undergo dysfunction, those of the indirect (striatopalladial) pathway seem to be affected earliest in adult onset patients. This explains the impairment of motor control and dyskinesia, whereas blockade of the direct (striatonigral) pathway leads to bradykinesia (21). *Drd2* is one of the primary markers of indirect pathway MSNs, so its specific study not only ensures that my population is as uniform as possible, but represents the cells hit earliest and hardest by mHTT toxicity.

I have, however, demonstrated that my technique can be used to evaluate at least two other fluorescent models (D1tdTomato and CDG2GFP), in at least two different tissues (striatum and cortex). It stands to reason that any neuronal population of interest could be monitored accurately for the dysregulation of a marker of choice, provided a fluorescent protein-expressing strain exists. Also, at least two markers can be monitored simultaneously, provided they occupy different fluorescent spectra. Finally, other neurological diseases also demonstrate transcriptional dysregulation. In Alzheimer's Disease patients and mouse models, Sp1 is elevated, potentially producing

wide ranging effects on relevant genes including APP and Tau (42). Furthermore, EGR1 transcription factor binding sites are common among dysregulated genes (43), suggesting a pathogenic mechanism whose progress could be followed by monitoring one or more downstream dysregulated transcripts, similar to the approach taken in HD for REST/NRSF or Sp1 dysregulation. Meanwhile, FoxO1-regulated genes are upregulated in Parkinson's Disease (PD), and there may be an impact on PD age of onset for certain SNPs in FoxO1 itself (44). It remains to be seen whether other disease models can leverage transcriptional dysregulation for a quantitative fluorescent marker, but there is nothing about this assay or the underlying biology to suggest that the techniques are only relevant for HD models.

The robustness of HD transcriptional profile alterations is remarkable, but it can't be ignored that it does not appear to be ubiquitous. As others have shown (37) and I verified, BACHD animals have no dysregulation of *Drd2*. There is no simple explanation for why every single mouse model of HD that has been tested has demonstrated transcriptional profile changes other than BACHD. The closest strain to it, YAC128, was also generated by transgenic implantation of full-length *mHTT* with a large span of surrounding genome, and these mice have reproducible transcriptional alterations. It is formally possible that the transgene insertion site may have impacted a modifier, or that differences in the genomic regions surrounding *mHTT* can be modulating the transgene's effects. These are difficult to investigate, and the latter would likely only affect the transgene's levels, which would primarily alter the age of onset. On the other hand, because they were generated using two different individuals' HTT genes, there are different SNP markers between the two strains (45). Notably, there is little evidence

that SNPs within the HTT region can affect age of onset (46). Instead, it seems most likely that a SNP the BACHD transgene subtly alters either the proteolysis of mHTT or its posttranslational modifications, impacting its subcellular localization. Indeed, in spite of their identical strain background (FVB) and similar mHTT expression levels, BACHD mHTT produces very few striatal intranuclear inclusion bodies, while YAC128 mice have pervasive striatal aggregation (36,37,39). This at least demonstrates a difference in subcellular localization of the N-terminal fragment. Furthermore, because Sp1 aberrantly interacts with N-terminal mHTT (47), it seems most likely that mHTT spends too little time in the nucleus of BACHD mice to significantly impact Sp1-regulated transcripts, including *Drd2*. That these animals demonstrate other pathological sequelae common to HD tells us that the dysregulation of Sp1 targets is not necessary for many HD symptoms. That being said, the fact that virtually every other model of HD shows both intranuclear inclusions and a similarly altered transcriptional profile strongly suggests that the failure to produce such a phenotype from BACHD mice may simply be an artifact of a unique transgene in that strain, rather than evidence of the irrelevance of transcriptional dysregulation to HD pathology.

The inconsistency of the N171-82Q D2GFP phenotype is another matter. N171-82Q mice have demonstrable transcriptional profile alterations, with striking similarity to that of R6/2 animals (48), though interestingly, *Drd2* showed variability in this study as well, as one replicate produced significant downregulation, while the other showed no change. The variability could be due to the breeding scheme, which involves crossing a male in each generation to an F1 animal from a C57BL/6 x C3H mating. A similar scheme is used for R6/2 animals (C57BL/6 x CBA F1 offspring), but this strain has a

consistent phenotype, so a mixed genetic background alone cannot explain it. However, a polymorphism within the C3H background could be impacting dysregulation. I have not initiated any of the kinds of crossing studies, such as those using recombinant inbred lines, to investigate this in detail, but one example is of particular interest. It is known that C3H mice lack the Tlr4 receptor (49), impacting their response to inflammatory stimuli. Because there is substantial evidence for a role of inflammation in neurodegenerative diseases, including HD, this is a reasonable candidate, and is being actively investigated in our group.

All told, I have developed an assay method for following HD progression in model mice, whose consistency in many of the most commonly used strains is unparalleled by conventional methodology, and that can be assayed in a fraction of the time. That killing the animal is required for the assay precludes its use for longitudinal studies (unless substantial improvements are made in *in vivo* fluorescent imaging methods), and only one gene of many relevant choices is assayed, which are its chief limitations. Nevertheless, only one piece of striatal tissue is required to rapidly analyze for GFP alteration, leaving the other parts of the animal available for more detailed, lengthy, and costly analyses should the D2GFP assay suggest value to such studies. Every common measure of pathogenic process (inclusion body formation, volumetric alterations [as measured by ventricle enlargement], motor impairment, weight loss, diminished lifespan, and consistent transcriptional alterations) has been demonstrated in HD mice carrying the D2GFP transgene, so its presence clearly fails to alter pathology and hence allows other analyses to take place without fear of being modified by GFP transgene expression. These experiments provide sensitive, quantitative data on the dysregulation

of a relevant gene representative of the early stages of polyglutamine toxicity, but further testing must take place before the assay can be recommended as a commonplace inclusion in preclinical drug development. Chapter 5 will cover my efforts to both induce and ameliorate this phenotype with viral vector delivered transgenes, as well as an attempt to use D2GFP dysregulation for the evaluation of a small molecule's efficacy at reducing neuropathology.

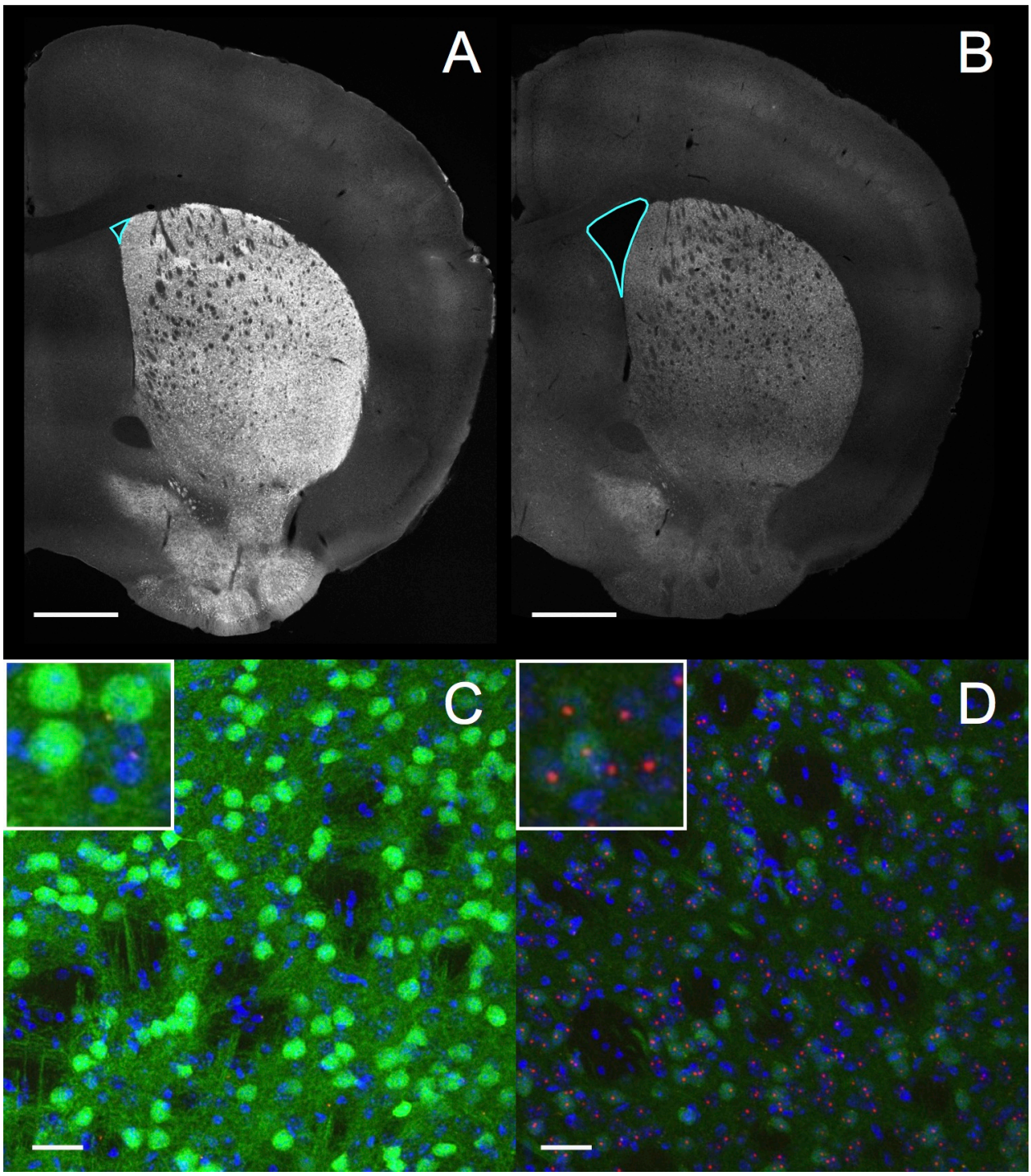

Figure 1: D2GFP mice bred to HD model mice demonstrate visible reduction in GFP, and apparent mHTT aggregates. (A) Coronal sections of brains from mice (12 weeks of age) carrying the D2GFP transgene demonstrate robust GFP expression in the striatum, including visible axons travelling through the ventral striatum towards the globus pallidus. **(B)** A littermate of the animal in (A) but expressing N-terminal *mHTT* (strain R6/1) has reduced absolute GFP expression with a similar anatomic pattern. Note the enlarged lateral ventricle (outlined in cyan in (A) and (B)). **(C)** DAPI (blue,

nuclear DNA), GFP, and EM48 (red, anti-mHTT antibody) co-staining of the animal from (A) indicates that GFP+ cells only represent ~1/2 of the cells in the striatum, the other half presumably made of direct MSNs expressing D1 but not D2 dopamine receptors. No EM48 staining is apparent. **(D)** In the animal from (B), a similar pattern (~1/2 of neurons are GFP+) is observed with reduced absolute GFP expression. EM48+ intranuclear inclusions are pervasive in neurons, but are largely absent from nuclei that make up the neuron-poor axon fiber bundles, suggesting that mHTT is less aggregation prone in oligodendrocytes. Scale bars represent 1 mm in (A) and (B), 32 μm in (C) and (D) (12 μm in the inset).

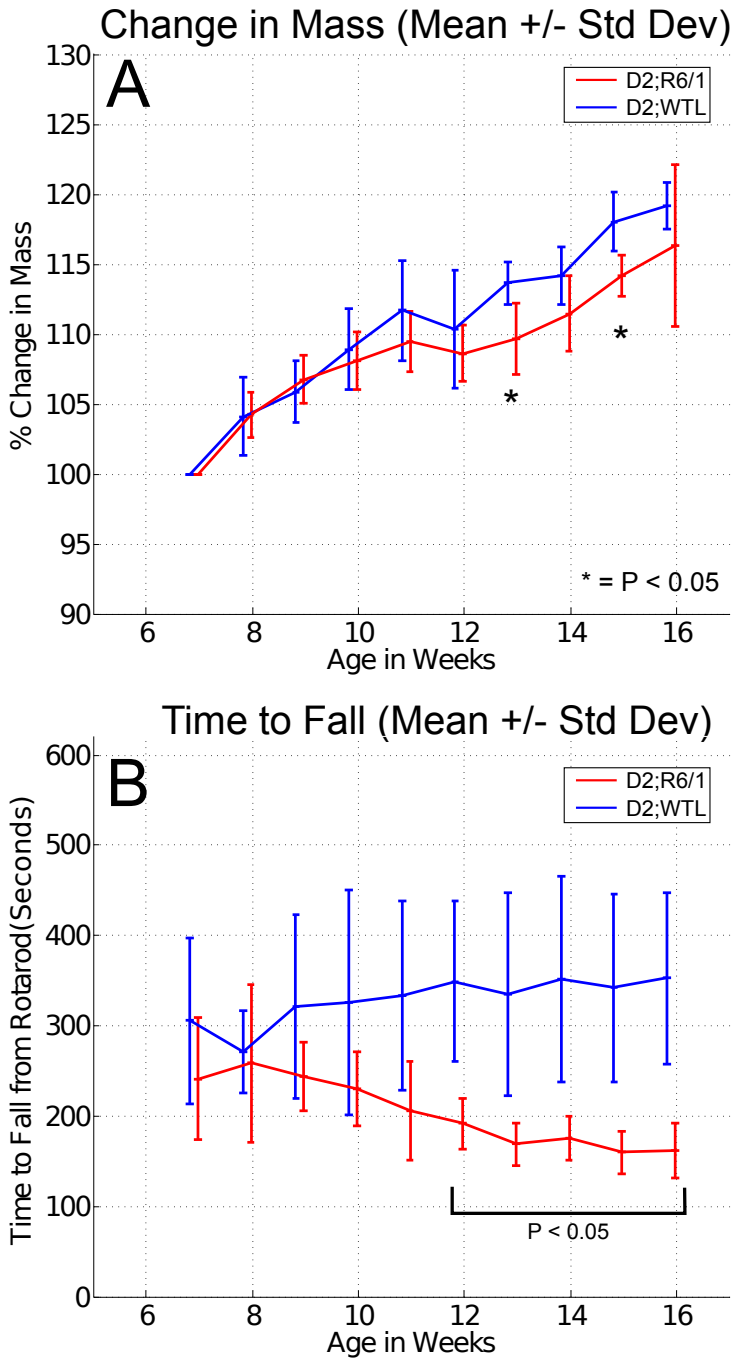

Figure 2: HD model mice carrying the D2GFP transgene demonstrate progressive motor performance decline. (A) Male mice carrying the D2GFP transgene either with or without N-terminal mHTT (D2;R6/1 or D2;WTL) demonstrate only minor weight differences as they age. **(B)** D2;R6/1 mice do, however, show progressive decline in performance on the accelerating rotarod beginning at approx. 12 weeks of age. N = 5 per genotype. WTL = wild type littermate.

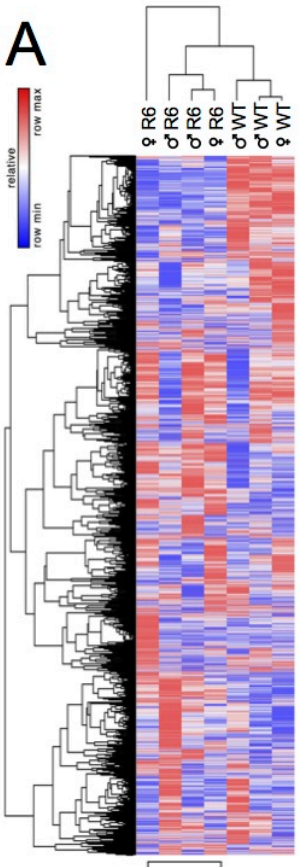

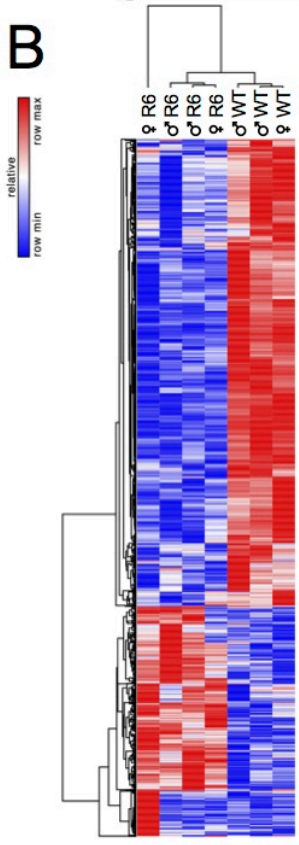

C

Downregulated Gene (N = 829) Associated Topics

Ingenuity Canonical Pathways	P-value
G-Protein Coupled Receptor Signaling	7.94E-15
cAMP-mediated signaling	2.00E-13
Gαi Signaling	1.15E-07
Dopamine-DARPP32 Feedback in cAMP Signaling	1.86E-06
Gαq Signaling	2.24E-06
VDR/RXR Activation	2.95E-06
Synaptic Long Term Potentiation	9.55E-06
Calcium Signaling	1.41E-05

Upstream Regulator	P-value
HTT	1.22E-56
dopamine	1.91E-15
CREB1	2.00E-14
BDNF	3.83E-14
HDAC4	4.36E-10
CREM	1.56E-09
BCL11B	5.85E-09
quinolinic acid	6.54E-09

Component	P-value
neuron part	9.66E-25
neuron projection	2.21E-22
cell projection	5.28E-20
synapse part	5.79E-17
cell projection part	1.63E-15
synapse	1.90E-14
cell junction	1.97E-14
synaptic membrane	4.84E-14

Function	P-value
protein binding	7.52E-28
binding	1.94E-21
metal ion transmembrane transporter activity	2.00E-13
cation channel activity	1.17E-12
GTPase regulator activity	2.74E-12
voltage-gated cation channel activity	2.98E-12
nucleoside-triphosphatase regulator activity	8.39E-12
ion channel activity	9.98E-12

Process	P-value
regulation of cell communication	4.09E-24
regulation of signaling	7.45E-24
regulation of ion transport	5.89E-23
regulation of localization	3.09E-20
single-organism behavior	1.03E-19
regulation of system process	1.83E-19
regulation of transport	1.13E-18
behavior	2.01E-18

Upregulated Gene (N = 406) Associated Topics

Ingenuity Canonical Pathways	P-value
Axonal Guidance Signaling	3.63E-03
Triacylglycerol Degradation	9.77E-03
Glutathione-mediated Detoxification	1.15E-02
Glutamate Receptor Signaling	1.32E-02
Neuroprotective Role of THOP1 in Alzheimer's Disease	1.35E-02
Vitamin-C Transport	2.51E-02
Glutamate Removal from Folates	2.51E-02
Anandamide Degradation	2.51E-02

Upstream Regulator	P-value
NFE2L2	1.22E-03
APP	1.95E-03
WNT1	3.47E-03
HTT	6.45E-03
PRDM8	8.39E-03
BDNF	1.46E-02
beta-estradiol	1.53E-02
NKX2-1	1.92E-02

Component	P-value
extracellular region part	5.20E-07
synapse	3.37E-05
unconventional myosin complex	7.28E-05
extracellular matrix	9.51E-05
proteinaceous extracellular matrix	1.82E-04
basement membrane	3.36E-04
extracellular matrix part	3.73E-04
cell surface	4.47E-04

Function	P-value
transporter activity	1.10E-05
substrate-specific transporter activity	2.40E-05
transmembrane transporter activity	2.92E-05
substrate-specific transmembrane transporter activity	5.92E-05
metal ion transmembrane transporter activity	7.22E-05
peptide hormone binding	1.59E-04
calcium ion binding	2.26E-04
substrate-specific channel activity	2.46E-04

Process	P-value
single-organism transport	1.97E-05
positive regulation of smoothened signaling pathway	2.63E-05
anatomical structure morphogenesis	2.76E-05
symbiont intracellular protein transport in host	2.96E-05
intracellular transport of viral proteins in host cell	2.96E-05
intracellular protein transport in other organism involved in symbiotic interaction	2.96E-05
establishment of localization	4.59E-05
regulation of BMP signaling pathway	4.87E-05

Figure 3: Transcriptional profiling of D2GFP;R6/1 mice reveals canonical HD-associated pathways. (A) Hierarchical clustering of all protein-coding genes (N = 15,416) in the samples produces a separation of wild type and HD mice. **(B)** When focusing on genes that are significantly differentially expressed (N = 1235), this clustering does not change, indicating a significant change in global transcriptional profile in HD mice. **(C)** The top 8 listings for selected topics are shown when downregulated (left column) or upregulated (right column) genes were analyzed by Ingenuity Pathway Analysis or GOrilla gene set enrichment tools. Many are commonly associated with dysregulated pathways and processes in HD. R6 = R6/1; WT = Wild type littermate.

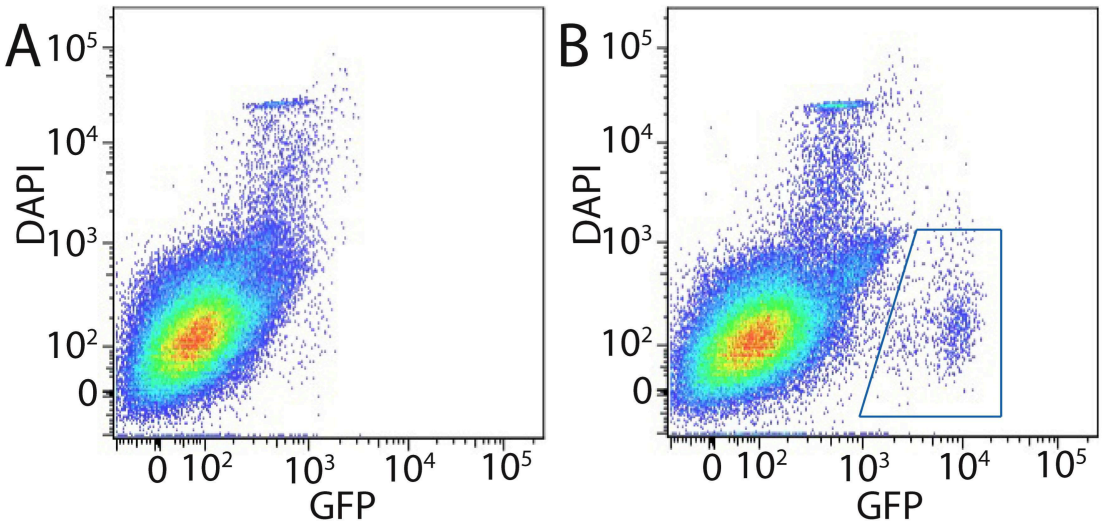

Figure 4: GFP+ events are visible by flow cytometry only in mice carrying the D2GFP transgene. Striata were dissected and neurons processed into single cell suspension as described in the Methods. When analyzed by flow cytometry, a population of GFP+ (X axis), DAPI- (Y axis) events is only visible in mice carrying the D2GFP transgene **(B)**, and is absent in animals lacking the transgene **(A)**.

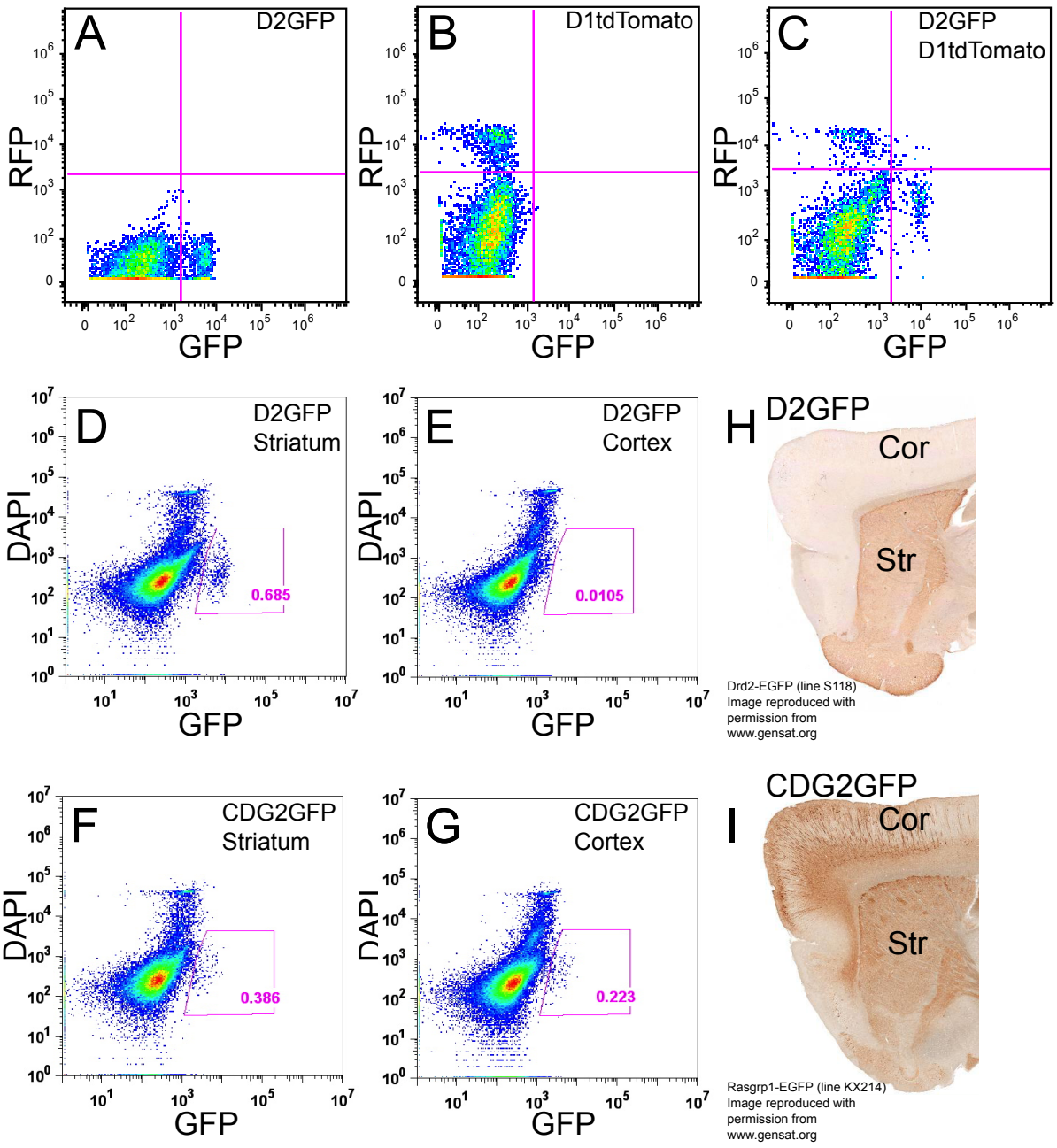

Figure 5: In mice carrying D2GFP, D1tdTomato, and/or CDG2GFP, the appropriate populations are visible by flow cytometry. Mice carrying D2GFP only **(A)**, D1tdTomato only **(B)**, or both transgenes **(C)** were analyzed by flow cytometry. Events fitting the forward scatter and side scatter profile of MSNs were analyzed for GFP (X axis) and RFP (Y axis). Mice carrying only the D2GFP transgene (A) showed GFP+ events but no RFP+ events, while those carrying only the D1tdTomato transgene (B) showed no GFP+ events but a population of RFP+ events. Double transgenic mice (C) showed both populations, but very few events positive for both events, consistent with

the fact that MSNs typically express either D1 or D2 receptors but rarely both. Separately, either cortical or striatal tissue from mice expressing either D2GFP or CDG2GFP were subjected to flow cytometry for detection of GFP+, DAPI- events (gated). In D2GFP mice (D and E), such events were only seen in the striatum, while CDG2GFP animals (F and G) had GFP+ events in both cortex and striatum. This agrees with the immunostaining patterns of GFP from these strains (H and I), as obtained from the GENSAT database (reproduced with permission from www.gensat.org).

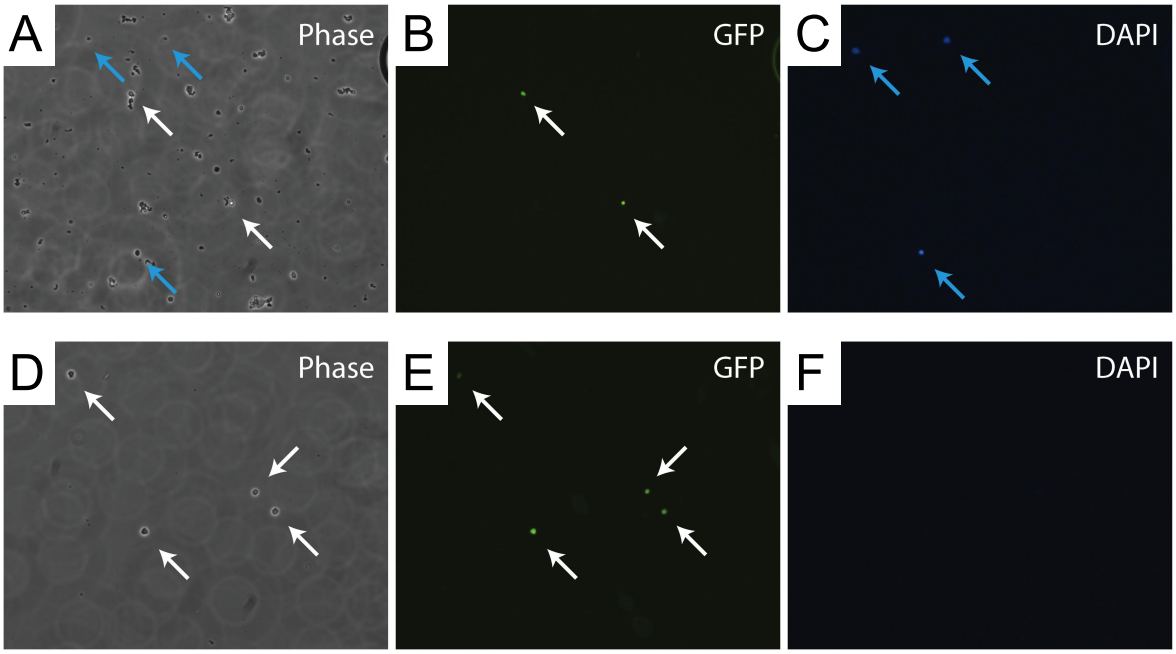

Figure 6: GFP+ events can be sorted, eliminating debris and dead (DAPI+) events. **(A)** Striata from D2GFP mice, when processed into single cell suspension, contain largely debris. **(B)** Rare GFP+ events, with a size and shape reasonable of a cell, are visible, while **(C)** some other events are DAPI+. Consistent with flow cytometry analysis, no cells contain both GFP and DAPI. **(D)** After sorting, no debris is visble, and all of the visible cells are **(E)** GFP+ and **(F)** DAPI-.

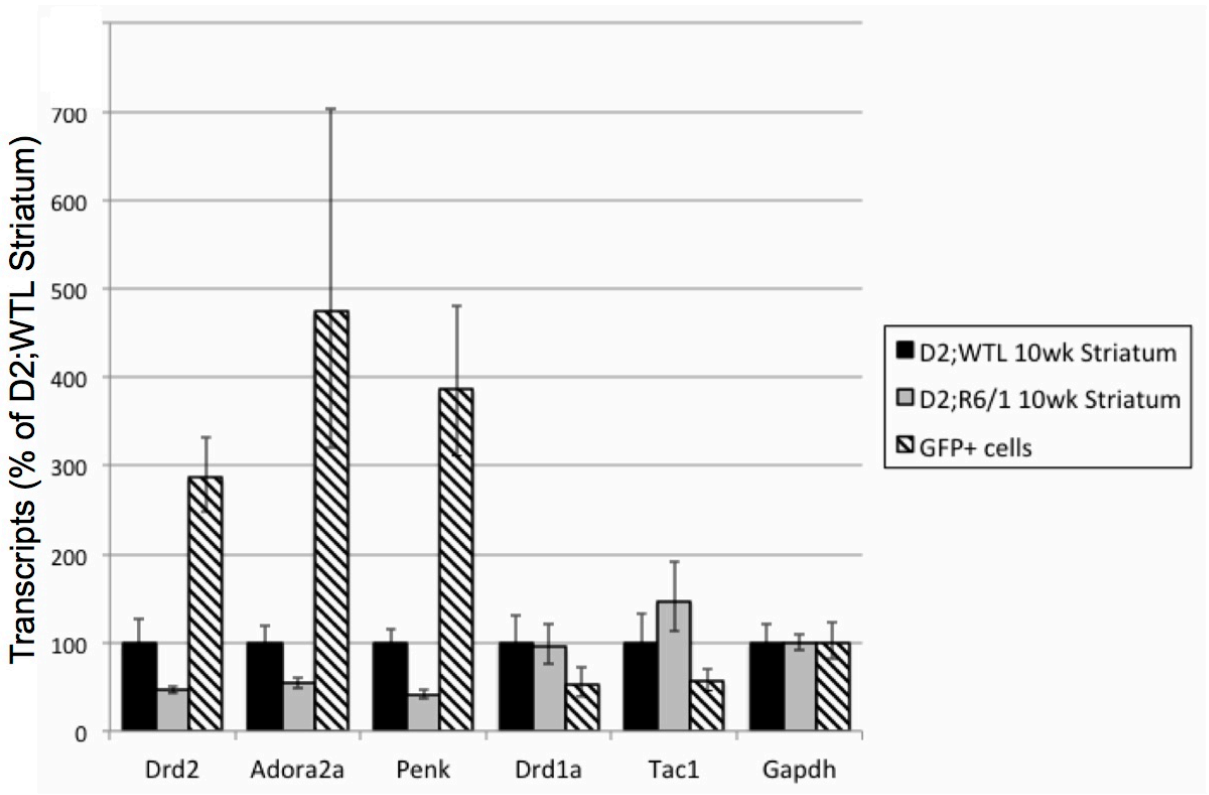

Figure 7: GFP+, DAPI- events sorted from D2GFP striatal suspensions have mRNA profiles consistent with indirect MSNs. After sorting, GFP+, DAPI- events from D2GFP mice (striped bars) show enrichment of *Drd2*, *Penk*, and *Adora2a* transcripts compared to whole striatum (black bars). These transcripts are known to be present in MSNs of the indirect pathway, while those of *Drd1a* and *Tac1* are enriched in direct MSNs and are depleted in D2GFP events compared to whole striatum. Additionally, *Drd2*, *Penk*, and *Adora2a* were reduced in R6/1 striatum compared to wild type striatum (grey bars), as would be expected based on previous studies.

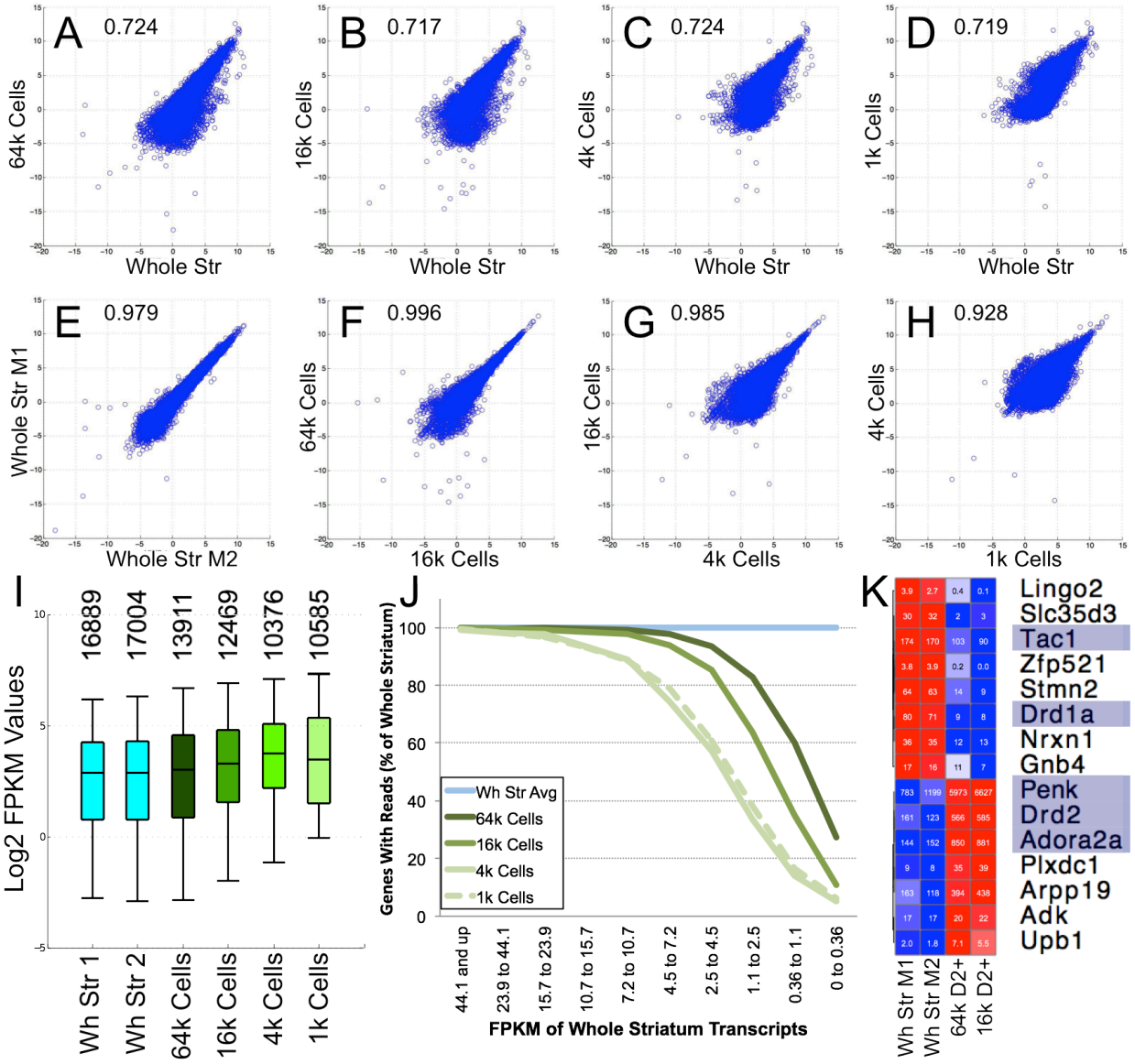

Figure 8: Flow-sorted D2GFP events can produce viable RNAseq libraries. (A-D) Plotted versus the transcripts in whole striatum (X axis), sorted D2GFP RNAseq libraries (Y axis) have significant similarities to non-sorted tissue. **(E-H)** Striatal replicates have striking similarities, as do libraries prepared from either 64,000 or 16,000 D2GFP cells. Further dilutions reveal weaker correlations (16,000 vs. 4000, or 4000 vs. 1000 cell libraries). **(I)** Not only are fewer total genes mapped in sorted cell libraries (top), but genes with >0 reads have higher absolute FPKM values on the lower and upper ends of libraries from fewer cells. **(J)** Low abundance transcripts in whole striatum are completely absent from RNAseq libraries made from fewer sorted cells. **(K)** Transcripts reportedly enriched in direct (top eight) or indirect (bottom seven) MSNs also demonstrate either depletion or enrichment in D2GFP MSNs compared to whole striatum. Highlighted genes were tested by QPCR (Figure 7).

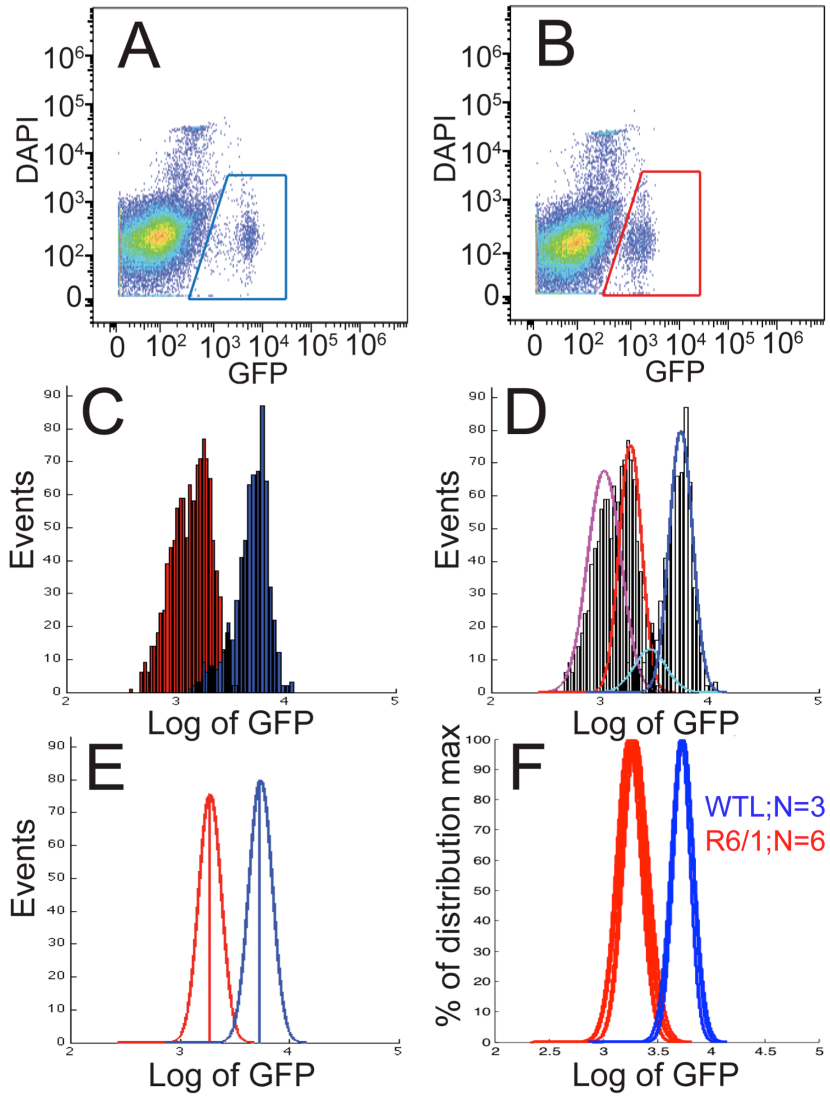

Figure 9: GFP content from D2GFP neurons can be accurately quantitated using Gaussian means regression (GMR). (A) The GFP (X axis) and DAPI (Y axis) profiles of wild type mice show a clear population of GFP+ MSNs. **(B)** Similar profiles from 16 week old R6/1 animals are nearly identical, except for the reduced GFP content of the cells. **(C)** When viewed as a histogram, the GFP+ events appear to each contain two distributions. **(D)** These distributions can be computationally separated using Gaussian means regression (in red and magenta, the two distributions from an R6/1 mouse; in blue and cyan, the distributions from a wild type mouse). **(E)** For the purposes of quantification, the mean of the higher (right-most) distribution is used as an animal's GFP level. **(F)** When such analysis is performed, animals within a cohort can demonstrate striking similarity within a genotype. For (C) through (F), R6/1 is plotted in red/magenta, and WTL is plotted in blue/cyan. WTL = wild type littermate.

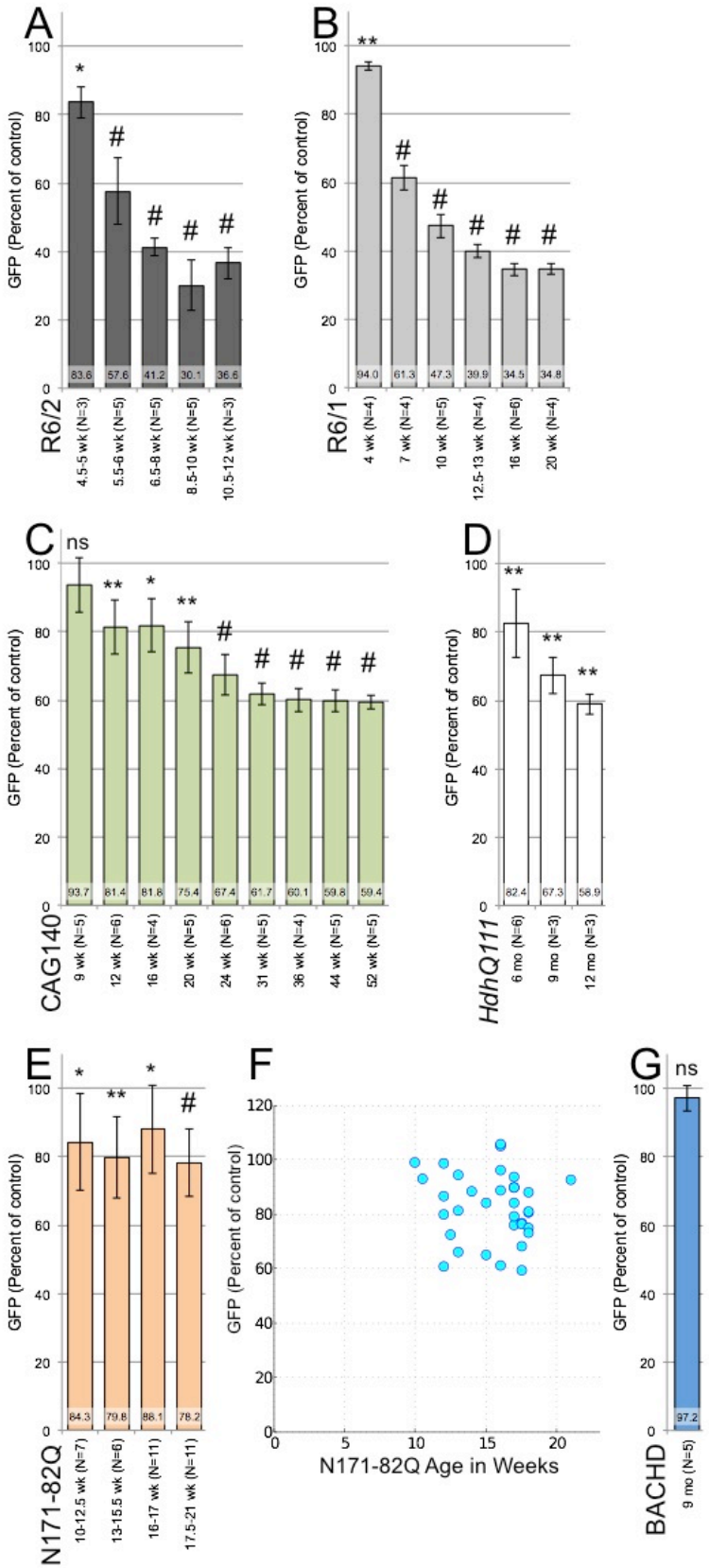
A
B
C
D
E
F
G
GFP (Percent of control)
R6/2
4.5-5 wk (N=3)
5.5-6 wk (N=5)
6.5-8 wk (N=5)
8.5-10 wk (N=5)
10.5-12 wk (N=3)
83.6
57.6
41.2
30.1
36.6
R6/1
4 wk (N=4)
7 wk (N=4)
10 wk (N=5)
12.5-13 wk (N=4)
16 wk (N=6)
20 wk (N=4)
94.0
61.3
47.3
39.9
34.5
34.8
CAG140
9 wk (N=5)
12 wk (N=6)
16 wk (N=4)
20 wk (N=5)
24 wk (N=6)
31 wk (N=5)
36 wk (N=4)
44 wk (N=5)
52 wk (N=5)
93.7
81.4
81.8
75.4
67.4
61.7
60.1
59.8
59.4
HdhQ111
6 mo (N=6)
9 mo (N=3)
12 mo (N=3)
82.4
67.3
58.9
N171-82Q
10-12.5 wk (N=7)
13-15.5 wk (N=6)
16-17 wk (N=11)
17.5-21 wk (N=11)
84.3
79.8
88.1
78.2
N171-82Q Age in Weeks
BACHD
9 mo (N=5)
97.2
ns

Figure 10: When quantified by Gaussian means regression, most strains of HD model mice show remarkable intra-cohort consistency in their GFP declines. MSNs from D2GFP mice crossed to the R6/2 **(A)** and R6/1 **(B)** strains show a rapid and consistent decline in GFP levels, reaching a floor of approximately 35% of control levels in both strains by end stage. Two knockin strains, CAG140 **(C)** and HdhQ111 **(D)**, also demonstrate a decline in MSN GFP levels, though it is less consistent in young animals. Both strains have a similar floor of ~60% of control levels. However, this phenotype is not universal in HD model mice. D2;N171-82Q animals **(E)** have a highly inconsistent phenotype in spite of statistically significant differences. Looking at each individual N171-82Q's normalized GFP levels **(F)**, it is clear that penetrance is incomplete and the degree of impairment is highly variable; also, there appears to be no worsening as mice age. Additionally, mice of the strain BACHD **(G)** show no significant decline in GFP at 9 months of age. (ns) = not significant; (*) = $P < 0.05$; (**) = $P < 0.01$; (#) = $P < 0.001$. For strains R6/2, R6/1, CAG140, N171-82Q, and BACHD, comparisons were between hemi- or heterozygous mice and wild type littermates. For strain HdhQ111, comparisons were between homozygotes and heterozygotes.

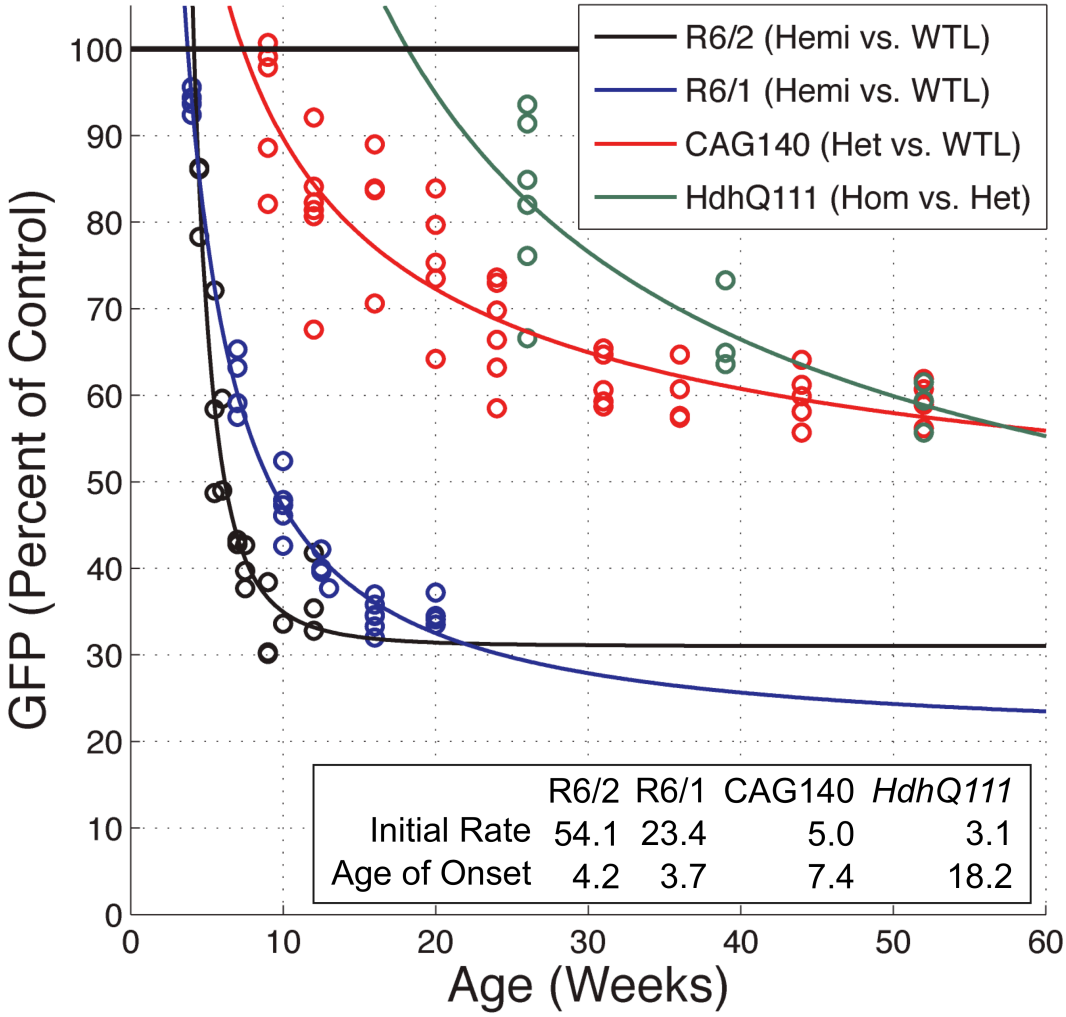

Figure 11: GFP analysis can be used to predict age of onset and rate of GFP loss for strains at a given age. The data from Figure 10, when scatter plotted and curve fitted, can be used to predict the age of onset for a given strain (the age at which the curve crosses the 100 value, representing the latest age at which the genotypes are expected to have equal GFP levels to controls). In addition, this fit curve can give the rate of decline at a given age, shown calculated for the initial rate of decline (the slope at the age of onset). The different floors of the strains as well as the differences between the strains' variance at different ages is also clear when plotted this way.

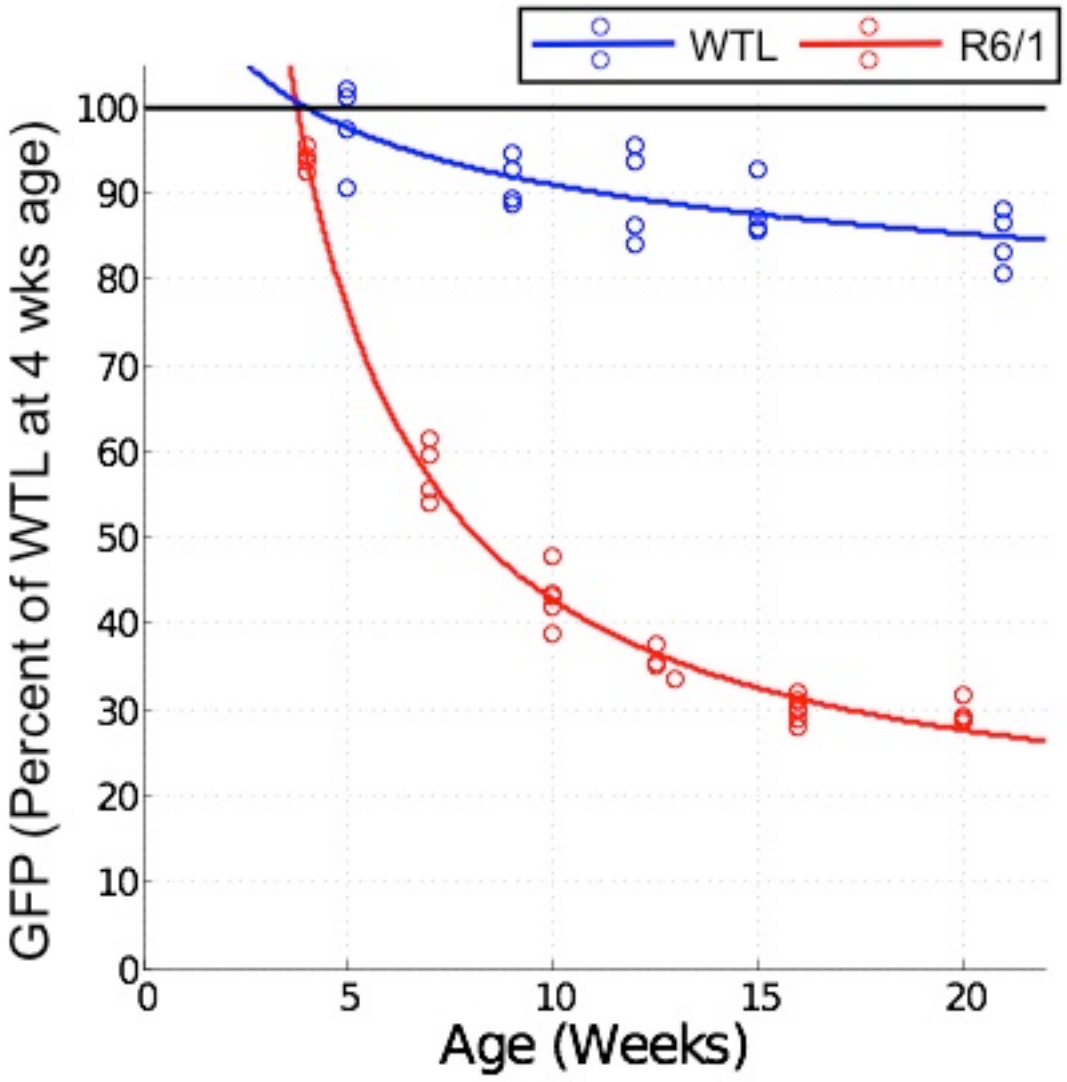

Figure 12: D2GFP levels decline over time in wild type mice. Because each sample collection is internally calibrated to control littermates, there is no reliable way to compare the absolute GFP values between cohorts gathered on different days, as the cytometer settings can be altered, producing significant differences. For this reason, to analyze GFP changes in wild type animals, several cohorts of different ages (blue) were analyzed on the same day, demonstrating a weak decline in GFP values over 21 weeks (two animals per age, analyzed in duplicate). For comparison, the decline of R6/1 mice is plotted (red), having been readjusted to the wild type values expected from the longitudinal curve.

			N to conclude % rescue		
Model	**Age**	**Mean±SD GFP**	**5%**	**10%**	**20%**
R6/2	6.5-8 wk	41.2±2.5	6	2	1
	8.5-10 wk	30.1±7.4	36	9	3
	10.5-12 wk	36.6±4.6	17	5	2
R6/1	7 wk	61.3±3.6	28	7	2
	16 wk	34.5±1.8	3	1	1
CAG140	31 wk	61.7±3.1	21	6	2
	36 wk	60.1±3.4	24	6	2
	44 wk	59.8±3.2	20	5	2
HdhQ111	12 mo	58.9±2.9	17	5	2
Q94 AAV	4 wk	53.8±4.1	26	7	2

Table 1: Power analyses for D2GFP levels versus control in HD models. Based on the mean and standard deviations of the normalized GFP levels (Mean±SD GFP) for selected cohorts, power analysis was carried out (power = 80%, P = 0.05) to determine how many animals would be required to reliably (80% chance) detect a given degree of therapeutic D2GFP rescue at a significance of $P \leq 0.05$. PI = Post-infection. Note: the final experiment listed (Q94 AAV) is described in Chapter 5, but was included in this table for context.

Bibliography

1. Luthi-Carter R, Strand A, Peters NL, Solano SM, Hollingsworth ZR, Menon AS, et al. Decreased expression of striatal signaling genes in a mouse model of Huntington's disease. Hum Mol Genet. 2000 May 22;9(9):1259–71.

2. Kuhn A, Goldstein DR, Hodges A, Strand AD, Sengstag T, Kooperberg C, et al. Mutant huntingtin“s effects on striatal gene expression in mice recapitulate changes observed in human Huntington”s disease brain and do not differ with mutant huntingtin length or wild-type huntingtin dosage. Hum Mol Genet. 2007 May 20;16(15):1845–61.

3. Hodges A, Hughes G, Brooks S, Elliston L, Holmans P, Dunnett SB, et al. Brain gene expression correlates with changes in behavior in the R6/1 mouse model of Huntington's disease. Genes Brain Behav. 2008 Apr 1;7(3):288–99.

4. Strand AD, Baquet ZC, Aragaki AK, Holmans P, Yang L, Cleren C, et al. Expression profiling of Huntington's disease models suggests that brain-derived neurotrophic factor depletion plays a major role in striatal degeneration. J Neurosci. 2007 Oct 24;27(43):11758–68.

5. Raymond LA, Andre VM, Cepeda C, Gladding CM, Milnerwood AJ, Levine MS. Pathophysiology of Huntington's disease: time-dependent alterations in synaptic and receptor function. Neuroscience. 2011 Aug 27.

6. Andrews TC, Weeks RA, Turjanski N, Gunn RN, Watkins LH, Sahakian B, et al. Huntington's disease progression. PET and clinical observations. Brain. 1999 Dec 1;122 (Pt 12):2353–63.

7. Glass M, Dragunow M, Faull RL. The pattern of neurodegeneration in Huntington“s disease: a comparative study of cannabinoid, dopamine, adenosine and GABA(A) receptor alterations in the human basal ganglia in Huntington”s disease. NSC. 2000;97(3):505–19.

8. Cha JH, Kosinski CM, Kerner JA, Alsdorf SA, Mangiarini L, Davies SW, et al. Altered brain neurotransmitter receptors in transgenic mice expressing a portion of an abnormal human huntington disease gene. Proc Natl Acad Sci USA. 1998 May 26;95(11):6480–5.

9. Cha JH, Frey AS, Alsdorf SA, Kerner JA, Kosinski CM, Mangiarini L, et al. Altered neurotransmitter receptor expression in transgenic mouse models of Huntington's disease. Philos Trans R Soc Lond, B, Biol Sci. 1999 Jun 29;354(1386):981–9.

10. Turmaine M, Raza A, Mahal A, Mangiarini L, Bates GP, Davies SW. Nonapoptotic neurodegeneration in a transgenic mouse model of Huntington's disease. Proc Natl Acad Sci USA. 2000 Jul 5;97(14):8093–7.

11. Hickey MA, Kosmalska A, Enayati J, Cohen R, Zeitlin S, Levine MS, et al.

Extensive early motor and non-motor behavioral deficits are followed by striatal neuronal loss in knock-in Huntington's disease mice. NSC. 2008 Nov 11;157(1):280–95.

12. Cyr M, Sotnikova TD, Gainetdinov RR, Caron MG. Dopamine enhances motor and neuropathological consequences of polyglutamine expanded huntingtin. The FASEB Journal. 2006 Dec;20(14):2541–3.

13. Stack EC, Dedeoglu A, Smith KM, Cormier K, Kubilus JK, Bogdanov M, et al. Neuroprotective effects of synaptic modulation in Huntington's disease R6/2 mice. J Neurosci. 2007 Nov 21;27(47):12908–15.

14. Gong S, Zheng C, Doughty ML, Losos K, Didkovsky N, Schambra UB, et al. A gene expression atlas of the central nervous system based on bacterial artificial chromosomes. Nature. 2003 Oct 30;425(6961):917–25.

15. Shuen JA, Chen M, Gloss B, Calakos N. Drd1a-tdTomato BAC transgenic mice for simultaneous visualization of medium spiny neurons in the direct and indirect pathways of the basal ganglia. J Neurosci. 2008 Mar 12;28(11):2681–5.

16. Kramer PF, Christensen CH, Hazelwood LA, Dobi A, Bock R, Sibley DR, et al. Dopamine D2 receptor overexpression alters behavior and physiology in Drd2-EGFP mice. J Neurosci. 2011 Jan 5;31(1):126–32.

17. Chan CS, Peterson JD, Gertler TS, Glajch KE, Quintana RE, Cui Q, et al. Strain-specific regulation of striatal phenotype in Drd2-eGFP BAC transgenic mice. J Neurosci. 2012 Jul 4;32(27):9124–32.

18. Brooks SP, Janghra N, Workman VL, Bayram-Weston Z, Jones L, Dunnett SB. Longitudinal analysis of the behavioural phenotype in R6/1 (C57BL/6J) Huntington's disease transgenic mice. Brain Res Bull. 2011 Jan 25.

19. Bayram-Weston Z, Jones L, Dunnett SB, Brooks SP. Light and electron microscopic characterization of the evolution of cellular pathology in the R6/1 Huntington's disease transgenic mice. Brain Res Bull. 2011 Jul 23.

20. van Dellen A, Blakemore C, Deacon R, York D, Hannan AJ. Delaying the onset of Huntington's in mice. Nature. 2000 Apr 13;404(6779):721–2.

21. Graybiel AM. The basal ganglia: learning new tricks and loving it. Curr Opin Neurobiol. 2005 Dec;15(6):638–44.

22. Lobo MK, Karsten SL, Gray M, Geschwind DH, Yang XW. FACS-array profiling of striatal projection neuron subtypes in juvenile and adult mouse brains. Nat Neurosci. 2006 Mar;9(3):443–52.

23. Crittenden JR, Cantuti-Castelvetri I, Saka E, Keller-McGandy CE, Hernandez LF, Kett LR, et al. Dysregulation of CalDAG-GEFI and CalDAG-GEFII predicts the

severity of motor side-effects induced by anti-parkinsonian therapy. Proc Natl Acad Sci USA. 2009 Feb 24;106(8):2892–6.

24. Gerfen CR, Engber TM, Mahan LC, Susel Z, Chase TN, Monsma FJ, et al. D1 and D2 dopamine receptor-regulated gene expression of striatonigral and striatopallidal neurons. Science. 1990 Dec 7;250(4986):1429–32.

25. Schiffmann SN, Vanderhaeghen JJ. Adenosine A2 receptors regulate the gene expression of striatopallidal and striatonigral neurons. J Neurosci. 1993 Mar;13(3):1080–7.

26. Mangiarini L, Sathasivam K, Seller M, Cozens B, Harper A, Hetherington C, et al. Exon 1 of the HD gene with an expanded CAG repeat is sufficient to cause a progressive neurological phenotype in transgenic mice. Cell. 1996 Nov 1;87(3):493–506.

27. Li JY, Popovic N, Brundin P. The use of the R6 transgenic mouse models of Huntington's disease in attempts to develop novel therapeutic strategies. NeuroRx : the journal of the American Society for Experimental NeuroTherapeutics. 2005 Jul 1;2(3):447–64.

28. Gil JM, Rego AC. The R6 lines of transgenic mice: a model for screening new therapies for Huntington's disease. Brain research reviews. 2009 Mar;59(2):410–31.

29. Carter RJ, Lione LA, Humby T, Mangiarini L, Mahal A, Bates GP, et al. Characterization of progressive motor deficits in mice transgenic for the human Huntington's disease mutation. J Neurosci. 1999 Apr 15;19(8):3248–57.

30. Wheeler VC, Auerbach W, White JK, Srinidhi J, Auerbach A, Ryan A, et al. Length-dependent gametic CAG repeat instability in the Huntington's disease knock-in mouse. Hum Mol Genet. 1999 Jan;8(1):115–22.

31. Menalled LB, Sison JD, Dragatsis I, Zeitlin S, Chesselet M-F. Time course of early motor and neuropathological anomalies in a knock-in mouse model of Huntington's disease with 140 CAG repeats. J. Comp. Neurol. 2003 Oct 6;465(1):11–26.

32. Rising AC, Xu J, Carlson A, Napoli VV, Denovan-Wright EM, Mandel RJ. Longitudinal behavioral, cross-sectional transcriptional and histopathological characterization of a knock-in mouse model of Huntington's disease with 140 CAG repeats. Experimental Neurology. 2011 Apr;228(2):173–82.

33. Wheeler VC, Gutekunst C-A, Vrbanac V, Lebel L-A, Schilling G, Hersch S, et al. Early phenotypes that presage late-onset neurodegenerative disease allow testing of modifiers in Hdh CAG knock-in mice. Hum Mol Genet. 2002 Mar 15;11(6):633–40.

34. Schilling G, Becher MW, Sharp AH, Jinnah HA, Duan K, Kotzuk JA, et al. Intranuclear inclusions and neuritic aggregates in transgenic mice expressing a mutant N-terminal fragment of huntingtin. Hum Mol Genet. 1999 Mar 1;8(3):397–407.

35. Yu Z-X, Li S-H, Evans J, Pillarisetti A, Li H, Li X-J. Mutant huntingtin causes context-dependent neurodegeneration in mice with Huntington's disease. J Neurosci. 2003 Mar 15;23(6):2193–202.

36. Gray M, Shirasaki DI, Cepeda C, André VM, Wilburn B, Lu X-H, et al. Full-length human mutant huntingtin with a stable polyglutamine repeat can elicit progressive and selective neuropathogenesis in BACHD mice. J Neurosci. 2008 Jun 11;28(24):6182–95.

37. Pouladi MA, Stanek LM, Xie Y, Franciosi S, Southwell AL, Deng Y, et al. Marked differences in neurochemistry and aggregates despite similar behavioural and neuropathological features of Huntington disease in the full-length BACHD and YAC128 mice. Hum Mol Genet. 2012 Feb 27.

38. Hersch SM, Ferrante RJ. Translating therapies for Huntington's disease from genetic animal models to clinical trials. NeuroRx : the journal of the American Society for Experimental NeuroTherapeutics. 2004 Jul;1(3):298–306.

39. Slow EJ, van Raamsdonk J, Rogers D, Coleman SH, Graham RK, Deng Y, et al. Selective striatal neuronal loss in a YAC128 mouse model of Huntington disease. Hum Mol Genet. 2003 Jul 1;12(13):1555–67.

40. Weiss A, Klein C, Woodman B, Sathasivam K, Bibel M, Régulier E, et al. Sensitive biochemical aggregate detection reveals aggregation onset before symptom development in cellular and murine models of Huntington's disease. J Neurochem. 2008 Feb;104(3):846–58.

41. Hickey MA, Gallant K, Gross GG, Levine MS, Chesselet M-F. Early behavioral deficits in R6/2 mice suitable for use in preclinical drug testing. Neurobiology of Disease. 2005 Oct;20(1):1–11.

42. Citron BA, Dennis JS, Zeitlin RS, Echeverria V. Transcription factor Sp1 dysregulation in Alzheimer's disease. J Neurosci Res. 2008 Aug 15;86(11):2499–504.

43. Gómez Ravetti M, Rosso OA, Berretta R, Moscato P. Uncovering molecular biomarkers that correlate cognitive decline with the changes of hippocampus“ gene expression profiles in Alzheimer”s disease. PLoS ONE. 2010;5(4):e10153.

44. Dumitriu A, Latourelle JC, Hadzi TC, Pankratz N, Garza D, Miller JP, et al. Gene expression profiles in Parkinson disease prefrontal cortex implicate FOXO1 and genes under its transcriptional regulation. PLoS Genet. 2012 Jun;8(6):e1002794.

45. Southwell AL, Warby SC, Carroll JB, Doty CN, Skotte NH, Zhang W, et al. A fully humanized transgenic mouse model of Huntington disease. Hum Mol Genet. 2012 Oct 5.

46. Lee J-M, Ramos EM, Lee J-H, Gillis T, Mysore JS, Hayden MR, et al. CAG repeat expansion in Huntington disease determines age at onset in a fully dominant fashion. Neurology. 2012 Mar 6;78(10):690–5.

47. Cornett J, Smith L, Friedman M, Shin J-Y, Li X-J, Li S-H. Context-dependent dysregulation of transcription by mutant huntingtin. J Biol Chem. 2006 Nov 24;281(47):36198–204.

48. Luthi-Carter R, Strand AD, Hanson SA, Kooperberg C, Schilling G, La Spada AR, et al. Polyglutamine and transcription: gene expression changes shared by DRPLA and Huntington's disease mouse models reveal context-independent effects. Hum Mol Genet. 2002 Aug 15;11(17):1927–37.

49. Poltorak A, He X, Smirnova I, Liu MY, van Huffel C, Du X, et al. Defective LPS signaling in C3H/HeJ and C57BL/10ScCr mice: mutations in Tlr4 gene. Science. 1998 Dec 11;282(5396):2085–8.

CHAPTER 5 – ASSESSING AAV AND CYSTAMINE MODULATION OF D2GFP LOSS

Introduction

My D2GFP flow cytometry assay has potential as a preclinical assay. For further validation, I wished to see whether the phenotype could be altered genetically or pharmacologically. For genetic modulation, there is a substantial literature on the ability to introduce, upregulate, or downregulate potential modifiers of HD in mice in order to investigate the therapeutic potential in altering a given gene or pathway. A sampling of such studies accomplished purely through crossbreeding is given in Table 1. Studies are often done genetically because relatively few proteins of interest have an activity that can be drugged with enough specificity and proper pharmacokinetics to obtain a relevant result. Such drugs can often be developed through a concerted effort including small molecule library screening and medicinal chemistry, but the research community must be sure that modulating a given target will actually have a beneficial impact in HD models before devoting the time and resources to identifying such a molecule.

The studies in Table 1 were each designed based on the belief that knockout or overexpression of a given gene is expected to modulate a pathway relevant to mHTT toxicity. While most were able to come to conclusive results, they require a tremendous amount of resources in the form of time and material investment. With my D2GFP flow cytometry assay, there is now a rapid way of measuring the progression of a single disease-relevant phenotype in small cohorts of animals. At minimum, there is potential here for using this assay as a pre-screen of sorts. Clearly, proper preclinical trials require careful behavioral and neuropathological analyses to detect improvement, but

many of the trials in Table 1 demonstrated transcriptional improvements in addition to the motor, behavioral, and/or survival benefits. Importantly, none tested for and failed to detect transcriptional rescue while succeeding in demonstrating behavioral normalization. Because of the pleiotropic nature of transcriptional dysregulation and its appearance prior to most behavioral symptoms, it is plausible that rescue of the HD transcription profile (as measured by rescue of D2GFP loss) would be an ideal early signal that a given modifier or drug warrants further study.

While this could be achieved by crossing knockout or transgenic strains into the D2GFP;HD background, there are several advantages to using viral vectors for the introduction of transgenes. Rather than working to acquire and breed knockout or transgenic strains into D2GFP;HD model mice, transgenes or knockdown constructs can be cloned and validated rapidly in tissue culture prior to delivery to D2GFP;HD animals. There would be less of an opportunity to test for behavioral improvements, which would require significant infectivity in the tissue, but as I will demonstrate, the flow cytometry protocol allows for conclusive results to be generated despite minimal tissue infectivity. This only requires that the vector co-delivers a fluorescent protein in a different fluorescence spectrum to that of GFP (in this case, RFP).

Therefore, to further test and validate the potential of my D2GFP flow cytometry assay in preclinical therapeutic testing, I constructed viral vectors to both induce and ameliorate this phenotype, and assayed for protection as either single vectors or in a pool. Additionally, I tested a small molecule (currently in clinical trials), cystamine, for an ability to alter transcriptional dysregulation as reported by D2GFP levels. It is my hope that the availability of a rapid, quantitative reporter system in the mouse brain for HD

pathology will improve the rapidity with which therapeutic interventions for HD can be discovered, validated and made ready for human clinical use.

Methods

Mice breeding, rotarod, flow cytometry of MSNs, QPCR, and RNAseq: Please see the Methods section of Chapter 4 for detailed protocols on our mouse breeding schemes, rotarod analysis, papain dissociation of MSNs, and transcriptional analysis by QPCR and RNAseq.

Cystamine treatment: Cystamine dihydrochloride (Sigma) was prepared to 15 mg/mL in PBS and filter sterilized (0.2 μm), and was either used fresh or stored at -20°C. PBS vehicle was prepared identically. Mice were dosed IP to 150 mg/kg by giving 0.01 mL per 1 g weight. On days when mice were tested on the rotarod, dosage came after all three rotarod trials.

Small-scale AAV production and purification: Viral capsids were assembled by cotransfection (TransIT LT1, Mirus, or calcium phosphate) of 32 μg AAV vector with 96 μg AAV rep2/cap1 helper plasmid (pDP1rs, PlasmidFactory) into a pair of 15 cm dishes of AAV-293 cells (Stratagene). Media was changed 24 hours post-transfection, and virus harvested 72 hours post-transfection. Cells were scraped, spun down (1100xg for 5 mins), and pellets resuspended in 5 mL PBS while media was kept and set aside. Next, cells were lysed by three successive freeze-thaw cycles (freeze in dry ice / ethanol, thaw in 37˚C water bath). Finally, the lysate was clarified by spinning at 3700xg

for 20 mins at 4˚C. Clarified lysate was mixed with media, and precipitated with a PEG – NaCl solution (5x solution contained 40% PEG-8000, 2.5 M NaCl, sterilized by autoclaving, and stored at RT). Precipitation took place at 4°C for >2 hrs, then pellets were spun at 2500xg for 30 mins at 4°C. Pellets were resuspended thoroughly in 4 mL PBS. AAV was next purified from the resuspended PEG precipitate using a stepwise iodixanol density gradient. Iodixianol (OptiPrep, 60% iodixanol solution, Sigma) buffers of various concentrations were prepared and underlayed into Beckman Ultra-Clear tubes (Catalog # 344085) as follows. First (top) layer, 3 mL: 15% iodixanol in PBS / 1 mM $MgCl_2$ (PBSM) with 0.86 M NaCl. Second layer, 2 mL: 25% iodixanol in PBSM. Third layer, 2 mL: 40% iodixanol in PBSM. Fourth (bottom) layer, 2 mL: 54% iodixanol in 1x PBSM. Viral lysate was then added up to the top of the tubes. The tubes were sealed with appropriate caps, and centrifuged at 40,000 rpm (150,000xg average) for 3.5 hrs at 18˚C. Layer 3 (second-to-bottom, 40% iodixanol) was collected with a syringe (18G) and concentration / LRS buffer exchange was carried out with 2-3 successive spins in Amicon Ultra-4 100K columns (Millipore), first 1500xg for ~25 mins, then 4000xg for ~15 mins, at 18˚C. Concentrated virus was titered by QPCR (PCR primers directed against the CAG promoter) and used for delivery *in vivo*. Viral titers were 1-2 x 10^{12} vector genomes/mL.

Stereotaxic delivery of AAV to mouse striatum: Animals (4 or 5 weeks of age) were given preemptive analgesia (0.1 mg/kg buprenorphine, 1.5 mg/kg meloxicam) and anesthetized (10 mg/kg xylazine, 120 mg/kg ketamine). The head was shaved, the animal was mounted into a stereotaxic frame, and the scalp sterilized prior to a 1 cm

midline incision to the scalp. Stereotaxic coordinates (left striatum) were 0.7 mm anterior, 1.8 mm left, and 3.5 mm ventral to bregma. A syringe (5 µL, Hamilton) carrying 3 µL virus was lowered and left in place for 5 mins. Virus was injected at 0.2 µL/min, and the needle was left in place for 3 mins post-injection, raised by 0.5 mm, then left for a further 4 mins before removal and wound closure. Animals were fed wet food for the first day post-op, and were singly housed after surgery until euthanasia.

Direct PCR of shRNA transgenes from flow sorted neurons: PCR amplification of the shRNA transgenes from sorted cells was specifically designed to perform only the minimal number of cycles required to gel isolate the amplified band. Cells were collected and spun down (2000xg), and the supernatant removed. 50 µL reactions of PCR Reaction 1 were prepared (Phire Direct PCR kit: 25 µL 2x Mix, 22 µL H_2O, 2 µL of a 5 µM barcoded primer stock, 1 µL Phire DNA polymerase). These 50 µL reaction mixes were added to the pelleted cells and mixed thoroughly, then incubated at RT for 5 mins. PCR Reaction 1 was performed for 22 cycles using the following cycling parameters:

Step 1: 50°C, 2 min

Step 2: 95°C, 10 min

Step 3: 98°C, 10 seconds

Step 4: 71°C, 1 min

Repeat of Steps 3-4 for a total of 22 cycles

PCR Reaction 2 was prepared (Phire Direct PCR kit: 30 µL 2x Mix, 23.3 µL H_2O, 2.4 µL of a 5 µM barcoded primer stock, 1.2 µL Phire DNA polymerase), enough for 60 µL

reactions per sample, and 3.1 μL of Reaction 1 was added to the appropriate PCR Reaction 2 (taking care to match the barcoded primers used), while the remainder of Reaction 1 was kept on ice. All Reaction 2 samples were mixed thoroughly and split into four 15 μL sub-reactions, which were cycled as follows:

Step 1: 50°C, 2 min

Step 2: 95°C, 10 min

Step 3: 98°C, 10 seconds

Step 4: 71°C, 1 min

Repeat of steps 3-4, total of either 4, 8, 12, or 16 cycles.

The sub-reactions were run on a 2% agarose gel to determine how many additional cycles of PCR Reaction 1 are required for proper amplification of the shRNA transgene (180 bp including primers), which is represented by first identifying the reaction at which this band is just clear enough for proper gel cutting, and then subtracting 4 from this (as PCR Reaction 2 includes 1/16 of PCR Reaction 1). PCR Reaction 1 was then cycled additionally (Steps 3-4) as appropriate, and was loaded in its entirety and run on a 2% gel for isolation of the 180 bp band. This band was submitted for Illumina sequencing, and reads were mapped to the predicted PCR products for each hairpin vector and counted.

Barcoded PCR primers used were as follows:

Forward primer (uniform, terminates immediately before shRNA sequence):

5'- AATGATACGGCGACCACCGAGATCTTGTGTTTTGAGACTATAAATATCCCTT…

…GGAGAAAGCCTTGTTTG-3'

Reverse primer (NNNNN designates barcode for multiplex analysis, and terminates right after shRNA sequence):

5'- CAAGCAGAAGACGGCATACGAGATNNNNNNGCGTATTGGGCGATCGCGGCG…

…CGCC-3'

Results

Adeno-associated Viral Vector Production and Purification

To deliver exogenous transgenes by AAV vector, I chose to produce the vectors myself rather than have them made for me by an outside group. This was because I anticipated needing many different vector preps, and both industrial and academic viral core facilities are expensive (~$2000-$5000 per prep by a survey of various sources) and slow (no less than 2 months). Thus, I adapted previous protocols (1) and began subcloning and producing my own AAV vectors capable of use *in vivo*. For most small-scale preps, the producer cell line is the standard HEK293, for many reasons. They are commonly available in most labs, are easy to culture, and are readily transfected. Importantly, they also naturally express an essential protein for AAV production, adenoviral E1 (the cell line was originally immortalized by introduction of sheared adenoviral DNA, as E1 inhibits p53 and Rb in a similar mechanism to SV40 large T antigen). Because AAV production requires E1 and several other adenoviral proteins, plus the two essential AAV cistrons (Rep and Cap), those not already in the cell line can be transiently transfected along with the vector plasmid for efficient AAV production and encapsidation.

A schematic for the production and purification is presented in Figure 1A, and is discussed in detail in the Materials and Methods. In short, virus is found both in the cytosol and in the media due to cell rupturing. To collect both, the clarified lysate is combined with the cell media, and viral particles in both are precipitated with polyethylene glycol. After centrifugation, this pellet contains many cellular proteins and vector particles, which are further purified by stepwise iodixanol density gradient ultracentrifugation. Vectors equilibrate in the third layer, and can be concentrated and buffer exchanged by dialysis or spin column concentrated (100 kDa MW cutoff) prior to delivery. A sample of the proteins present at each stage is shown in Figure 1B. As AAV infectivity is highly variable in culture (2), it is poorly predictive of *in vivo* infectivity; hence, rather than infectious units, titers are usually simply reported as genome copies per mL (GC/mL), determined by dot blot or QPCR.

AAV-delivered Transgenes Require 2 weeks for Activation in MSNs

To establish both the ability to identify AAV-infected cells by flow cytometry and the minimal incubation time, mice were injected with AAV vectors and incubated for 1, 2, 3, or 4 weeks, then harvested and their striata processed for flow cytometry (Figure 2A-D). All four demonstrated RFP fluorescence only in the injected hemisphere (uninjected not shown), but substantial transgene expression was not reached until two weeks post-injection. Cells identifiable as infected (Figure 2E) were specifically checked for the amount of visible RFP, which also required at least 2 weeks for maximum cell-by-cell transgene expression. This means the delay is not one of variable infectivity (some cells becoming infected sooner than others and reaching maximal transgene

expression quickly thereafter), but instead is a delay of transgene expression within the infected cells.

Exon 1 of *HTT* is Cytosolic, and Forms Perinuclear Inclusions Only with an Expanded polyQ

To demonstrate whether AAV-delivered transgenes can alter D2GFP levels, first I tested whether it can be induced acutely by exogenously-delivered mHTT. To do so, I cloned exon 1 of *HTT* into an AAV vector that I had prepared for shRNA delivery (Figure 3A). Because I wanted to be able to identify infected cells on the flow cytometer, I cloned the *HTT* fragment in frame with an RFP (specifically, AsRed) separated by a self-cleaving T2a peptide. There is evidence that this peptide cleaves, but incompletely (3), and I also observed this pattern. Transiently transfected HEK293 cells expressing the Q20-2a-RFP construct demonstrated significant cytosolic and nuclear fluorescence (Figure 3B), but nuclear RFP is the result of post-cleavage diffusion, as demonstrated by the absence of nuclear fluorescence in cells transfected by a similar construct missing the 2a peptide (Figure 3B inset). Meanwhile, *HTT* exon 1 with a pathogenic polyQ repeat (Q94-2a-RFP) shows similar cytosolic and nuclear fluorescence, but also the presence of inclusion bodies. This means the RFP present there is either fluorescing after becoming caught in the inclusions, or is the result of non-cleaved fusion proteins associating with inclusions through mHTT. The latter seems more likely, because fluorescent proteins are highly β-sheet rich, but if they associated with inclusions without the aid of fused mHTT, they would likely become denatured to the point of non-fluorescence. Histological sections from D2GFP mice carrying *mHTT*

transgenes support this, as there is no evidence of GFP flurescence in EM48+ inclusion bodies (Chapter 4, Figure 1D). Cells transfected with Q94-RFP constructs lacking the 2a peptide (Figure 3C inset) show similar inclusions, mostly found in cells without any other cytosolic or nuclear fluorescence, suggesting that most of the mHTT in these cells finds its way into inclusions.

mHTT Exon 1 Induces an Acute Drop in D2GFP Levels

The Q20-2a-RFP and Q94-2a-RFP constructs were packaged into AAV2/1 (genomic cis-elements from AAV2, capsid from AAV1) as described above, and delivered to the striatum of adult D2GFP animals (5 weeks of age). After a brief 4-week incubation period, where the transgene would only be expected to be fully active for 2 weeks, the mice were sacrificed and their striata processed for flow cytometry. In spite of low infectivity, RFP+ MSNs were visible in both groups (Figure 4A-B). However, because of the single-cell nature of the analysis, I do not rely on whole-tissue assessment of pathologic changes, so I can rapidly assess the specific impact of the transgene on infected cells, with the uninfected cells serving as an internal control. By separating the populations and analyzing their respective D2GFP levels (Figure 4C-D), I observed a significant reduction of GFP only in cells infected with the Q94 construct. When quantified (Figure 4E), this resulted in a 54% loss ($P = 0.0013$).

Closer inspection of the profiles of the Q94 infected mice suggested a possible correlation between higher RFP levels and lower GFP levels within the population. Because RFP and *mHTT* are monocistronic in the vector, they are produced in a 1:1 ratio, so cells with twice as much RFP fluorescence can be expected to have twice as

much mHTT, perhaps leading to more severe pathology and D2GFP loss. Analyzing these Q94 RFP+ populations (Figure 4F-I) revealed a significant correlation in 2 of 3 mice, and for the three populations analyzed as one. Significance was interrogated by permuting the RFP values 100,000 times and counting how often the resulting randomized population demonstrated stronger correlation than the original. These results demonstrate that transcriptional dysregulation can be acutely induced by expression of *mHTT* in adulthood, that AAV represents a rapid means of assessing the impact of *mHTT* on transcript levels, and that the amount of *mHTT* present in a given cell impacts the severity of the D2GFP loss.

Demonstration of Therapeutic Impact of an AAV-delivered shRNA Using the D2GFP FACS Assay

To further determine whether the observed progressive loss of GFP in D2GFP-expressing HD model mice is dependent on mHTT expression and could be alleviated by therapeutic intervention, I produced AAV vectors delivering two genes: RFP, and one of two short hairpin RNAs (shRNAs) (Figure 5A). shRNAs are short transcripts consisting of sense and antisense sequences of ~21 nucleotides separated by a small loop sequence, and they engage the RNAi machinery in the cell (4), degrading target mRNAs for which perfect complementarity is present. I generated two shRNA sequences, one negative control targeting a transcript absent in MSNs (*LacZ*, called shLacZ) and one targeting the polyCAG tract of *HTT* (called DhEx1_5). DhEx1_5 can effectively reduce HTT exon 1 protein product (Figure 5B) by 74% versus shLacZ, as assessed using an *mHTT* exon 1 fusion with luciferase. These AAV genomes were

separately packaged into viral particles (AAV2/1 as above) and delivered to the striatum of 4-week-old R6/2 mice in the D2GFP background, 3 mice per vector, and samples were harvested at 8 weeks of age (4 weeks post-infection).

Note that the expected rescue depends not just on the efficacy of the hairpin, but also on the duration of exposure, constrained in this case by the AAV life cycle. As demonstrated in Figure 2, AAV-delivered transgenes take at least 2 weeks for peak expression. I have not yet systematically assessed how long it takes an shRNA transgene to reach peak knockdown ability after AAV infection, but if we generously assume that the time course is similar to that of RFP expression, it may take 2 weeks for *mHTT* expression to be significantly reduced, and for D2GFP levels to stabilize post-infection. In this case, I can use the R6/2 progression curve (Chapter 4, Figure 10) to predict the maximum rescue. For this experiment, D2;R6/2 mice were injected at 4 weeks of age and harvested at 8 weeks of age. Halting of D2GFP decline by 2 weeks post-infection might cause infected cells' D2GFP levels to resemble those of 6-week-old mice, estimated to be ~51.9% of control, as opposed to ~39.2% of control in uninfected cells at 8 weeks of age. This would represent a 21% rescue (reduction in the amount of D2GFP lost) under ideal conditions, a small dynamic range for most behavioral assays but well above the detection threshold for my D2GFP assay.

After the brief 4-week incubation, the 8-week-old mice were sacrificed, striata were harvested and MSNs analyzed for GFP content. Comparisons were made within each striatum between the GFP content of RFP^+ (infected) and RFP^- (uninfected) cells. DhEx1_5 partially protected cells from GFP loss upon aging (Figure 5C). DhEx1_5 expressing cells' GFP levels were reduced to 47% of WT levels, while uninfected cells

had 39% of WT GFP (Figure 5E), perfectly agreeing with predictions from the time course and representing a rescue of 14 ± 4% in infected cells (P = 0.0014, Paired 2-tailed Student's T-test). This result is consistent with our power analysis (Chapter 4, Table 1), which suggests 8-week-old R6/2 mice require only 2 mice to detect a 10% rescue in D2GFP loss. Also, this is ~2/3 of the maximum rescue (21%) under the aforementioned assumptions of a 2-week post-infection delay in shRNA expression and arrest of D2GFP loss. The control AAV (shLacZ) had no effect on GFP loss (Figure 5D).

The shRNA data suggest that this AAV system can be used as a rapid, efficient system to assess cell autonomous effects of the modulation of a target gene on HD transcriptional dysregulation. However, it is worth emphasizing the importance of the disease model's rapidity for the therapeutic window and dynamic range. R6/2 mice have an extremely rapid progression, particularly in the D2GFP dysregulation assay, in which their levels bottom out by only 8 weeks of age. If an AAV is going to reach peak expression prior to the onset of D2GFP loss (4 weeks of age), the vector must be introduced to either embryos or pups, which complicates the protocol. On the other hand, if the same experimental paradigm were attempted in CAG140 mice (a strain whose D2GFP decline begins at ~7.5 weeks of age, as seen in Chapter 4, Figure 10), complete rescue of D2GFP dysregulation is plausible, with the tradeoff that this model requires ~7 months before reaching sufficient power to allow for small cohorts (Chapter 4, Table 1).

Knockdown Constructs Delivered as a Pool Reveal Hairpins Against mHTT as Enriched in Rescued Cell Populations

The power of this assay in using small cohorts to reliably detect subtle changes in D2GFP levels was an unexpected bonus and was worth exploring in detail, as there is definitely a paucity of rapid, highly quantitative assays for therapeutic efficacy in HD model mice. However, a goal of this project from the beginning was to use GFP rescue and flow cytometry as a way of detecting therapeutic rescue within a mixed pool of constructs. This has had tremendous power in cancer models (5,6), through which genes and pathways specifically relevant to medically relevant to topics like chemoresistance can be interrogated in an unbiased way, without the need for candidate genes. An obvious advantage that cancer models have for this technique is that infections can take place in millions of cells in tissue culture, and enrichment or depletion of relevant genes are related to the cell population's survival, under selective pressure in the mouse. Unfortunately for my goals, HD mice do not have significant cell death to use survival as a simple genetic selection criterion, which is why D2GFP loss is used as a surrogate disease progression measure, allowing rescued cells to be studied in isolation.

With this in mind, I investigated the potential for this assay to detect disease modifying genes by delivering shRNA pools to D2GFP;HD model mice. The experimental model is given in Figure 6. Pools of shRNA would be cloned into AAV vectors and delivered to the striata of HD model mice in the D2GFP background (Figure 6A). Upon initial infection (Figure 6B), all cells robustly express GFP, while those infected with the virus also express RFP. After the animal ages and pathology begins to impact D2GFP levels (Figure 6C), in theory, only those cells infected with therapeutic constructs are protected from GFP loss. To practically and powerfully interrogate

constructs present in this rescued population, I delivered such pools to R6/2 mice and littermate controls, in a small cohort (as the assay robustness suggests few mice are required). As illustrated in Figure 6D, I collected the cells with the highest GFP levels as a population, and amplified the pool of viral shRNA constructs within by PCR. The primers contained bardcodes and adaptors to facilitate multiplex Illumina sequencing. In this way, I asked whether given hairpins are found more often in this “high GFP” population in HD mice, where selective pressure for loss of GFP is present, versus wild type cells under no such pressure.

Knockdown constructs against genes of a variety of pathways (Table 2) were cloned into the AAV vector. Most of the shRNAs cloned had been pre-validated for knockdown efficacy in lentivectors delivered to 3T3 fibroblasts by The RNAi Consortium of the Broad Institute, and I re-validated a subset of them to confirm that shRNA expression is not impacted in the AAV vector plasmid setting. This was challenging because, unlike lentivectors, generating a separate AAV prep for each construct was not practical, so infection *in vitro* was not attempted. However, the cell type used, Neuro2a murine neuroblastoma cells, did not transfect efficiently enough to use the whole population for knockdown efficacy analysis. Hence, after subcloning into the AAV vector plasmid, I transfected cells in culture, and flow sorted the RFP+ cells before RNA purification and QPCR (Figure 7). For a large majority of the hairpins, subcloning into the AAV vector did not impair their activity.

After knockdown validation, a pool was constructed containing 2 shRNAs versus each of these 16 genes, plus five against exon 1 of *mHTT* and one control against *LacZ*. Mice (5 R6/2, 3 wild type, in the D2GFP background) were injected at 4 weeks of

age and harvested at 8 weeks of age. Preparation of vector shRNA sequence libraries from high-GFP neurons took place as described in Figure 6. Reads of each shRNA were analyzed as a population of the total pool, were compared between R6/2 and wild type populations, and were reported as enrichment over wild type (Figure 8). In other words, if a construct makes up 2% of the library in WTL MSNs but 3% of the library in R6/2 MSNs, the enrichment would be reported as 1.5-fold.

Only one shRNA was enriched significantly ($P = 0.011$), as calculated with an FDR of 0.2, while two others trended towards enrichment ($P < 0.1$). Admittedly, this is a very generous FDR, but because I reported the data as enrichment based on population composition, it necessitates that there appears to be as much enrichment as there is depletion (an increase in one hairpin's percentage of the pool means one or all of the remaining hairpins must make up less of the total population). Therefore, it is likely that enrichment is underreported by this method, and that, unless there are hairpins in the population that exacerbate toxicity, depletion may be largely an artifact.

It is, however, notable that all three of the enriched or trending hairpins target exon 1 of *mHTT* (Table 2), and the top hairpin (and only one significantly enriched) is DhEx1_5, validated alone *in vivo* (Figure 5). The presence of 3 of 5 hairpins against *mHTT* from a pool of 38, all within the top 3, seems highly unlikely by chance. Indeed, by arithmetic permutation predictions, one might see this this (the top 3 items of a ranked list of 38 all coming from a specific group of 5 items) by random chance at a rate of 1.185×10^{-3}. I further tested this possibility computationally by simulating this randomization 5,000,000 times, and produced this result (the top 3 contained only hairpins against *mHTT*) 5,873 times for a rate of 1.175×10^{-3}, closely agreeing with the

mathematical predictions.

In all, this was a small cohort experiment with limited scope, but there is clear demonstration of an ability to apply pooled screening protocols amenable to populations under extreme selection to a neurodegeneration model, provided that a population of rescued cells can be collected and specifically studied. In D2GFP rescue, we have a disease-relevant phenotype to be rescued, and flow cytometry allows it to be measured rapidly, quantitatively, and on a single cell level, allowing collection and both simple and complex analysis of interesting subpopulations.

A Small Molecule Therapeutic Candidate, Cystamine, Failed to Produce Demonstrable Rescue by D2GFP and QPCR in a Small Cohort

While the use of D2GFP dysregulation to identify and validate genetic modifiers of toxicity is a powerful tool, the method also has the accuracy and speed to potentially allow for rapid small molecule candidate assessment in small cohorts. Indeed, there is no shortage of candidate therapeutics, but most studies analyzing their efficacy utilize cohorts of roughly 20 per group. The requirement for large cohort size makes it a significant drain on resources and scientist time to evaluate more than a small number of such compounds. Hence, as a proof of principle, I evaluated D2GFP flow cytometry as a means of evaluating the rescue effects of cystamine in small cohorts. Cystamine is a small molecule with transglutaminase inhibitory and antioxidant capabilities which is currently in clinical trials. Cystamine is easily administered to HD model mice in drinking water or by intraperitoneal injection, and has established preclinical efficacy, including some transcriptional rescue effects (7-10).

A pair of small cohorts (15 mice total) was dosed with cystamine (6 R6/1 mice; 150 mg/kg/day, 5 days/week) or PBS vehicle (4 R6/1 mice and 5 wild type mice). A note on the dosing regimen: one of the previous studies (10) reported efficacy at a dose of 112.5 mg/kg/day, but also demonstrated some toxicity at higher doses that was ameliorated by giving a "drug holiday" (a week off of drugs). Hence, I tried incorporating this into my dosing regimen, giving drug in a "5 days on, 2 days off" pattern at a dose (150 mg/kg/day for 5 days/week) that should be roughly equivalent to the previously effective weekly dose of 112.5 mg/kd/day for 7 days/week.

During dosing, I monitored weight loss and performance on the rotarod. While there appears to be a trend towards worsening rotarod performance by week 12 (when mice were sacrificed), which would agree with data from a previous D2GFP;R6/1 cohort (Chapter 4, Figure 2), the difference was not significant at any age, nor was there a difference in weight gain in this cohort before euthanasia. I sacrificed the animals at 12 weeks of age, prior to obvious motor problems, because their D2GFP loss is expected to be nearing its maximum by this point. This is important because if a treatment delays onset without altering its rate of progression, assessing D2GFP fluorescence in older mice may miss this effect, as the drug simply shifted the progression curve to the right. However, this necessitated tissue collection early enough that significant behavioral dysfunction or weight loss were not seen, so rescue there could not be evaluated.

There were reports that cystamine could alter the transcriptional profile of HD model mice (7), so it was plausible that D2GFP levels would be altered. One of the cohorts of mice was sacrificed 72 hours after the final dose (Figure 10A), and D2GFP levels were analyzed by flow cytometry. Initially, the 72 hour after final dose time was

chosen because I did not want any acute effects of injection or handling to impact the data. Although I observed the expected change of D2GFP in R6/1 mice versus wild type, there was no demonstrable difference between cystamine treated and PBS treated mice.

However, some of the transcriptional effects of cystamine previously published (8,9) were acute and rapidly changed, so by giving the animals 72 hours drug-free, interesting transcriptional changes could be normalizing. Hence, I decided to sacrifice and analyze the second cohort 1 hour after the final dose (Figure 10B). This also failed to demonstrate any significant difference between cystamine treated and PBS treated R6/1 mice in D2GFP fluorescence, although there were only two animals per group, so only a substantial and consistent difference in GFP levels would be seen as significant.

There is a significant preclinical literature on the benefits of cystamine treatment in HD model mice, particularly in R6/2 mice, a sister strain to R6/1. There was no behavioral alteration to begin with, so the failure to alter a nonexistent phenotype was not notable. However, the lack of demonstrable transcriptional alteration on *Drd2* prompted more detailed analysis. First, QPCR was used to assay a few genes of specific interest. *Bdnf, Capn2*, *Dnajb2*, and *Ntrk2* are all reported to increase in cystamine-treated R6/2 mice (8,9). Meanwhile, *Drd1a* and *Drd2* are of particular interest to me as demonstration of transcriptional dysregulation in the direct and indirect MSNs, respectively, and the *Drd2* reduction is clearly expected from the D2GFP loss. There was a significant decrease in R6/1 mice for the transcripts *Bdnf*, *Drd1a*, and *Drd2* in the mice euthanized 72 hours after the final dose (Figure 11A). These transcripts, plus *Ntrk2*, were also reduced in mice euthanized 1 hour after the final dose. (Figure 11B).

However, in no case was there a significant difference between the transcripts in PBS-treated R6/1 mice and cystamine-treated R6/1 mice.

RNAseq Revealed Subtle Transcriptomic Rescue by Cystamine Treatment

While there was no significant differences from cystamine treatment in D2GFP or in the six transcripts tested by QPCR (including *Drd2*), it is possible that this dosage of cystamine either was too low or is less effective with 2 days off per week, so to look for particularly subtle changes on a global transcriptional level, I performed RNAseq analysis. I focused on the 72 hour after final injection cohort to be confident that any changes seen are the result of altered physiology from the near-continuous cystamine treatment.

Overall analysis demonstrated very few significant ($q < 0.05$, fold change $>\log_2(0.5)$) differences between R6/1 mice treated with cystamine versus those treated with PBS, as only 138 genes were differentially expressed out of >16,000 total genes with mapped reads (Figure 12A). Compared to the >1000 genes differentially expressed between the wild type littermates and R6/1 mice, this is a very subtle transcriptomic change. The transcriptional changes were subtle enough that hierarchical clustering failed to differentiate cystamine-treated with PBS-treated R6/1 animals, within those genes differentially expressed between R6/1 and wild type littermates (Figure 12B).

However, there is an indication that this cohort showed some minor transcriptional benefit from cystamine treatment (Figure 12C). Of the 138 genes significantly altered by cystamine treatment, 38 of them are found within those genes dysregulated in R6/1 mice versus wild type, a highly significant overlap ($P = 7.9 \times 10^{-18}$).

Furthermore, of those 38 genes differentially expressed in both comparisons (WTL-PBS vs. R6/1-PBS, and R6/1-PBS vs. R6/1-cystamine), 34 of them are altered in opposite directions in both datasets (reduced in R6/1 vs WTL but increased in Cys vs PBS, or vice versa), suggesting rescue. This improvement was similar enough within the overlapping gene set that cystamine-treated R6/1 mice clustered more closely to wild type mice than to PBS-treated R6/1 mice. Therefore, it may be concluded that with this dosing regimen, sacrifice delay, strain, and age, cystamine may have only very subtle effects. Nevertheless, what few effects cystamine does seem to have (that are detectable by deep sequencing of mRNA) in this setting strongly suggest rescue. This agrees with previous reports that cystamine not only rescues overt neuropathology and behavior, but the dysregulation of selected transcripts as well. That the D2GFP assay failed to detect this effect (Figure 10) is likely not a failure of detection but rather a successfully determined negative result, in that cystamine treatment by this regimen had no effect on most transcripts, including *Drd2*.

Discussion

Chapter 4 presented a method for rapidly measuring transcriptional dysregulation in HD model mice, and I have expanded on this by demonstrating the ability for virally delivered genes to modify this phenotype. This provides a small but significant demonstration of my assay as a potential tool for screening genetic modifiers of HD rapidly and in small cohorts of mice. The standard set of tools for measuring disease progression in HD model mice remains the most medically relevant way of predicting a modifier's effect, but such studies require significant resource investments. Many simply

reveal a candidate to be ineffective at affecting HD pathology. Clearly a negative result is as significant a contribution to the existing literature as a positive result is, but I hope that my assay and others like it can help groups pre-screen their candidates in small cohorts with minimal time and resource investment before devoting additional resources to more detailed and time-intensive analysis. For example, the group of Gillian Bates at King's College in London has had a long-standing interest in the repair of altered transcription profiles for therapeutic testing, and hence her group and others have made great strides in testing HDAC inhibitors such as SAHA and sodium butyrate (11,12). Because these drugs are relatively non-specific in their inhibition, a more targeted approach may produce fewer off-target effects, but this requires careful dissection of the many HDACs potentially involved in HD, which is in progress (13-16) but has thus far only succeeded in eliminating candidates. To be fair, using my D2GFP flow cytometry assay as a rapid replacement for this systematic crossing of knockout strains into R6/2 mice and careful phenotypic assessment would deny the field much of what we now know about the intersection of transcriptional control and disease pathology. However, from a clinical perspective, it may be a better use of time and resources to prioritize those modifiers with the most therapeutic potential. Continuing this example, if a researcher can use this technique to sift through the various HDACs to find those that most efficiently modify HD-relevant transcriptional dysregulation through D2GFP rescue, it may at least focus initial study on certain HDACs, rather than use a systematic approach to their elimination from consideration. Alternatively, if none of the HDACs individually has a significant effect on D2GFP loss, this could inform researchers that multiple HDACs may require simultaneous inhibition, and the speed of

experimentation allowed by viral delivery could facilitate the pairwise (or more) assessment in short order.

Meanwhile, from a small molecule testing approach, a truly efficacious therapy often requires the use of a combination of therapeutic interventions. Such may be the case for HD, as single therapeutic tests rarely produce more than a 20% improvement in R6/2 lifespan, while one of the most successful preclinical trials to date, effecting a 32% increase of R6/2 lifespan, was a combination of remacemide and coenzyme Q10 (17). To systematically evaluate the interaction and synergy between two or more therapies, particularly in the rapid R6/2 strain for which the therapeutic window is quite narrow, requires a readout that is highly quantitative and reproducible, and D2GFP dysregulation assays would facilitate this. Therefore, the strategies described here could be of particular use in optimizing a therapeutic approach for HD even if several targets or modes of action are necessary to achieve an optimal effect.

Another use for my novel assay was demonstrated by the ability to induce an HD-like phenotype by exogenous delivery of an *mHTT* transgene. Viral models of HD are relatively commonplace (18,19), and are often used for animals for which genetic models are uncommon or impractical. All demonstrate a common symptomology, at least on a cellular level, validating the gain-of-toxic-function aspect of HD. An additional advantage that could potentially be exploited involves the co-delivery of genes, demonstrated in a simple form by *mHTT* and RFP. Modifier testing, commonly involving the crossing of knockout or overexpression strains to genetic models of HD (Table 1), could potentially be expedited or even carried out in other animal models rapidly using monocistronic vectors. *mHTT*, plus a candidate cDNA or shRNA, can be delivered in the

same vector particle, guaranteeing that every infected cell expresses both transgenes, allowing for well-controlled assessment of therapeutic impact. This can be analyzed by flow cytometry (requiring a fluorescent gene included in the vector) or by classical neuropathological methods, but flow cytometry would facilitate the collection of infected cells, which I and others (20) have demonstrated can be reliably studied by transcriptionally profiling.

The flow cytometry approach presented here allows for not just the rapid identification and study of cells carrying a viral transgene, but for the study of subpopulations within a group of infected cells. The observation that there is correlation between high RFP expression and low GFP expression in the monocistronic mHTT-2a-RFP vector could facilitate the detailed study of the specific effects on cells of low levels or high levels of mHTT. Similar studies have been carried out in some detail using YAC128 mouse models, because in its initial characterization multiple lines were created. Some happen to express more mHTT than others (21), and this can also be induced by breeding mice to homozygosity, but the ability to do this rapidly without constructing new strains of mice is inviting, making viral models attractive. Additionally, there is much known about the effects of posttranslational modifications on HD because additional strains have been created with point mutations at interesting residues (22). Competition studies are commonplace in the cancer field, and could be rapidly adapted to my flow cytometry system. One could imagine the preparation of pairs of *mHTT* transgenes with subtle mutation differences, which are then co-delivered to a single piece of tissue, allowing for perfectly controlled analysis of the populations of cells best protected from pathology.

The pairwise delivery of genes (*mHTT* variants or potential modifier genes) is elegant, but the pooled delivery demonstrated here could not only expedite modifier searches by a significant margin, but with enough improvements to the protocol, could potentially even facilitate unbiased screening. The chief limitations to the assay in its current form are both mathematical and practical. There is limited tissue for infection; even with high infectivity (~50%), only ~10,000 infected cells from a single striatum would be recovered under ideal conditions, unless tremendous strides are made in the improvement of MSN yield from my already improved protocol. Furthermore, selective collection of only a subset of these cells (those with highest GFP levels, as was used here) further reduces cell yield. This places limits on the potential pool size; for example, delivery of 1000 genes of interest may only allow infection of an average of 5-15 collectible neurons, leaving it at risk for substantial randomness in determining enrichment. Additionally, the collection of only a few thousand cells places crucial importance on the post-flow-sort workup, namely the PCR of the shRNA pool. One mistake in the complex protocol results in a wasted experiment (an eventuality with which I have much experience), and these experiments can be time consuming to replicate given the breeding schemes involved.

A potential solution to these issues could come from the delivery of *mHTT*. There is nothing saying this analysis must take place in previously established genetic mouse models of HD. By using viral *mHTT*, D2GFP animals could be bred in substantial quantities for smaller pools of vectors carrying both *mHTT* and various shRNAs to be delivered to reasonably sized cohorts, without the need for age synchronization. Additionally, this D2GFP dysregulation assay is demonstrated in an animal carrying a

large BAC transgene containing GFP and the genomic region surrounding murine *Drd2*. It may be possible to identify a smaller region of transcriptional control responsive to *mHTT* expression, place it in front of GFP, then co-deliver this with *mHTT* and an shRNA. In this way, this kind of experiment to take place in rats or larger animal models, from which more cells would be available for flow cytometry collection.

One of the most immediate uses for an assay like this is facilitating preclinical drug trials to take place more rapidly and with greater power. The speed and consistency of this assay (Chapter 4, Table 1) could allow for rapid candidate assessment in small cohorts. I wished to demonstrate this using a small molecule currently in late stage clinical trials and with published transcriptional profile alterations, so I chose cystamine. However, it demonstrated only subtle rescue effects.

Given previous preclinical success with this drug, the most likely reason for my inability to demonstrate benefit would be the drug-dosing regimen. Cystamine is tolerated at a wide range of doses, but no other successful preclinical study used a “5 days on, 2 days off” regimen. It was a reasonable idea to include a weekly drug holiday given reports of toxicity at high doses, as other cytotoxic drugs like chemotherapeutics are administered at reduced frequencies to limit side effects. Nevertheless, it is possible that the effects of cystamine are only maintained in the R6 mouse lines by daily dosing. There is only weak evidence that cystamine has an effect on the clearance or production of mHTT (in that there is some minor reduction in aggregation) (10), many of the transcriptional changes are transient (8,9), and it is rapidly cleared from serum (23,24), so its effects may indeed be short-lived and subtle enough that dosage only 5 of 7 days a week abrogates its therapeutic effects. Furthermore, the most advanced

clinical trial of cystamine is using a formulation specifically designed for delayed, consistent release, placing further emphasis on constant dosage.

Re-testing this to establish the proper dosing regimen using previous studies would be possible, and the small cohort sizes necessary for confident efficacy determination using D2GFP would be perfect for such a study, but it is still necessary to breed up the D2GFP;HD model cohorts. Perhaps taking advantage of viral or toxin models of HD would be more useful here, as virally delivered *mHTT* rapidly induces D2GFP loss, and 3-NP, a well-tested chemical model of HD, has already been demonstrated to be less toxic in animals pre-treated with cystamine (25). I have not tested whether 3-NP or quinolinic acid (the two most common chemical models of HD) induce a D2GFP loss, and this would be a valuable continuation of my genetic model work. Regardless of the potential problems with the chosen dosing regimen, it should not be ignored that the D2GFP assay demonstrated no significant rescue by a small molecule, and more detailed inspection only succeeded in revealing a very subtle effect. Therefore, whether or not the drug itself has potential, it can be stated that the D2GFP assay successfully determined that this particular drug and dosage regimen had no effect on the HD phenotype.

Being a novel assay with successful but limited validation, there is much more to do going forwards if this assay is to significantly aid in the testing of potential HD therapeutics. Nevertheless, mice carrying the D2GFP transgene faithfully present HD symptoms when mHTT is present, and measurement of GFP in their MSNs represents a rapid and valid way of assessing cellular health that could potentially be leveraged in countless ways.

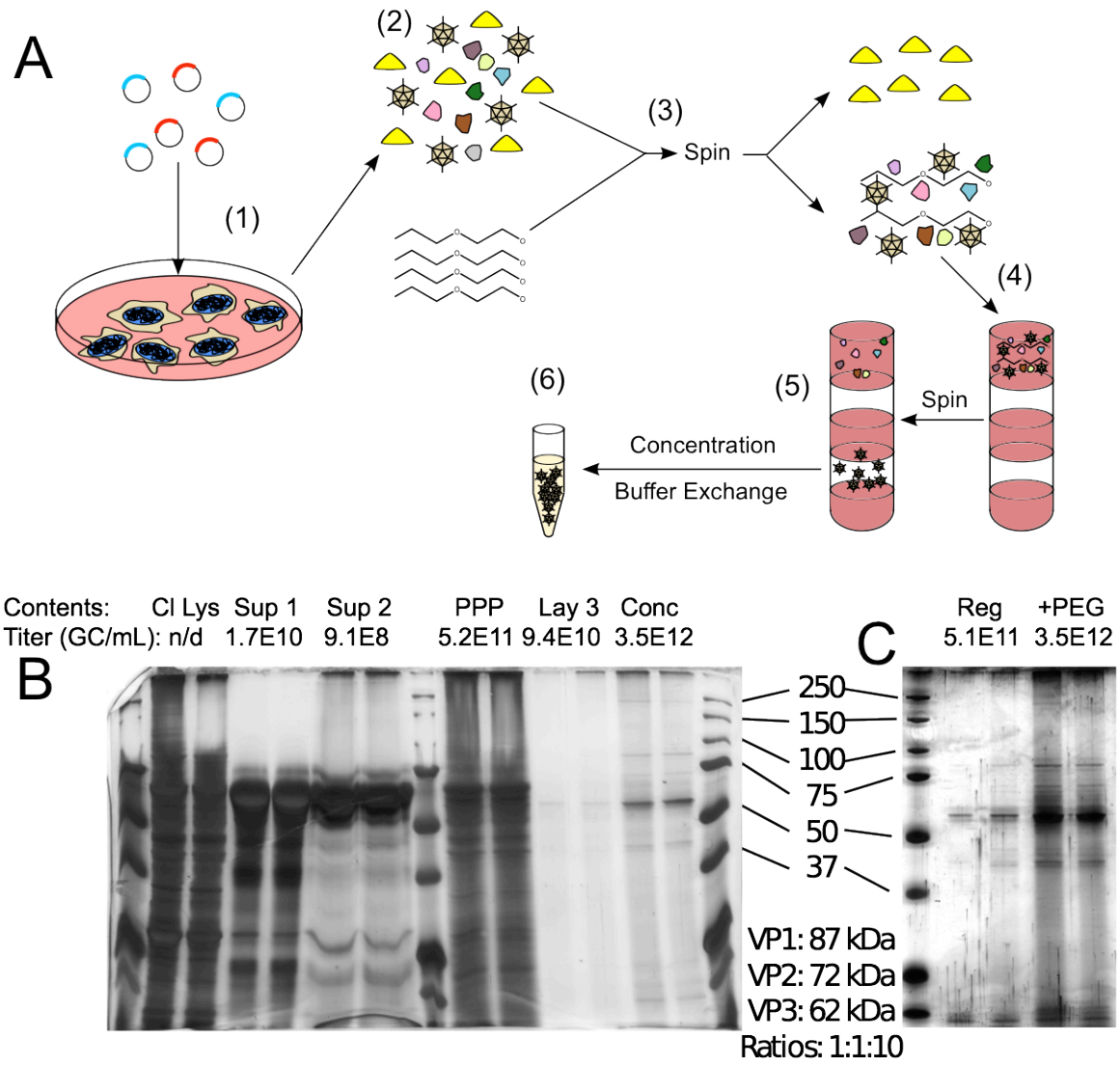

Figure 1: Production and purification of adeno-associated viral vectors. (A) Schematic depicting the steps of adeno-associated viral (AAV) vector production and purification. AAVs are produced in HEK293 cells transiently transfected by standard methods (calcium phosphate or commercial reagents). (1) Plasmids encoding AAV Rep and Cap, and adenoviral helper proteins, are cotransfected with the vector plasmid, containing the gene(s) of interest flanked by AAV ITR sequences. (2) After a 3-day incubation period, media is collected and set aside, and cells are lysed by freeze-thaw cycles and clarified. The media and clarified lysate each contain serum proteins (primarily albumin), cellular proteins, and viral particles. (3) Precipitation with polyethylene glycol (PEG) followed by centrifugation concentrates the viral particles and serves to remove much of the serum proteins. (4) This PEG precipitate, containing cellular proteins and viral particles, is laid on top of a stepwise iodixanol density gradient. (5) After ultracentrifugation, viral particles are in a lower layer, which can be isolated. (6) This layer contains viral particles and is relatively free of cellular proteins,

and after concentration and buffer exchange, is ready for delivery *in vivo*. **(B)** Proteins from the various purification steps were silver stained. The clarified cell lysate (Cl Lys) contains many cell proteins, while the media (Sup 1) has several proteins with a prominent albumin band (~65 kDa); titration reveals a significant amount of vector. After PEG precipitation, the supernatant (Sup 2) shows a removal of ~95% of the vector genomes, and a strong albumin band. The PEG precipitation pellet (PPP) has some albumin but not much more than the original clarified lysate. Density gradient ultracentrifugation places the vectors into layer 3 (Lay 3), which has only dilute proteins and low vector titer, but after concentration (Conc), the most prominent protein visible corresponds to the expected molecular weight of AAV capsid protein VP3 (62 kDa). **(C)** Two different pairs of AAV preps, prepared with (+PEG) or without (Reg) PEG precipitation, reveal similar proteins and differ mainly in titer, where the titer also corresponds to an increase in viral proteins (VP1, VP2, and VP3)

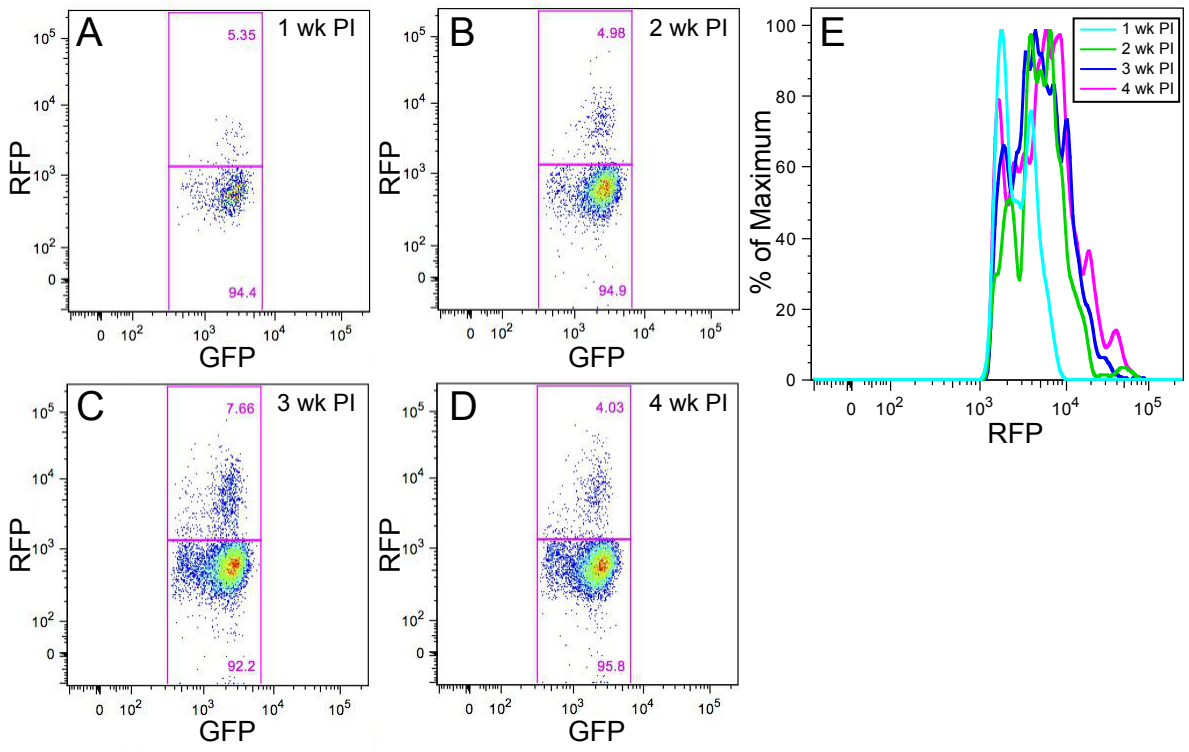

Figure 2: AAV-delivered transgenes require at least 2 weeks for significant transgene expression. (A-D) GFP vs RFP cytometer profiles of MSNs from mice receiving AAV delivering RFP demonstrate weakly-expressing RFP+ cells after 1 week (A), and significant numbers of RFP+ cells by 2 weeks (B), without a tangible increase in numbers or RFP levels at 3 weeks (C) or 4 weeks (D). **(E)** Plotted as a histogram for better visibility, the amount of transgene produced (level of RFP in the infected MSN population) requires at least 2 weeks to reach near-maximal levels.

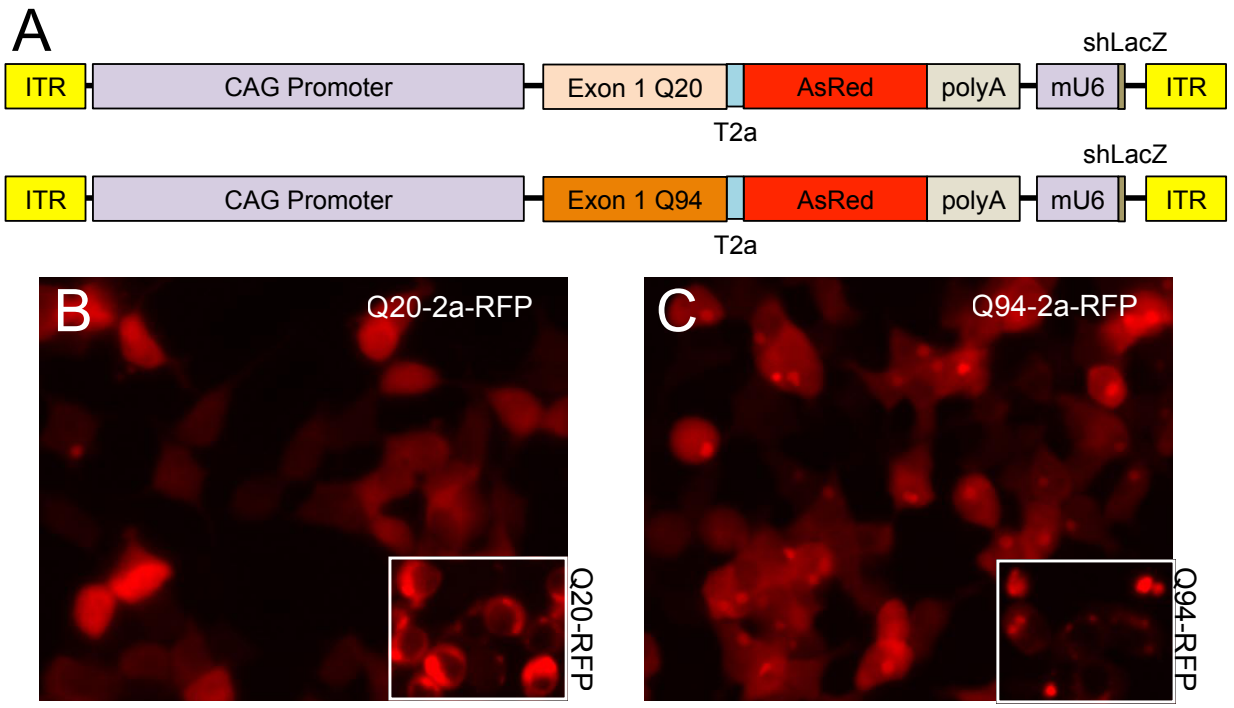

Figure 3: Exon 1 mHTT cloned into an AAV vector forms visible inclusions. (A) A map of the AAV vector used for introduction of exon 1 constructs, which was based on an shRNA-delivery vector. The inverted terminal repeats (ITRs) flank the delivered elements, consisting of a CAG promoter driving expression of Exon 1 of *HTT* in frame with the red fluorescent protein AsRed. The two protein sequences are separated by a self-cleaving T2a peptide. Irrelevant to this experiment, an shRNA expression cassette (mU6 promoter driving an innocuous hairpin against LacZ) is also present. **(B)** In transfected HEK293 cells, the Q20 construct demonstrates free diffusion of RFP into the nucleus, not seen for a similar construct missing the T2a peptide (inset). **(C)** The Q94 construct also demonstrates free diffusion of RFP, but the T2a peptide cleavage is incomplete, as some RFP is present in inclusion bodies. A construct missing the T2a peptide (inset) shows that most transfected cells have either inclusions or diffuse RFP.

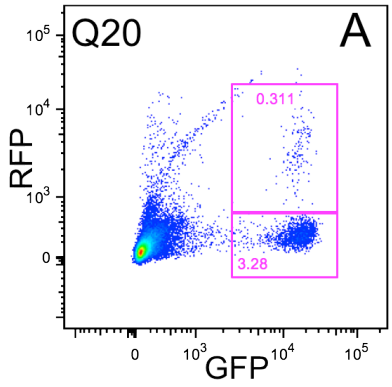

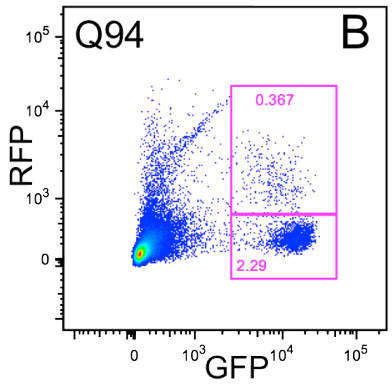

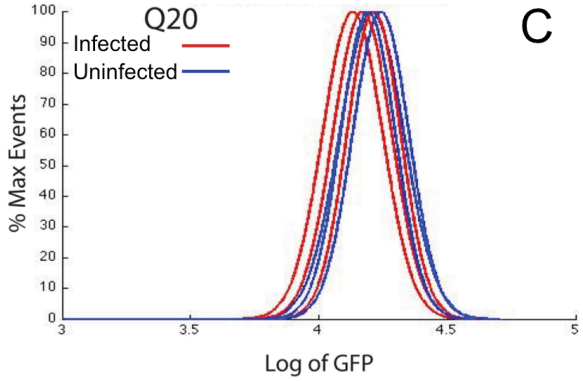

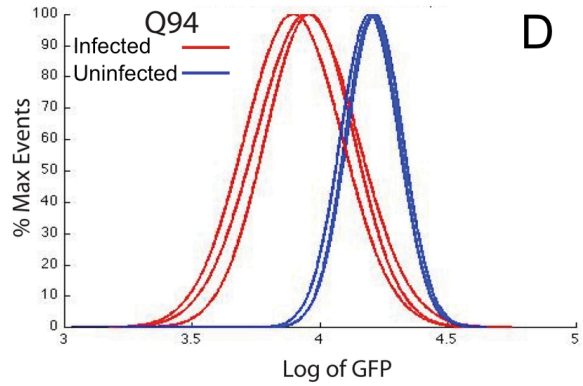

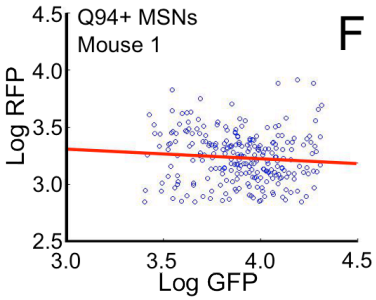

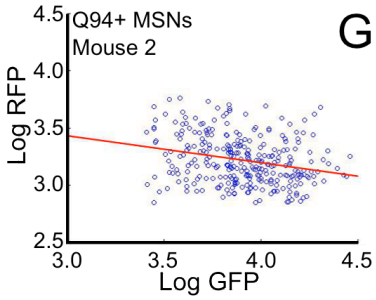

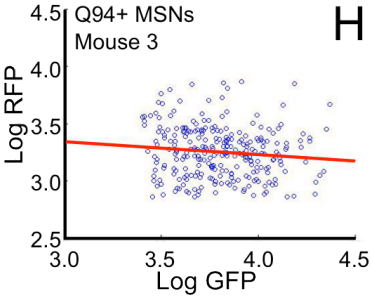

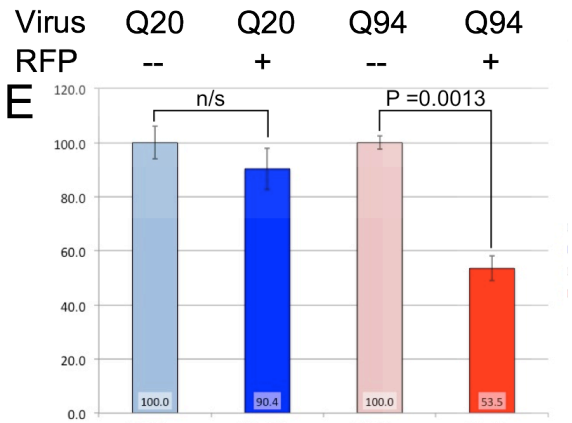

I	R	P value
Mouse 1	–0.0839	0.09
Mouse 2	–0.2561	$<1x10^{-5}$
Mouse 3	–0.1091	0.0366
All mice	–0.1622	$<1x10^{-5}$

Figure 4: AAV-delivered mHTT exon 1 causes significant D2GFP declines, while wtHTT exon 1 does not. (A and B) Flow cytometry profiles (X axis: GFP; Y axis: RFP) of striatal suspensions from D2GFP mice injected with AAV delivering either exon 1 wtHTT (Q20) (A) or mHTT (Q94) (B) after a 4-week incubation. **(C and D)** The GFP+ MSNs were divided into RFP+ (infected) or RFP- (uninfected) populations, which were quantified for GFP levels. The Gaussian means regression profiles are plotted. Q20 had no significant effect on the profiles (C), but Q94 caused a significant decline (D). **(E)** Quantification of the GFP changes which demonstrate both minimal variance of the assay and a significant loss of GFP only in cells infected with the Q94 construct. **(F-I)** Cytometry profiles of the Q94-infected cells revealed a correlation between high RFP expression and low GFP expression, which was significant ($P < 0.05$) in 2 of 3 mice and in all three summed together.

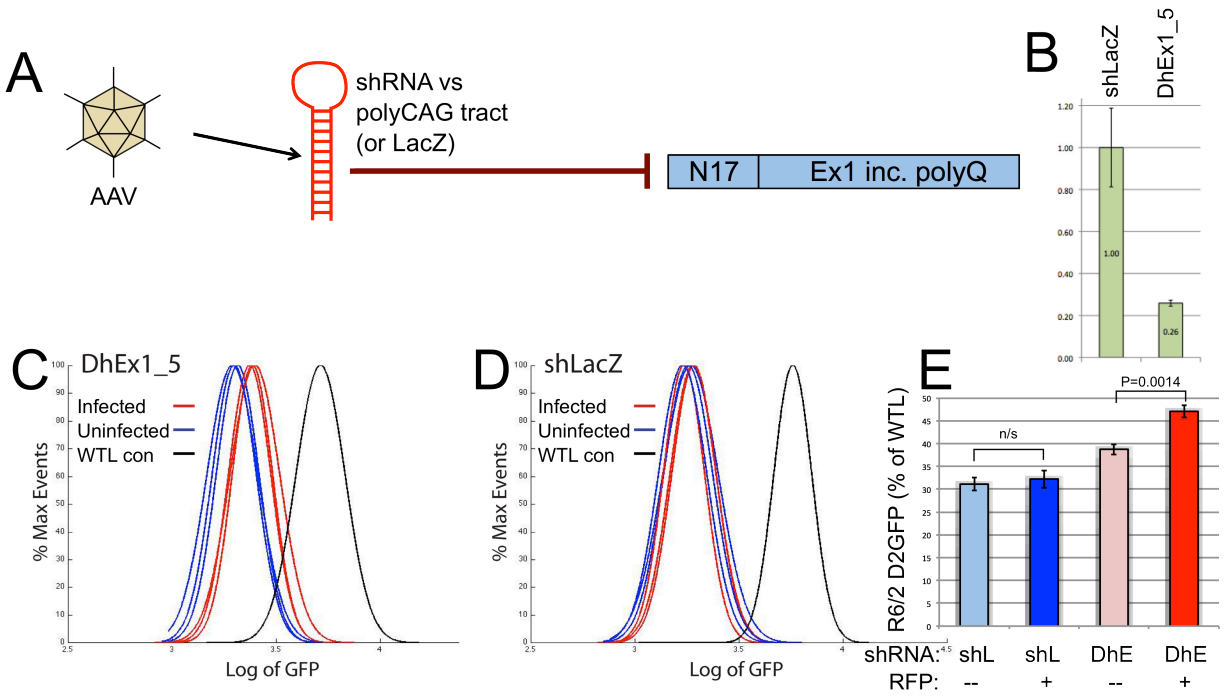

Figure 5: Knockdown of mHTT partially prevents the D2GFP loss seen in mice carrying the R6/2 mHTT transgene. (A) Schematic of the strategy, where AAV will deliver an shRNA knockdown construct either targeting the polyCAG tract of mHTT or an innocuous LacZ sequence. **(B)** The shRNA used reduces levels of an exon 1 mHTT luciferase fusion protein by 75% compared to the LacZ hairpin. **(C)** Upon delivery to 4 week old D2GFP;R6/2 mice and harvest 4 weeks later, GFP profiles from RFP+ (infected) or RFP- (uninfected) MSNs were plotted. Infected MSNs from mice receiving the polyCAG-targeting hairpin AAV demonstrated less GFP loss than uninfected MSNs. **(D)** No such rescue was seen in cells infected with AAV delivering the shLacZ hairpin. **(E)** A significant rescue of GFP loss (14 +/- 4% reduction, P = 0.0014)) was seen for the DhEx1_5 hairpin. No significant change was seen from the shLacZ hairpin.

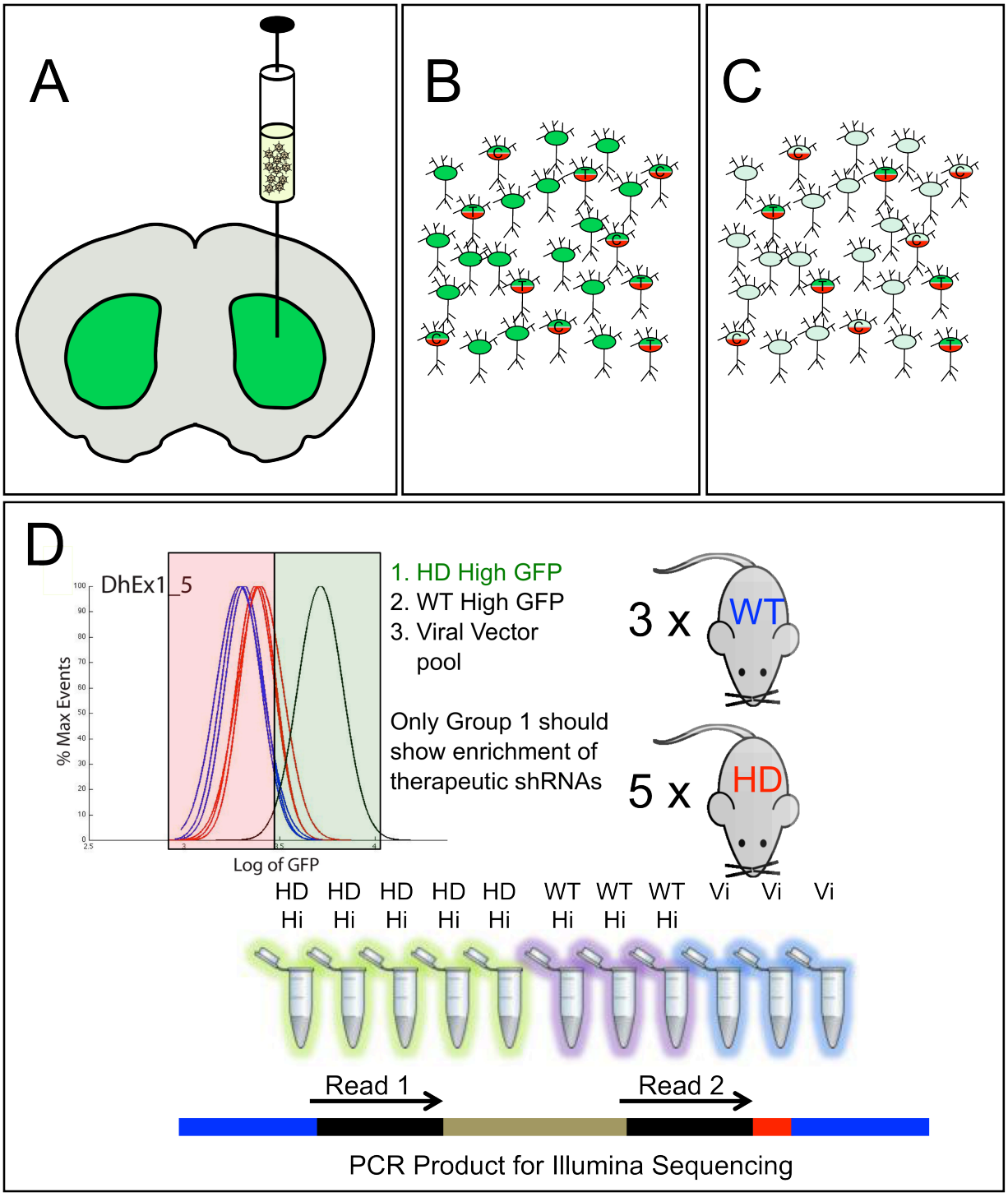

Figure 6: Strategy for pooled vector delivery to HD mice and interrogation of therapeutic construct enrichment using high throughput sequencing. (A) Pools of virus are delivered to the striatum of HD mice expressing D2GFP. **(B)** In young *mHTT*-expressing animals, some cells are infected with non-therapeutic constructs "C" while constructs with therapeutic potential "T" infect others. **(C)** After aging, both uninfected

cells and cells infected with “C” constructs lose GFP expression, but cells infected with “T” constructs are protected. **(D)** These protected cells were collected by sorting only the neurons with high GFP expression (green box). Three wild type and 5 mutant mice received the pools, and those high GFP cells were compared to each other and to the original AAV pool for library composition and enrichment. This is done by PCR amplifying the shRNA sequences using primers with animal-specific barcodes, and reading all by Illumina sequencing.

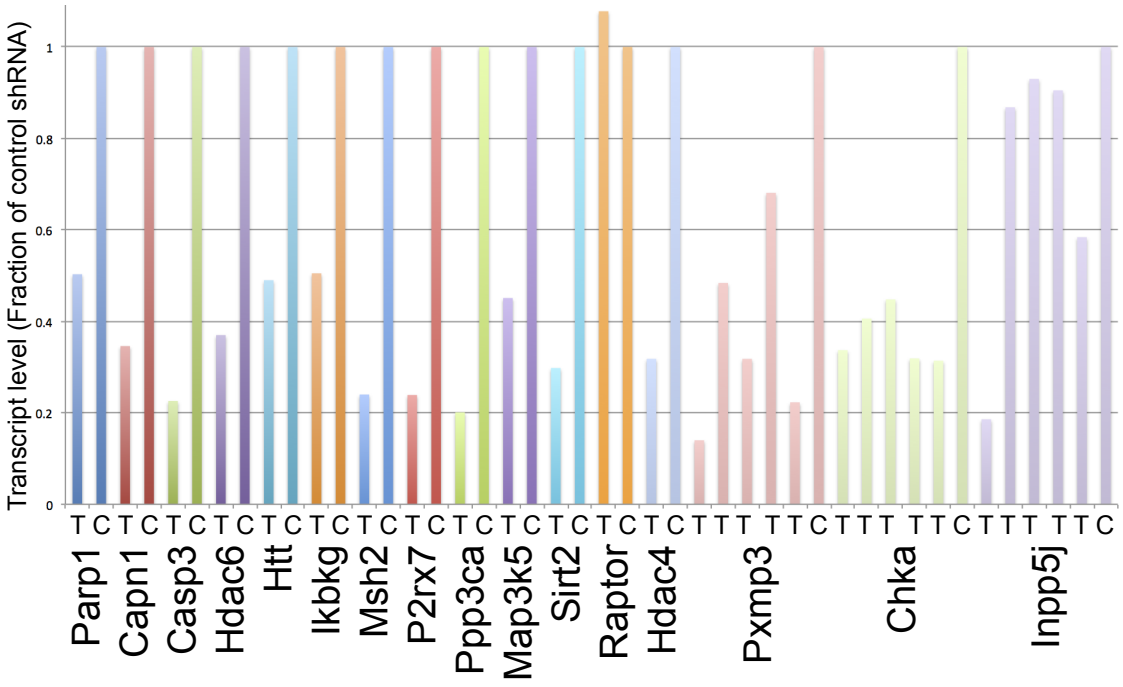

Figure 7: shRNAs from lentivectors possess similar knockdown potential in AAV vectors. A selection of the shRNAs used in the pool were re-validated after cloning into the AAV vector. Most demonstrated similar knockdown capability to that seen from lentivector experiments (not shown). Knockdown was evaluated in Neuro2a cells after transfection and sorting of RFP+ cells, followed by RNA isolation and QPCR. For each gene, transcript levels are shown compared between one or more targeting hairpins (T) and the control shLacZ hairpin (C).

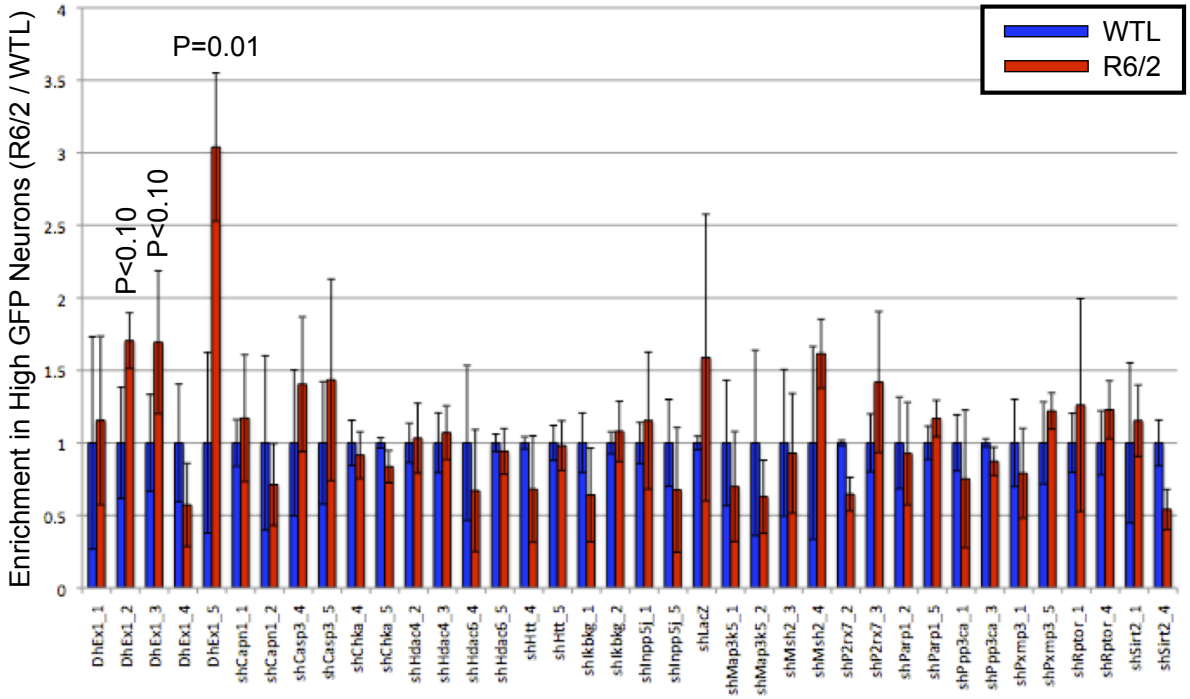

Figure 8: Pooled shRNA delivery demonstrates an enrichment of hairpins targeting mHTT within MSNs with high GFP levels. shRNA-infected MSNs with high GFP levels were collected and hairpins were analyzed by Illumina sequencing as illustrated in Figure 6. Data is presented as enrichment in R6/2 MSNs versus WTL MSNs. For example, if a construct makes up 2% of the library in WTL MSNs but 3% of the library in R6/2 MSNs, the enrichment would be reported as 1.5-fold. Only one hairpin was significantly enriched (P = 0.01, significant by FDR) while two hairpins trended towards enrichment (P < 0.1). All three target exon 1 of *mHTT*.

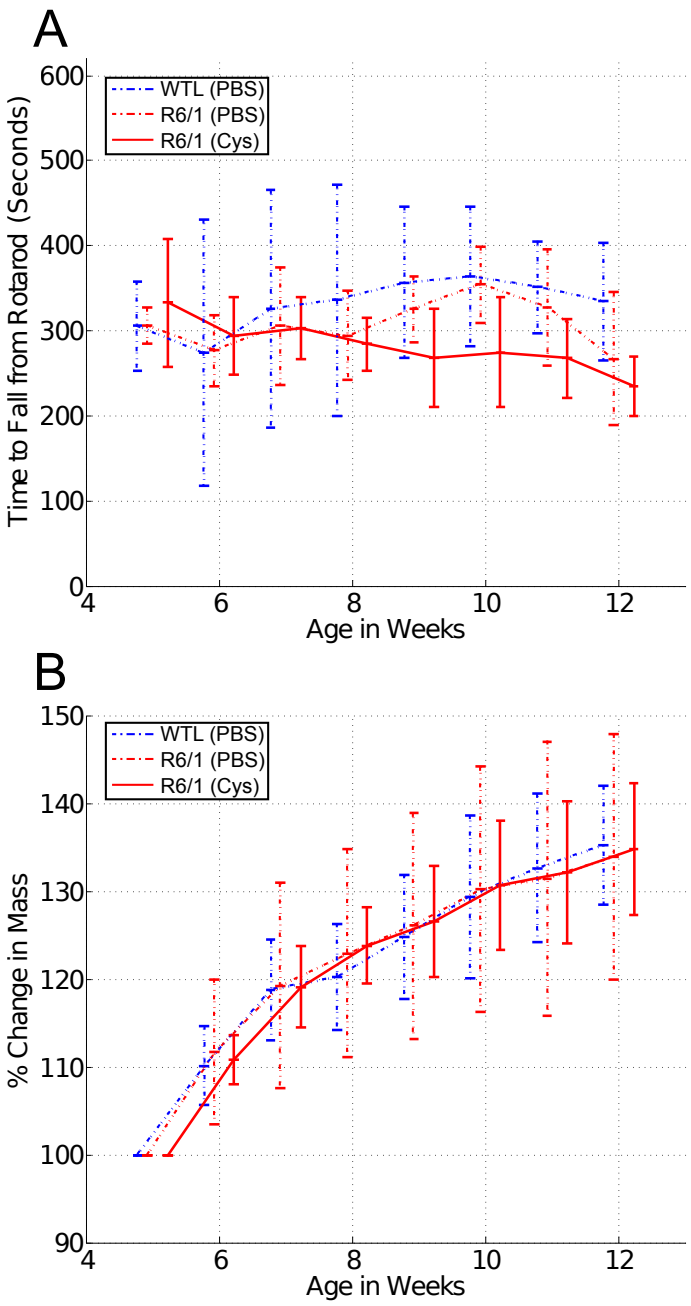

Figure 9: In the small cohort of cystamine treated animals, there was no difference in rotarod performance or weight by 12 weeks of age. Mice treated with either cystamine (150 mg/kg/day, 5 days/wk) or vehicle (PBS alone) were tested on the rotarod and weighed weekly. The cohort was euthanized at a young age (12 weeks), and in this cohort, no difference in weight or rotarod performance was observed by the age of euthanasia. N = 5 WTL(PBS) mice, 4 R6/1(PBS) mice, 6 R6/1(Cys) mice. WTL = wild type littermate.

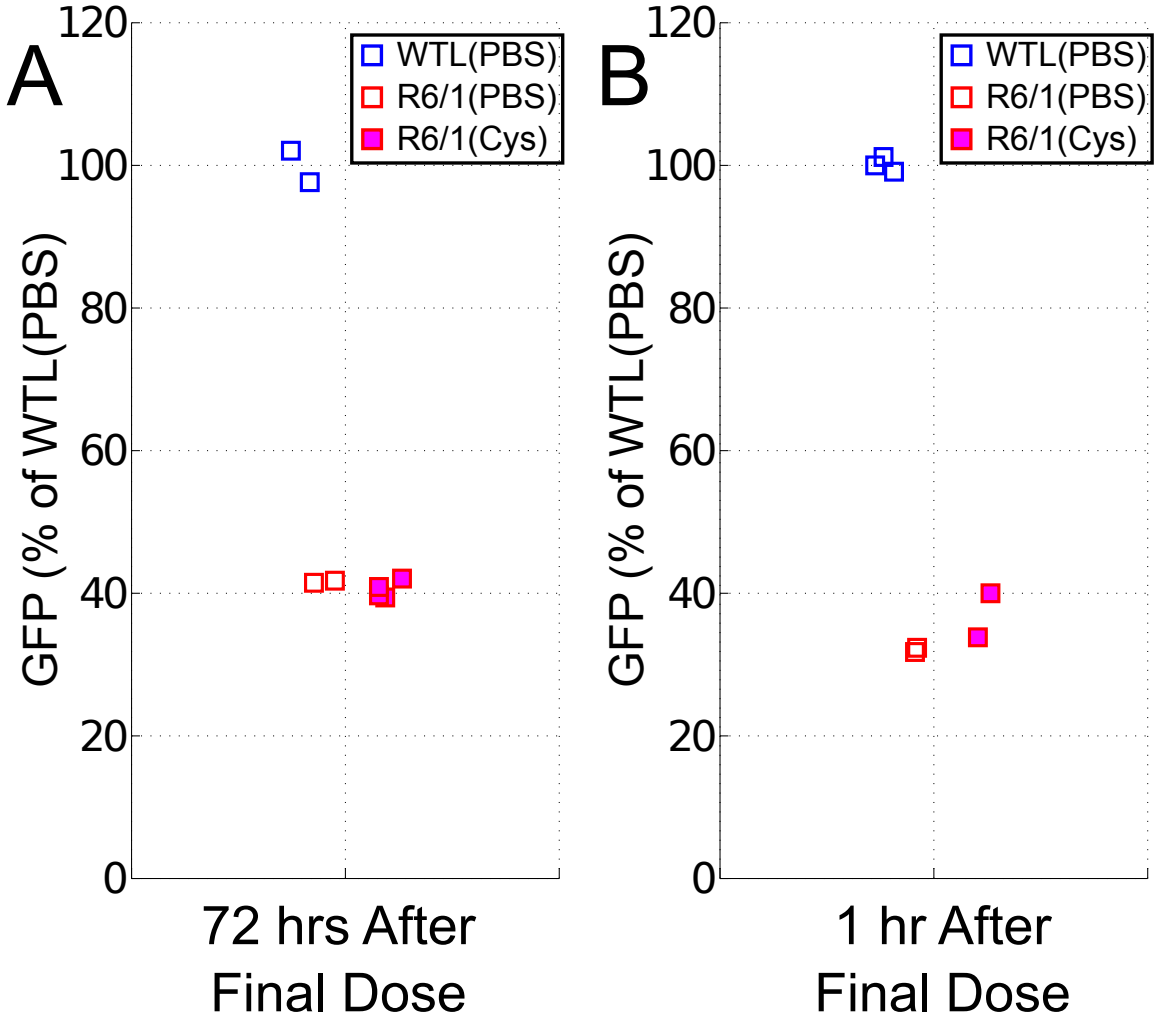

Figure 10: By D2GFP flow cytometry, cystamine did not alter GFP levels. (A) In the first set of mice, animals were euthanized 72 hours after the final dose, to allow for any transient response to cystamine to normalize. While there was a robust reduction in GFP in the R6/1 (N = 6) mice versus WTL (N = 2), cystamine did not alter this reduction (N = 4 Cys, N = 2 PBS). **(B)** To see if the response is actually transient, the second cohort was euthanized 1 hour after the final dose of the week. No obvious alteration in the GFP loss was observed, though the numbers were too low to have statistical relevance (N = 3 WTL, N = 2 R6/1-PBS, N = 2 R6/1-Cys). WTL = wild type littermate.

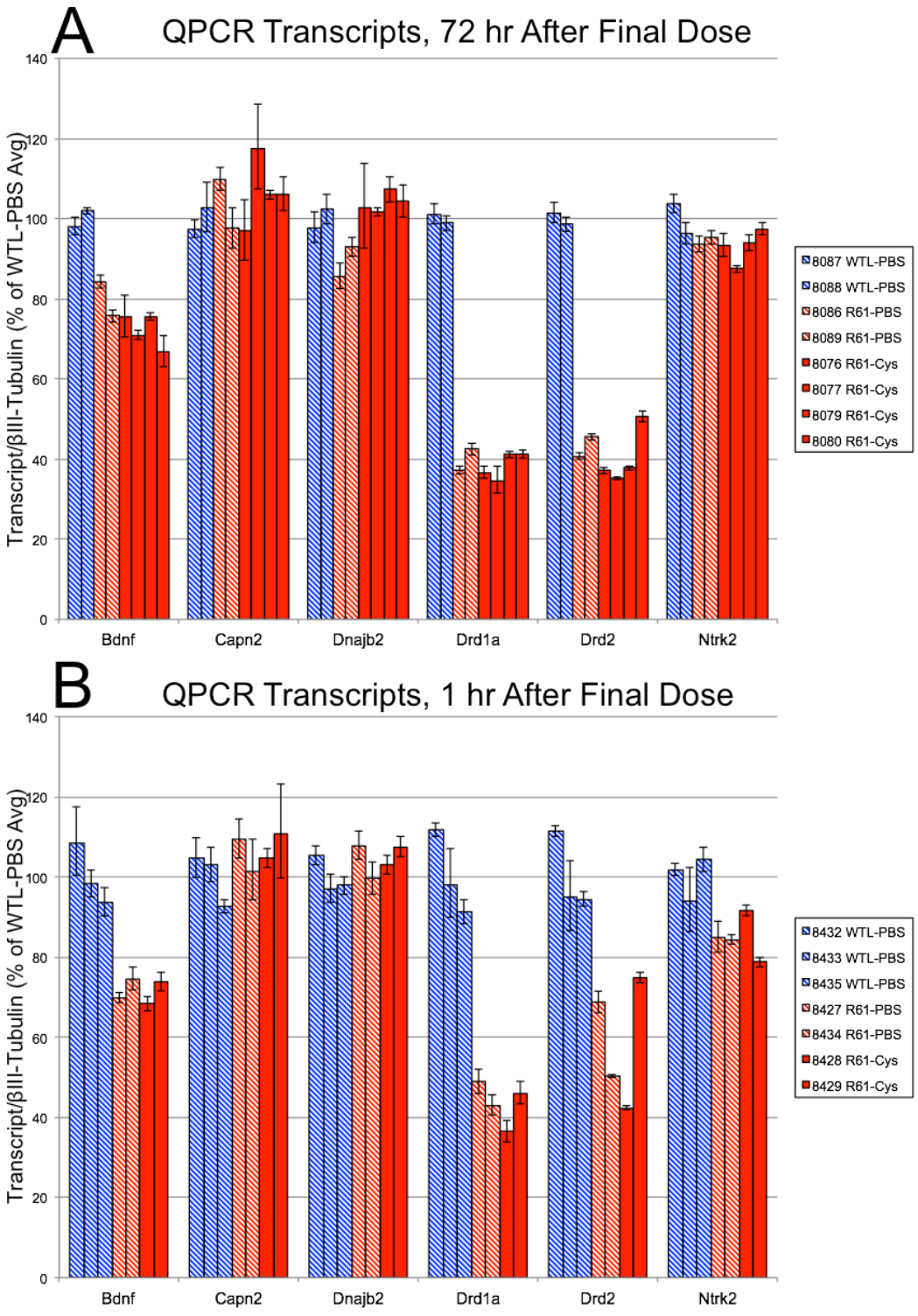

Figure 11: QPCR validated both the GFP loss and the lack of demonstrable response to cystamine. Striatal and cortical samples from cystamine or PBS treated mice were tested by QPCR for several genes. Cortical RNA was used for *Bdnf*, *Capn2*, and *Dnajb2*, and striatal RNA was used for *Drd1a*, *Drd2*, and *Ntrk2*.

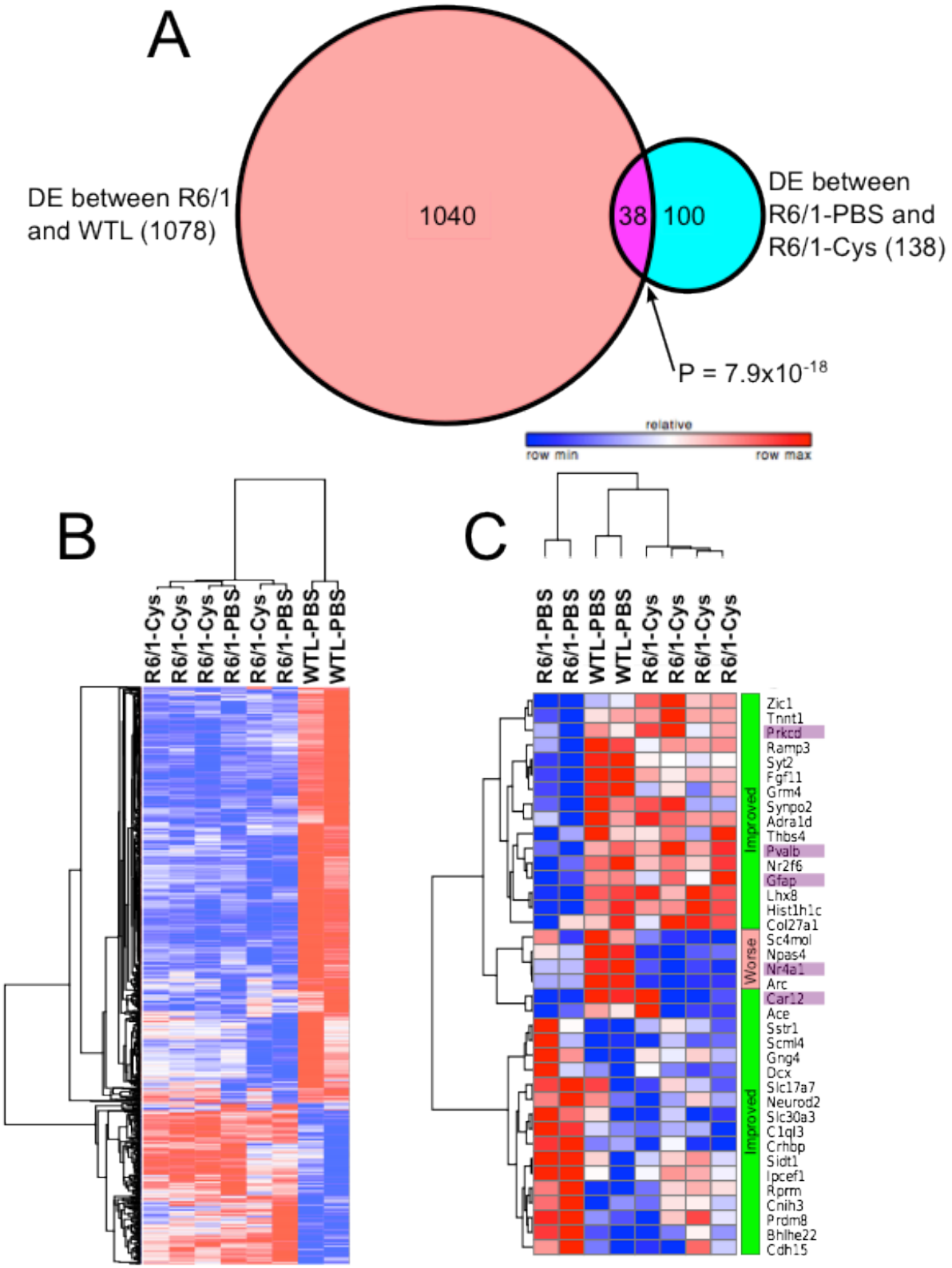
A
DE between R6/1 and WTL (1078)
1040
38
100
DE between R6/1-PBS and R6/1-Cys (138)
P = 7.9x10-18
relative
row min
row max
B
C
R6/1-Cys
R6/1-Cys
R6/1-Cys
R6/1-PBS
R6/1-Cys
R6/1-PBS
WTL-PBS
WTL-PBS
R6/1-PBS
R6/1-PBS
WTL-PBS
WTL-PBS
R6/1-Cys
R6/1-Cys
R6/1-Cys
R6/1-Cys
Improved
Worse
Improved
Zic1
Tnnt1
Prkcd
Ramp3
Syt2
Fgf11
Grm4
Synpo2
Adra1d
Thbs4
Pvalb
Nr2f6
Gfap
Lhx8
Hist1h1c
Col27a1
Sc4mol
Npas4
Nr4a1
Arc
Car12
Ace
Sstr1
Scml4
Gng4
Dcx
Slc17a7
Neurod2
Slc30a3
C1ql3
Crhbp
Sidt1
Ipcef1
Rprm
Cnih3
Prdm8
Bhlhe22
Cdh15

Figure 12: Cystamine treatment produced subtle effects detectible through deep sequencing of striatal mRNA. (A) Differential expression (DE) called 1078 genes as dysregulated between PBS-treated R6/1 and WTL mice (pink), but only called 138 genes as altered by cystamine treatment in R6/1 mice (blue). The overlap (38 genes) was highly significant ($P = 7.9x10^{-18}$). **(B)** Among the R6/1 vs WTL DE gene set, there was poor differentiation between cystamine-treated and PBS-treated R6/1 animals, as demonstrated by hierarchical clustering, meaning the effect of cystamine on the HD transcriptional phenotype was subtle overall. **(C)** However, focusing on the 38-gene overlap set not only differentiated the three groups readily as expected, but R6/1-Cys animals clustered closer to WTL-PBS mice than to R6/1-PBS mice. This is because, of the 38 genes dysregulated in both comparisons, 34 demonstrate improvement (rescue towards wild type levels) in R6/1-Cys mice and only 4 demonstrate worsening. All analysis was performed on the male 12-week-old cohort sacrificed 72 hours after final dose, so acute effects of dosage will not be seen. Genes reported as part of the HTT network by Ingenuity Pathway Analysis are highlighted in purple; this network includes ~11% of all transcripts reported as DE between R6/1 and WTL. WTL = wild type littermate.

Gene	Alt Name	Method	Model	Effect	Reference
Adora2a	A2a Receptor	Hom KO	3-NP	Improved lesions and toxicity	(26)
Bag1		Tg OE	N171-82Q	Improved motor deficit	(27)
Bdnf		Tg OE	YAC128	Improved motor, neuropathological, transcriptional defects	(28)
Casp2	Caspase 2	Hom KO	YAC128	Improved behavioral symptoms, not neuropathology	(29)
Cnr2	CB2 Receptor	Hom KO	R6/2	Exacerbates motor and survival deficit	(30)
Hdac3		Het KO	R6/2	No alteration (motor, weight, transcriptional defects)	(13)
Hdac6		Hom KO	R6/2	No alteration (motor, weight, transcriptional defects)	(14)
Hdac7		Het KO	R6/2	No alteration (motor, weight, transcriptional defects)	(15)
Hsf1		Tg OE	R6/2	Improved survival, weight, aggregates	(31)
Hsp27		Tg OE	R6/2	No alteration (motor, weight, oxidative damage)	(32)
Hsp70		Tg OE	3-NP	Improved lesions and toxicity	(33)
		Tg OE	R6/2	Minor weight improvement	(34)
		Hom KO	R6/2	Exacerbates motor and survival deficit	(35)
Msh2		Hom KO	HdhQ111	Delayed neuropathology	(36)
Nos1	nNOS	KO (Het or Hom)	R6/2	Het KO improved motor + weight, Hom KO exacerbated both	(37)
Ppargc1a	PGC1α	KO (n/s)	CAG140	Exacerbates motor and neuropathological defects	(38)
Ppid	Cyclophilin D	KO (Het or Hom)	R6/2	No alteration (motor, weight, survival)	(39)
Psme3	REGγ	KO (Het or Hom)	R6/2	No alteration (motor, weight)	(40)
Sirt1		Tg OE	BACHD	Improved motor, neuropathological defects	(41)
Sirt2		KO (Het or Hom)	R6/2	No alteration (motor, weight, transcriptional defects)	(16)
Sp1		Het KO	R6/2, N171	Improved survival, transcriptional defects	(42)
Tgm2	Tissue trans-glutaminase	Hom KO	R6/1	Improved survival, neuropathological defects	(43)
		Hom KO	R6/2	Improved survival, motor defects	(44)
		Tg OE	R6/2	No alteration (motor, weight, neuropathology)	(45)
Ubc	Polyubiquitin C	Het KO	R6/2	Minor behavioral improvements.	(46)

Key:

Hom KO	Homozygous knockout
Het KO	Heterozygous knockout
KO (n/s)	Knockout (zygosity unspecified)
KO (Het or Hom)	Tested both heterozygous and homozygous knockout
Tg OE	Overexpression from a transgene

Table 1: Selected examples of genetic modifiers, evaluated through genetic crosses of knockout or transgenic overexpression strains.

Hairpin	WTL %	R6/2 %	Fold Enrich	P-val
DhEx1_5	0.41	1.26	3.04	0.011
DhEx1_2	3.61	6.16	1.70	0.068
DhEx1_3	0.98	1.65	1.69	0.078
shMsh2_4	0.91	1.46	1.62	0.246
shLacZ	0.71	1.13	1.59	0.320
shCasp3_5	0.85	1.21	1.43	0.354
shP2rx7_3	3.04	4.31	1.42	0.191
shCasp3_4	1.56	2.19	1.40	0.335
shRptor_1	0.79	0.99	1.26	0.540
shRptor_4	2.30	2.83	1.23	0.229
shPxmp3_5	1.84	2.25	1.22	0.311
shCapn1_1	0.97	1.13	1.17	0.514
shParp1_5	1.81	2.11	1.17	0.130
DhEx1_1	1.17	1.35	1.15	0.779
shInpp5j_1	3.42	3.94	1.15	0.575

Table 2: Top 15 enriched hairpins in R6/2 versus WTL amplified from high GFP MSNs. Hairpins from *in vivo* shRNA enrichment were ranked, and the top 15 are listed. Of this list, the top 3 all target exon 1 of *mHTT*, highly unlikely by chance (P = 0.0012).

Bibliography

1. Zolotukhin S, Byrne BJ, Mason E, Zolotukhin I, Potter M, Chesnut K, et al. Recombinant adeno-associated virus purification using novel methods improves infectious titer and yield. Gene Ther. 1999 Jun 1;6(6):973–85.

2. Grimm D, Kay MA, Kleinschmidt JA. Helper virus-free, optically controllable, and two-plasmid-based production of adeno-associated virus vectors of serotypes 1 to 6. Mol Ther. 2003 Jun 1;7(6):839–50.

3. Kim JH, Lee S-R, Li L-H, Park H-J, Park J-H, Lee KY, et al. High cleavage efficiency of a 2A peptide derived from porcine teschovirus-1 in human cell lines, zebrafish and mice. PLoS ONE. 2011;6(4):e18556.

4. Xia H, Mao Q, Paulson HL, Davidson BL. siRNA-mediated gene silencing in vitro and in vivo. Nat Biotechnol. 2002 Oct;20(10):1006–10.

5. Meacham CE, Ho EE, Dubrovsky E, Gertler FB, Hemann MT. In vivo RNAi screening identifies regulators of actin dynamics as key determinants of lymphoma progression. Nat Genet. Nature Publishing Group; 2009 Sep 27;41(10):1133–7.

6. Silva JM, Li MZ, Chang K, Ge W, Golding MC, Rickles RJ, et al. Second-generation shRNA libraries covering the mouse and human genomes. Nat Genet. 2005 Nov;37(11):1281–8.

7. Karpuj MV, Becher MW, Springer JE, Chabas D, Youssef S, Pedotti R, et al. Prolonged survival and decreased abnormal movements in transgenic model of Huntington disease, with administration of the transglutaminase inhibitor cystamine. Nat Med. 2002 Feb;8(2):143–9.

8. Borrell-Pagès M, Canals JM, Cordelières FP, Parker JA, Pineda JR, Grange G, et al. Cystamine and cysteamine increase brain levels of BDNF in Huntington disease via HSJ1b and transglutaminase. J Clin Invest. 2006 May;116(5):1410–24.

9. Gibrat C, Bousquet M, Saint-Pierre M, Lévesque D, Calon F, Rouillard C, et al. Cystamine prevents MPTP-induced toxicity in young adult mice via the up-regulation of the brain-derived neurotrophic factor. Prog. Neuropsychopharmacol. Biol. Psychiatry. 2010 Feb 1;34(1):193–203.

10. Dedeoglu A, Kubilus JK, Jeitner TM, Matson SA, Bogdanov M, Kowall NW, et al. Therapeutic effects of cystamine in a murine model of Huntington's disease. J Neurosci. 2002 Oct 15;22(20):8942–50.

11. Hockly E, Richon VM, Woodman B, Smith DL, Zhou X, Rosa E, et al. Suberoylanilide hydroxamic acid, a histone deacetylase inhibitor, ameliorates motor deficits in a mouse model of Huntington's disease. Proc Natl Acad Sci USA.

2003 Feb 18;100(4):2041–6.

12. Ferrante RJ, Kubilus JK, Lee J, Ryu H, Beesen A, Zucker B, et al. Histone deacetylase inhibition by sodium butyrate chemotherapy ameliorates the neurodegenerative phenotype in Huntington's disease mice. J Neurosci. 2003 Oct 15;23(28):9418–27.

13. Moumné L, Campbell K, Howland D, Ouyang Y, Bates GP. Genetic knock-down of HDAC3 does not modify disease-related phenotypes in a mouse model of Huntington's disease. PLoS ONE. 2012;7(2):e31080.

14. Bobrowska A, Paganetti P, Matthias P, Bates GP. Hdac6 knock-out increases tubulin acetylation but does not modify disease progression in the R6/2 mouse model of Huntington's disease. PLoS ONE. 2011;6(6):e20696.

15. Benn CL, Butler R, Mariner L, Nixon J, Moffitt H, Mielcarek M, et al. Genetic knock-down of HDAC7 does not ameliorate disease pathogenesis in the R6/2 mouse model of Huntington's disease. PLoS ONE. 2009 Jan 1;4(6):e5747.

16. Bobrowska A, Donmez G, Weiss A, Guarente L, Bates G. SIRT2 Ablation Has No Effect on Tubulin Acetylation in Brain, Cholesterol Biosynthesis or the Progression of Huntington's Disease Phenotypes In Vivo. PLoS ONE. 2012;7(4):e34805.

17. Schilling G, Coonfield ML, Ross CA, Borchelt DR. Coenzyme Q10 and remacemide hydrochloride ameliorate motor deficits in a Huntington's disease transgenic mouse model. Neurosci Lett. 2001 Nov 27;315(3):149–53.

18. de Almeida LP, Ross CA, Zala D, Aebischer P, Déglon N. Lentiviral-mediated delivery of mutant huntingtin in the striatum of rats induces a selective neuropathology modulated by polyglutamine repeat size, huntingtin expression levels, and protein length. J Neurosci. 2002 May 1;22(9):3473–83.

19. DiFiglia M, Sena-Esteves M, Chase K, Sapp E, Pfister E, Sass M, et al. Therapeutic silencing of mutant huntingtin with siRNA attenuates striatal and cortical neuropathology and behavioral deficits. Proc Natl Acad Sci USA. 2007 Oct 23;104(43):17204–9.

20. Lobo MK, Karsten SL, Gray M, Geschwind DH, Yang XW. FACS-array profiling of striatal projection neuron subtypes in juvenile and adult mouse brains. Nat Neurosci. 2006 Mar;9(3):443–52.

21. Slow EJ, van Raamsdonk J, Rogers D, Coleman SH, Graham RK, Deng Y, et al. Selective striatal neuronal loss in a YAC128 mouse model of Huntington disease. Hum Mol Genet. 2003 Jul 1;12(13):1555–67.

22. Gu X, Greiner ER, Mishra R, Kodali R, Osmand A, Finkbeiner S, et al. Serines 13 and 16 are critical determinants of full-length human mutant huntingtin induced disease pathogenesis in HD mice. Neuron. 2009 Dec 24;64(6):828–40.

23. Pinto JT, van Raamsdonk JM, Leavitt BR, Hayden MR, Jeitner TM, Thaler HT, et al. Treatment of YAC128 mice and their wild-type littermates with cystamine does not lead to its accumulation in plasma or brain: implications for the treatment of Huntington disease. J Neurochem. 2005 Aug;94(4):1087–101.

24. Tennezé L, Daurat V, Tibi A, Chaumet-Riffaud P, Funck-Brentano C. A study of the relative bioavailability of cysteamine hydrochloride, cysteamine bitartrate and phosphocysteamine in healthy adult male volunteers. Br J Clin Pharmacol. 1999 Jan;47(1):49–52.

25. Mao Z, Choo YS, Lesort M. Cystamine and cysteamine prevent 3-NP-induced mitochondrial depolarization of Huntington's disease knock-in striatal cells. Eur J Neurosci. 2006 Apr;23(7):1701–10.

26. Fink JS, Kalda A, Ryu H, Stack EC, Schwarzschild MA, Chen J-F, et al. Genetic and pharmacological inactivation of the adenosine A2A receptor attenuates 3-nitropropionic acid-induced striatal damage. J Neurochem. 2004 Feb;88(3):538–44.

27. Orr AL, Huang S, Roberts MA, Reed JC, Li S, Li X-J. Sex-dependent effect of BAG1 in ameliorating motor deficits of Huntington disease transgenic mice. J Biol Chem. 2008 Jun 6;283(23):16027–36.

28. Xie Y, Hayden MR, Xu B. BDNF overexpression in the forebrain rescues Huntington's disease phenotypes in YAC128 mice. J Neurosci. 2010 Nov 3;30(44):14708–18.

29. Carroll JB, Southwell AL, Graham RK, Lerch JP, Ehrnhoefer DE, Cao L-P, et al. Mice lacking caspase-2 are protected from behavioral changes, but not pathology, in the YAC128 model of Huntington Disease. Mol Neurodegener. 2011 Aug 19;6(1):59.

30. Palazuelos J, Aguado T, Pazos MR, Julien B, Carrasco C, Resel E, et al. Microglial CB2 cannabinoid receptors are neuroprotective in Huntington's disease excitotoxicity. Brain. 2009 Nov;132(Pt 11):3152–64.

31. Fujimoto M, Takaki E, Hayashi T, Kitaura Y, Tanaka Y, Inouye S, et al. Active HSF1 significantly suppresses polyglutamine aggregate formation in cellular and mouse models. J Biol Chem. 2005 Oct 14;280(41):34908–16.

32. Zourlidou A, Gidalevitz T, Kristiansen M, Landles C, Woodman B, Wells DJ, et al. Hsp27 overexpression in the R6/2 mouse model of Huntington's disease: chronic neurodegeneration does not induce Hsp27 activation. Hum Mol Genet. 2007 May 1;16(9):1078–90.

33. Dedeoglu A, Ferrante RJ, Andreassen OA, Dillmann WH, Beal MF. Mice overexpressing 70-kDa heat shock protein show increased resistance to malonate and 3-nitropropionic acid. Experimental Neurology. 2002 Jul 1;176(1):262–5.

34. Hansson O, Nylandsted J, Castilho RF, Leist M, Jäättelä M, Brundin P. Overexpression of heat shock protein 70 in R6/2 Huntington's disease mice has only modest effects on disease progression. Brain Res. 2003 Apr 25;970(1-2):47–57.

35. Wacker JL, Huang S-Y, Steele AD, Aron R, Lotz GP, Nguyen Q, et al. Loss of Hsp70 exacerbates pathogenesis but not levels of fibrillar aggregates in a mouse model of Huntington's disease. J Neurosci. 2009 Jul 15;29(28):9104–14.

36. Wheeler VC, Lebel L-A, Vrbanac V, Teed A, Riele te H, Macdonald ME. Mismatch repair gene Msh2 modifies the timing of early disease in Hdh(Q111) striatum. Hum Mol Genet. 2003 Feb 1;12(3):273–81.

37. Deckel AW, Tang V, Nuttal D, Gary K, Elder R. Altered neuronal nitric oxide synthase expression contributes to disease progression in Huntington's disease transgenic mice. Brain Res. 2002 Jun 7;939(1-2):76–86.

38. Cui L, Jeong H, Borovecki F, Parkhurst CN, Tanese N, Krainc D. Transcriptional repression of PGC-1alpha by mutant huntingtin leads to mitochondrial dysfunction and neurodegeneration. Cell. 2006 Oct 6;127(1):59–69.

39. Perry GM, Tallaksen-Greene S, Kumar A, Heng MY, Kneynsberg A, van Groen T, et al. Mitochondrial calcium uptake capacity as a therapeutic target in the R6/2 mouse model of Huntington's disease. Hum Mol Genet. 2010 Sep 1;19(17):3354–71.

40. Bett JS, Goellner GM, Woodman B, Pratt G, Rechsteiner M, Bates GP. Proteasome impairment does not contribute to pathogenesis in R6/2 Huntington's disease mice: exclusion of proteasome activator REGgamma as a therapeutic target. Hum Mol Genet. 2006 Jan 1;15(1):33–44.

41. Jiang M, Wang J, Fu J, Du L, Jeong H, West T, et al. Neuroprotective role of Sirt1 in mammalian models of Huntington's disease through activation of multiple Sirt1 targets. Nat Med. 2012 Jan;18(1):153–8.

42. Qiu Z, Norflus F, Singh B, Swindell MK, Buzescu R, Bejarano M, et al. Sp1 is up-regulated in cellular and transgenic models of Huntington disease, and its reduction is neuroprotective. J Biol Chem. 2006 Jun 16;281(24):16672–80.

43. Mastroberardino PG, Iannicola C, Nardacci R, Bernassola F, de Laurenzi V, Melino G, et al. 'Tissue‘ transglutaminase ablation reduces neuronal death and prolongs survival in a mouse model of Huntington’s disease. Cell Death Differ. 2002 Sep 1;9(9):873–80.

44. Bailey CDC, Johnson GVW. Tissue transglutaminase contributes to disease progression in the R6/2 Huntington's disease mouse model via aggregate-independent mechanisms. J Neurochem. 2005 Jan 1;92(1):83–92.

45. Kumar A, Kneynsberg A, Tucholski J, Perry G, van Groen T, Detloff PJ, et al. Tissue transglutaminase overexpression does not modify the disease phenotype of the R6/2 mouse model of Huntington's disease. Experimental Neurology. 2012 Jun 12.

46. Bett JS, Benn CL, Ryu K-Y, Kopito RR, Bates GP. The polyubiquitin Ubc gene modulates histone H2A monoubiquitylation in the R6/2 mouse model of Huntington's disease. J Cell Mol Med. 2009 Aug;13(8B):2645–57.

CHAPTER 6 – FUTURE DIRECTIONS FOR THE (PRE)CLINIC IN HD

Introduction

In dissecting the *Drd2* dysregulation phenotype in HD mice, my work has provided three key findings to the HD community. First, that transcriptional dysregulation of *Drd2* is a consistent, highly predictable phenotype in many mouse models of HD. Second, that flow cytometric analysis of virally transduced cells can facilitate rapid analysis of candidate genetic modifiers. Third, that flow cytometry of neurons allows their collection and characterization, whether as a whole population or as sub-populations. Whether these methods and data are used directly, or as evidence of their feasibility for others to adapt their own techniques, the HD preclinical and clinical fields can hopefully benefit in a meaningful way from what I have learned and produced. Here I will discuss my thoughts on the future of therapeutic development for HD in patients and mouse models, including whether (and how) my novel assay can play a role.

Toward a UHDRS for Mouse Models

One of the main factors facilitating the determination of efficacy in HD clinical trials is the use of a standard method for monitoring phenotypic progression, the UHDRS (1). While it has its disadvantages (some subjectivity in the ratings, partly inherent to medication state and other variables), its focus on quality of life measurements while remaining relatively fast to administer makes it a clear favorite for clinicians. Postmortem neuropathology is similarly standardized by the Vonsattel

Grading System, through which disease state is assessed by careful classification of cell populations in different regions of the brain (2). These systems require training and expertise to administer reproducibly enough to maintain similarity across multiple centers and by different clinicians and pathologists. Nevertheless, they are essential to the study of a rare disease that almost always requires the combined efforts of patients and doctors in different parts of the world to assemble meaningful data sets.

Preclinical trials, on the other hand, lack this standardized set of assays for monitoring progression and postmortem disease state. While mice can be bred to substantial quantities and can include comparisons to (often inbred) wild type littermates, the interpretation of data is not the same. In the clinic, studies can be cross-compared by assessing changes in a patient cohort's UHDRS Motor Subscore, for example. However, when analyzing mouse data, improvement is somewhat of a binary determination, either beneficial or not beneficial. An improvement of rotarod score requires an understanding of many lab- and study-specific variables such as animal weight, specific rotarod protocol, and even the material on the rod itself. Neuropathology, similarly, can have some standard analytical measures (volumetric increases of the lateral ventricle, for example), but even here, histological assessment can change based on coronal section location, while MRI techniques and calculations can change upon a software update, let alone between laboratory facilities. Clearly, an improvement in multiple measures in a given mouse study often bodes well for others who repeat the experiments in mice to demonstrate improvement in their own hands. That being said, I believe the field would benefit greatly from a standard set of behavioral, molecular, and neuropathological measures from which a generalized

assessment of efficacy could be assigned. This would not only allow the research community to determine a drug or modifier gene's ability to improve (or worsen) the phenotype, but would allow the direct comparison of multiple such interventions done by different groups. In short, it would let clinicians prioritize the drugs that will enter clinical trials based on which ones perform best in animals, without having to consider the particulars of the techniques used.

The individual measures of the UHDRS were chosen by selecting those with the greatest ease at standardization (minimizing subjectivity) and speed of assessment. Those that best represent patient quality of life were then chosen, with an additional emphasis on those that change most rapidly in the early stages of the disease. In simple terms, this assigns a set of numbers to how a patient's manifest disease is affecting his or her life. With mouse models, we are less adept at determining how "bad" a mouse is feeling on a given day (for example, it is not uncommon for sick animals to feign health in an attempt to fool potential predators). Hence, it is not a simple task to assign a preclinical measure with a human quality of life. However, certain techniques are more robust than others, in that a reproducible change in performance is present in most mouse models as neuropathology progresses.

For the UHDRS, all measurements are by their nature longitudinal, in that patients are measured over the course of the disease to quantify progression. In mice, standard measurements of survival, weight loss, and clasping phenotype, when applicable, are simple and generalizable, even though survival can differ based on various mouse research facilities' definitions for the need to euthanize a given sick animal. Additionally, mouse models have several longitudinal quantitative behavioral

measurements, but the two most common methods, accelerating rotarod and balance beam, both measure balance and coordination. They each contain confounding variables, such as the specific rotarod duration. For example, we use a 4 to 40 RPM over 10 mins protocol, while others may use a 0 to 44 over 5 mins method (3). Additionally, the time to run will typically encounter a ceiling effect, in that wild type animals will often remain on the rod for longer than the acceleration protocol, complicating quantitation. Finally, the material of the beam (wood, plastic, or even bicycle innertubes over other materials can be used) can change how the mouse grips and drastically change how often it falls. Balance beam, on the other hand, can give different results for time to cross or foot slips based on the width and style of the beam. Some use tapered beams, others use a uniform width; the beam can be square or circular, and can be of a variety of lengths and angles. Overall, though, the main advantage that the rotarod provides is ubiquity, because it has been used in virtually every preclinical study for alteration of phenotypic progression. However, rotarod only provides one set of measurements (time to remain on rotarod), while the balance beam can measure time to turn when the mouse is placed backwards on it, the speed of the crossing, and number of foot slips. Overall, both are useful and demonstrate changes in performance across many models, but if forced to choose, I would propose to make balance beam (of a given length, width, style, and angle) a standard motor performance measure, if only for its multiple measurements and the speed with which it is analyzed, facilitating larger cohorts to be tested in a given time. There are many other tests for motor activity, but many of them either require substantial time, such as open field activity monitoring (which can require 30 minutes or more of observation), while others

require equipment that can be difficult to acquire and maintain, as is the case for swimming test apparatuses.

Much like volumetric imaging and the Vonsattel Grading Scale, neuropathological measurements in mice are consistent in that advanced disease state correlates worsening performance at behavioral tasks with greater neurodegeneration. For mouse studies, it may be impractical to expect researchers to have access to advanced *in vivo* volumetric imaging equipment (i.e. MRI), but brain weight could be a standard, simple, and relevant measure, and histological assessment is commonplace and relevant enough to patient data to be included. If a given set of locations within the brain were standardized for ideal analysis of certain structures, it would allow rapid assessment of differences in brain structure volumes. For example, the cortex, striatum, lateral ventricle, and hippocampus have demonstrable volumetric changes by MRI in multiple models (4), and could be quantitated with only two sections of mouse brain. Additionally, if they could be measured without the need for tissue fixation, the remaining tissue to be either used for other analyses that require protein or nucleic acid purification. mHTT inclusions are also commonly assessed and could be considered. While I agree that they are a rapid and quantitative indicator of proteotoxic stress, I would be hesitant to include their analysis in a standard measurement for disease pathology. This is due to the weight of data suggesting their limited direct role in neurotoxicity and the poor correlation across models between their appearance and the appearance of motor symptoms. However, for studies that are specifically evaluating a reduction in mHTT levels or investigating aggregation kinetics, it clearly remains useful.

On the molecular level, I believe my and others' work have unequivocally

demonstrated the ubiquity and progressive nature of transcriptional dysregulation. It is not yet well established which genes' alterations are the direct result of pathological processes (let alone which specific ones) and which are compensatory changes from a cell under stress. However, there are some whose alterations are well established as not only a byproduct of disruption, but as potential drivers. For example, transcripts for PGC1α were reported to be reduced in HD patients and models (5), with direct binding of mHTT to the *Ppargc1a* promoter thought to be the cause of this downregulation. This is likely not a passive alteration, given that PGC1α knockout within an HD mouse model exacerbates toxicity (5) in addition to the number of mitochondrial toxins modeling HD. mHTT also disrupts many transcription factors, such as REST/NRSF and Sp1, with direct physiological consequences. While whole transcriptome analysis by array profiling or RNAseq may be preferable in terms of data complexity, perhaps it would be more practical to limit analysis to a few select transcripts with the highest reproducibility among many samples, and representing many different factors' disruption of activity. *Drd2* is a candidate for which I have the most data, with relatively well-defined control by Sp1 (6), while genes such as *Chrm4* are REST/NRSF targets in the striatum (7) with demonstrable reductions in my striatal RNAseq profiles. QPCR would be a cost-effective, rapid, and simple way of analyzing a select few genes, and this could potentially be done with the leftover tissue from any volumetric analysis, conserving animal tissues.

In all, what could help is a standard, disease-relevant, and relatively easy set of measurements that can be administered without having to devote significant amounts of tissue. Ideally, this would allow lab- and study-specific analysis through other methods. I

wish to emphasize that the point of this is not to unseat a given lab's "favorite" techniques, in favor of a ubiquitous singular measurement system; even clinical trials often have primary endpoints other than UHDRS score improvements. It is only to add a set of data to each study that would facilitate cross-study analysis, without being a significant burden. This would certainly require thorough discussion in the HD research and clinical community, but a reasonable starting point for such a discussion might be as follows:

1) Longitudinal measurements: survival, weight, suspended limb clasping (submeasures age of onset and duration of suspension until clasp), and balance beam (submeasures time to turn around, time to cross, and number of foot slips) and/or rotarod (with a standard acceleration protocol and rod material).
2) Postmortem neuropathology: brain weight, cortical area (two sections), striatal area, ventricle area, and hippocampus area, taken from very specific coronal sections based on standard guides of mouse neuroanatomy.
3) Molecular pathology: transcriptional alterations of at least one Sp1 target (e.g. *Drd2*), at least one REST/NRSF target (e.g. *Chrm4* in striatum, *BDNF* in cortex), at least one direct target (e.g. *Ppargc1a*), and others deemed most relevant, normalized to one or more standard neuronal markers (e.g. *Tubb3* [βIII Tubulin]). For those treatments with whole-body exposure, it would also be wise to assess a similar set of genes in skeletal muscle.

All of these measurements (with the exception of clasping) are relatable to the human disease condition, require little in the way of specific equipment (a balance beam can be

purchased or constructed for little money), are simple to assess and standardize, and are not resource-intensive in either time or tissue. Importantly, they all have demonstrated sufficient power that reasonable cohort sizes are allowed.

The above assumes a relatively standard rate of progression in the various mouse models, but we know that there is significant variance among the mouse models for the onset and severity of such phenotypes. Hence, it would also be necessary to standardize the mouse strains used for rigorous preclinical studies. In general, they can be roughly divided into the N-terminal transgenic strains (R6/2, R6/2, and N171-82Q) versus the full-length strains (either transgenic, such as YAC128 or knockin, such as CAG140). While the N-terminal transgenic strains properly model the severe motor impairment, loss of brain tissue, and lethality present in HD patients, they do not model the genetic condition of patients or the slow progression of disease, which are faithfully recapitulated in full-length models. For this reason, it seems reasonable to make testing one of each standard practice. Among the N-terminal transgenic models, R6/2 have been most thoroughly studied, primarily due to their rapid progression, allowing even survival studies to be performed in a 3-4 month period. However, given the difficulty of producing even a modest phenotypic improvement in R6/2 mice, plus the speed at which pathogenic markers appear (mHTT aggregates by birth (8) and severe *Drd2* dysregulation by 6 weeks of age), I believe the slower R6/1 model would be more forgiving and sensitive to alterations. Its phenotypic progression appears nearly identical to that of R6/2 (9), albeit slower, and it has three added advantages: reduced rates of triplet repeat expansion (10), increased fecundity, and an inbred background. These make it both more genetically tractable than R6/2 and easier to breed in large numbers.

For full-length strains, there is great variability in the genetic structures. Testing a human full-length model like the well-studied YAC128 seems preferable due to the ability for human-specific interventions (such as oligonucleotides) to have an effect, but it has the downside of an altered genetic dosage, in that both wild type alleles of mouse *Htt* are also present. It would perhaps be possible to humanize YAC128 mice on a knockout *Htt* background, as has been done with BACHD (a similar strain but one which produces no transcriptional dysregulation and has very little intranuclear mHTT) (11,12), but the strength of the currently existing models is the glut of literature defining their expected phenotypes. The "best" full-length strain might not exist, but it seems reasonable to use YAC128 mice when the intervention requires human mHTT. Meanwhile, a pure murine knockin strain like HdhQ150 (also known as CHL2) (13) can be used when human mHTT is not essential, but emphasis is placed on the proper genetic balance of mutant and wild type *Htt*.

Pharmaceutical Interventions: When is the Target Specific Enough?

One of the primary reasons for the lack of an effective disease altering therapeutic in HD may be the diverse number of cellular pathways impacted by mHTT. For drug trials, both preclinical and clinical, it is often difficult to specify the target and its effects, but with HD, careful targeting may not always be desirable. Given the diverse suite of symptoms, a drug with multiple effects may be ideal. For example, the compounds that are furthest along in the clinic (cysteamine, coenzyme Q10, and creatine) are all antioxidants, but coenzyme Q10 and creatine aid mitochondrial function (14,15), while cysteamine has documented transcriptional rescue effects (16,17).

Meanwhile, a specific Hsp90 inhibitor, geldanamycin and its analogs, can be dosed to primarily affect HSF1 binding (18,19). However, this specific interaction is only powerful from an HD perspective because it alters the expression of several chaperone genes and alters the proteasomal degradation rate of several Hsp90 client proteins, important in the context of the limited ability of single chaperones to significantly impact mouse model pathology (20). With this in mind, a viable strategy would be to identify those drugs with the greatest pleiotropic impact on the various phenotypes, which would be facilitated by the standardized assessments presented above. An additional example of this would be the green tea extract compound EGCG, which not only can alter mHTT aggregation and toxicity in cell and fly models of HD, but also has antioxidant properties (21).

However, there are also situations where target specificity is required. A prime example for this is in the histone deacetylase (HDAC) field. General HDAC inhibitors may target many such proteins due to similarities in the binding sites, but often with toxic effects in HD mice despite some relief of the transcriptional phenotype (22,23). Parsing out the specific HDAC whose activity is most responsible for the relevant transcriptional alterations has been a goal for several labs, which has required a sizeable effort. The strengths of the assay I have developed are its sensitivity, low required cohort sizes, and the ability to pool candidates and assess their efficacy en masse. In the face of classical genetic techniques, this could be a rapid method of sorting out candidates as effective or ineffective at altering *Drd2* levels, which could lead to closer studies of the genes' impact on other phenotypic measures. HDACs are not the only large, druggable family of proteins for which specificity of inhibition could be

useful. Some kinases, like IKK (24), already have well-defined roles, but important phosphosites both within and outside of mHTT may be discovered by screening shRNA libraries directed against families of kinases or phosphatases. Given the necessity of specificity with kinase inhibitors in the clinic, this could be of great use from a medicinal chemistry perspective.

The specific targeting of a given protein to modify neurodegeneration is enticing, but the difficulty in this approach is that, to date, the only well-validated single target is mHTT itself. Others have been tested (Chapter 5, Table 1), and many have beneficial effects. Worth considering, though, is whether any single non-mHTT target truly provides enough therapeutic potential to justify the development of specific drugs or gene therapies to alter its activity. This is perhaps more of a philosophical question beyond the scope of a thesis, but it is clear that certain modifiers are better candidates than others. For example, one of the prevailing theories for the specificity of striatal degeneration in HD relies on the withdrawal of trophic support, specifically that of BDNF. As BDNF is not only poorly transported from the cortex, but is also downregulated (25,26) in HD, this is an attractive explanation, and transcriptional analysis of striatal tissue suggests a striking similarity between *Bdnf* knockout mice and HD models (27). Even amongst growth factors, though, there are many whose augmentation could be beneficial as single therapeutics. A rapid, small-cohort technique for assessing therapeutic impact would facilitate not only single-candidate testing, but combination therapeutics as well in order to investigate synthetic effects of multiple growth factor administration. Once promising single or combination growth factor regimens are selected, standardized phenotypic techniques could help carry successful

regimens to the clinic.

This is not to imply that mHTT itself is not the ideal target, and as *in vivo* oligonucleotide delivery or gene therapy improves, this will become a very attractive choice. However, allele specificity has become a point of (polite) contention in this subfield. Most of the tools for reducing *mHTT* RNA *in vivo* have demonstrated efficacy in an allele non-specific manner (28-30), but this has come with it the need to demonstrate the safety and tolerability of reduction of wild type HTT levels (31,32). Allele specific knockdown approaches would clearly be desirable, but there are only two ways of accomplishing this, each with drawbacks. One method is to identify highly polymorphic single nucleotide polymorphisms (SNPs) and utilize a small number of allele specific oligonucleotide (ASO) molecules with the greatest population coverage. The two downsides from this approach would be the fact that not every patient would be a candidate for this (e.g. homozygotes for the appropriate markers), and also that this would necessitate stratification of patient populations for clinical trials, which not only adds a degree of difficulty to recruitment, but puts the study at risk of artificial results due to a shared ancestry within this stratified population. Alternatively, targeting the poly(CAG) repeat would be applicable to every patient, and possibly more efficacious in those patients with highly expanded repeats. The risk with this approach would be the presence of poly(CAG) microsatellites in other genes, so off target effects would need to both be accounted for, and tested for disease influence. For any of these approaches, my novel assay could facilitate the specific collection of cells infected with a viral shRNA targeting the desired region. D2GFP rescue could be used as a first-pass therapeutic measure, but after collected, QPCR or RNAseq can be performed to document off

target effects.

Beating Back mHTT on Multiple Fronts

Toxicity in HD affects multiple pathways, and I have discussed drugs known to affect multiple disrupted functions. However, there is nothing to say that multiple drugs cannot be co-administered. In truth, I believe it makes more sense to approach HD the same way one would approach cancer. Historically, only modest improvements in survival were achieved in patients when single drugs are given, with only rare drugs like Gleevec improving survival drastically, even when added to existing regiments. It is often only when multiple drugs, combined with radiotherapy and/or surgical resection, are administered that significant gains in survival have been made. This is because to even become a cancer cell, several checkpoints to growth, division, and migration have to be overcome. Targeting only one of these pathways with single agents, however effective they are, can often be brushed off by a tumor cell on its way to regrowth.

Neurons in HD do not divide, nor do they encounter selective pressure to maintain mHTT toxicity in the face of therapeutics. However, the progressive degeneration is still the result of the disruption of multiple pathways, so it is only logical that multi-drug regimens should be more thoroughly explored. This has already been attempted with coenzyme Q10 (an antioxidant with added benefits to mitochondrial energetics) administered with remacemide (an NMDA receptor antagonist) (33,34). While this combination had no significant protective effect after 30 months of treatment in patients, it is remarkable in that it provided the best increase to survival for a non-surgical intervention in mice yet tested, greater than 30% in R6/2 mice. I would

comment here that, because the best improvement of survival for this strain has been only 30%, this leads me to the view that R6/2 is not the ideal model for a disorder with comparatively subtle effects over decades of life in patients.

The paucity in clinical success for HD to date may well be due to the consequences of toxic effects on multiple cellular pathways. There are two reasons to consider these multiple pathways in the context of HD therapeutics. First, it may prove extremely difficult to directly eliminate the mutant protein while also preventing its expression from the point of therapeutic intervention onwards. Second, the impact of mutant protein may have had profound effects on the neurons, to the point that their eventual death will not be reversed by simply eliminating mHTT protein. For these reasons, I believe it is important to continue to focus on determining in detail the pathological impact of mHTT on cellular function at all stages of development and disease progression.

The different pathways to toxicity can be categorized any number of ways, but for simplicity's sake, I will divide them into four: trophic support, mitochondrial health (including Ca^{2+} homeostasis defects), transcriptional dysregulation, and proteostasis (both protein folding and degradation). All four of these categories contain both genetic modifier studies and pharmaceutical trials that significantly alter the motor phenotype and/or survival. For trophic support, *Bdnf* overexpression is protective, as is the administration of agonists for its receptor (35,36). Mitochondrial health was impaired by *Ppargc1a* (the gene for PGC1α) knockout and is boosted by creatine and coenzyme Q10 (5,14,15). Transcriptional dysregulation is improved (albeit confusingly) by *Sp1* knockout and by a number of HDAC inhibitors, such as SAHA (37,38). Finally,

proteostasis is aided by *Hsf1* overexpression and modestly improved in a different polyglutamine disease model (polyQ androgen receptor) by the Hsp90-inhibitor and geldanamycin analog 17-AAG (19,39).

Considering that all of these individually aid HD mice, some of which with crossover effects in other pathways (cysteamine, a mitochondrial energetic booster and andioxidant, also improves BDNF protein levels in the brain) (16), it should be fairly straightforward to test combinations of them. The best candidates, with the fewest predicted contraindications, can be selected and initially tested pairwise and singly. If, for example, a group were to focus on the four pathways I described above, this would mean four single-drug groups, six pair-wise drug groups, and at least one no-drug cohort. Through conventional drug studies, it is complicated to test even one therapeutic, so 11 trials would require a monumental effort. However, let us assume it could be established that the four drugs would individually have even subtle effects on *Drd2* levels. In this case, it would be reasonable to use only 5 or fewer D2GFP;R6/1 mice (which could detect an improvement of less than 10% with great confidence) in each test, so a synthetic effect could be confidently ascertained. Alternatively, if behavioral and neuropathological effects also should be taken into account, the beam crossing and histological volumetric assays proposed above could maximize clinical relevance and information with a minimum of hands on time by the researchers, and would likely necessitate only modestly larger cohort sizes. This is only an example (and an optimistic one at that), but it illustrates the fact that experimental throughput, not just information content, is one of the chief impediments to preclinical science. The bottleneck may not be on this end, given the difficulties in establishing a clinical trial

protocol and gathering a suitable patient population. Nevertheless, clinical trials might produce more success if they are not dependent on a significant health improvement to neurons arising from only a single pathway's repair.

Gene Therapeutics: Risks, Progress Remaining, and Potential

Pharmaceutical approaches have a long history of success for many diseases, and are often simple to test in mice, but for a disease like HD with a potentially long life of treatment in front of patients, it is worth exploring in greater detail those strategies that require one or a few interventions; namely, gene therapy. It also provides the only way for the administration of a complex protein whose isolation or synthesis in quantities adequate for consistent dosage would be prohibitively difficult or costly. Growth factors, for example, only have practical therapeutic potential in the context of either gene therapy or the surgical implantation of transduced cells secreting the growth factor, due to poor serum half-lives and the blood brain barrier. There is a growing literature on cell implantation in HD and other neurodegenerative diseases (in particular, Parkinson's Disease) (40), and the poor outcomes have come primarily from either failure of cells to survive, or overgrowth. This perhaps should not be surprising, but implanting neuronal progenitors or fibroblasts, and expecting them to remain living cells in a foreign environment but not to grow, is a difficult task even in ideal conditions. This might be improved in the near future with the advent of induced pluripotent stem cell technologies (41,42), from which patients' own cells provide the source material and hence preventing the necessity of immunosuppression. For the moment, however, AAV vector delivery, with good immune tolerance in the CNS and long-lived expression, is a

more viable option. The major downsides are the requirement of neurosurgery, and the inability to “turn off” the transgene should intolerable side effects arise. These effects can be minimized with proper GMP viral prep, skilled and accurate surgical implantation, and importantly, longitudinal preclinical studies in mice and longer-lived animals.

Of the options available for gene therapy, reduction of mHTT through small noncoding antisense RNA transgenes (e.g. shRNAs) is perhaps the most attractive choice. This was discussed in detail above, but given the difficulty in silencing viral transgenes, it is worth emphasizing the necessity of validating the safety and tolerability of HTT reduction if the construct is not allele-specific. Such efforts are underway with promising results (31,32).

Modulation of indirect modifiers, through either shRNA or cDNA transgene delivery, is more of an open question as to its utility. As outlined above, the ability of single factors to meaningfully alter disease progression is up for debate. However, a rapid, simple technique with which such factors could be evaluated in groups could aid in selecting those with the most potential. Particularly with shRNA screens and cDNA families whose members are likely to have cell-intrinsic effects (transcription factors, but not growth factors), pooled screens could rapidly assess these putative modifiers, and the single factors arising from these screens can be tested more rigorously individually.

Importantly, these pooled approaches need not be limited to known cDNAs or shRNAs against known genes. It is particularly enticing to screen small libraries generated from enriched therapeutic peptides tested in cell culture or lower organisms, for example. The polyglutamine binding protein QBP1 was screened in such a way and

has demonstrated therapeutic effects (43), but with a pooled *in vivo* approach, it would not be necessary to narrow down such libraries to only one or two top-performing candidates. Given the differences between disease progression *in vitro* and *in vivo*, some peptides with great clinical potential may be lost when researchers are forced for practical reasons to cull the promising hits down to only one or two top candidates.

A final note, which is relevant for any clinical trial, but particularly for gene therapy interventions that require neurosurgery, is the subject of when to administer the vector. It is well established that by the time symptoms set in, significant atrophy has occurred in the striatal cells that would presumably serve as the target for gene delivery. Fortunately, primary outcome measures of volumetric changes are substantial predictors of motor dysfunction in patients and mice (44-48) and can be measured prior to symptom onset. However, it would be no small task to convince regulatory agencies to allow a clinical trial to take place in a premanifest patient population, and for good reason. Neurosurgery, even when carefully and properly performed, carries with it significant risks. Asking patients to subject themselves to such a surgery prior even to any deficit in their quality of life is, at best, ethically challenging. Nevertheless, this may be the only setting in which meaningful phenotypic rescue would be expected, in that this is the setting where there are actually cells in substantial quantities (and quality) to be rescued at all by the transgene. For this reason, data from animal trials will need to be of extremely high quality, repeated several times, with demonstrable effects in premanifest and manifest animals, for any serious attempt to be made in the clinical setting. Even in this setting, it would be difficult to convince Institutional Review Boards to condone a gene therapy trial in premanifest patients, but this might be the only way

such a neuroprotective gene therapy trial even has a chance of success.

Conclusions

The article documenting the definitive cloning of *huntingtin*, the causative mutated gene in HD, was published just over 20 years ago. Initially, there was hope that the mutant protein can simply be drugged directly and either “fixed” or destroyed. In the years since, the field has learned of mHTT’s altered protein-protein interactions and the difficulty in altering them pharmaceutically. We have looked for more easily drugged modifier proteins whose function facilitates mHTT toxicity, to learn that many such proteins exist but that no one protein seems to be the a key “spoke” other than mHTT itself. Animal models have been developed in great numbers, with different genetic bases and backgrounds allowing the core phenotypic effects to be more carefully studied. Finally, clinicians have made tremendous strides in the study of pathology in patients, if not yet in their ultimate outlook. This last step is all that remains, but for the next great drug to find success in the clinic, it must first have demonstrated effects in animal models, namely mice. My novel assay has provided further detail for a well-documented and consistent phenotype, dysregulation of *Drd2*, as well as demonstrated the means to leverage this assessment for preclinical candidate evaluation using minimal cohort sizes with great sensitivity. My hope is that my method can make the task of sifting through several candidate drugs or modifiers less daunting, and will ultimately provide the basis for HD or other disease researchers to leverage flow cytometry in the adult neuronal setting for sensitive phenotyping and specific cell population collection alike.

Bibliography

1. The Huntington's Study Group. Unified Huntington's Disease Rating Scale: reliability and consistency. Huntington Study Group. Mov Disord. 1996 Mar;11(2):136–42.

2. Vonsattel JP, Myers RH, Stevens TJ, Ferrante RJ, Bird ED, Richardson EP. Neuropathological classification of Huntington's disease. J Neuropathol Exp Neurol. 1985 Nov;44(6):559–77.

3. Brooks SP, Janghra N, Workman VL, Bayram-Weston Z, Jones L, Dunnett SB. Longitudinal analysis of the behavioural phenotype in R6/1 (C57BL/6J) Huntington's disease transgenic mice. Brain Res Bull. 2011 Jan 25.

4. Aggarwal M, Duan W, Hou Z, Rakesh N, Peng Q, Ross CA, et al. Spatiotemporal mapping of brain atrophy in mouse models of Huntington's disease using longitudinal in vivo magnetic resonance imaging. Neuroimage. 2012 Feb 9;60(4):2086–95.

5. Cui L, Jeong H, Borovecki F, Parkhurst CN, Tanese N, Krainc D. Transcriptional repression of PGC-1alpha by mutant huntingtin leads to mitochondrial dysfunction and neurodegeneration. Cell. 2006 Oct 6;127(1):59–69.

6. Goold R, Hubank M, Hunt A, Holton J, Menon RP, Revesz T, et al. Down-regulation of the dopamine receptor D2 in mice lacking ataxin 1. Hum Mol Genet. 2007 Sep 1;16(17):2122–34.

7. Zuccato C, Belyaev N, Conforti P, Ooi L, Tartari M, Papadimou E, et al. Widespread disruption of repressor element-1 silencing transcription factor/neuron-restrictive silencer factor occupancy at its target genes in Huntington's disease. J Neurosci. 2007 Jun 27;27(26):6972–83.

8. Stack EC, Kubilus JK, Smith K, Cormier K, del Signore SJ, Guelin E, et al. Chronology of behavioral symptoms and neuropathological sequela in R6/2 Huntington's disease transgenic mice. J. Comp. Neurol. 2005 Oct 3;490(4):354–70.

9. Crook ZR, Housman DE. Huntington's Disease: Can Mice Lead the Way to Treatment? Neuron. 2011 Feb 10;69(3):423–35.

10. Goula A-V, Stys A, Chan JPK, Trottier Y, Festenstein R, Mérienne K. Transcription Elongation and Tissue-Specific Somatic CAG Instability. PLoS Genet. 2012 Nov;8(11):e1003051.

11. Gray M, Shirasaki DI, Cepeda C, André VM, Wilburn B, Lu X-H, et al. Full-length human mutant huntingtin with a stable polyglutamine repeat can elicit progressive and selective neuropathogenesis in BACHD mice. J Neurosci. 2008 Jun 11;28(24):6182–95.

12. Southwell AL, Warby SC, Carroll JB, Doty CN, Skotte NH, Zhang W, et al. A fully humanized transgenic mouse model of Huntington disease. Hum Mol Genet. 2012 Oct 5.

13. Lin CH, Tallaksen-Greene S, Chien WM, Cearley JA, Jackson WS, Crouse AB, et al. Neurological abnormalities in a knock-in mouse model of Huntington's disease. Hum Mol Genet. 2001 Jan 15;10(2):137–44.

14. Matthews RT, Yang L, Browne S, Baik M, Beal MF. Coenzyme Q10 administration increases brain mitochondrial concentrations and exerts neuroprotective effects. Proc Natl Acad Sci USA. 1998 Jul 21;95(15):8892–7.

15. Andreassen OA, Dedeoglu A, Ferrante RJ, Jenkins BG, Ferrante KL, Thomas M, et al. Creatine increase survival and delays motor symptoms in a transgenic animal model of Huntington's disease. Neurobiology of Disease. 2001 Jun;8(3):479–91.

16. Borrell-Pagès M, Canals JM, Cordelières FP, Parker JA, Pineda JR, Grange G, et al. Cystamine and cysteamine increase brain levels of BDNF in Huntington disease via HSJ1b and transglutaminase. J Clin Invest. 2006 May;116(5):1410–24.

17. Gibrat C, Bousquet M, Saint-Pierre M, Lévesque D, Calon F, Rouillard C, et al. Cystamine prevents MPTP-induced toxicity in young adult mice via the up-regulation of the brain-derived neurotrophic factor. Prog. Neuropsychopharmacol. Biol. Psychiatry. 2010 Feb 1;34(1):193–203.

18. Sittler A, Lurz R, Lueder G, Priller J, Lehrach H, Hayer-Hartl MK, et al. Geldanamycin activates a heat shock response and inhibits huntingtin aggregation in a cell culture model of Huntington's disease. Hum Mol Genet. 2001 Jun 1;10(12):1307–15.

19. Waza M, Adachi H, Katsuno M, Minamiyama M, Sang C, Tanaka F, et al. 17-AAG, an Hsp90 inhibitor, ameliorates polyglutamine-mediated motor neuron degeneration. Nat Med. 2005 Oct;11(10):1088–95.

20. Hansson O, Nylandsted J, Castilho RF, Leist M, Jäättelä M, Brundin P. Overexpression of heat shock protein 70 in R6/2 Huntington's disease mice has only modest effects on disease progression. Brain Res. 2003 Apr 25;970(1-2):47–57.

21. Ehrnhoefer DE, Duennwald M, Markovic P, Wacker JL, Engemann S, Roark M, et al. Green tea (-)-epigallocatechin-gallate modulates early events in huntingtin misfolding and reduces toxicity in Huntington's disease models. Hum Mol Genet. 2006 Sep 15;15(18):2743–51.

22. Ferrante RJ, Kubilus JK, Lee J, Ryu H, Beesen A, Zucker B, et al. Histone deacetylase inhibition by sodium butyrate chemotherapy ameliorates the

neurodegenerative phenotype in Huntington's disease mice. J Neurosci. 2003 Oct 15;23(28):9418–27.

23. Hockly E, Richon VM, Woodman B, Smith DL, Zhou X, Rosa E, et al. Suberoylanilide hydroxamic acid, a histone deacetylase inhibitor, ameliorates motor deficits in a mouse model of Huntington's disease. Proc Natl Acad Sci USA. 2003 Feb 18;100(4):2041–6.

24. Thompson LM, Aiken CT, Kaltenbach LS, Agrawal N, Illes K, Khoshnan A, et al. IKK phosphorylates Huntingtin and targets it for degradation by the proteasome and lysosome. The Journal of Cell Biology. 2009 Dec 28;187(7):1083–99.

25. Gauthier LR, Charrin BC, Borrell-Pagès M, Dompierre JP, Rangone H, Cordelières FP, et al. Huntingtin controls neurotrophic support and survival of neurons by enhancing BDNF vesicular transport along microtubules. Cell. 2004 Jul 9;118(1):127–38.

26. Zuccato C, Ciammola A, Rigamonti D, Leavitt BR, Goffredo D, Conti L, et al. Loss of huntingtin-mediated BDNF gene transcription in Huntington's disease. Science. 2001 Jul 20;293(5529):493–8.

27. Strand AD, Baquet ZC, Aragaki AK, Holmans P, Yang L, Cleren C, et al. Expression profiling of Huntington's disease models suggests that brain-derived neurotrophic factor depletion plays a major role in striatal degeneration. J Neurosci. 2007 Oct 24;27(43):11758–68.

28. McBride JL, Boudreau RL, Harper SQ, Staber PD, Monteys AM, Martins I, et al. Artificial miRNAs mitigate shRNA-mediated toxicity in the brain: Implications for the therapeutic development of RNAi. Proc Natl Acad Sci USA. 2008 Apr 15;105(15):5868–73.

29. Franich NR, Fitzsimons HL, Fong DM, Klugmann M, During MJ, Young D. AAV vector-mediated RNAi of mutant huntingtin expression is neuroprotective in a novel genetic rat model of Huntington's disease. Mol Ther. 2008 May;16(5):947–56.

30. Boudreau RL, McBride JL, Martins I, Shen S, Xing Y, Carter BJ, et al. Nonallele-specific silencing of mutant and wild-type huntingtin demonstrates therapeutic efficacy in Huntington's disease mice. Mol Ther. 2009 Jun;17(6):1053–63.

31. McBride JL, Pitzer MR, Boudreau RL, Dufour B, Hobbs T, Ojeda SR, et al. Preclinical Safety of RNAi-Mediated HTT Suppression in the Rhesus Macaque as a Potential Therapy for Huntington's Disease. Mol Ther. 2011 Dec;19(12):2152–62.

32. Grondin R, Kaytor MD, Ai Y, Nelson PT, Thakker DR, Heisel J, et al. Six-month partial suppression of Huntingtin is well tolerated in the adult rhesus striatum. Brain. 2012 Apr;135(Pt 4):1197–209.

33. Ferrante RJ, Andreassen OA, Dedeoglu A, Ferrante KL, Jenkins BG, Hersch SM, et al. Therapeutic effects of coenzyme Q10 and remacemide in transgenic mouse models of Huntington's disease. J Neurosci. 2002 Mar 1;22(5):1592–9.

34. Huntington Study Group. A randomized, placebo-controlled trial of coenzyme Q10 and remacemide in Huntington's disease. Neurology. 2001 Aug 14;57(3):397–404.

35. Xie Y, Hayden MR, Xu B. BDNF overexpression in the forebrain rescues Huntington's disease phenotypes in YAC128 mice. J Neurosci. 2010 Nov 3;30(44):14708–18.

36. Jiang M, Peng Q, Liu X, Jin J, Hou Z, Zhang J, et al. Small-molecule TrkB receptor agonists improve motor function and extend survival in a mouse model of Huntington's disease. Hum Mol Genet. 2013 Mar 6.

37. Qiu Z, Norflus F, Singh B, Swindell MK, Buzescu R, Bejarano M, et al. Sp1 is up-regulated in cellular and transgenic models of Huntington disease, and its reduction is neuroprotective. J Biol Chem. 2006 Jun 16;281(24):16672–80.

38. Mielcarek M, Benn CL, Franklin SA, Smith DL, Woodman B, Marks PA, et al. SAHA decreases HDAC 2 and 4 levels in vivo and improves molecular phenotypes in the R6/2 mouse model of Huntington's disease. PLoS ONE. 2011;6(11):e27746.

39. Fujimoto M, Takaki E, Hayashi T, Kitaura Y, Tanaka Y, Inouye S, et al. Active HSF1 significantly suppresses polyglutamine aggregate formation in cellular and mouse models. J Biol Chem. 2005 Oct 14;280(41):34908–16.

40. Cicchetti F, Soulet D, Freeman TB. Neuronal degeneration in striatal transplants and Huntington's disease: potential mechanisms and clinical implications. Brain. 2011 Mar;134(Pt 3):641–52.

41. The Hd Ipsc Consortium. Induced Pluripotent Stem Cells from Patients with Huntington's Disease Show CAG-Repeat-Expansion-Associated Phenotypes. Cell Stem Cell. 2012 Jun 28.

42. An MC, Zhang N, Scott G, Montoro D, Wittkop T, Mooney S, et al. Genetic Correction of Huntington's Disease Phenotypes in Induced Pluripotent Stem Cells. Cell Stem Cell. 2012 Jun 26.

43. Bauer PO, Goswami A, Wong HK, Okuno M, Kurosawa M, Yamada M, et al. Harnessing chaperone-mediated autophagy for the selective degradation of mutant huntingtin protein. Nat Biotechnol. 2010 Mar;28(3):256–63.

44. Jurgens CK, van de Wiel L, van Es ACGM, Grimbergen YM, Witjes-Ané M-NW, van der Grond J, et al. Basal ganglia volume and clinical correlates in 'preclinical' Huntington's disease. J Neurol. 2008 Nov;255(11):1785–91.

45. Cheng Y, Peng Q, Hou Z, Aggarwal M, Zhang J, Mori S, et al. Structural MRI detects progressive regional brain atrophy and neuroprotective effects in N171-82Q Huntington's disease mouse model. Neuroimage. 2011 Jun 1;56(3):1027–34.

46. Kassubek J, Juengling FD, Ecker D, Landwehrmeyer GB. Thalamic atrophy in Huntington's disease co-varies with cognitive performance: a morphometric MRI analysis. Cereb. Cortex. 2005 Jun;15(6):846–53.

47. Kassubek J, Juengling FD, Kioschies T, Henkel K, Karitzky J, Kramer B, et al. Topography of cerebral atrophy in early Huntington's disease: a voxel based morphometric MRI study. J Neurol Neurosurg Psychiatr. 2004 Feb;75(2):213–20.

48. Rattray I, Smith E, Gale R, Matsumoto K, Bates GP, Modo M. Correlations of Behavioral Deficits with Brain Pathology Assessed through Longitudinal MRI and Histopathology in the R6/2 Mouse Model of HD. PLoS ONE. 2013;8(4):e60012.

APPENDIX: TARGETING HTT RNA SECONDARY STRUCTURE

Introduction

Many hereditary diseases, including Huntington's Disease (HD) and Myotonic Dystrophy (DM), involve a toxic gain of function. While DM type 1 (DM1) is brought on by an RNA gain of function mechanism, including muscleblind proteins aberrantly binding expanded CUG repeats in the 3' untranslated region of DMPK (1), HD toxicity is encoded by an expanded poly(CAG) tract causing a polyglutamine expansion in the N-terminus of huntingtin (HTT) (2). Both diseases are progressive in nature with pleiotropic symptoms (3,4), and as gain of toxic function disorders, could be treated by reducing the toxic species. In the case of DM1, this can only reasonably be accomplished by trying to either reduce the levels of the toxic RNA, potentially by treatment with oligonucleotides that engage RNase H (5), or by prevention of the poly(CUG) repeat in DMPK from interacting with the splicing factor MBNL, which also has tremendous potential (6-8). However, in HD, because the toxic species is a protein with aberrant protein-protein interaction tendencies, much of the attention has been at the level of removing the toxic protein. This might be done indirectly through modulation of protein folding pathways (9,10) or directly by administering transgenes that interact with mutant HTT (11-13), causing degradation machinery like the proteasome and autophagosome to destroy it more efficiently.

However, because the toxic species is a protein, a similar strategy to that of DM1 can be attempted, targeting the mRNA directly. The conventional method for targeting mutant HTT RNA (*mHTT*) involves knockdown or oligonucleotide-based approaches.

Engaging the RNAi machinery of the cell using virally delivered short hairpin RNAs has had preclinical efficacy in several studies (14-17). Alternatively, using oligonucleotides to engage target RNA sequences through RNase H has promise because it would not risk altering miRNA homeostasis (through engaging the RNAi machinery), and there is also evidence of preclinical rescue through such methods (18).

There may be an intersection of these two strategies, and it relies on two facts. One is that poly(CAG) repeats can be highly structured with high melting temperatures (19). The other is that there are interesting sequences within the 5' untranslated region (UTR) of *HTT* that modulate its transcription rate, such as an upstream open reading frame (uORF) whose ablation increases downstream HTT translation (20). Because of our lab's longstanding interest in both DM and HD, we looked more closely at the 5' region of *HTT*, both coding and noncoding, from an RNA structure perspective. In doing so, we noticed that the 5' region of *HTT* appears highly structured, particularly a hairpin encompassing its start codon. While much of the efforts for DM1 have gone into interacting with repeat structures with the intent of freeing binding factors like MBNL, here, the strategy could be to stabilize the secondary structure of *HTT*, reducing translation. I therefore tested whether two separate predicted hairpins can be modulated in a fashion that would reduce translation rates, first genetically, then pharmaceutically using both oligonucleotides and small molecule libraries. This work is preliminary in nature and will be continued by the lab in the coming years, but demonstrates in principle that *HTT* RNA structure is an additional target for reducing the production of mHTT protein.

Methods

Cloning and T7 transcription of constructs: The firefly luciferase vector pGL4.13 (Promega) was the base vector for *HTT* construct cloning, while pGL4.73 (Promega) was used for generating renilla luciferase transcripts. Wild type sequences of *HTT* were PCR amplified from cDNA generated from patient lymphoblastoid cell lines. These were cloned into pGL4.13 using In-Fusion (Clontech) to generate the exon 1 constructs (Q20, Q47, and Q96), as well as the wild type UTR construct. The Strong hairpin, Weak hairpin, and start codon mutants were generated from the wild type UTR construct by site-directed mutagenesis using overlapping PCR primers amplifying in the opposite directions. Transcripts were produced by PCR amplifying the appropriate luciferase or *HTT*-luciferase gene from these plasmids using primers that caused the product to include a T7 consensus binding site upstream (5'-TACGTACGTTAATACGACTCACTATAGGGAGAGCCACC-3') and 20 (dA) bases downstream. RNA (uncapped) is produced by T7 *in vitro* transcription (Epicentre) according to manufacturer directions, incubating 250 ng of PCR product for 1 hr. RNA is purified from the reactions with RNeasy columns (Qiagen) according to manufacturer instructions. Aliquots were dissolved in H_2O to desired concentrations and stored at -80°C until use.

Oligonucleotides for translation inhibition: The following oligonucleotides (unmodified DNA oligos, IDT) were tested; those in bold were used for dose escalation and as screening controls.

UTR Oligo 1: GTTTTTGGCATCTTCTGGCCTCGGGCCG

UTR Oligo 2: GTTTTTGGCATCTTCTGCCTCGGGCCG

UTR Oligo 3: GTTTTTGGCATCTTCGGCCTCGGGCCG

UTR Oligo 4: GTTTTTGGCATCTTCGCCTCGGGCCG

UTR Oligo 5: GTTTTTGGCATCTTCTAGGCCTCGGGCCG

UTR Oligo 6: GTTTTTGGCATCTTCTTGGCCTCGGGCCG

UTR Oligo 7: GTTTTTGGCATCTTCTTAGGCCTCGGGCCG

UTR Oligo Scrambled: TGTGAGTTTGCTCTGCCTGGCCGTGCTC

CAG Oligo 1: TGAGGAAGCTGAGGAGTGGAAGGACTTG

CAG Oligo 2: TGAGGAAGCTGAGGAGGGAAGGACTTG

CAG Oligo 3: TGAGGAAGCTGAGGATGGAAGGACTTG

CAG Oligo 4: TGAGGAAGCTGAGGAGGAAGGACTTG

CAG Oligo 5: TGAGGAAGCTGAGGAGCTGGAAGGACTTG

CAG Oligo 6: TGAGGAAGCTGAGGAGGTGGAAGGACTTG

CAG Oligo 7: TGAGGAAGCTGAGGAGGCTGGAAGGACTTG

CAG Oligo Scrambled: ATAGTGCGTGGAGGAATGAGGGAGGTAC

Cell-free translation systems: Wheat germ extract and Rabbit reticulocyte lysate (Promega) were used to generate active luciferase for quantitation of translation. Reactions were run in 15 μL volumes using 300 ng/well firefly luciferase RNA (various clones) as well as 0.3 ng/well renilla luciferase RNA (unmodified). For oligonucleotide or compound incubations, RNA and drug were pre-incubated in a total volume of 3 μL. The concentrations assayed are that seen by the RNA in this 3 μL volume, but after a 15 min incubation at 37°C, the cell free extract was added to a total volume of 15 μL. This

reaction was incubated for a further 45 mins, and then was frozen at -20°C before assaying in a Dual Luciferase System (Promega).

Luciferase quantification: All firefly data was internally normalized to the renilla value from that same well. 10 μL of the cell free translation reaction was added to each well of a white-bottom plate compatible with the Varioskan Flash (Thermo Scientific) 96-well luminometer. Reading time was 8 seconds after a 2 second lag time following reagent injection, and samples were read at room temperature. For screening, all plates contained at least 6 no drug (water) control wells, 3 Strong Hairpin wells, and 3 wells containing the exon 1 (Q47) construct as well as 10 fold excess inhibitory oligo. Plates were re-run if all positive controls were not at least 4 standard deviations below the mean of the no drug controls, and all drug wells were reported as a percentage of luciferase seen in the averaged no drug wells. Data was analyzed in Microsoft Excel.

Results

The 5' Region of *HTT* is Highly Structured

mFOLD RNA structure prediction software (21) was used to investigate any potential secondary structure present in exon 1 of *HTT*, a region whose expression is sufficient for toxicity when expressed in mice (22). In doing so, the first 160 bases of the transcript present three highly structured and stable predicted hairpins (Figure 1A). This region of *HTT* is highly conserved between humans, chimpanzees, mice, and rats (Figure 1B), including the non-coding sequences, suggesting potential function that could exist on a structural level. The first such hairpin contains the start codon for an

upstream open reading frame (uORF), whose expression levels modulate downstream *HTT* levels (20). However, the third hairpin contains the *HTT* start codon, and is predicted to be the most stable of the three. Hence, we reasoned that this hairpin in particular could be amenable to small molecule or oligonucleotide targeting, as there are three bulges or loops into which a small molecule could potentially insert and stabilize the structure, on top of the base pairing apparent that could be altered through an agent that intercalates or rests in the major groove. This region was subcloned into luciferase vectors and transcribed *in vitro* for further study in cell-free translation systems, so as to screen for an ability to inhibit translation exogenously. Cell-free translation systems were favored for these studies in order to separate the activities of transcription and translation, ensuring that any activities observed are on the post-transcriptional level. Additionally, this provides the practical advantages of using compounds with poor cell penetrance in primary screening.

Genetic Modulation of the Start Codon-containing Hairpin has Strong Effects on the Translation Rate.

Before attempting to target the secondary structure of *HTT* exon 1 pharmacologically, I needed to establish that altering the strength of this hairpin would, in fact, impact translation rates. Hence, the first 160 bases of *HTT* (from the transcription start site through the first 5 codons of *HTT*, pictured in Figure 1) were cloned upstream of firefly luciferase, while additional clones were modified to either strengthen or weaken the hairpin containing the start codon (Figure 2A). Originally with a free energy of -31.33 kcal/mol, five sites were mutated to strengthen this hairpin,

producing a new “Strong hairpin” with 50% increased stability (-47.23 kcal/mol). Encouragingly, the features whose alteration contributed most strongly to the predicted stability, the bulges, are those that may serve as the most attractive targets for drugging. Reciprocal alterations were made by creating a construct with extremely weak structure through similar mutations. Whereas the wild type hairpin shown (Figure 2A) is always present in mFOLD prediction permutations, the structure for this weakened structure (“Weak hairpin”) is predicted to be highly variable; the most stable such prediction was shown.

These constructs, plus two more that mutated the two start codons present (the uORF start codon, and that of *HTT*), were tested for translation rates by first *in vitro* transcribing the construct and then adding a set concentration of the purified transcript into cell free translation systems. In both systems (wheat germ extract and rabbit reticulocyte lysate), the strong hairpin reduced translation rates by >95%, almost as strongly as the construct with the mutated start codon. In addition, the weakened hairpin had a three to four fold increase of translation. An increase was also seen by removing uORF translation, indicating that both the secondary structure of the start codon-containing UTR hairpin and uORF usage may be relevant regulatory cis elements in the *HTT* transcript. This is plausible considering the strong conservation of this sequence (both coding and non-coding) in humans, chimpanzee, mice, and rats (Figure 1B).

Targeted Impairment of *HTT* Transcript Expression

The above results encouraged further analysis of *HTT* RNA structure as a therapeutic target. Looking more broadly at the *HTT* transcript, specifically the exon 1

region (Figure 3A), it is apparent that the poly(CAG) repeat, encoding polyglutamine, also has substantial potential structure. This is not surprising; a poly(CUG) repeat forms hairpins in DM1 (1), while there is evidence that expanded poly(CAG) androgen receptor and poly(CAG) *HTT* can form RNA foci in nuclei of fibroblasts (23). Hence, there are two potential hairpins in the 5' region of *HTT* that may be amenable to stabilization with small molecules or oligonucleotides (Figure 3B). To identify such molecules, two approaches are reasonable. Targeted design requires substantial computational predictive ability for the 3D structure of the resulting hairpin, but such approaches have been fruitful for identifying first generation compounds to target the poly(CUG) repeat of *DMPK* in DM1 (6), and may be potentially useful for the poly(CAG) repeat of *HTT*. Oligonucleotide approaches, on the other hand, may be initiated with only knowledge of the base pairs to which we want them to anneal, "locking" the base of the hairpin and possibly stabilizing it to mimic the effects demonstrated genetically.

Figure 4 demonstrates my testing with several oligonucleotides (oligos), designed against the base of the UTR hairpin (Figure 4A-B) or the base of the poly(CAG) hairpin (Figure 4C-D) in the context of cell-free extracts translating luciferase constructs with the appropriate sequence upstream. Two details are apparent. First, several such oligos have substantial efficacy, capable of reducing luciferase by >60% in many cases or even as much as 80%. Second, the effects are blunted in rabbit reticulocyte lysate versus wheat germ extract. That plant and mammalian cell free systems have differences in oligo interaction is not surprising, but there are two particularly intriguing possibilities for how this difference could be seen. If steric hindrance by "locking" the hairpin is the mechanism of action, there may be differences

in the kinds or activities of helicases between the two preps. On the other hand, if RNase H is mediating the reduction by degrading mRNA found in RNA-DNA hybrids, this could be seen if the two systems have different RNase H activity. I am unaware of any detailed studies on the differing helicase activities of the two systems, but RNase H is much more active in wheat germ extract than in rabbit reticulocyte lysate (24). The actual mechanism of action of these oligomers, whether steric hindrance or nuclease engagement, is currently under investigation in our group.

Screening a Small Molecule Library for Inhibitors of *mHTT* Translation

Other than rationally designed approaches for identifying translation inhibitors, unbiased compound library screens can be attempted. As a proof of principle for this, I acquired a library of ~1800 natural compounds from the laboratory of Jerry Pelletier at McGill University and attempted to identify compounds within that naturally suppress luciferase translation in a manner specific to *mHTT* sequence elements. From extensive tests of the values produced by negative controls (*HTT* exon 1 (Q47) – Firefly fusion) and positive controls (Strong Hairpin – Firefly fusion), I determined that the screen has an appropriate variance and dynamic range to facilitate screens (Z-score = 0.55). Hence, singlet tests using 20 μM of each compound were conducted to identify those that reduced luciferase levels (Figure 5A). Several such compounds were identified, which were validated in triplicate. However, because the compounds were not removed from solution prior to luciferase activity testing, it is likely that many of them are simply inhibitors of luciferase rather than suppressors of translation. Hence, these 34 positive compounds were further tested for an ability to suppress luminescence when pre-

incubated with a luciferase transcript with no *HTT* sequences (Figure 5B). Many remained effective in this setting (suggesting an activity related to luciferase enzymatic activity), but others were ineffective, and hence appear to have inhibitory effects that were *HTT* sequence-specific. Four such compounds (isobavachalcone, gancaonin G, alpinumisoflavone, and glyasperin H) inhibited luciferase with exon 1 (Q47) upstream by >40% but were at least 1.5-fold less effective at inhibiting luciferase alone. All are highly aromatic, which may lend itself to intercalation. Isobavachalcone, in particular, was 4.4 fold more effective at inhibiting activity of the exon 1 (Q47) transcript than that of luciferase alone. There is evidence of anti-inflammatory and anti-tumorigenic activity of this compound (25,26), but interestingly for us, it has also been directly demonstrated to relax supercoiled DNA (27), demonstrating a potential ability to interact with double stranded nucleic acids.

Discussion

Inhibiting *HTT* translation is amongst the most promising therapeutic options for HD, because while there are several pathways downstream of mHTT that contain pharmaceutical targets (such as creatine for mitochondrial defects or *BDNF* cell and gene therapy for trophic factor starvation), an ideal solution that would resolve all of the varied toxicities would be reducing the amount of mHTT present in neurons. Efforts aimed at directly removing mHTT are ongoing and promising (11,13), but prevention of translation may reduce protein levels with the fewest side effects. The aromatic small molecules identified from preliminary screening efforts may be specific to the *HTT* transcript, but it is more likely that they simply interact with double stranded RNA.

However, this kind of screening could be generally used to inform us about secondary structures in RNA and what kinds of compounds efficiently interact with them. Additional structured RNA sequences can be cloned into luciferase, and similar screens for prevention of translation can be attempted. Perhaps more powerfully, small molecule microarrays could rapidly assess direct binding to transcripts in a sequence-specific manner, and hit compounds could be rapidly validated in cell free systems and in tissue culture for translation inhibition. Sequence specificity may not be easily ascertained, but learning what kinds of compounds interact with what kinds of structures could allow for better rational drug design, such as scaffolding approaches (28).

The predicted secondary structures in *HTT* RNA require tremendous work for validation and further screening efforts to identify interactors, but there is also potential here for avoiding off target effects present in standard knockdown approaches. Targeting *HTT* transcripts with RNAi engaging small RNAs, such as AAV-delivered shRNA transgenes (14-16,29), presents the risk for off target toxicity due to the nature of the RISC complex, as the 6-base seed sequence mediates much of the specificity. Promiscuous sequences can result in the reduction of many unintended targets, often with toxic consequences (30). However, if either oligo or small molecule approaches identify compounds that require a particular secondary structure for their inhibitory effects, it would provide additional specificity in the form of structure in addition to sequence. In the case of the UTR hairpin, there is preliminary data from our group to suggest that oligo binding to the sequence immediately upstream of the hairpin is sufficient for inhibitory effects. Furthermore, not only is the effect likely RNase H mediated, but importantly, it may be dependent on an intact RNA hairpin downstream of

the binding site. If validated, this could provide a suitable binding site within the *HTT* transcript for oligonucleotide therapeutic approaches, but one for which off-target effects would be blunted in those transcripts without sufficient adjacent secondary structure.

Testing for therapeutic efficacy requires a demonstration of improvement in neuropathology and behavior. The oligos identified here may have more immediate therapeutic potential than the aromatic compound hits, and there have been recent strides in oligonucleotide therapeutics for mouse models of HD (18). We have preliminary data that backbone modifications to protect the oligos from nuclease degradation do not impair its efficacy, and delivery to tissue culture for knockdown validation is ongoing. For testing *in vivo*, it my D2GFP assay could be used in mouse models of HD to evaluate oligos, primarily because of its sensitivity. This allows small cohorts to give conclusive results, and because oligos can be modified in many ways, multiple iterations may need to be tested *in vivo* to demonstrate a substantial protective effect before it becomes worthwhile to invest in larger behavioral studies.

In all, this work is at early stages but demonstrates that, on top of sequence specificity, structure specificity might be leveraged to make prevention of *HTT* translation as safe as possible from off target effects. Further studies, *in vitro* and *in vivo*, are in progress, but my small cohort D2GFP dysregulation assay would be an ideal test for efficacy given the modular and rapidly modifiable nature of such oligos.

Acknowledgements

The work in this chapter was done with tremendous help from Theresa Gipson. Dr. Jerry Pelletier donated both materials and advice for the library screen.

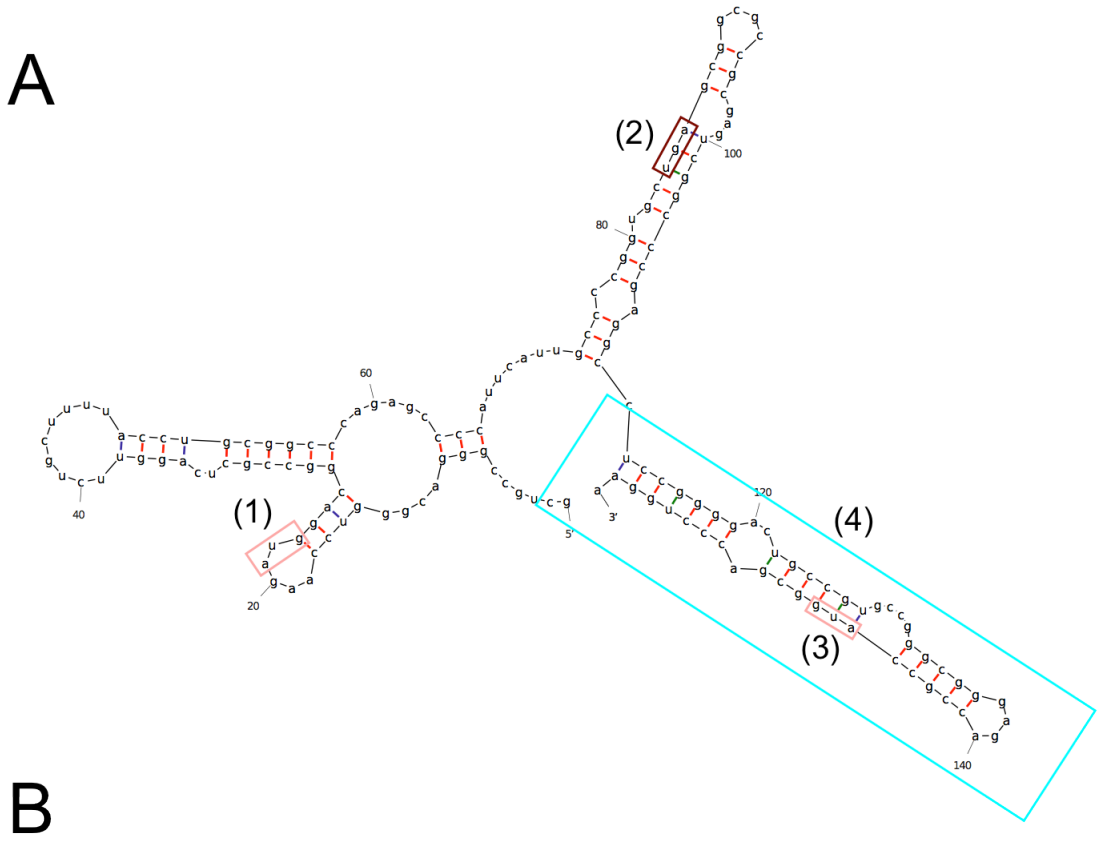

Figure 1: The 5' HTT mRNA sequence is predicted to contain significant secondary structure. (A) mFOLD structure prediction was applied to the 5' *HTT* mRNA sequence, from the transcription start site to through the 5th codon of *HTT*. An upstream open reading frame is present, with a start codon **(1)** and stop codon **(2)** within structured regions. The strongest structured region **(4)** contains the *HTT* start codon **(3)**. **(B)** There is significant homology of this region in human, chimpanzee, mouse, and rat *huntingtin* (labeled HsHTT, PtHTT, MmHtt, and RnHtt, respectively), even among the noncoding sequences. The blue shaded region is the upstream open reading frame, while the red shaded region is the beginning of the *HTT* coding sequence. The green dot designates the published transcription start site in human *HTT*.

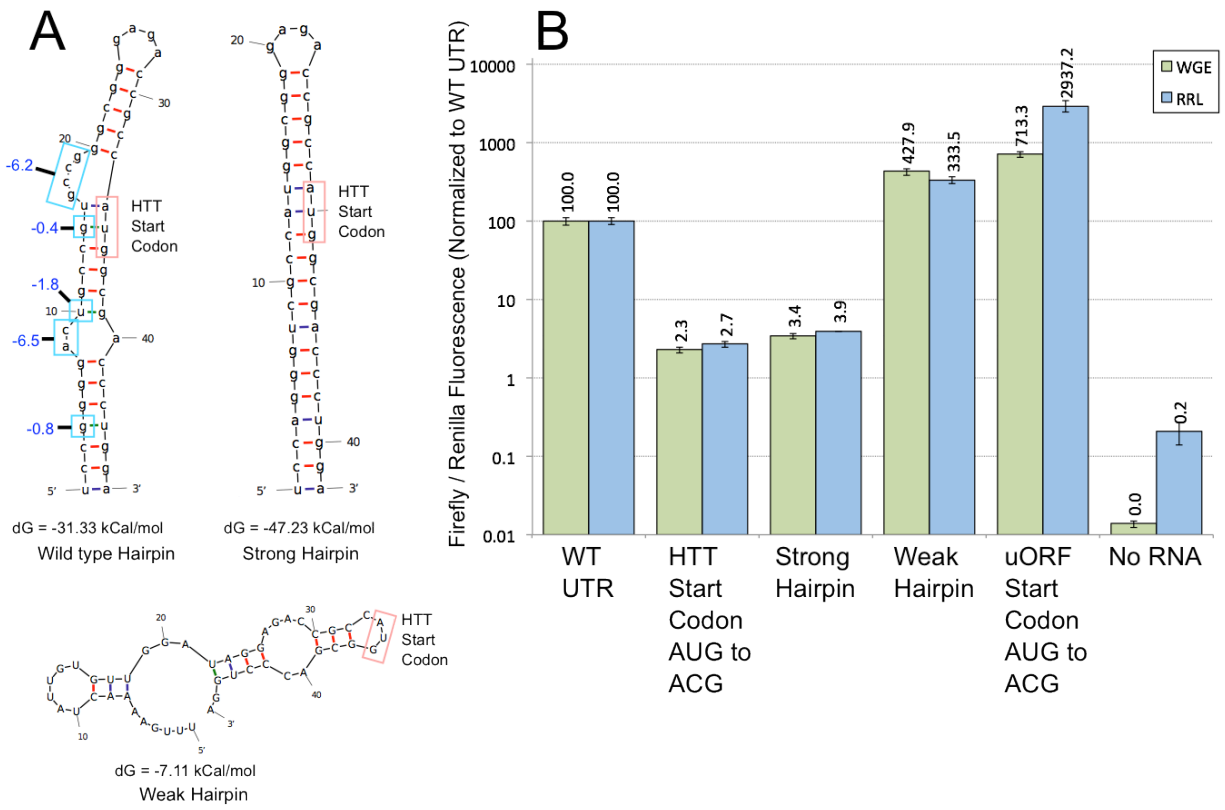

Figure 2: Modifying the start codon-containing hairpin structure impacts its translation rate. (A) The start codon in the wild type *HTT* transcript is within a hairpin with a predicted energy of -31.33 kCal/mol ("Wild type Hairpin"). Five sites (blue boxes) were mutagenized to raise the melting temperature ("Strong Hairpin"); the kCal/mol changes of each mutation are indicated in blue. Alternatively, a weakened version was made that abrogated most of the strong base pairing ("Weak Hairpin"). Neither the Strong nor the Weak hairpins have an altered protein coding sequence. **(B)** When placed upstream of firefly luciferase, translation rates were measured as luminescence from cell free extracts. WGE = wheat germ extract, RRL = rabbit reticulocyte lysate. Luciferase data presented as firefly (*HTT* constructs) normalized to renilla (unmodified).

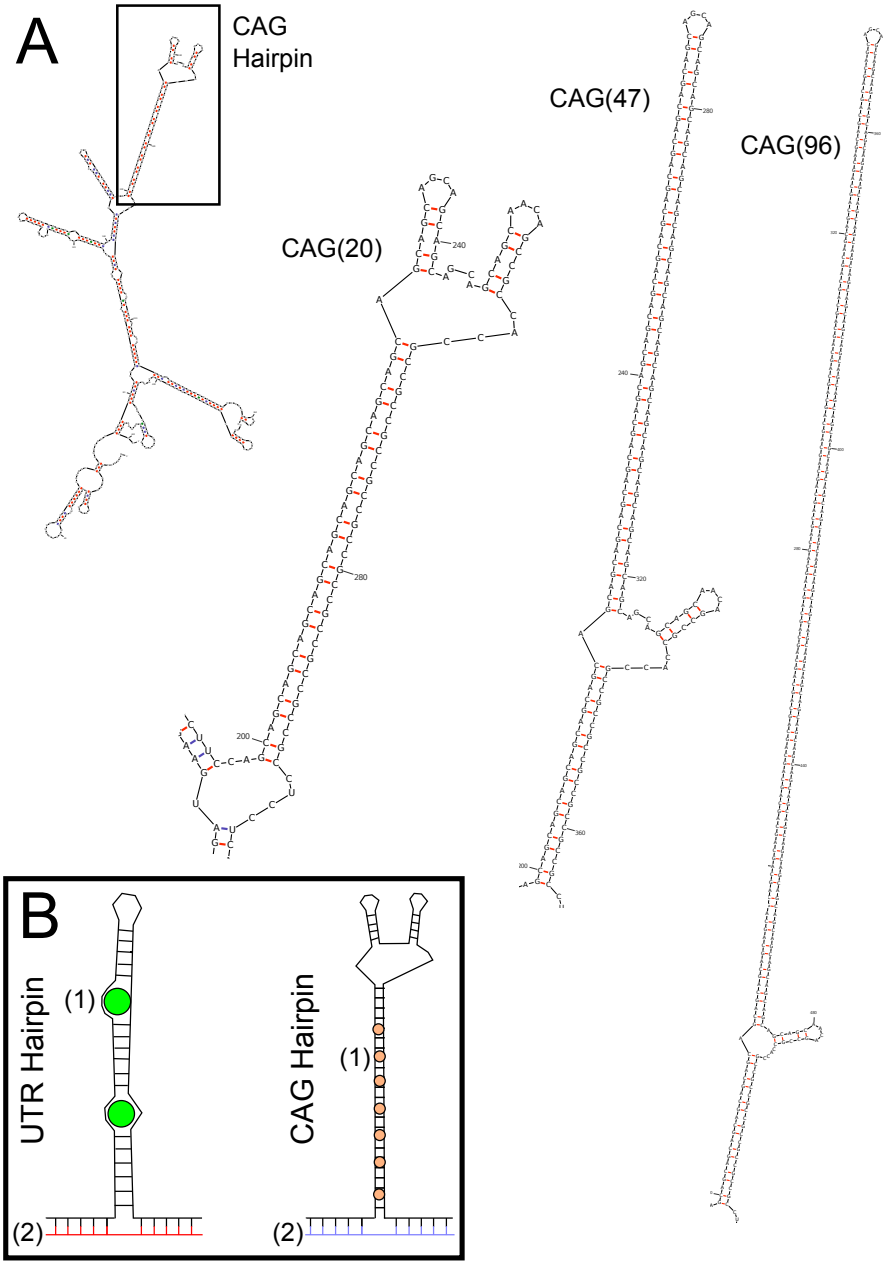

Figure 3: Hairpins formed in the 5'UTR and by the CAG repeat may be targetable by drugs or oligonucleotides. (A) Apart from the hairpin containing the start codon (Figures 1 and 2), another hairpin formed by the CAG repeat may serve as a target. The *HTT* transcript up to intron 1, when structure is predicted by mFOLD, has such a predicted hairpin, whose size only increases as the CAG repeat length increases without affecting the rest of the structure. **(B)** Strategies for targeting these secondary structures (UTR hairpin on the left, poly(CAG) on the right) could include finding an intercalating drug that stabilizes the annealed hairpin **(1)**, or finding oligonucleotides that span the base of the structure to "lock" it in place **(2)**.

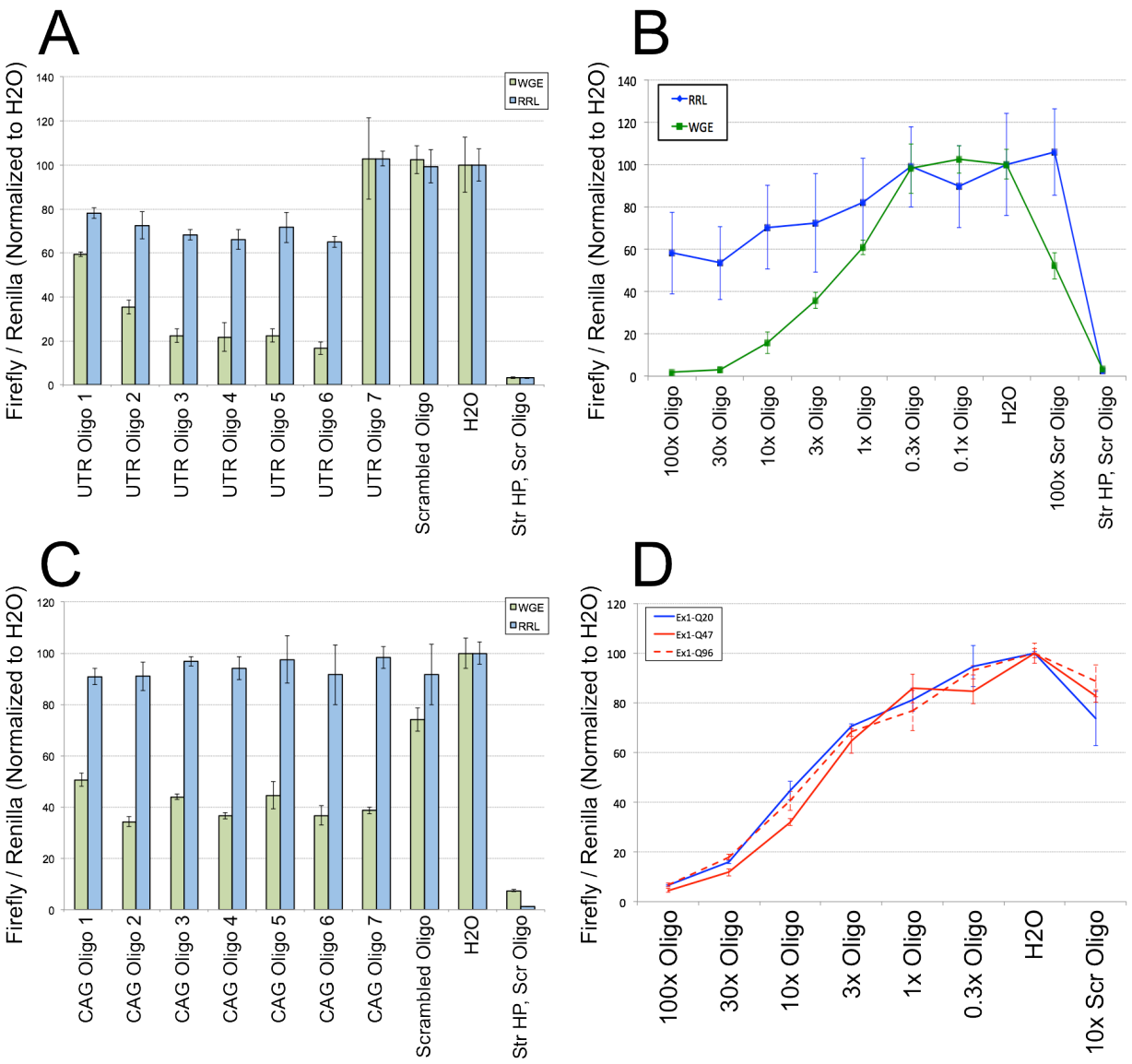

Figure 4: Oligonucleotides targeting the base of the hairpins can suppress translation. (A) Oligonucleotides (oligos) versus the UTR hairpin were screened. The most effective one (Oligo 6) was tested for dose response **(B)** in both WGE and RRL. **(C)** A similar strategy was attempted for oligos targeting the base of the CAG repeat hairpin, with oligo 2 tested more thoroughly in WGE. **(D)**. Interestingly, in WGE, there was no altered dose response in the exon 1 constructs with longer poly(CAG) tracts. The dosage curves in (B) and (D) were completed by adding oligo in the given fold excess, while the data in (A) and (C) used a 10 fold excess of oligo. Str HP = strong hairpin, Scr = scrambled. WGE = wheat germ extract, RRL = rabbit reticulocyte lysate. All luciferase data presented as firefly (*HTT* constructs) normalized to renilla (unmodified), and all oligos were pre-incubated with target transcripts prior to addition of cell free translation systems.

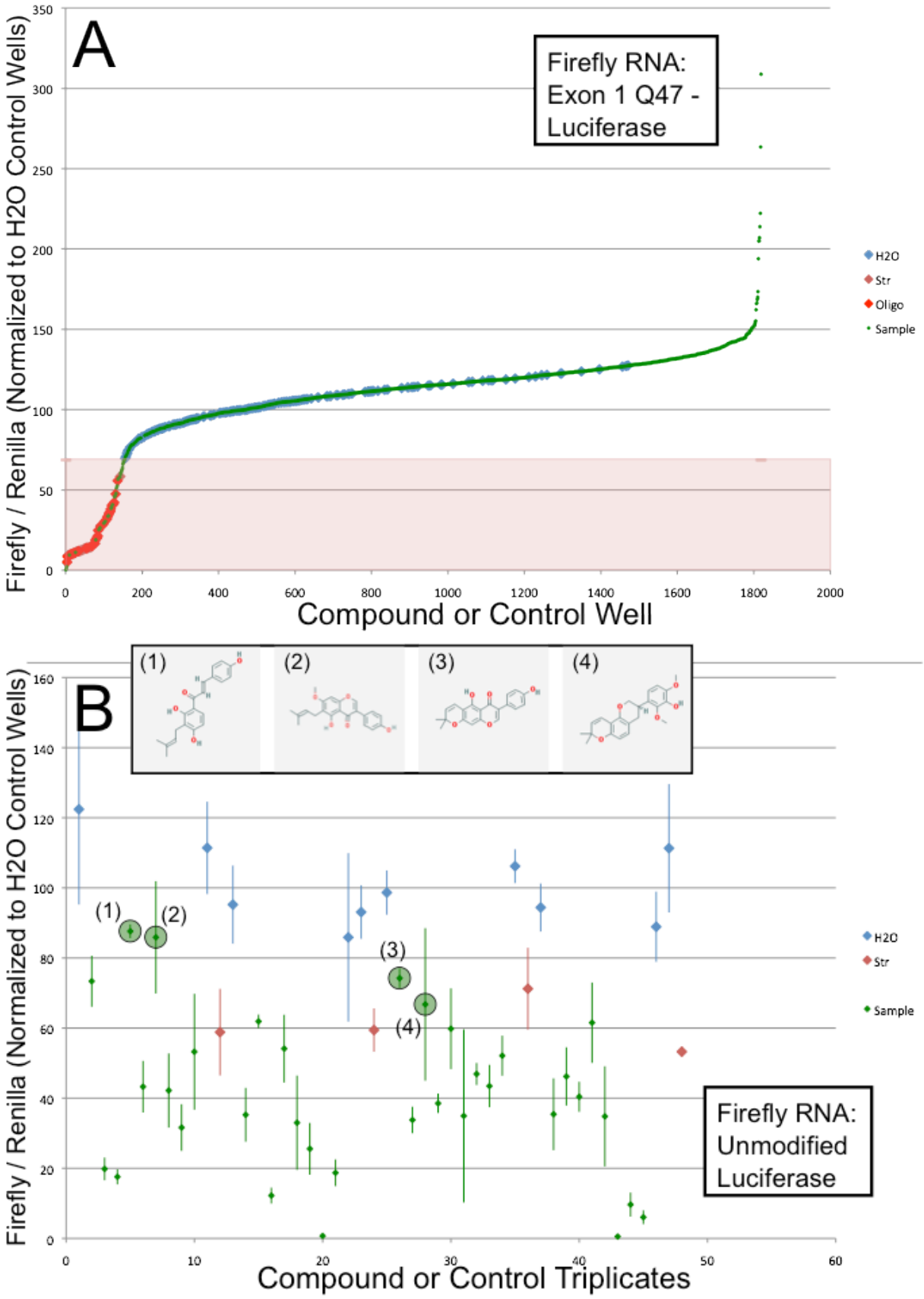
A
Firefly RNA:
Exon 1 Q47 -
Luciferase
Firefly / Renilla (Normalized to H2O Control Wells)
Compound or Control Well
H2O
Str
Oligo
Sample
B
(1)
(2)
(3)
(4)
Firefly / Renilla (Normalized to H2O Control Wells)
Compound or Control Triplicates
Firefly RNA:
Unmodified
Luciferase

Figure 5: The exon 1-luciferase fusion transcript can be screened for compounds that specifically inhibit the translation of exon 1. (A) A small molecule library of ~1800 compounds was screened for an ability to inhibit luminescence produced by *in vitro* transcription of the *HTT* exon 1 (Q47) – luciferase construct. Compounds were tested further if they resulted in lower luciferase activity than all of the water controls (pink shaded region). **(B)** When tested against a transcript encoding firefly luciferase alone, many of the hits from the primary screen (34 of which also re-validated in triplicate) failed to inhibit luciferase activity when the transcript lacked *HTT* exon 1 sequences, suggesting sequence specificity to inhibiting *HTT* translation. Four such compounds were isobavachalcone (1), gancaonin G (2), alpinumisoflavone (3), and glyasperin H (4).

Bibliography

1. Miller JW, Urbinati CR, Teng-Umnuay P, Stenberg MG, Byrne BJ, Thornton CA, et al. Recruitment of human muscleblind proteins to (CUG)(n) expansions associated with myotonic dystrophy. EMBO J. 2000 Sep 1;19(17):4439–48.

2. The Huntington's Disease Collaborative Research Group. A novel gene containing a trinucleotide repeat that is expanded and unstable on Huntington's disease chromosomes. Cell. 1993 Mar 26;72(6):971–83.

3. Cho DH, Tapscott SJ. Myotonic dystrophy: emerging mechanisms for DM1 and DM2. Biochim Biophys Acta. 2007 Feb;1772(2):195–204.

4. Penney JB, Vonsattel JP, MacDonald ME, Gusella JF, Myers RH. CAG repeat number governs the development rate of pathology in Huntington's disease. Ann Neurol. 1997 May;41(5):689–92.

5. Lee JE, Bennett CF, Cooper TA. RNase H-mediated degradation of toxic RNA in myotonic dystrophy type 1. Proc Natl Acad Sci USA. 2012 Mar 13;109(11):4221–6.

6. Childs-Disney JL, Parkesh R, Nakamori M, Thornton CA, Disney MD. Rational design of bioactive, modularly assembled aminoglycosides targeting the RNA that causes myotonic dystrophy type 1. ACS Chem. Biol. 2012 Dec 21;7(12):1984–93.

7. Leger AJ, Mosquea LM, Clayton NP, Wu I-H, Weeden T, Nelson CA, et al. Systemic delivery of a Peptide-linked morpholino oligonucleotide neutralizes mutant RNA toxicity in a mouse model of myotonic dystrophy. Nucleic Acid Ther. 2013 Apr;23(2):109–17.

8. Warf MB, Nakamori M, Matthys CM, Thornton CA, Berglund JA. Pentamidine reverses the splicing defects associated with myotonic dystrophy. Proc Natl Acad Sci USA. 2009 Nov 3;106(44):18551–6.

9. Fujimoto M, Takaki E, Hayashi T, Kitaura Y, Tanaka Y, Inouye S, et al. Active HSF1 significantly suppresses polyglutamine aggregate formation in cellular and mouse models. J Biol Chem. 2005 Oct 14;280(41):34908–16.

10. Hay DG, Sathasivam K, Tobaben S, Stahl B, Marber M, Mestril R, et al. Progressive decrease in chaperone protein levels in a mouse model of Huntington's disease and induction of stress proteins as a therapeutic approach. Hum Mol Genet. 2004 Jul 1;13(13):1389–405.

11. Southwell AL, Ko J, Patterson PH. Intrabody gene therapy ameliorates motor, cognitive, and neuropathological symptoms in multiple mouse models of Huntington's disease. J Neurosci. 2009 Oct 28;29(43):13589–602.

12. Wang C-E, Tydlacka S, Orr AL, Yang S-H, Graham RK, Hayden MR, et al.

Accumulation of N-terminal mutant huntingtin in mouse and monkey models implicated as a pathogenic mechanism in Huntington's disease. Hum Mol Genet. 2008 Sep 1;17(17):2738–51.

13. Bauer PO, Goswami A, Wong HK, Okuno M, Kurosawa M, Yamada M, et al. Harnessing chaperone-mediated autophagy for the selective degradation of mutant huntingtin protein. Nat Biotechnol. 2010 Mar;28(3):256–63.

14. Rodriguez-Lebron E, Denovan-Wright EM, Nash K, Lewin AS, Mandel RJ. Intrastriatal rAAV-mediated delivery of anti-huntingtin shRNAs induces partial reversal of disease progression in R6/1 Huntington's disease transgenic mice. Mol Ther. 2005 Oct;12(4):618–33.

15. McBride JL, Pitzer MR, Boudreau RL, Dufour B, Hobbs T, Ojeda SR, et al. Preclinical Safety of RNAi-Mediated HTT Suppression in the Rhesus Macaque as a Potential Therapy for Huntington's Disease. Mol Ther. 2011 Dec;19(12):2152–62.

16. Franich NR, Fitzsimons HL, Fong DM, Klugmann M, During MJ, Young D. AAV vector-mediated RNAi of mutant huntingtin expression is neuroprotective in a novel genetic rat model of Huntington's disease. Mol Ther. 2008 May;16(5):947–56.

17. Boudreau RL, Martins I, Davidson BL. Artificial microRNAs as siRNA shuttles: improved safety as compared to shRNAs in vitro and in vivo. Mol Ther. 2009 Jan;17(1):169–75.

18. Kordasiewicz HB, Stanek LM, Wancewicz EV, Mazur C, McAlonis MM, Pytel KA, et al. Sustained therapeutic reversal of Huntington's disease by transient repression of huntingtin synthesis. Neuron. 2012 Jun 21;74(6):1031–44.

19. Sobczak K, Krzyzosiak WJ. CAG repeats containing CAA interruptions form branched hairpin structures in spinocerebellar ataxia type 2 transcripts. J Biol Chem. 2005 Feb 4;280(5):3898–910.

20. Lee J, Park EH, Couture G, Harvey I, Garneau P, Pelletier J. An upstream open reading frame impedes translation of the huntingtin gene. Nucleic Acids Res. 2002 Dec 1;30(23):5110–9.

21. Zuker M. Mfold web server for nucleic acid folding and hybridization prediction. Nucleic Acids Res. 2003 Jul 1;31(13):3406–15.

22. Mangiarini L, Sathasivam K, Seller M, Cozens B, Harper A, Hetherington C, et al. Exon 1 of the HD gene with an expanded CAG repeat is sufficient to cause a progressive neurological phenotype in transgenic mice. Cell. 1996 Nov 1;87(3):493–506.

23. de Mezer M, Wojciechowska M, Napierala M, Sobczak K, Krzyzosiak WJ. Mutant

CAG repeats of Huntingtin transcript fold into hairpins, form nuclear foci and are targets for RNA interference. Nucleic Acids Res. 2011 Jan 18;39(9):3852–63.

24. Cazenave C, Frank P, Büsen W. Characterization of ribonuclease H activities present in two cell-free protein synthesizing systems, the wheat germ extract and the rabbit reticulocyte lysate. Biochimie. 1993;75(1-2):113–22.

25. Matsuda H, Kiyohara S, Sugimoto S, Ando S, Nakamura S, Yoshikawa M. Bioactive constituents from Chinese natural medicines. XXXIII. Inhibitors from the seeds of Psoralea corylifolia on production of nitric oxide in lipopolysaccharide-activated macrophages. Biol Pharm Bull. 2009 Jan 1;32(1):147–9.

26. Nishimura R, Tabata K, Arakawa M, Ito Y, Kimura Y, Akihisa T, et al. Isobavachalcone, a chalcone constituent of Angelica keiskei, induces apoptosis in neuroblastoma. Biol Pharm Bull. 2007 Oct 1;30(10):1878–83.

27. Chen Y-G, Song X-P, Hai L-N, Lv Y-P, Fang A, Halaweish F, et al. Compounds with DNA cleaving activity from Kadsura ananosma. Pharmazie. 2006 Oct;61(10):891–2.

28. Disney MD, Lee MM, Pushechnikov A, Childs-Disney JL. The role of flexibility in the rational design of modularly assembled ligands targeting the RNAs that cause the myotonic dystrophies. Chembiochem. 2010 Feb 15;11(3):375–82.

29. Boudreau RL, McBride JL, Martins I, Shen S, Xing Y, Carter BJ, et al. Nonallele-specific silencing of mutant and wild-type huntingtin demonstrates therapeutic efficacy in Huntington's disease mice. Mol Ther. 2009 Jun;17(6):1053–63.

30. Boudreau RL, Spengler RM, Davidson BL. Rational Design of Therapeutic siRNAs: Minimizing Off-targeting Potential to Improve the Safety of RNAi Therapy for Huntington's Disease. Mol Ther. 2011 Sep 27.

ACKNOWLEDGMENTS

I have many people to thank for my time here. My advisor David has given me all the support and advice I could hope to receive in my graduate studies, and I thank him for allowing me the freedom to explore my scientific interests in a welcoming and open-minded environment. The postdocs and research scientists in the lab (and in our collaborators' labs) have been my advisors-on-the-ground, giving freely of their reagents, protocols, mice, and minds, so I am indebted to Julia Alberta, Eric Wang, Jill Crittenden, Ferah Yildirim, Ruth Bodner, and Brad Friedman. Particular thanks need to go to Kelly Knee and Oksana Sergeeva, who have been a tremendous outside-of-lab resource for ideas and for stress reduction. My friends and fellow students in the department, particularly in the labs of Angelika Amon and Mike Hemann, have helped keep me sane through this process while also providing crucial tidbits of advice, and they continually remind me that this was the right graduate program for me. Furthermore, Betsey Walsh and Janice Chang in the Graduate Program Office have helped keep me organized and on track, so thanks to them. Theresa Gipson joined the lab in 2010, and has been my labmate and the yin to my emotional yang for these past three years. Her insights, protocols, and computational skills have been almost as helpful to my development as has her positive attitude and sense of humor, and I truly appreciate the opportunity to have shared a bay with her. Theresa: If you read this, I'm sorry for all the dirty jokes over the years. I'll pay for your therapy if needed. Hilary Bowden and Shanie Coven Easter have been as helpful as they have been friendly, full of advice in both my scientific and social lives, and it would not have been as fun a lab without them. Our small but growing army of undergraduates and technicians has helped make the lab feel whole, so thank you to Thomas Wang, Destie Provenzano, Jordan Taylor, Sabine Schneider, and too many more to name. My committee members and collaborators, namely Mike Hemann, Susan Lindquist, Marian Difiglia, Leslie Thompson, and Gillian Bates, have been an invaluable resource, and I hope to return the favor in my future ventures. My parents Doug and Lisa, my brother Daniel, and my in-laws Bob and Maryann have been supporting me for years, reminding me that there is life outside of MIT without for a second allowing me to think that I have been doing anything other than my best. I love them all and am proud to call them family. Lastly and most importantly, I want to thank my wife Melissa. It would seem disingenuous to try to compress all the thanks that I owe you into this space. Just know that I love you. You have made this journey only one portion of a wonderful life, and have never let it become my life.